Reprinted from Hinz, K., Winterer, E. L., et al., 1984
Initial Reports of the Deep Sea Drilling Project, Volume LXXIX, Washington (U. S. Government Printing Office)

3. SITE 545[1]

Shipboard Scientific Party[2, 3]

HOLE 545

Date occupied: 23 April 1981

Date departed: 1 May 1981

Time on hole: 7 days, 13 hr., 21 min.

Position: 33°39.86′N; 09°21.88′W

Water depth (sea level; corrected m, echo-sounding): 3142

Water depth (rig floor; corrected m, echo-sounding): 3152

Bottom felt (m, drill pipe): 3160 (beneath rig floor)

Penetration (m): 701

Number of cores: 75

Total length of cored section (m): 701

Total core recovered (m): 354.01

Core recovery (%): 50.59

Oldest sediment cored:
Depth sub-bottom (m): 530.7
Nature: Limestone
Age: Middle Jurassic or Oxfordian
Measured velocity (km/s): 3.2 to 5.3

Basement: Not reached

Principal results: Site 545 lies in 3150 m water depth at the foot of the steep Mazagan Plateau escarpment (Fig. 1); 701 m were drilled, consisting of (Fig. 2):

0–85.6 m: Pleistocene clayey foraminiferal–nannofossil ooze.

85.6–181 m: upper Miocene to Pliocene firm, clayey nannofossil ooze with a few layers of breccia containing Jurassic carbonate-platform clasts. Rests with unconformity on

181–252 m: lower to middle Miocene greenish clayey radiolarian-bearing nannofossil chalk. Rests with unconformity on

252–530.7 m: middle or upper Cenomanian through upper Aptian green nannofossil claystone showing slump folds and microfaults and cut by low-angle sliding surfaces, with both stratigraphic repetition and omission. The lowest few meters are dolomitized nannofossil chalk. Rests with unconformity on

530.7–635.5 m: Upper Jurassic to Neocomian(?) dolomitized limestone, mainly showing high-energy shallow water features: coral debris, algal fragments, oolites, miliolids, mollusks, echinoderms. Much brecciated with iron-stained fissure fillings. Grades downward into:

635.5–701 m (total depth [T.D.]): Middle (?) Jurassic to Oxfordian dolomitized sandy limestone with ammonites. Very angular quartz and fresh feldspar, to granule size. Terrigenous component increases to 90% in last core.

Drilling stopped because the bit would not turn. After about 80 hr. of rotation, the bit lost all four cones and had only jagged and twisted cone supports left. Carbonate breccias are tough on bits.

BACKGROUND AND OBJECTIVES

Objectives at Site 545

The prime objectives at Site 545 (close to planning Site MAZ-4; Figs. 1 and 2) were to reach and, if possible, core through the Mesozoic platform carbonate rocks that underlie what we expected to be Cenozoic, Cretaceous, and perhaps Jurassic pelagic and hemipelagic sediments.

Oxfordian reddish oncoidal limestones were dredged from the Mazagan Escarpment about 10 km southeast of Site 545 (Renz et al., 1975), and we expected to encounter these at Site 545, on the assumption that the carbonate platform rocks have been displaced by seaward-dipping normal faults, as suggested by the irregular, steplike geometry of the deepest seismic reflector seen on *Meteor* profile *M* 53-08 (Fig. 21, later).

The results at Site 544 (Fig. 3) showed reddish limestone resting directly on a thin sequence of nonmarine sediments which in turn lie on crystalline basement. At Site 545 we expected a thicker section of Jurassic carbonate rocks in which the red limestone might lie within a datable sequence that would establish its age limits.

We hoped to core a carbonate sequence that would record the history of subsidence and drowning of this margin. The seismic profile suggested the possibility of an angular unconformity between the carbonate platform rocks and the overlying hemipelagic sediments. The cores would also place limits on the age at which major normal faulting ceased.

Within the sequence that came after the carbonate platform was laid down, we wanted to pin down the ages of the sedimentary units between prominent seismic reflectors. We strongly suspected that the seismic boundary Ma 1/Ma 2—the so-called Red reflector (see

---

[1] Hinz, K., Winterer, E. L., et al., *Init. Repts. DSDP*, 79: Washington (U.S. Govt. Printing Office).

[2] Karl Hinz (Co-Chief Scientist), Bundesanstalt für Geowissenschaften und Rohstoffe, 3 Hannover, Postfache 510153, Federal Republic of Germany; E. L. Winterer (Co-Chief Scientist), Geological Research Division, Scripps Institution of Oceanography, La Jolla, CA 92093; Peter O. Baumgartner, Geological Research Division, Scripps Institution of Oceanography, La Jolla, CA 92093 (present address: Escuela Centroamericana de Geologia, Apartado 35, Ciudad Universitaria Rodrigo Facio, San José, Costa Rica); Martin J. Bradshaw, Department of Geological Sciences, University of Aston, Birmingham B4 7ET, United Kingdom (present address: Shell International Petroleum Company, The Hague, The Netherlands); James E. T. Channell, Lamont-Doherty Geological Observatory, Columbia University, Palisades, New York (present address: Department of Geology, 1112 GPA Building, University of Florida, Gainesville, Florida 39611); Michel Jaffrezo, Département de Géotectonique, Université Pierre et Marie Curie, 4 place Jussieu, 75230 Paris Cedex 05, France; Lubomir F. Jansa, Geological Survey of Canada, Bedford Institute of Oceanography, Dartmouth, Nova Scotia, Canada; Robert Mark Leckie, Department of Geological Sciences, University of Colorado, Boulder, Colorado 80309 (present address: Department of Geology and Geography, University of Massachusetts, Amherst, Massachusetts 01003); Johnnie N. Moore, Department of Geology, University of Montana, Missoula, Montana 59812; Jürgen Rullkötter, Institut für Erdöl und Organische Geochemie, ICH-5, KFA Jülich, Postfach 1913, D-517 Jülich, Federal Republic of Germany; Carl H. Schaftenaar, Department of Geophysics, Texas A&M University, College Station, Texas 77843 (present address: Chevron, U.S.A., 700 S. Colorado Blvd., Denver, Colorado 80222); Torsten H. Steiger, Institut für Paläontologie und Historische Geologie, Universität München, Richard-Wagner-Strasse 10, D-800 München 2, Federal Republic of Germany; Vassil T. Vuchev, Kansas Geological Survey, University of Kansas, Lawrence, Kansas 66044 (present address: Geological Institute, Bulgarian Academy of Sciences, UL. Academy G. Bonchev, Block 2, 1113 Sofia, Bulgaria); and George E. Wiegand, Department of Geology, Florida State University, Tallahassee, Florida 32306.

[3] The descriptions of sites, cores, and data included in these site reports were completed within one year of the cruise, but many of the topical chapters that follow were completed at a later date. More data were acquired and authors' interpretations matured during this interval, so readers may find some discrepancies between site reports and topical papers. This is particularly true of biostratigraphic age assignments. The timely publication of the *Initial Reports* series, which is intended to report the early results of each leg, precludes incurring the delays that would allow the site reports to be revised at a later stage of production.

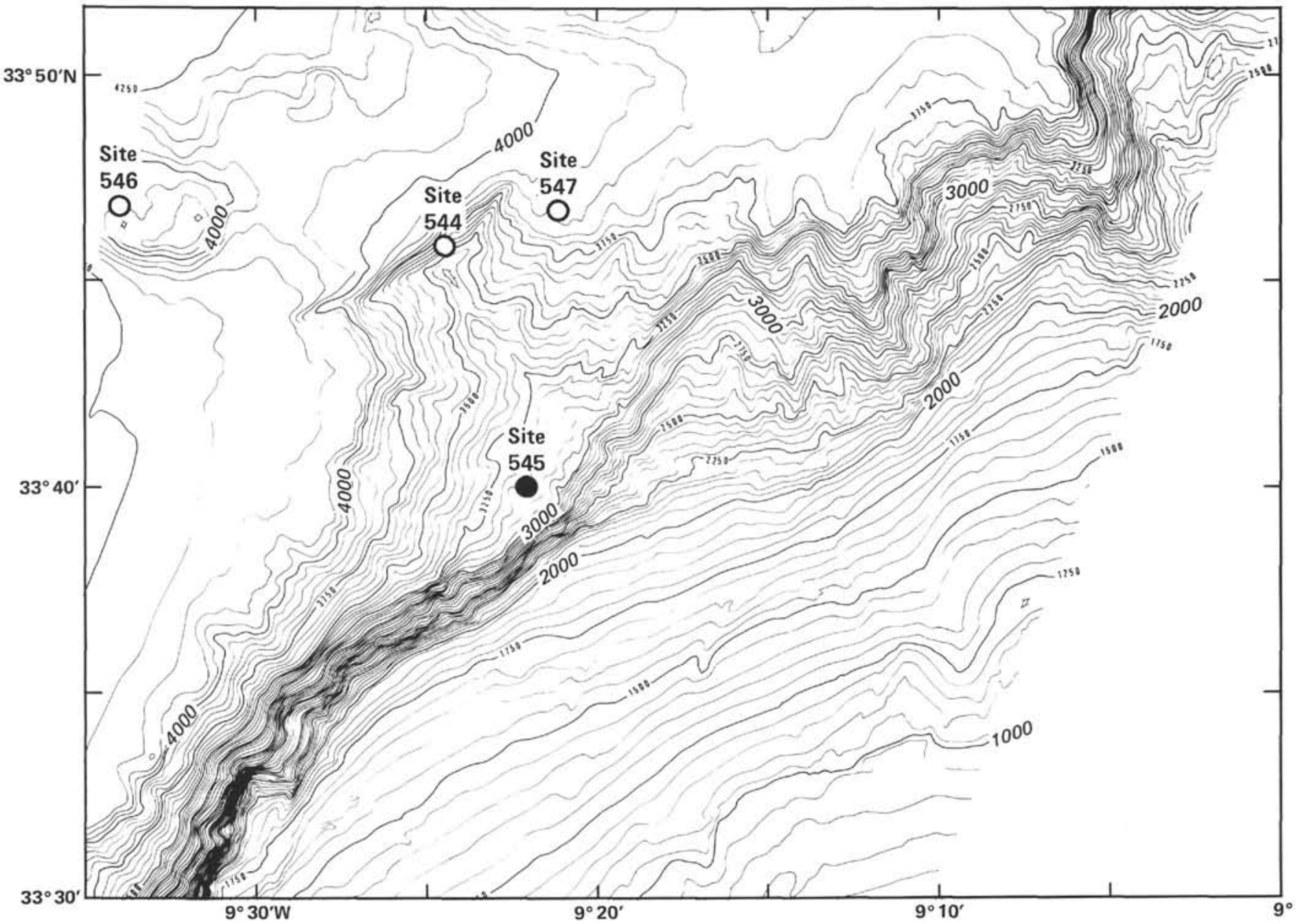

Figure 1. Bathymetry around Site 545, based on SEAZAGAN Seabeam map (Auzende et al., this volume). Depths in m.

Seismic Stratigraphy section, this chapter)—would cut out most of the Upper Cretaceous, as it does in the adjacent Morocco Basin at Sites 415 and 416 (Lancelot and Winterer, 1980). Whether Paleogene beds were present at Site 545 above this reflector was unknown.

We reasoned that the history of erosional shaping of the steep Mazagan Escarpment would be echoed, in part at least, in the stratigraphy of the Cretaceous and Cenozoic slope sediments to be cored at Site 545.

OPERATIONS

Approach

The approach to Site 545 was by a circuitous route, to allow a brief survey over a structural high about 10 km west of Site 544. This structure looks very similar to the gneissic fault block drilled at Site 544 and we were very keen now to drill the other structure if it could be done safely. The *Challenger* left Site 544 at 0245 GMT on 23 April, and after streaming the seismic gear passed back near the acoustic beacon at 0337 GMT. The survey took only about 4 hr., and we then returned to the acoustic beacon at Site 544 and attempted to follow *Meteor* seismic line *M* 53-08, to reach MAZ-4 (see Fig. 4). A satellite fix at 0758 GMT showed us to be a little east of the *Meteor* line. At 0815 GMT we made a correction to a new course that took us a little east of MAZ-4, so we steamed ahead, made a right turn, and came back on a reciprocal course in order to arrive directly over MAZ-4. Instead, the ship's drift carried us off this intended line, so when we reached what appeared on the *Glomar Challenger* seismic profiler (Fig. 5) to be a position equivalent to MAZ-4 with respect both to the foot of the Mazagan Escarpment and to the reflection time to the Red reflector (the deepest reflector consistently visible on the *Glomar Challenger* profiles), we dropped the beacon for Site 545, at 0944 GMT (1044 hr. local time). After a day or two at Site 545, the weighted average of the satellite fixes showed our position to be about 1 km west of MAZ-4.

The echo sounder at Site 545 showed an echo at 4.17 s; we used this echo to calculate our depth, even though we knew this might be a side echo from a reflector on the slope. With a correction of 8 m for the speed of sound in water at this depth in this region (Matthews, 1939), the depth below sea level was estimated as 3142 m.

Coring Operations

The pipe was lowered to a little above 3152 m below the derrick floor and slowly advanced to find the sea-

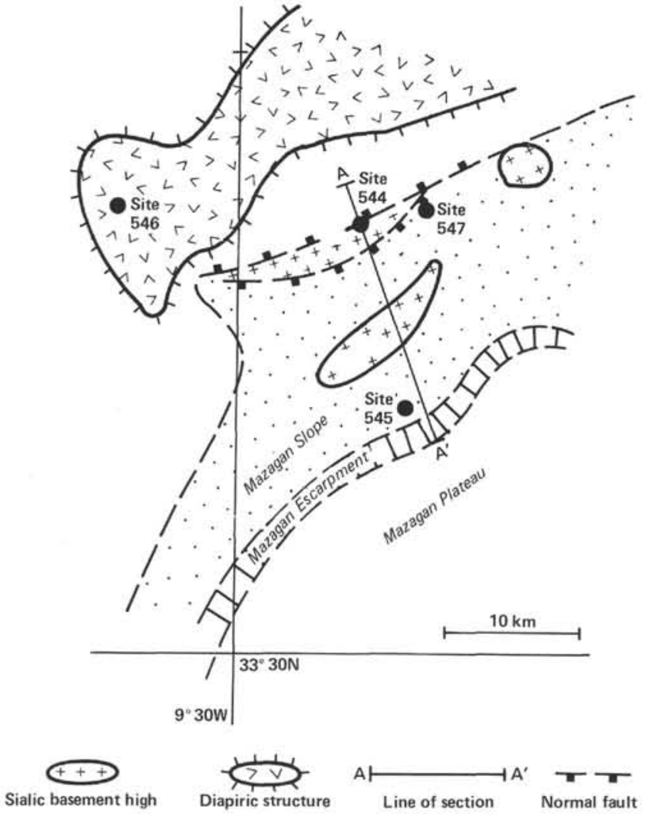

Figure 2. Map of Mazagan Escarpment area, showing Leg 79 sites and major geologic features. Line A-A′ is line of seismic reflection profile *M* 53-08.

floor. A core at 3159.0 to 3168.5 m contained 8.5 m of sediment and the seafloor depth was thus established as 3160 m below the derrick floor, or 3150 m below sea level.

Continuous coring proceeded without incident, with gradually increasing pump pressure, weight on the bit, and torque limit as the bit met firmer sediments.

At about 93 m below the seafloor (BSF), the coring slowed markedly and the pipe began to bounce and vibrate. This was the first of a series of limestone and dolomite breccia layers between 93 and 180 m BSF, and drilling through these doubtless damaged the bit.

At about 252 m BSF, drilling slowed and we entered Cretaceous clayey chalk and calcareous claystone. These became progressively harder through the 287.7-m thickness of this unit: coring rates at the top were about 7 min./m, and at the base were about 12 min./m.

At 530.7 m, the bit entered Jurassic carbonate rocks, which were drilled surprisingly rapidly: about 2–7 min./m, down to about 641 m BSF. Cores from this interval contained dolomite that was much brecciated, and recovery rates were poor. We believe the brecciation to be an original feature of the rocks. This type of material was also probably very rough on the bit.

Below 641 m the coring rate slowed markedly, to about 12–14 min./m in hard dolomite that became sandier below. The deterioration of the bit now became apparent as the core diameter progressively decreased to 48 mm in Cores 72 and 73 and to only about 40 mm in Core 74. Meanwhile, the actual cored material became progressively softer and more friable. Clearly the bit was failing. When we began to cut Core 75, at a depth of 700.5 m BSF, the bit would not rotate, so this core barrel was retrieved (with about 40 cm of limey fossiliferous sandstone) and the hole abandoned. The total depth was 701.0 m BSF.

When the bit arrived on deck (Fig. 6), it was without any of the four cones, and presented only the jagged and twisted cone supports and throat guards. Small wonder that it would go not farther.

Plots of elapsed time versus core depth and versus bit rotation time are shown in Figure 7. A summary of the coring operations, giving core numbers and depths, is shown in Table 1.

SEDIMENT LITHOLOGY

Introduction

The sedimentary succession encountered at Site 545 (Fig. 2) is subdivided into the four lithologic units and nine subunits (Fig. 23, later) described here in descending order.

Unit I: 0–181 m; 545-1 to 545-20-1, 43 cm

Foraminiferal nannofossil clay and ooze with layers of carbonate gravel

Lithologic Unit I extends from the seafloor to 545-20-1, 43 cm; consideration of drilling rate data (see below) suggests that the true sub-bottom depth of this horizon is 181 m. The principal sediment types composing the unit are yellowish brown foraminiferal-nannofossil-rich clay and very clayey, foraminiferal-nannofossil-rich and nannofossil-rich ooze, which range in age from middle Miocene or early late Miocene to late Pleistocene. Calcium carbonate, chiefly in the form of nannofossils, does not exceed 77% of the sediment and decreases upward through the Pleistocene section to less than 40%; terrigenous clay-sized material composes most of the remainder. Intervals of limestone gravel occur in the lower half of the unit, and two subunits have been distinguished on this basis; their boundary is drawn above the highest limestone pebble at 545-10-1, 106 cm (85.6 m sub-bottom depth), which is also approximately the Pliocene/Pleistocene boundary.

Subunit IA; 0–85.6 m; 545-1 to 545-10-1, 106 cm

The upper part of Subunit IA consists of foraminiferal-nannofossil-rich and nannofossil-rich clays, which pass downward around 67 m to very clayey foraminiferal nannofossil ooze. This transition reflects the calcium carbonate content of the sediment, which increases from 41% around 46.5 m (Core 6) to approximately 65% at the base of the subunit (Core 10); calcium carbonate contents above Core 6 mostly vary between 35 and 42%. Apart from dolomite rhombs, medium-silt-sized or finer, which constitute up to 2% of the sediment, the carbonate fraction consists entirely of foraminifers and nannofossils. Foraminifer abundance (measured as the volumetric percentage of foraminifers within the biogenic carbonate fraction) averages 15% but falls to 7% in

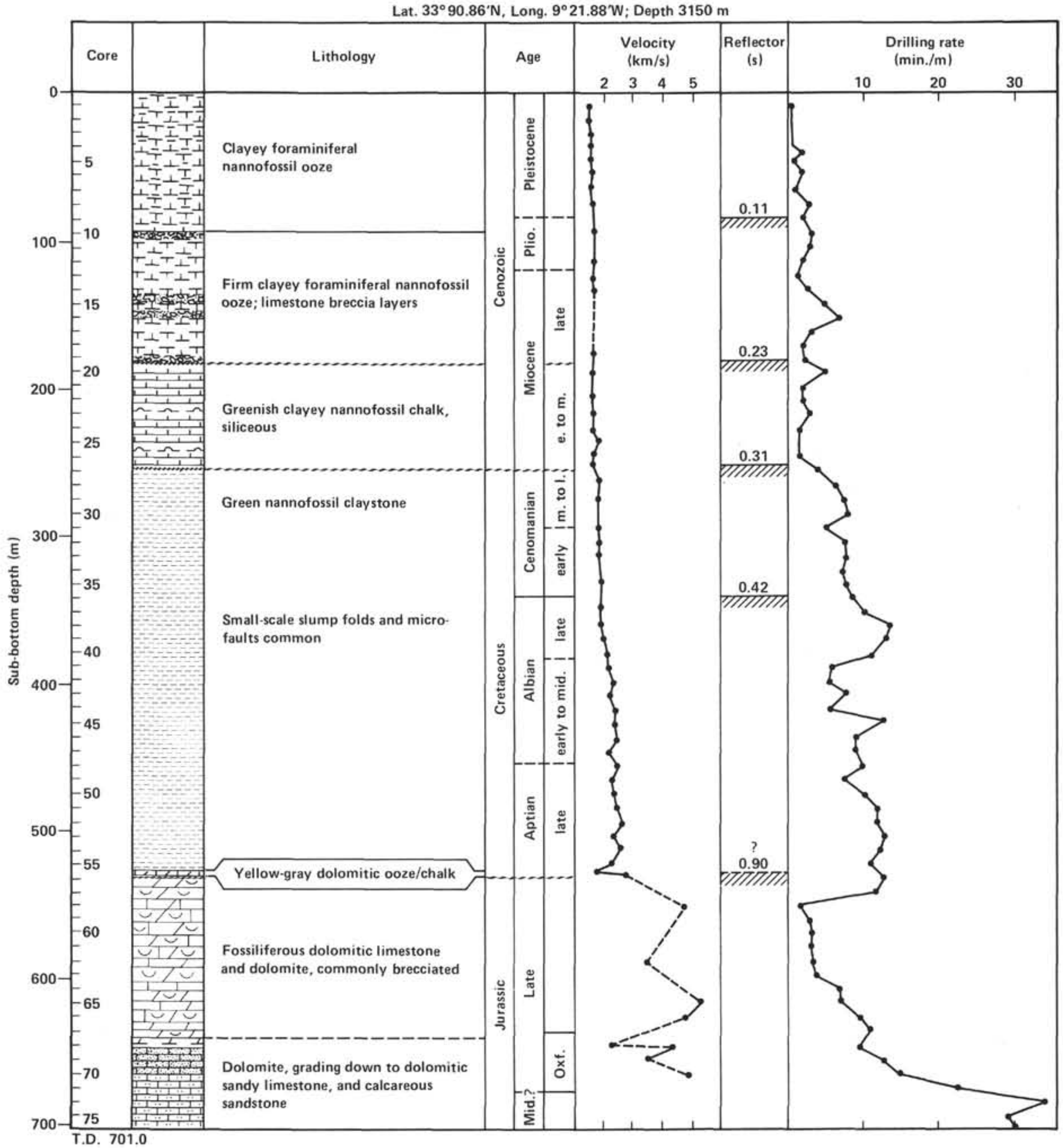

Figure 3. Summary graphic log of Site 545.

Core 6 and Section 545-4-1. Siliceous biogenic debris appears confined to Cores 1 to 4 (0–37 m). This component decreases downward from 0.3% in Core 1; sponge spicules are accompanied by a tiny proportion of radiolarians and trace quantities of diatoms. Silt forms around 5% of the terrigenous sediment fraction, but very fine sand-grade quartz is extremely rare; quartz silt is omnipresent, accompanied by muscovite, but feldspar is rare. Glauconite grains form a very tiny but consistent component of the silt-grade material.

Core recovered from Subunit IA was considerably disturbed by drilling and in places mixed to a slurry. Color banding or interlayering was, however, discerned in the less disturbed Cores 2, 3, and 8. Yellowish brown is the dominant sediment color of the subunit, and alternating paler (10YR 6/2) and darker (10YR 4/2) layers, 40–60 cm thick, characterize Core 3; layer contacts are both sharp and gradational. These color alternations do not reflect fluctuations in the clay: carbonate ratio but appear to be related to varying pyrite content. Framboidal pyrite is concentrated in thinner, light olive gray and greenish gray layers (less than 1 cm and generally 1–2 mm thick), which are abundant in the less disturbed cores. Light olive gray to medium dark gray, pyrite-rich, simple burrow fills, up to 4 mm in diameter, are also common throughout Subunit IA; in places they display coalesced pyrite octahedra, whereas others consist of a pyrite-cemented foraminifer sand. Many burrows dis-

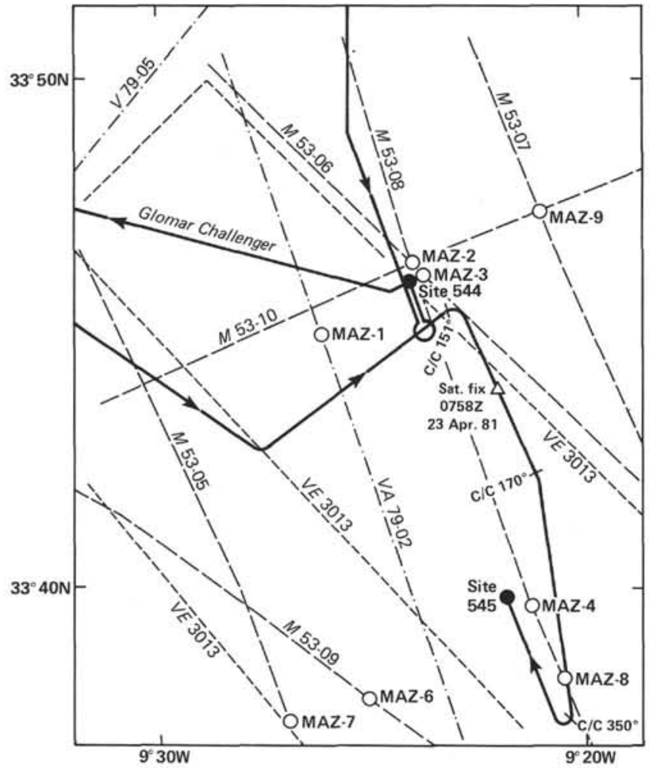

Figure 4. Approach to Site 545.

play longitudinal striations which may reflect scraping by either annelid hairs or crustacean appendages, as in some *Spongeliomorpha.*

Subunit IB; 85.6–181 m; 545-10-1, 106 cm to 545-20-1, 43 cm

Unfortunately, owing to the greatly differing resistance to drilling of soft ooze and limestone gravel, core recovery in parts of Subunit IB was poor (6.8% for 131–170 m), and much ooze was washed out. Consideration of drilling rate enables a tentative reconstruction of the sequence (Fig. 8). The sediment beneath the gravels consists of a very clayey and clayey foraminiferal nannofossil ooze in the upper 18 m of the subunit (85.6–103.5 m), but grades down into clayey nannofossil ooze and then very clayey nannofossil ooze below 151 m (Core 16). The calcium carbonate content of the sediment initially increases downward from 62% in Core 10 to an average of 75% in Cores 11 to 15, but then drops steadily toward 50% near the base of the subunit, where thin layers of dusky brown nannofossil-rich clay are common. As in Subunit IA, dolomite rhombs constitute up to 2% of the sediment, but foraminifer abundance within the remaining carbonate fraction is lower in IB, only exceeding 10% near the top of the subunit and averaging 6% elsewhere, except for two 4-cm-thick, foraminifer-rich layers in Samples 545-19-3, 47–51 cm and 545-19-6, 62–66 cm. Subunit IB is devoid of siliceous biogenic debris and the composition of the terrigenous sediment fraction is the same as that in IA. Once again much of the core was considerably disturbed by drilling, but the 8 m of ooze in Core 19 is the least disturbed interval recovered from Unit I and also the most consolidated, reflecting increased burial pressure. Color interlayering of light olive gray with dark yellowish brown, and pale yellowish brown with greenish gray, light olive gray, and dark yellowish brown is well developed here, 14 such alternations occurring within 7.7 m. Contacts are both sharp and gradational; like Unit I sediments in general, many are slightly to moderately bioturbated. Cores 12 and 13 also display color interlayering on a slightly larger scale, but of pale yellowish brown with pinkish gray in Core 12 and grayish orange pink with pinkish gray in Core 14. As in Subunit IA, thin olive gray and greenish gray pyrite-rich layers are abundant in the less disturbed cores and pyrite-rich burrow fills abound.

In the interpolated section for Subunit IB presented in Figure 8, four main units of limestone gravel are recognized, the lowest resting directly on the hiatus between Units I and II. Although some of the pebbles and cobbles have not been excessively fragmented by drilling, are subrounded to rounded (terminology of Powers, 1953) and commonly display bivalve borings on their exterior, others may be the remains of larger cobbles, or perhaps even boulders, and their roundness is partly the result of abrasion within the core barrel. No undisturbed matrix from the main gravelly units was recovered and hence important features such as their degree of packing and textural class are unknown. However, the lack of atypical sediments within the gravels and drilling breccias recovered, also the occurrence of scattered pebbles (which may be the representatives of quite widespread but thin pebbly layers) sitting in unexceptional ooze between the main gravel units, suggests to us that their matrix was also clayey nannofossil ooze or foraminiferal nannofossil ooze. The limestone gravel displays considerable petrographic variety, but dominant is a suite of white, occasionally glauconitic, skeletal, oncoidal, and intraclastic wackestones and packstones which commonly display a "merged" peloidal texture. Oolitic, peloidal, and intraclastic grainstones also belong to this suite of limestones, which contain a shallow-water macrofaunal assemblage of colonial scleractinian coral debris, echinoderms, calcified siliceous sponges, thick-shelled bivalves, foraminifers (*Trocholina alpina* and *T. elongata*), and rare algae (*Acicularia, Salpingoporella pygmaea*). Common calpionellids (*Calpionella, Crassicollaria, Tintinnopsella*) indicate a Tithonian to Berriasian age. These calpionellids, along with abundant pelagic bivalve fragments, ammonites, and belemnites, indicate an open marine depositional environment. Two particularly notable rock types are each represented by only a single clast. A rounded pebble of glauconite-bearing microsparite (545-10-1, 106 cm) yielded *Nannoconus colomi* of Berriasian to Barremian age (Thierstein, 1976), and another pebble consists of angular clasts of calpionellid-bearing peloid grainstone reworked into a (?)-Santonian micrite matrix.

Discussion: Pelagic sediment of Unit I was deposited above the foraminiferal lysocline. Terrigenous input is greater than at Site 544 and reflects a settling closer to the continental shelf.

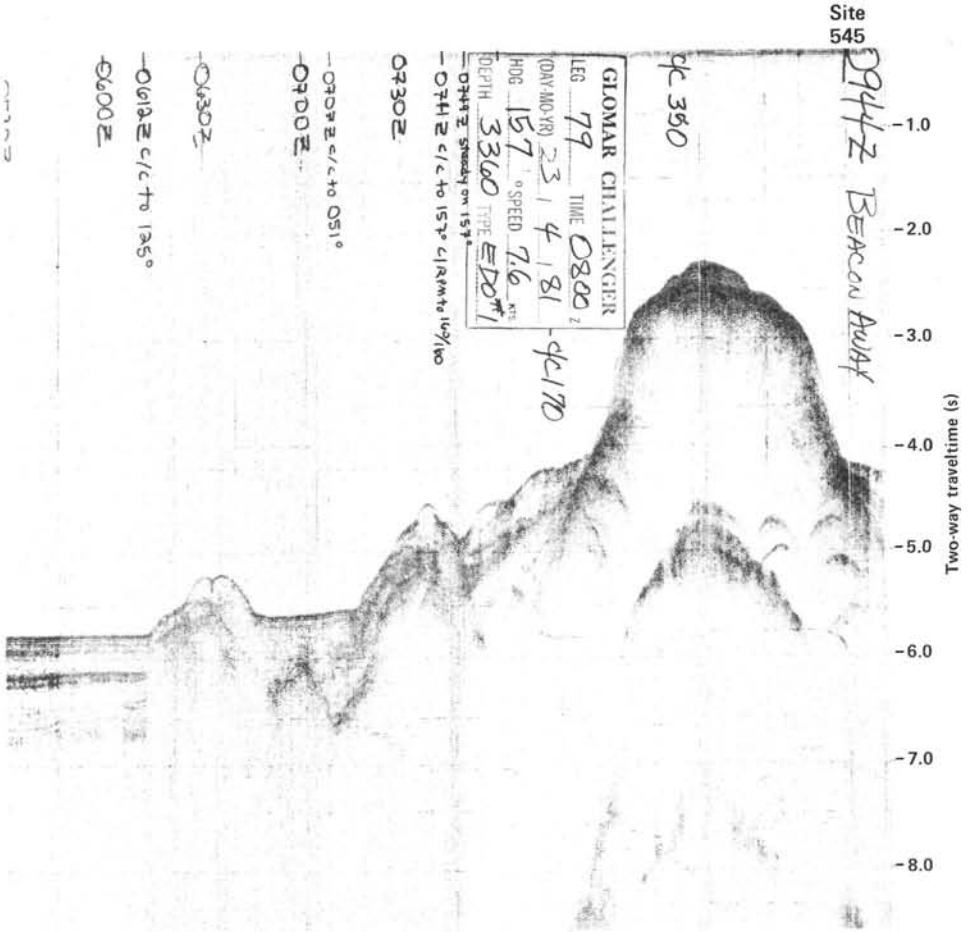

Figure 5. Seismic reflection profile made by *Glomar Challenger* during approach to Site 545.

Thin, light olive gray and darker pyrite-rich layers reflect vertical variation in the organic component of the sediment, probably because of temporal variations in organic productivity; larger-scale fluctuations in pyrite content gave rise to color interlayering and suggest regular changes in oxygenation of the bottom sediments that are linked to organic productivity; these alternations were not detected at Site 544. The generally increased pyrite content of Site 545 compared to Site 544 reflects either closer proximity to sites of high organic productivity on the shelf, or less-oxygenated bottom waters.

The petrography of the limestone clasts in the gravel units at the base of Unit I indicates their derivation from the nearby Mazagan Plateau. The discrete gravel-rich units must represent the deposits of subaqueous debris flows or incoherent slumps, and their inferred matrix of unexceptional ooze further indicates that the flows began at the face of the escarpment, rather than on the shelf.

The inception of the debris flows and their coincidence with sharp lithological change between Units I and II reflects a change in basin morphology and/or current dynamics. During the time interval between the units, erosion probably removed the Cretaceous to middle Miocene fine-grained sediments which had blanketed the escarpment; subsequently currents continued to sweep the escarpment, where gravity effects and bioerosion combined to deface the slope. The cessation of gravelly gravity flows in the late Pliocene reflects either complete blanketing of the escarpment face by ooze, or less active erosion of the exposed carbonates. Continued redeposition of higher-slope oozes may, however, have continued.

Unit II: 181–252 m; 545-20-1, 43 cm through 545-27

Clayey foraminiferal nannofossil chalk and nannofossil-rich claystone, glauconite-bearing and basally slightly siliceous.

Lithologic Unit II, which ranges in age from early to middle or early late Miocene, is clearly distinguishable from Unit I by a higher degree of induration, a preponderance of green and gray hues rather than yellowish brown colors, a conspicuous and more diverse ichnofauna, and a higher content of siliceous biogenic sediment, especially at the base. The lower boundary of Unit II with darker, olive nannofossil-rich Cenomanian claystone was not recovered, but in view of the marked change in penetration rate experienced while drilling Core 27, we place the boundary within that interval and immediately below the recovered sections at a sub-bottom depth of 252 m. The more consolidated nature of Unit II when compared to Unit I is reflected by less severe drilling disturbance. However, fragmentation into 2–8 cm lengths with some reorientation occurred locally and is

Figure 6. Drill bit used at Site 545.

particularly well developed below 236.5 m, where the heaving of the drilling bit with each passing ocean swell resulted in the injection of regularly spaced clay seams which cross-cut and offset bedding and bioturbational structures (Fig. 9A).

The upper part of Unit II consists of clayey nannofossil chalk and minor amounts of foraminiferal nannofossil chalk, which become very clayey below 208.0 m and pass gradationally down around 238.0 m into nannofossil-rich claystone. This transition reflects a general downward decrease in the carbonate content of the sediment, from 70 to 80% at the top of the unit to approximately 43% at the base. Silt-sized dolomite rhombs are ubiquitous but never exceed 1% of the total sediment, and apart from these the carbonate fraction consists entirely of foraminifers and nannofossils. Foraminifer abundance within the biogenic carbonate is generally low compared to Unit I, but exceeds 10% between 198.5 and 221.5 m and between 227.6 and 231.1 m (37% of the total unit), elsewhere averaging 5%. The fall in carbonate content from over 60 to around 50% within the upper part of Core 25 coincides with the appearance of a significant proportion of siliceous biogenic debris. This latter component constitutes an average of 5% (as high as 7.5% locally) of the total sediment between 227.07 and 249.0 m, but then falls away to less than 2% in the lower meters of the unit. Radiolarians dominate, consistently forming between 60 and 75% of the siliceous biogenic fraction, and are accompanied by sponge spicules and smaller proportions of diatoms and silicoflagellates. The terrigenous sediment component of Unit II is texturally a clay; on average it contains 4% silt-sized material, mostly quartz, accompanied by less muscovite than in Unit I. Minor but important components of Unit II, which were virtually unrecorded in Unit I, are fish remains and plant cuticle debris.

Greenish gray colors (5GY 6/1, 5G 6/1, 5GY 8/1) characterize the upper five cores of Unit II (181.0-227.0 m), the different shades picking out thin lamination which is best developed at the top of the unit and becomes progressively more obscured by bioturbation downward. Lighter-colored intervals are firmer and slightly more calcareous; in them the nannoplankton, especially discoasters, commonly display incipient carbonate overgrowths. Associated softer lithologies verge on the ooze classification. Three 1-cm layers of olive black nannofossil-rich claystone occur within the chalks of Core 20, and similar dusky yellow brown layers occur in Core 23 between 215.18 and 215.91 m. Pale green, grayish green, and greenish gray intercalations persist below 227.0 m, but yellow green and olive colors characterize the lower three cores of Unit II. Examination of color trends within the unit generally suggests that although there is no absolute correlation between color and terrigenous sediment content, the duskier or more olive colored intervals within a particular core contain between 5 and 10% more detrital clay. Another very important factor appears to be the variable pyrite content of the sediment. Pyrite occurs commonly as framboids but is also more finely dispersed within the sediment and shows a preference for plant debris and especially radiolarian tests. Particularly pyrite rich layers are olive gray or medium gray in color and display notably less bioturbation. In addition, the range in shades of green, greenish gray, and grayish green is clearly controlled by the glauconite content of the sediment. Glauconite is much more abundant than in Unit I and averages at least 1% of most sediment. Though it is dominantly of medium silt to medium sand size, larger lumps up to medium pebble size also occur and locally, where concentrated in patches with the finer grade of glauconite, would appear to be *in situ*. Glauconite sand is also abundant and suspected to be *in situ* in the paler greenish gray intercalations within the lower part of the unit.

Unit II is strongly bioturbated, except for the uppermost meters and the lowermost meter, which retain a well-developed, thin lamination. Especially toward the base of the unit, the ichnofauna is picked out by olive colors (5Y 5/2, 5Y 3/2, 10Y 6/2, 5Y 4/1, 5Y 6/1), which apparently reflect a higher pyrite content. Simple burrows such as Planolites (0.3-1.3 cm diameter) abound, along with Chondrites and Zoophycos, including "pelleted" varieties of the latter. Rind burrows and composite burrows (both sensu Chamberlain, 1978) are also common; the latter are large tubular burrows, up to 1 cm in diameter, containing either Chondrites or pellets (Fig. 9B). Pyritic burrows similar to those described from Unit I are particularly conspicuous in the more calcareous sediments above 227.0 m.

Four units of intraformational conglomerate occur in Cores 25 and 26 (230.36-230.61, 231.15-231.50, 235.76-

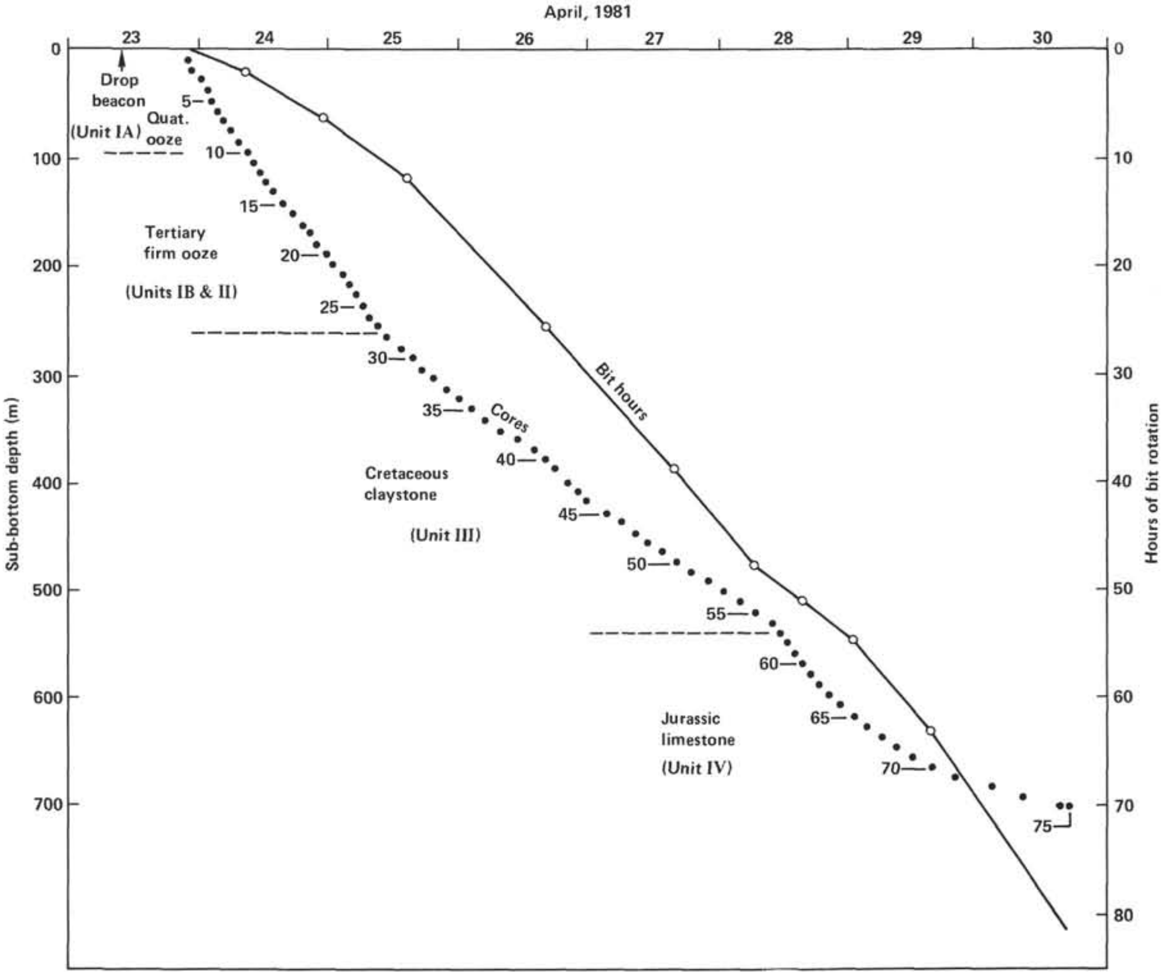

Figure 7. Elapsed time on Site 545 versus core depth (core numbers and lithologic units shown) and hours of rotation on bit at Site 545.

235.91, and 238.85–239.14 m; Fig. 9C). Texturally they are clayey, large-pebble conglomerates with a range of phenoclast composition embracing all the lithologies of Unit II; their matrices are similarly unexceptional claystones and chalks. Pebbles are highly deformed because of bedding compaction but an original clast-support is obvious. Maximum phenoclast size within a 25-cm unit generally grades; above this point, the pebbles fine upward and the tops of the units are extensively bioturbated. Sand- and pebble-sized glauconite is common within the conglomerates, where it may have a derived origin, but the concentration and texture of the glauconite within and immediately above the conglomerate tops (see again, Fig. 9C) suggests *in situ* growth.

Discussion: The pelagic sediment of Unit II was deposited above the foraminiferal lysocline; the presence of Seilacher's (1967) Nereites ichnofacies reflects the deep bathymetric position but mainly indicates a low-energy environment.

The conglomeratic layers are interpreted as subaqueous debris flows or incoherent slumps, the downslope edges of slumped sediment masses from higher up the slope which have mixed with water to the extent that stratification is destroyed, and a chaotic mixture of mud and water and chunks of the remaining coherent sediment results. Some sorting is apparent; it presumably reflects the liquified nature, virtually without cohesion, of the flow: the fining-upward trend reflects waning flow.

The boundary between Units I and II is contained within a hiatus in Site 544 (Core 7). The higher depositional rate at Site 545 reflects a basal slope setting, whereas Site 544 represents a more distal high at the foot of the main slope. The contrast in induration between Units I and II suggests that much of the induration was acquired prior to deposition of Unit I, and therefore the amount of sediment removed in the mid to late Miocene was considerable.

Units II and I are glauconite-rich and glauconite-poor respectively. Though glauconite may form by several processes, an association with organic material is frequent (Burst, 1968a, b). Unit II sediments at Site 545 contain in addition significant amounts of biogenic silica whereas the glauconite-poor higher sequence is also silica-poor. These trends and the relative abundance of fish and plant remains in the earlier unit all point to a marked change in climate or oceanography in the mid- to late Miocene, which radically affected organic productivity and hence the early diagenetic environment.

Table 1. Coring summary, Site 545.

Core no.	Date (April 1981)	Time	Depth from drill floor (m) Top Bottom	Depth below seafloor (m) Top Bottom	Length cored (m)	Length recovered (m)	Percentage recovered
1	23	2128	3160.0–3168.5	0.0–8.5	8.5	7.8	92
2	23	2220	3168.5–3178.0	8.5–18.0	9.5	9.3	98
3	23	2338	3178.0–3187.5	18.0–27.5	9.5	8.7	93
4	24	0100	3187.5–3197.0	27.5–37.0	9.5	7.7	85
5	24	0202	3197.0–3206.5	37.0–46.5	9.5	6.4	67
6	24	0311	3206.5–3216.0	46.5–56.0	9.5	1.5	20
7	24	0412	3216.0–3225.5	56.0–65.5	9.5	1.8	19
8	24	0538	3225.5–3235.0	65.5–75.0	9.5	8.7	92
9	24	0652	3235.0–3244.5	75.0–84.5	9.5	0.01	0.1
10	24	0822	3244.5–3254.0	84.5–94.0	9.5	4.1	43
11	24	0942	3254.0–3263.5	94.0–103.5	9.5	6.8	72
12	24	1054	3263.5–3273.0	103.5–113.0	9.5	7.6	80
13	24	1209	3273.0–3282.5	113.0–122.5	9.5	9.4	100
14	24	1331	3282.5–3292.0	122.5–132.0	9.5	7.0	74
15	24	1519	3292.0–3301.5	132.0–141.5	9.5	0.4	4
16	24	1730	3301.5–3311.0	141.5–151.0	9.5	1.5	16
17	24	1858	3311.0–3320.5	151.0–160.5	9.5	0.3	2
18	24	2018	3320.5–3330.0	160.5–170.0	9.5	0.4	4
19	24	2139	3330.0–3339.5	170.0–179.5	9.5	8.0	84
20	24	2328	3339.5–3349.0	179.5–189.0	9.5	2.3	24
21	25	0044	3349.0–3358.5	189.0–198.5	9.5	3.1	34
22	25	0204	3358.5–3368.0	198.5–208.0	9.5	0.6	6
23	25	0322	3368.0–3377.5	208.0–217.5	9.5	9.6	102
24	25	0434	3377.5–3387.0	217.5–227.0	9.5	8.2	87
25	25	0550	3387.0–3396.5	227.0–236.5	9.5	9.7	102
26	25	0700	3396.5–3406.0	236.5–246.0	9.5	6.0	63
27	25	0836	3406.0–3415.5	246.0–255.5	9.5	5.6	59
28	25	1035	3415.5–3425.0	255.5–265.0	9.5	1.0	11
29	25	1302	3425.0–3434.5	265.0–274.5	9.5	2.3	24
30	25	1526	3434.5–3444.0	274.5–284.0	9.5	1.0	11
31	25	1717	3444.0–3453.5	284.0–293.5	9.5	2.0	21
32	25	1924	3453.5–3463.0	293.5–303.0	9.5	0.8	8
33	25	2146	3463.0–3472.5	303.0–312.5	9.5	1.2	14
34	25	2359	3472.5–3482.0	312.5–322.0	9.5	4.1	43
35	26	0216	3482.0–3491.5	322.0–331.5	9.5	3.0	32
36	26	0432	3491.5–3501.0	331.5–341.0	9.5	4.2	44
37	26	0711	3501.0–3510.5	341.0–350.5	9.5	3.6	38
38	26	1025	3510.5–3520.0	350.5–360.0	9.5	4.4	46
39	26	1326	3520.0–3529.5	360.0–369.5	9.5	6.5	68
40	26	1612	3529.5–3539.0	369.5–379.0	9.5	8.1	85
41	26	1809	3539.0–3548.5	379.0–388.5	9.5	5.3	57
42	26	2003	3548.5–3558.0	388.5–398.0	9.5	8.8	93
43	26	2214	3558.0–3567.5	398.0–407.5	9.5	9.8	103
44	27	0007	3567.5–3577.0	407.5–417.0	9.5	3.1	3
45	27	0315	3577.0–3586.5	417.0–426.5	9.5	8.7	92
46	27	0558	3586.6–3595.0	426.5–436.0	9.5	8.0	84
47	27	0824	3596.0–3605.5	436.0–445.5	9.5	9.0	95
48	27	1058	3605.5–3615.0	445.5–455.0	9.5	9.8	103
49	27	1326	3615.0–3624.5	455.0–464.5	9.5	8.8	92
50	27	1612	3624.5–3634.0	464.5–474.0	9.5	8.8	93
51	27	1908	3634.0–3643.5	474.0–483.5	9.5	8.4	87
52	27	2202	3643.5–3653.0	483.5–493.0	9.5	9.7	102
53	28	0102	3653.0–3662.5	493.0–502.5	9.5	8.1	85
54	28	0356	3662.5–3762.0	502.5–512.0	9.5	9.7	102
55	28	0655	3672.0–3681.5	512.0–521.5	9.5	8.6	91
56	28	0958	3681.5–3691.0	521.5–531.0	9.5	9.3	98
57	28	1117	3691.0–3700.5	531.0–540.5	9.5	1.5	16
58	28	1241	3700.5–3710.0	540.5–550.0	9.5	0.2	2
59	28	1402	3710.0–3719.5	550.0–559.5	9.5	0.7	7
60	28	1550	3719.5–3729.0	559.5–569.0	9.5	0.2	1
61	28	1716	3729.0–3738.5	569.0–578.5	9.5	0.6	6
62	28	1852	3738.5–3748.0	578.5–588.0	9.5	0.8	8
63	28	2033	3748.0–3757.5	588.0–597.5	9.5	1.1	12
64	28	2245	3757.5–3767.0	597.5–607.0	9.5	2.8	29
65	29	0103	3767.0–3776.5	607.0–616.5	9.5	1.3	14
66	29	0339	3776.5–3786.0	616.5–626.0	9.5	2.3	25
67	29	0629	3786.0–3795.5	626.0–635.5	9.5	1.5	16
68	29	0902	3795.5–3805.0	635.5–645.0	9.5	3.7	39
69	29	1213	3805.0–3814.5	645.0–654.5	9.5	3.3	35
70	29	1542	3814.5–3824.0	654.5–664.0	9.5	1.7	18
71	29	2033	3824.0–3833.5	664.0–673.5	9.5	5.0	53
72	30	0301	3833.5–3842.5	673.5–682.5	9.0	3.3	37
73	30	0939	3842.5–3851.5	682.5–691.5	9.0	2.5	28
74	30	1533	3851.5–3860.5	691.5–700.5	9.0	1.3	14
75	30	1748	3860.5–3861.0	700.5–701.0	0.5	0.4	80
					701.0	354.01	51

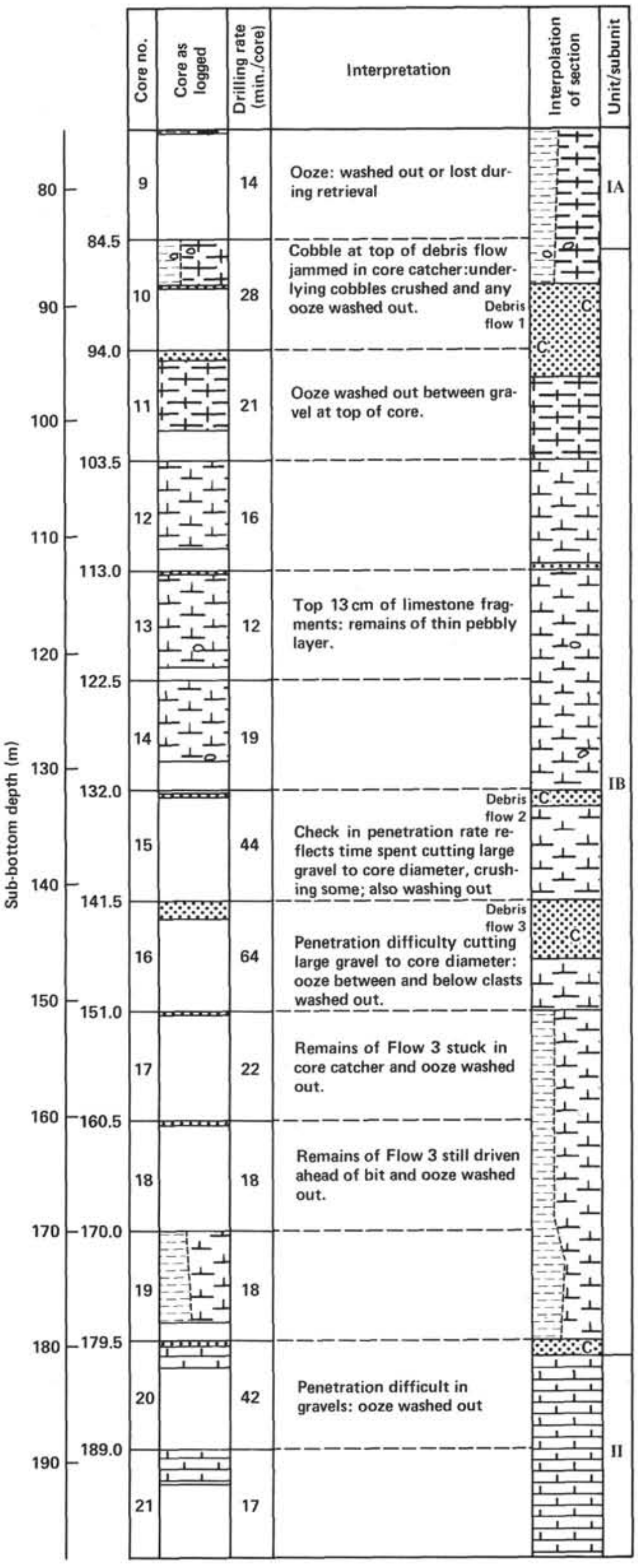

Ooze: washed out or lost during retrieval

Cobble at top of debris flow jammed in core catcher: underlying cobbles crushed and any ooze washed out.

Ooze washed out between gravel at top of core.

Top 13 cm of limestone fragments: remains of thin pebbly layer.

Check in penetration rate reflects time spent cutting large gravel to core diameter, crushing some; also washing out

Penetration difficulty cutting large gravel to core diameter: ooze between and below clasts washed out.

Remains of Flow 3 stuck in core catcher and ooze washed out.

Remains of Flow 3 still driven ahead of bit and ooze washed out.

Penetration difficult in gravels: ooze washed out

Figure 8. Attempted reconstruction for the true sequence within Subunit IB.

Unit III: 252–530.7 m; 545-28 to 545-56-7, 20 cm

Nannofossil claystone and clayey nannofossil chalk, slightly siliceous in places, dolomitic toward the base, with pebble conglomerates.

The Cretaceous system at Site 545 is represented by Lithologic Unit III, which is 278.7 m thick, of early late Aptian to middle or late Cenomanian age, and rests unconformably on pale orange Jurassic limestones at 545-56-7, 20 cm. The principal sediment types composing the unit are grayish olive green, grayish olive, and

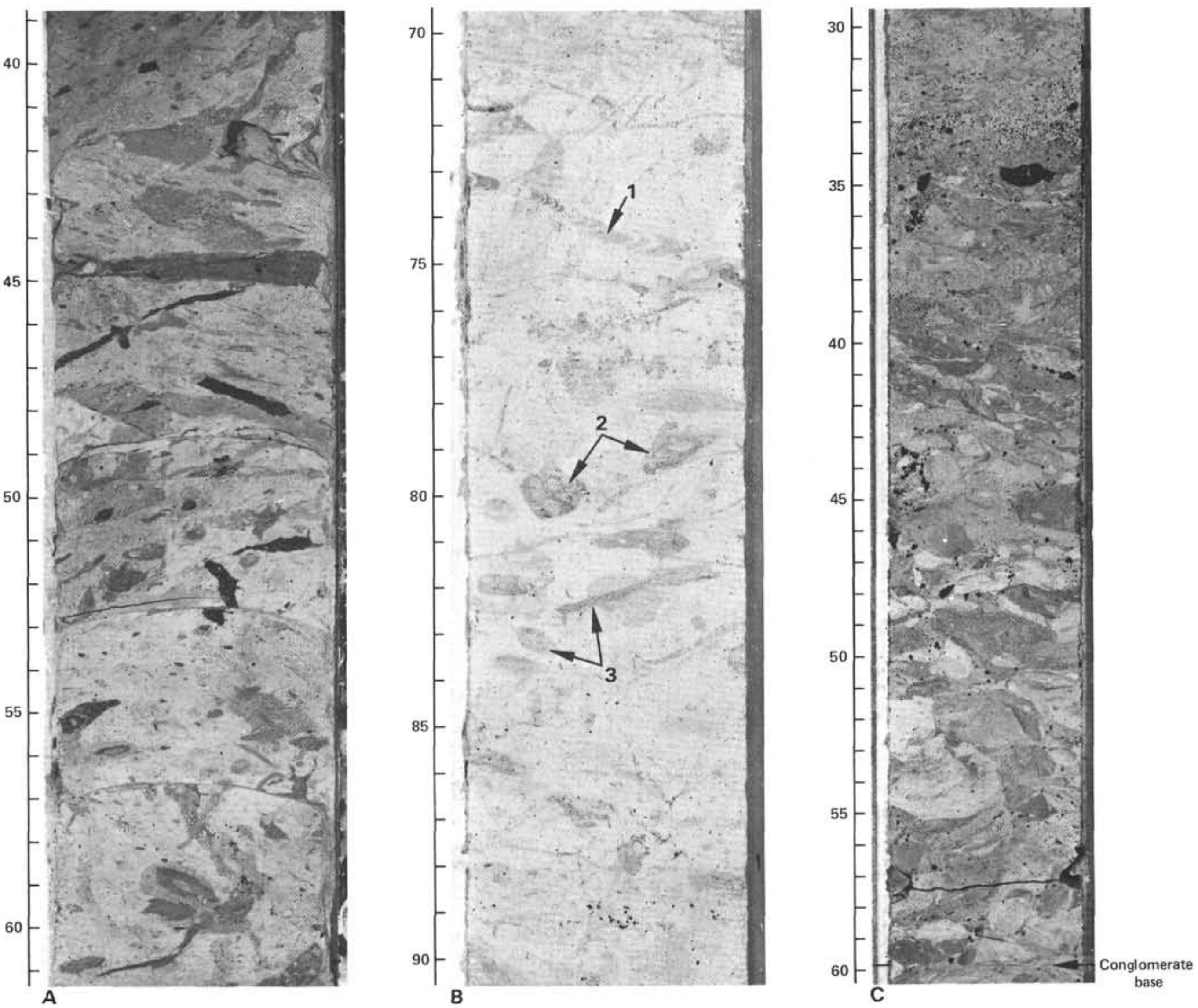

Figure 9. Features of Unit II: A. "Drilling cake" structure: rising and falling of the drilling bit with the ocean swell fragmented the core, reoriented fragments slightly, and induced the injection of thin clay seams between the fragments. Sample 545-27-1, 39-61 cm. B. A conspicuous ichnofauna is dominated by Planolites and Chondrites, but also contains abundant Zoophycos (1) and larger composite burrows containing either Chondrites (2) or pellets (3), both picked out in pale tones. Sample 545-25-3, 69-91 cm. C. Intraformational conglomerates are clast-supported and pebbles are highly deformed by bedding compaction. Maximum clast size occurs a few centimeters above the sharp bases of the clasts, and pebbles fine upward to the tops of the units, which are extensively bioturbated (in this case by "pelleted" Zoophycos). Glauconite (black in photograph) is concentrated within and immediately above the conglomerate tops. Sample 545-25-3, 29-63 cm.

dark greenish gray nannofossil claystones and nannofossil-rich claystones, with subordinate greenish gray and grayish green, very clayey, nannofossil chalks. In general, Unit III becomes more calcareous downward, though the carbonate sediment content rarely exceeds 60%. Siliceous biogenic debris is important only between 407.5 and 464.5 m, where planktonic foraminifers are relatively uncommon. Tectonic deformation and disturbance increases downward through the unit, and three subunits are recognized largely on this basis. Hence Subunit IIIA (252-418.2 m) is largely undisturbed, whereas Subunit IIIB (418.2-520.3 m) is characterized by pervasive microfaulting, and IIIC (520.3-530.7 m) is a heterogeneous unit containing a major fault mélange.

Subunit IIIA; 252-418 m; 545-28 to 545-45-1, 120 cm

The transition from mostly nannofossil claystone to nannofossil-rich claystone below 312.5 m reflects a downward increase in the calcium carbonate component of the sediment in Subunit IIIA. The grayish olive green nannofossil claystones of the upper part of the subunit average 25% carbonate (though locally they contain only 17%) and are accompanied by minor, lighter-colored intervals of nannofossil-rich claystone, which take the form of grayish green, greenish gray, and dusky yellow green laminae or thicker (up to 60 cm) layers. Grayish olive green colors still predominate in the nannofossil-rich claystones below 312.5 m. The carbonate content of these sediments is highest in Cores 37 to 40 (341–371 m), which contain units of grayish olive or light olive gray, very clayey nannofossil chalk, with up to 66% carbonate. A color change to olive gray within the lower part of Core 40 (below 374.4 m) marks a slight decrease in carbonate content (of 3–4% to ~37%). This is restored to over 40% within Core 43, from where grayish olive nannofossil-rich claystone continues to the base of the subunit. Thin sedimentary lamination, picked out by subtle changes in color value, is discernible sporadically through most of Subunit IIIA but is frequently obscured by moderate to strong bioturbation.

The nature and degree of drilling disturbance displayed by recovered cores from Subunit IIIA reflect a downward increase in sediment induration. As induration increases, deformation decreases, and most of the sediments below Core 38 (below 360 m) are disturbed by fracture and fragmentation but rarely deformed. Increased induration is correlated with recrystallization of nannofossils to calcite microspar, which was first detected in smear slides from Core 37 and markedly increases in importance below Core 38, where calcite microspar commonly forms 50% of the carbonate sediment fraction. Within the lower part of Subunit IIIA, recrystallization has affected the more calcareous lithologies to a greater extent.

Although nannofossils constitute most of the carbonate sediment fraction, silt-sized dolomite rhombs are omnipresent, forming between 1 and 3% of the total sediment. Foraminifer abundance exceeds 10% of the biogenic carbonate fraction only at the top of the subunit, in Core 28 and parts of Core 29, and falls sharply to around 3.5% by Core 30. A continued fall in foraminifer abundance below Core 36 (below 341 m) results in the virtual disappearance of planktonic foraminifers within the upper part of Core 41 (approximately 381 m); these eventually reappear in Core 44 (approximately 409 m) and reach an abundance of 2.5% by the base of the subunit. Apart from calcareous microfossils, Subunit IIIA contains a low-density, low-diversity macrofauna of thin-shelled *Inoceramus* s.l., ammonites, and rare belemnites. Through most of the subunit, siliceous biogenic debris constitutes only from a trace to 1% of the total sediment and consists mainly of sponge spicules. An increase within Core 41 coincides with the disappearance of planktonic foraminifers at approximately 381 m, and a further increase of the siliceous biogenic component to over 3% occurs at the base of Core 43 (407.5 m)—thus the use of the "slightly siliceous" qualifier for the lowest part of the subunit. Sponge spicules continue to dominate these lower intervals, though radiolarians become more important. Silt forms 1% or less of the terrigenous sediment fraction in the upper part of Subunit IIIA, increasing below 312.5 m to 3.2%; it is joined by a small amount of very fine sand. Both silt and sand fractions are dominated by quartz but contain some feldspar and muscovite. Glauconite grains form a very tiny but consistent component of the silt-grade material. The content of organic carbon within Subunit IIIA is high relative to Units I and II. Organic carbon increases from a mean of 1.02% in the nannofossil claystones above 312.5 m to 1.46% in the more calcareous lithologies below, and values in excess of 2% were recorded from claystone and chalk at 342.2 and 351.5 m respectively.

Bioturbation in Subunit IIIA is commonly expressed by dark, generally olive black, pyrite-rich wisps and recognizable burrow fills of Planolites, Chondrites, and Chondrites-like ichnofossils; burrow fills of pyrite-cemented sediment occur in the more calcareous lithologies below Core 35 (that is, below 331.5 m). Ichnofossils are absent from olive black, thinly laminated intervals in Cores 42 (389.85–390.45 m) and 43 (407.38–407.44 m), which are probably richer in organic-matter than the rest of the subunit. A greater amount of compaction in the more indurated sediments below 360 m is revealed by the more flattened appearance of Planolites and Chondrites there.

Two conglomerate-rich intervals occur with Subunit IIIA. The higher interval, between 312.7 and 322.6 m, contains sharp-based ungraded units, from 25 to 80 cm thick, which vary in texture from pebbly claystone to clayey pebble conglomerate (Fig. 10, A and B). The subrounded to well-rounded phenoclasts are very poorly sorted and range in size from granules to large cobbles (16 cm in diameter); they are supported by an unexceptional nannofossil-rich claystone matrix and are variably distorted by burial compaction. Three principal lithologic types are present:

1. Olive gray to dusky yellow brown firm nannofossil claystone or, less commonly, foraminiferal nannofossil claystone, homogeneous or displaying Chondrites-like burrow patterns. This lithology composes 40 to 50% of the phenoclasts and contains a relatively high proportion of organic matter (organic carbon exceeds 2%), also a relatively high proportion of quartz silt and very fine sand within the terrigenous sediment fraction (5%).
2. Grayish yellow green, occasionally greenish gray nannofossil-rich claystone, bordering on chalk. This lithology composes approximately 40% of the phenoclasts and is harder because the nannoplankton component is partially recrystallized to calcite microspar. Foraminifers are absent and quartz silt forms only a trace of the terrigenous sediment component. *Nannoconus* indicates an Early Cretaceous age (an isolated small cobble of this lithology was also encountered above the main conglomerate-rich interval at 284.1 m).
3. Light olive gray firm claystone, rich in nannofossils and containing approximately 40% carbonate, but lacking any evidence of nannoplankton recrystallization. This lithology composes only 10% of the phenoclasts; foraminifers form 4% of its biogenic carbonate fraction and quartz silt approximately 3% of the terrigenous sediment fraction.

The lower conglomerate-rich interval, between 362.2 and 386.3 m, contains pebbly units, 1–42 cm thick, which display sharp and in places scoured bases (Fig. 10C). Phenoclasts are rounded to well rounded and range in size from very coarse sand to small cobbles, but are highly deformed by burial compaction. These lower conglomerates are clast supported and contain little matrix; they are moderately sorted and display fining-upward trends which define multiple flows within a single con-

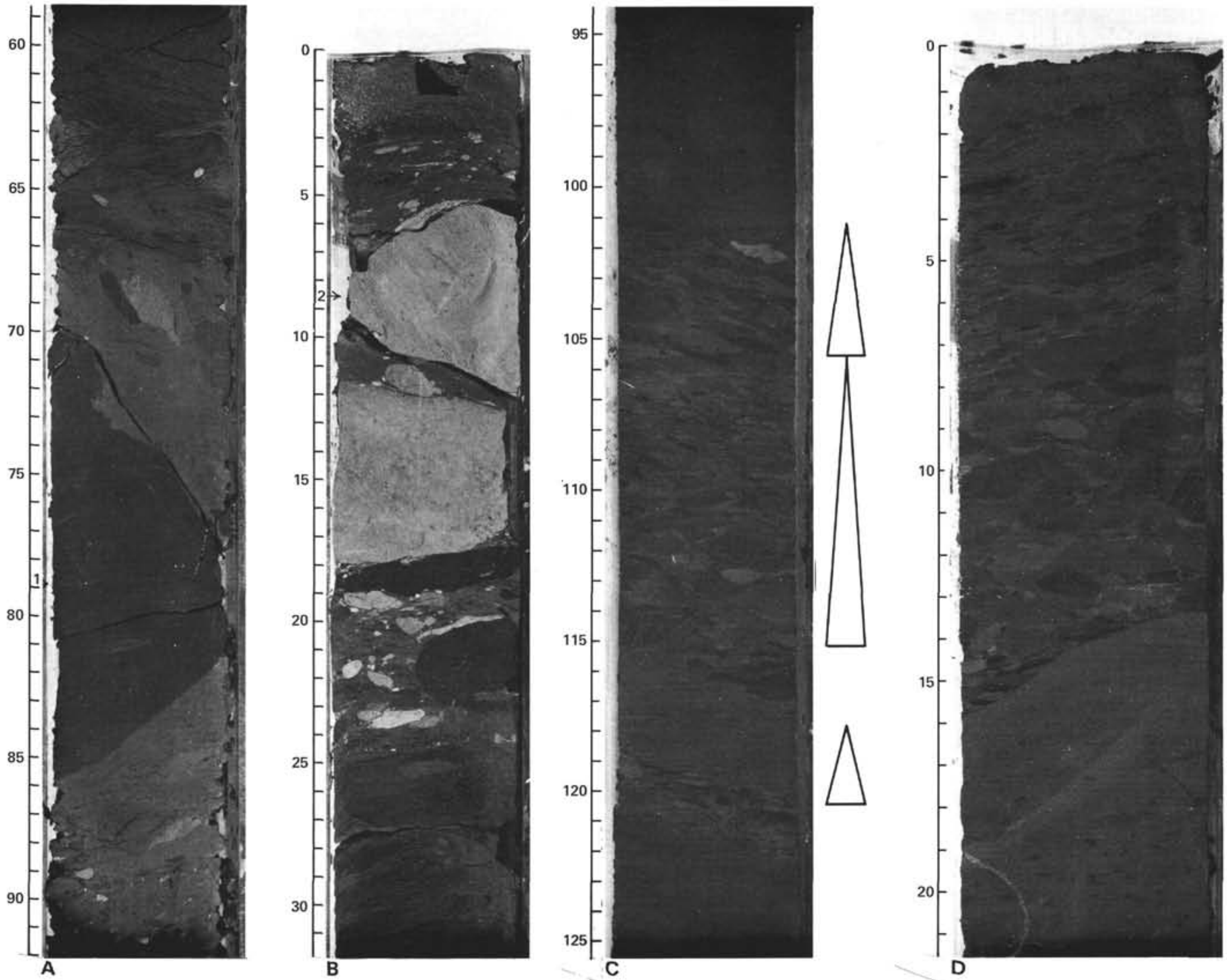

Figure 10. Features of Unit III conglomerates. A, B. Conglomeratic units in the upper part of Subunit IIIA are 25-80 cm thick, sharp-based, and vary texturally between pebbly claystone (A, Sample 545-34-1, 59-92 cm) and clayey pebble conglomerate (B, Sample 545-34-2, 0-30 cm). The subrounded to well-rounded phenoclasts are of three main lithological types (clast types 1 and 2 are illustrated; see text), were variably compacted after deposition, and are generally matrix supported. C, D. Pebble conglomerates in the lower part of Subunit IIIA are sharp-based; a few display scour features (D, Sample 545-40-2, 0-21 cm). They are clast supported and contain little matrix, which accounts for the intense distortion of the clasts. Moderately sorted, they also display fining-upward trends which pick out multiple flows within a single conglomerate (C, Sample 545-40-1, 95-125 cm).

glomerate (Fig. 10D). Individual flows do not exceed 21 cm in thickness; flow thicknesses are directly proportional to the diameter of their largest phenoclast. Shell debris (*Inoceramus* s.l.) accompanies the phenoclasts, which consist of pale green, greenish black, dark greenish gray, brownish black, and dusky yellowish brown nannofossil-rich claystone.

Subunit IIIB; 418.2-520.2 m; 545-45-1, 120 cm to 545-55-6, 65 cm

At Site 545, core recovery was best in Subunits IIIB and IIIC (93 and 91% respectively). The lithologies of Subunit IIIB are basically those of the lower part of IIIA; the calcium carbonate sediment component varies only slightly around 50% (total range is 37-56%), claystones (53% of the recovered intervals) being slightly more common than chalks. The distinguishing feature of Subunit IIIB is its degree of tectonic disturbance. This takes the form primarily of pervasive microfaulting, which commonly disrupts laminae and burrow fills to give them a crenulated appearance (Fig. 11A). In addition, centimeter-scale folds overturned down bedding dip (which varies widely over short intervals, but is generally between 15 and 30°) display axial plane dislocations of a few millimeters to a few centimeters, and larger faults at 40 to 60° to the bedding are commonly marked by a slickensides. Larger overturned fold noses, up to 20 cm across, occur toward the base of Subunit IIIB, and veins filled with fibrous barite are scattered throughout. The smearing of claystone and chalk along many fault planes suggests that much disturbance occurred while the sediments were only moderately consolidated.

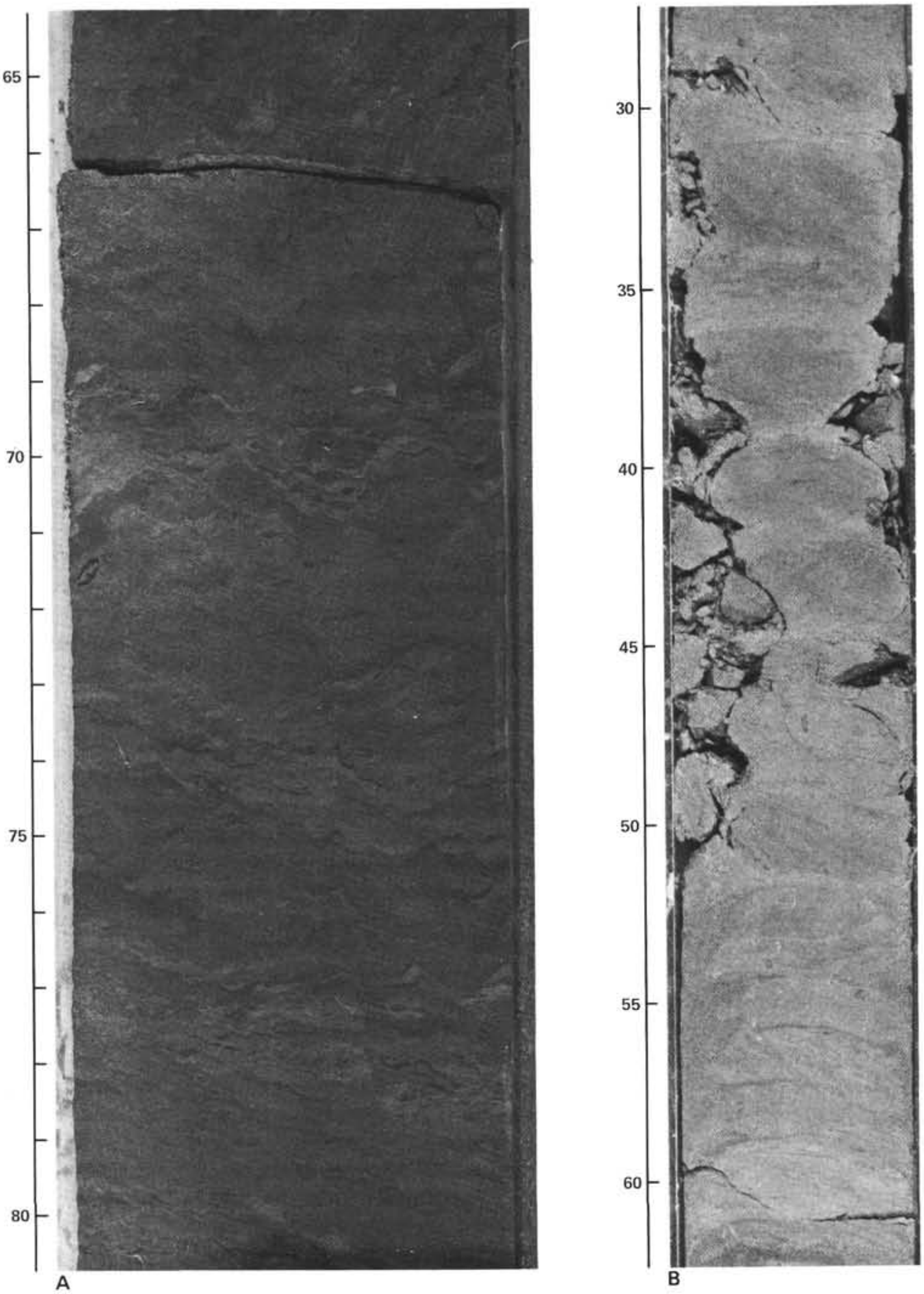

Figure 11. Tectonic disturbance in the lower part of Unit III. A. Subunit IIIB is characterized by pervasive microfaulting which commonly disrupts laminae and burrow fills to give them a crenulated appearance. Sample 545-45-3, 65–80 cm. B. Nannofossil-rich claystones in the lower part of Subunit IIIC contain sharp-based intervals of stacked claystone slivers, interpreted as intense, low-angle fault zones resulting from gravity-driven downslope movement. Sample 545-56-3, 29–55 cm.

The nannofossil-rich claystones of Subunit IIIB are slightly darker than their accompanying chalks. Grayish olive green, grayish olive, light olive gray, dark greenish gray, and greenish gray (5G 6/1) colors characterize the former, whereas greenish gray (5GY 6/1) and grayish green dominate the latter, with minor grayish olive and dusky yellow green. Olive colors are most common toward the top of the subunit. Thin sedimentary lamination is sporadically discernible by subtle changes in color value, but color interlayering is mostly the result of intense compaction of a profuse subhorizontal burrow network. Recognizable ichnofossils consist mainly of Planolites, Chondrites, and Chondrites-like burrows, but composite burrows containing Chondrites also occur and halo burrows (sensu Chamberlain, 1978) are a conspicuous feature below 455 m. Many burrow fills are dark in color (olive gray or greenish black) and pyrite-rich; some are pyrite-cemented.

The calcareous sediment component of Subunit IIIB is dominated by nannofossils. Foraminifer abundance is generally low, falling from approximately 2% of the biogenic carbonate fraction at the top of the subunit to less than 1% between 436 and 474 m, then rising steadily to 4.5% at the base of the subunit. Silt-sized dolomite is omnipresent, forming between 1 and 2% of the total sediment, and calcite microspar, resulting from recrystallization of part of the nannofossil fraction, generally comprises around 25% of the total carbonate sediment component. Subunit IIIB also contains scattered thin-shelled *Inoceramus* s.l. and rare belemnites. The upper 46 m of the subunit (to the base of Core 49) contains between 1 and 3.5% siliceous biogenic debris. Sponge spicules are the major component, but radiolarians are also abundant in the lower 28 m of this interval. Below 464.5 m (below Core 49), the siliceous biogenic sediment fraction varies from a trace to 1% and consists of sponge spicules and minor pyritized radiolarians. Pyrite is more common within the lower part of Subunit IIIB; in addition to pyritic burrow fills, pyrite aggregates up to 5 mm in diameter are scattered throughout. Silt and very fine sand average 3.3% of the terrigenous sediment fraction through most of the subunit, but increase in the basal meters to approximately 6%; a trace of feldspar and muscovite accompanies quartz. The content of organic matter is only one half that of Subunit IIIA; organic carbon averages 0.77%.

In further contrast to Subunit IIIA, IIIB contains only a single layer of conglomerate. This occurs between 440.27 and 440.50 m and is matrix supported, texturally resembling the upper conglomerates of the younger subunit. The phenoclasts, however, are smaller (granule to small pebble grade) and consist of nannofossil-rich claystone and light gray chalk.

Subunit IIIC 520.2–530.7 m; 545-55-6, 65 cm to 545-56-7, 20 cm

A 3-m-thick fault mélange forms the upper part of Subunit IIIC and is underlain by nannofossil-rich claystones containing two further zones of intense shearing; these claystones become increasingly oxidized and dolomitic downward to the contact with Unit IV.

The upper fault mélange (520.3–523.23 m) consists of a medial unit (521.63–522.44 m) of mostly dark greenish gray, nannofossil-rich claystone and greenish gray, very clayey nannofossil chalk, bounded above and below by a breccia containing pebble-sized fragments of olive gray nannofossil-rich claystone, light olive gray, very clayey nannofossil chalk, and medium to light gray, clayey microsparitic limestone (the latter lithology distinguished by almost total recrystallization of its nannofossil component) set in an olive black nannofossil-rich claystone matrix, probably rich in organic matter. Foraminifers form no more than a trace of the carbonate component within all these lithologies, whereas the extent of nannofossil recrystallization to calcite microspar is directly proportional to induration. Siliceous biogenic debris is virtually absent, but quartz silt comprises approximately 5.5% of the terrigenous sediment fraction. Slices and fragments of the olive black and light olive gray lithologies occur within the medial greenish gray unit, and the entire sequence is intensely fractured, with faults mostly subparallel to the bedding dip of the less disturbed adjacent sediments. Many of the faults display superimposed microfaulting.

Thin (1–3 cm thick) stacked fault slivers of the olive black and dark greenish gray claystones and the light olive gray and greenish gray chalks form the lower 23 cm of the fault mélange, which rests at 523.23 m on greenish gray nannofossil-rich claystone. This latter lithology displays an ichnofauna of compacted Planolites and Chondrites and resembles parts of Subunit IIIB, which is approximately of the same age. Siliceous biogenic debris, mainly sponge spicules, constitutes a trace to 1.5% of the total sediment, and foraminifers comprise only a trace of the carbonate fraction; 5% of the terrigenous sediment fraction consists of quartz silt. Microfaulting is pervasive and is accompanied by larger dislocations. This greenish gray claystone is separated from similar but grayish olive claystone below 524.95 m by a 45-cm interval of stacked fault slivers of both lithologies (Fig. 11B). Faults again trend at low angles to bedding. The grayish olive claystone becomes dark greenish gray downward and is separated from light gray nannofossil-rich claystone below 526.5 m by a comparable 30-cm interval of intense, low-angle faulting. The lower, paler claystone is petrographically similar to those above, but softer. Scattered concentrations of sand-sized glauconite occur, and a downward color transition to yellowish gray reflects increasing oxidation of the sediment, with expyritic burrows conspicuously oxidized to orange brown limonite. Silt-sized dolomite rhombs also increase in abundance below 528.8 m, and comprise the entire carbonate sediment component for the lowest 120 cm of Unit III. The contact with the pale orange limestones of Unit IV was not recovered intact but appears to be undisturbed by faulting.

Discussion: The pelagic sediments of Unit III were generally deposited well above the foraminiferal CCD. A low-density, benthos-poor macrofauna reflects the marked fall in nutrient supply normally detected in deep off-shelf settings, whereas the abundance of burrowing indicates well-oxygenated bottom waters, except during deposition of the two thin, fissile, black claystone intervals in Subunit IIIB. These two occurrences in the early to middle Albian may be the local reflection of the well-known mid-Cretaceous "Oceanic Anoxic Event" thought by Schlanger and Jenkyns (1976) to be caused by expansion of the oceanic oxygen minimum layer during times of climatic equability and global transgression. Further possible anoxic deposits are the black claystones of Subunit IIIC, but these are too deformed for bedding structure to be visible.

The mud-supported conglomeratic intervals preserved within the sequence are interpreted as debris flows in a continental-slope depositional environment. Clast-size analysis reveals breaks in the size distribution; these and the presence of poorly sorted, nongraded units are criteria for proximal settlement.

In spite of variable bedding dips and the pervasive microfaulting and folding of Subunit IIIC, biostratigraphic analysis reveals a fairly uniform age progression. We consider that the major dislocation present in Unit III is represented by the mélange zone at the top of Subunit IIIC. Gravity sliding on a glide plane of black claystones overrode middle to late Aptian chalks at Site 545. The sedimentary sequence below the mélange zone is thus concluded to be substantially *in situ*. The deformation in Subunit IIIC is thought to originate both by laterally uneven rates of movement across the sliding sediment wedge and by frictional drag through the lower part of the wedge that overturned microfolds and caused axial plane shear with displacement in a predominantly downslope direction.

Unit IV: 530.7–701.0 m; 545-56-7, 20 cm to 545-75, base

Intraclast skeletal grainstone, packstone, and wackestone, sandy toward base.

Unit IV consists of 170.3 m of mainly light gray, olive gray, light yellowish gray, yellowish orange, pale orange, and yellowish brown limestones. Core recovery was poor. We recognize two subunits on the basis of gross changes in lithologic composition; these subunits have gradational boundaries. Subunit IVA (104.8 m) consists mostly of dolomitized intraclast skeletal grainstone, packstone, and wackestone, containing a variety of shallow-water bioclastic material. Subunit IVB (65.5 m) is distinguished from the higher subunit by a more constant lithology and an abundance of terrigenous debris.

Subunit IVA: 545-56-7, 20 cm to 545-67, base

The upper part of Subunit IVA consists of intraclast skeletal grainstone, variably dolomitized. Skeletal debris includes dasycladacean algae (*Salpingoporella, ?Petrascula*) and other algae such as *Thaumatoporella* and *Cayeuxia*. Coral fragments, bryozoans, bivalves (including large pectinids), serpulids, and sessile foraminifers are also common. Vagile benthic foraminifers (*Textularia, Pseudocyclammina, Trocholina, Nautiloculina, Protopeneroplis*, and *Quinqueloculina*), echinoderm plates (including cidaroid spines), sponge spicules, and *Tubiphytes* are also present. Micritization of skeletal debris is common. Intraclasts consist mostly of subangular to subrounded pieces of peloidal calcisiltite, 1–3 mm in size. These limestones have a high interparticle and moldic porosity (20–30%). Dolomitization is moderate to intensive.

A greater diversity of lithofacies distinguishes the lower 57 m of Subunit IVA, that is, below Core 61; skeletal packstone and grainstone (commonly with coral fragments), oolitic grainstone, intraclast-skeletal grainstone, possible coral and serpulid boundstones, and peloidal calcisiltites all occur. The intraclast-skeletal grainstones are very similar to those higher in the subunit. Coated grains and intraclasts of peloidal calcisiltite (up to 3 cm in size) are common, and grapestone grains were also recorded; the skeletal component consists mainly of algal, coral, echinoderm, bivalve, and gastropod (cerithеid) debris, also *Tubiphytes* and rare ammonites. Grainstone cements show a first phase of bladed sparry calcite and a second phase of blocky calcite. Several possible coraliferous and serpulid-rich boundstones occur in the lower part of Subunit IVA. Corals include colonial *Thamnasteria* and branching phaceloid forms such as *Thecosmilia;* thick-walled mollusk debris is also present. Geopetal cavity-fill fabrics occur in some of the boundstone (545-66-2, 67–87 cm).

Brecciated zones in Subunit IVA contain angular clasts, frequently bounded by stylolites in a reddish dolomite matrix. This fabric may represent a solution-collapse breccia. Dolomitization varies from weak to intensive, and in places has affected 80% of the rock. Two types of dolomites were observed. Replacive pink to red dolomites are associated with stylolitization. A second very different type of dolomite is a dark yellowish orange (10YR 6/6) dolomicrosparite which in Section 545-67-1 is thinly laminated, with pyrite concentrated in some of the laminae. The laminated dolomite drapes coral debris at its base. Because of the similarity in color and mineralogy to some undisputed vein fillings, the laminite may represent the fill of a large cavity. An alternative explanation involving deposition in a high intertidal to supratidal remains a possibility.

Subunit IVB: 545-68, top to 545-75, base

Subunit IVB consists of less dolomitized, mostly tan-colored, sandy skeletal wackestones and packstones, with subordinate sandy grainstones and calcitic sandstones. Terrigenous content increases downward and is accompanied by a color change from pale yellowish orange to medium light gray near the base of the subunit.

The skeletal wackestones, which are the most common constituent of this subunit, contain a matrix of silt-sized peloids which often display a merged texture. Skeletal debris includes mollusk fragments (including ammonites), filaments, rare foraminifers, *Tubiphytes*, coral and echinoderm debris, and sponge spicules. Terrigenous grains (up to 4 mm in diameter) float in the carbonate matrix, but locally they are concentrated into thin layers (less than 5 cm), some with a sharp base. These grains are angular to subangular and consist of stretched metamorphic quartz, feldspar, weathered plagioclase, phyllite, and gneissic material, clearly demonstrating a regionally metamorphosed source. Some sandy layers contain variable admixture of skeletal and oolitic material; coral debris becomes suddenly abundant in the upper part of the subunit.

Discussion: We interpret Unit IV as a shallowing-upward sequence. The skeletal wackestones with a peloidal silt matrix at the base of the unit contain abundant ammonites and filaments; their ichnofauna of Zoophycos also supports a depositional environment of moderate depth, probably on the continental slope. Oolitic and terrigenous sand material within these limestones was introduced from the shelf. The upward increase in shallow-water bioclastic material through Core 69 indicates shallowing and an advancing carbonate platform. Changes in the abundance of coral and oolitic material and an intercalation of possible stromatolite may reflect sea level fluctuations.

BIOSTRATIGRAPHY

Biostratigraphic Summary and Synthesis

At Site 545, drilled at the foot of the Mazagan Escarpment, the bit was expected to drill through a Cenozoic and Late Mesozoic sequence of slope deposits and eventually reach the Jurassic carbonate platform and possibly even the underlying granitic basement.

Both sedimentology and biostratigraphy provide definite indications for gravity-driven redeposition and sliding. A number of successive limestone breccias in the Miocene (Cores 10 to 20) can be partly matched with minor biostratigraphic gaps indicating local erosion and/or nondeposition. The Aptian–Albian interval (Cores 45-46) also contains abundant microfracturing and sediment deformation suggesting unstable slope conditions.

Cenozoic

Cores 1 through 9 contain an 84.5-m-thick sequence of early Pleistocene or younger age.

Core 10 and 547-11-1, 0–80 cm contain probably three redeposited units, which contain Upper Jurassic limestone clasts and reworked middle and late Pliocene nannofossil assemblages.

The interval from 545-11-1, 86 cm through 545-13,CC contains early Pliocene to late Miocene nannofossil and foraminiferal assemblages, again associated with Mesozoic limestone clasts in Core 13. Faunal mixing is probable and at least Core 13 must be considered as a redeposited unit.

Cores 14 through 19 contain late Miocene nannofossil (mainly NN11) and foraminiferal (N16 and 17) assemblages. Cores 15, 16, and 17 contain coarse limestone breccias which probably represent one or more slope breccias (biostratigraphy of clasts discussed later). In Cores 20 through 22, difficulties in recognizing particular nannofossil zones again may indicate redeposition. In 545-20-1, 0–44 cm another limestone breccia possibly marks the regionally recognized hiatus between middle and late Miocene (see other sites). Foraminifers indicating a middle Miocene age (N10–N14) are present in Cores 20 through 22.

Cores 23–27 yielded early Miocene assemblages of foraminifers (N5–N8), whereas the nannoflora indicate an NN5–NN6 age for Core 23 (early middle Miocene and NN3–NN5 for Cores 24–27 (early Miocene). The Cenozoic units rest unconformably on Cenomanian sediments, first recovered in Core 28.

Biostratigraphy of the Mesozoic Limestone Clasts

Cores 10 through 20 contain redeposited limestone clasts with fossils of Late Jurassic to Late Cretaceous age. A succession of multiple reworking and downslope transport events can be deduced both from microfacies and from fossil distribution in the limestone clasts.

The first generation of redeposition is represented by white skeletal, oncoidal, and intraclast grainstones and packstones, containing a mixture of grains from various environments: scleractinian coral debris, dasycladacean algae, ooids, etc., reflect a very shallow, high-energy environment. The age of this material is most likely to be Late Jurassic. These clasts are mixed with calcified siliceous sponge debris and micritic clasts containing calpionellids, and seem to be embedded in a matrix commonly containing abundant calpionellids indicative of a late Tithonian age.

This first generation may still have been deposited on the shelf or at the shelf edge. However, calpionellid-bearing micrite and sponge debris suggest a deeper environment than the included algal and coral fragments. A pebble of glauconite-bearing microsparite with *Nannoconus colomi* attests a Neocomian deep-water environment on the Mazagan Plateau or at its edge.

The lithified first-generation limestones eventually became fractured and exposed, as indicated by the occurrence of rounded, bored clast surfaces. This reworking occurred, at least in part, in the Cretaceous: clasts of first-generation limestones are embedded in a micrite containing Late Cretaceous planktonic foraminifers. This constitutes the second-generation limestones.

During the Miocene and Pliocene, the second-generation breccias became again exposed and eroded to form the drilled Neogene slope deposits. Partial exhumation of first-generation clasts from nonlithified Late Cretaceous breccias may be indicated by the occurrence of reworked *Globotruncana sigali* (Core 15) and *G. coronata* (Core 24) in the muddy matrix of the Miocene slope breccias. Most pebbles in this final third generation in fact show only first-generation lithology. Only one thin section shows lithified Late Cretaceous of the second generation. A minor percentage of clasts consists of pink skeletal and oncoidal packstones with grainstone patches similar to those encountered *in situ* at Site 544 and probably identical with the Oxfordian limestones dredged on the Mazagan Escarpment (Renz et al., 1975).

Cretaceous

Cores 28 through 33 represent an age of middle to late Cenomanian. In Core 34 and Section 545-35-1, occur several beds of claystone conglomerate. They may be associated with a minor erosional or nondepositional event separating middle to late Cenomanian faunas above from early Cenomanian ones below. Cores 37 through 50 constitute an almost continuous Albian-upper Aptian sequence. There is a possibility of a hiatus in Core 40, where several thin beds of claystone conglomerates have been recovered. Throughout this interval there is a good stratigraphic control based on planktonic foraminifers, except for Cores 41 through 43, where their diversity is greatly reduced.

The paucity of planktonic foraminifers is accompanied by a sharp increase in sponge spicules and radiolarians. In Core 42 we also recovered some thin layers of black shale. In Cores 43 through 49, the planktonic foraminifers slowly increase and sponge spicules and radiolarians remain abundant down to Core 49. The fossil preservation almost certainly reflects paleoceanographic changes.

Cores 50 through 56 record a virtually complete sequence of late Aptian strata.

Jurassic

The top of the Jurassic limestone and dolomite sequence was recovered in 545-56,CC, and 170 m of limestones were drilled until the bit failed. Dasycladacean algae, corals, and lituolids testify to a shallow-water environment throughout much of the carbonate sequence. Strong dolomitization has altered most of the rock and makes fossil determination difficult. Nonetheless, a Late Jurassic age is suggested at least for the upper part of the drilled section by the presence of *Trocholina alpina, T. elongata*, and *Pseudocyclammina lituus*. If the limestones of Site 545 are of late Middle to Late Jurassic age, they would be, at least in part, synchronous with the deeper-water red limestone facies recovered at Site 544 and with the red ammonite limestones dredged from the nearby Mazagan Escarpment.

Nannofossils

Core 1 is of late Pleistocene age, placed within the *Emiliania huxleyi* Zone (NN21) (Gartner, 1977). Cores 2 through 9 contain calcareous nannofossils of the Pleistocene. The upper sediments may be younger in age, since older forms, such as *Calcidiscus macintyrei* and *Pseudoemiliania lacunosa*, are found in the late Pleistocene assemblage; this reworking may be due to downslope movement. The small size of the late Pleistocene marker fossil, *E. huxleyi*, warrants the use of a scanning electron microscope for exact age determination of Cores 2 through 9. The Pleistocene assemblages contain, in part, *C. macintyrei, Discolithina viginitiforata, Gephyrocapsa oceanica, G. caribbeanica, P. lacunosa*, and *Helicosphaera sellei.* The preservation is moderate and abundance is low. Sample 545-10-1, 10 cm contains nannofossils of late Pliocene age; but the upper portion of Section 1 is very disturbed and is probably reworked. This assemblage is given a Pleistocene age.

The interval from 545-10-1, 105-105 cm through 545-10-1, 144-145 cm contains a late middle Pliocene assemblage of the *Discoaster brouweri* Zone, *D. tamalis* Subzone (bottom half of NN16) (Okada and Bukry, 1980). The assemblage consists of *D. tamalis, D. brouweri, D. surculus, C. macintyrei*, and *C. leptopora;* the abundance is common and preservation is moderate to good.

The interval from 545-10-2, 5-6 cm through 545-10,CC consists, in part, of *D. surculus, Reticulofenestra pseudoumbilica, C. macintyrei*, and *Discolithina viginitiforata*. This assemblage is of mid-late Pliocene age, but can be placed in no particular zone.

The interval from 545-11-1, 86 cm through 545-12,CC is early Pliocene in age. The assemblage consists, in part, of *Amaurolithus primus, A. tricorniculatus, R. pseudoumbilica, Discoaster challengeri, C. macintyrei*, and *D. variabilis;* preservation is moderate and nannofossils are few to common.

The nannofossils in Core 13 through 545-19-1, 20-21 cm are placed in the *D. quinqueramus* Zone (NN11) (Okada and Bukry, 1980) of late Miocene age. A representative sample of this assemblage contains *D. quinqueramus, A. primus, R. pseudoumbilica, D. berggrenii, D. brouweri*, and *C. macintyrei*. Nannofossils are few to common, and preservation is moderate to good in these cores.

The interval from 547-19-2, 20-21 cm through Core 22 cannot be dated exactly by nannofossil zonations, but it appears to be of middle to early late Miocene age; nannofossils are common to few and preservation moderate. Contained within the assemblage are *C. macintyrei, D. variabilis, D. brouweri, Triquetrorhabdulus rugosus*, and *R. pseudoumbilica*. A hiatus may possibly be present in this part of the column, since no marker fossils are found for the interval in question; no apparent dissolution features are observed.

The nannofossils in Core 23 represent an early to middle Miocene age (NN5-NN6). *Sphenolithus heteromorphus, S. belemnos, C. macintyrei, Cyclicargolithus floridanus, D. variabilis*, and *D. deflandrei* are representative of this assemblage; nannofossils are common and preservation is moderate to good.

The interval from 545-24,CC to 545-26,CC is of early middle Miocene to late early Miocene age (NN3-NN5); assemblages cannot be zoned more precisely because marker fossils are absent. The assemblage is much like those above with the exclusion of *S. heteromorphus;* nannofossils are few and preservation is poor to good.

The nannofossil assemblage of the interval from 545-28-1, 9-10 cm through 545-38-1, 37-38 cm is Cenomanian in age and is of the *Lithraphidites alatus* biohorizon (Thierstein, 1976). The preservation is moderate to good with nannofossils being few to common. A representative sample of the assemblage consists of *Eiffellithus turriseiffeli, L. alatus, Prediscosphaera cretacea, Stephanolithion laffittei, Parhabdolithus angustus, Lithastrinus floralis, Tranolithus orionatus, T. gabalus, P. asper*, and *P. embergeri*.

The interval from 545-39-1, 98-99 cm through 545-40-1, 7-8 cm is defined by the *E. turriseiffeli* biohorizon (Thierstein, 1976) of late Albian age. A typical assemblage of this interval includes *E. turriseiffeli, Chiastozygus litterarius, Vagalapilla stradneri, L. floralis, P. asper, P. embergi*, and *L. carniolensis*. Preservation within this sequence is poor to moderate with preservation decreasing downhole; nannofossils are few.

The calcareous nannofossils of 545-40-2, 35-36 cm through 545-47-3, 30-31 cm are of early to middle Albian age; corresponding to the *Prediscosphaera cretacea* biohorizon of Thierstein (1976). The assemblage is the same as above, except for the absence of *E. turriseiffeli.* Nannofossils are few, and preservation is poor to moderate.

From 545-47-4, 47-48 cm to 545-56-5, 97 cm the interval is placed in the *L. floralis* biohorizon (Thierstein, 1976) of middle Aptian to early Albian age. Some reworking of late Barremian-early Aptian marker fossils is found; the remainder of the assemblage is typical of the ones above, except for the exclusion of *P. cretacea.* Preservation is poor to moderate and nannofossils are few.

The interval below 545-56-1, 20-21 cm comprises a dolomitized nannofossil ooze. Near the contact between the ooze and the underlying dolomitized limestone, preservation and abundance decrease down to 545-56-7, 2 cm, where the sample is barren of nannofossils. No calcareous nannofossils are found beneath this interval.

Neogene and Middle Cretaceous Foraminifers

The Neogene sequence of Site 545 contains minor diastems in the late Pliocene, near the late Miocene/middle Miocene boundary, and between the middle and early Miocene. The first two diastems correspond with lithology breaks between Units IA and IB, and IB and II, respectively. Both planktonic and benthic foraminifers are abundant and well preserved. The zonal scheme for the Cenozoic sediments is from Stainforth et al. (1975).

Unit IA, 85 m thick, represents the (?)Recent and Pleistocene, all lumped into the *Globorotalia truncatulinoides* Zone (NN22–NN23). Characteristic planktonic taxa are *G. truncatulinoides, G. hirsuta, G. crassiformis, G. inflata, Orbulina universa, Globigerina bulloides, G. glutinata, Globigerinoides conglobatus, G. ruber, G. trilobus, Globigerinella aequilateralis*, and *Neogloboquadrina pachyderma*. Benthics include Miliolidae, Nodosaridae, *Cibicides* spp., *Melonis* spp., *Pullenia* spp., *Anomalinoides* spp., and *Eponides* spp.

A minor diastem appears to be associated with the lithologic boundary between Units IA and IB (545-10-1, 106 cm). The upper Pliocene sediments may be very thin at this site. The early to middle Pliocene is represented by the *Globorotalia margaritae* Zone (N18–N19). Characteristic taxa include *G. margaritae, G. plesiotumida, G. acostaensis, Globigerina nepenthes, Sphaeroidinellopsis* spp., and *Orbulina universa.*

As in Site 544, the Miocene/Pliocene boundary is not clearly defined but is considered to be in the lower part of Core 13. Characteristic planktonics of the late Miocene *Globorotalia acostaensis* Zone (N16–N17) include *G. acostaensis, G. juanai, G. plesiotumida, G. continuosa, Globigerina nepenthes, Globoquadrina dehiscens, G. altispira, Sphaeroidinellopsis seminulina, S. subdehiscens, Globigerinoides trilobus*, and *Orbulina universa.*

A second minor diastem corresponds with the lithologic break between Units IB and II in 545-20-1, 43 cm. The middle Miocene (N10–N14) is represented in Cores 20 through 22. Planktonic foraminifers present include *Globorotalia siakensis, G. praemenardii, G. lenguaensis, G. conoidea, G. miozea, Globigerinoides trilobus, Orbulina universa, Sphaeroidinellopsis seminulina*, and *Globoquadrina dehiscens.*

A middle Miocene/lower Miocene hiatus may be present between Cores 22 and 23. The presence of *Globigerinoides sicanus* and *Praeorbulina glomerosa* represent the latest early Miocene *P. glomerosa* Zone (N8) in 545-23,CC. Lowermost middle Miocene (N9) sediments may be present in the large coring void between Cores 22 and 23. The *Catapsydrax stainforthi–C. dissimilis* Zones (N5–N6) are represented by 545-25,CC through 545-27,CC. Characteristic taxa include *Catapsydrax dissimilis, C. unicavus, Globigerina woodi, Globorotalia continuosa–opima nana* and *G. peripheroronda.*

The lower Miocene rests unconformably on the Middle Cretaceous sediments of Unit III. The contact was not recovered but lies in the coring void between Cores 27 and 28. Cretaceous faunas are in general moderately to well preserved and few to common in abundance. Cretaceous zones are after van Hinte (1976).

Cores 28 through 32 represent the *Rotalipora cushmani* Zone of middle to late Cenomanian age. A diverse assemblage of planktonic species characterize this zone: *R.* aff. *cushmani, R. appenninica, R. greenhornensis, Hedbergella delrioensis, H. planispira, H. amabilis, Praeglobotruncana* spp., *Schackoina cenomana, Globigerinelloides bentonensis, G. caseyi*, and *Clavihedbergella simplex.* The benthic fauna is also diverse and well preserved: *Dorothia, Ammodiscus, Lenticulina, Astacolus, Dentalina, Vaginulopsis, Gavelinella*, and Miliolidae. These genera suggest mixing of neritic and bathyal assemblages (Sliter, 1980).

An early Cenomanian age is suggested for Cores 33 through 36. The presence of *R. appenninica, R. gandolfii*, and *R. brotzeni* characterize this interval.

The late Albian is represented by the *Planomalina buxtorfi* Zone in 545-37,CC and Core 38, and the *Ticinella breggiensis* Zone in Cores 39 and 40. Planktonic species noted in the late Albian include *Planomalina buxtorfi, T. breggiensis, T. raynaudi aperta, T. raynaudi digitalis, T. primula, Rotalipora ticinensis, R. subticinensis, Hedbergella* spp., and *Globigerinelloides* spp.

Cores 41 through 49 demonstrate some interesting trends which are most likely oceanographically controlled. Cores 47 through 49 contain abundant sponge spicules and common radiolarians. The planktonic foraminifers of this interval are also common in abundance. This would appear to have been a time of upwelling and associated high productivity. In Cores 44 through 46, the planktonic foraminifers diminish, becoming few to common, and the radiolarians diminish to few, whereas sponge spicules remain abundant. In Cores 41 through 43 sponge spicules are few, radiolarians rare, and the diversity of planktonic foraminifers is greatly reduced.

No zones could be established for Cores 41 through 47, although a middle to early Albian age is probable. The early Albian–late Aptian *T. bejaouensis* Zone extends from 545-48,CC through Core 49. Characteristic species include *Ticinella bejaouensis* and/or *T. roberti, Hedbergella trocoidea, H. gorbachikae*, and *H. delrioensis.*

Core-catcher samples from Cores 50 and 51 yielded faunas of the late Aptian *Hedbergella trocoidea* Zone. The *Globigerinoides algerianus* Zone is represented from 545-52,CC through 545-54,CC.

A lithologic break between Units IVC and IVD in the lower part of Section 545-55-6 corresponds to an interpreted fault zone containing faunas of the early late Aptian *Schackoina cabri* Zone. This zone extends down through Core 56, where the top of the (?) Upper Jurassic limestones was recovered in 545-56,CC.

Middle Cretaceous Radiolarians

Cores 47 through 49 contain abundant, moderately to well preserved radiolarians. Sample 545-47,CC contains *Triactoma echoides, Acanthocircus trizonalis, Ultranapora praespinifera*, and ?*Archaeodictyomitra simplex.* This assemblage suggests a late Aptian or early Albian age.

Samples 545-48,CC and 545-49,CC both contain *Eucyrtis micropora*, indicating an age no younger than late Aptian.

Cores 50 through 55 contain mostly pyritized, but usually well preserved and determinable radiolarians. Further picking and SEM study are needed to substantiate the assemblages.

Sample 545-53,CC contains *Pseudodictyomitra carpatica, P. lilyae, Xitus spicularius, Thanarla pulchra*, and many other species suggesting a late Barremian or Aptian age.

Biostratigraphy of the Jurassic Limestones

Two groups of Jurassic limestones are distinguished at Site 545: Jurassic limestones *in situ*, from 545-56,CC through Core 74 (Table 2A), and limestone pebble and cobbles in Pliocene and Miocene ooze (Cores 10 to 20) (Table 2B).

In situ Limestones

Most of the samples from the *in situ* limestones are strongly dolomitized; this has affected the fossil preservation. Nonetheless, the preservation allows us to see that the limestones are generally rich in fragments of echinoderms and lamellibranchs. The upper part (from Cores 56 to 64) is characterized by the presence of algae (dasycladacean, codiacean, oncoids), but stratigraphically significant foraminifers and algae are rare and nondefinitive.

Fossils having age significance include, in Core 57, fragments of a dasycladacean algae which could be attributed to *Petrascula* and which occur together with *Trocholina alpina, T. elongata*, and *Pseudocyclammina lituus*, suggesting a Late Jurassic age for this core. In Cores 70 to 74, foraminifers include *Lenticulina* sp., some *Protopeneroplis* sp., and *Ammobaculites*. Among the ammonites, *Phylloceras* sp. is common (e.g., Sample 545-68-3, 14–16 cm), but this is a long-ranging genus (Sinemurian–Valanginian). The only other type of ammonite encountered is an indeterminate perisphinctacean (middle Bajocian–Valanginian age) in Sample 545-72-1, 137 cm.

Limestone Pebbles–Cobbles in Pliocene and Miocene Ooze

These are of two types, calpionellid-bearing (Jurassic or Early Cretaceous age), and microbreccia of Late Cretaceous age. Calpionellids are found in 10 of the 17 thin sections made from the limestone clasts in the Pliocene and Miocene. The observed genera are abundant *Crassicollaria* as well as *Calpionella* and *Tintinnopsella*. Thus, a late Tithonian age is indicated for the clasts containing calpionellids. Although it is impossible to give a very accurate age to the clasts without calpionellids, the

Table 2A. Summary of bioclast occurrences in thin sections of Jurassic limestone, Site 545.

Core-Section (interval in cm)	Lamellibranches	Echinids	Gastropods	Sponges	Bryozoans	Brachiopods	Ostracodes	Corals	Serpulid annelid worms	Oncoids	Dasyclads	Codiaceans	*Thaumatoporella*	*Protopeneropalis*	Miliolids	*Lenticulina* sp.	*Ammobaculites* sp.	*Pseudocyclammina* sp.	Textularids	*Trocholina* sp.	*Nauticoculina* sp.	
56-7, 22–24	x	x				x		x		x	x									x		
56,CC	x	x			x			x		x	x		x		x							
57-1, 28–31	x	x		x	x	x					x		x					x	x		x	*Pseudocyclammina lituus*
57-1, 45–50	x	x		x	x		x	x		x		x		x	x	x			x	x		
57-1, 133–135	x	x									x											
57-1, 136–142				x							x			x	x			x		x		
57-1, 146–150	x	x		x		x			x		x				x					x	x	*Petrascula*
59-1, 10–13	x	x																		x		
60-1, 13–15		x	x					x		x									x	x	x	Ammonite
62-1, 23–27	x	x						x		x	x									x		
62-1, 41–43	x	x								x	x	x								x		
63-1, 11–14	x	x						x														
63-1, 53–57	x	x						x														
63-1, 61–64	x	x			x				x			x	x							x		
64-1, 10–14	x	x																				
64-1, 63–65		x								x	x											
64-2, 47–51	x	x	x		x					x	x		x		x					x		
64-2, 88–91		x	x		x					x		x		x						x	x	
64-2, 105–108	x	x	x							x		x			x							
66-1, 39–42	x	x									x?											
66-2, 67–69	x	x					x		x													Ammonite
68-2, 134–139	x	x																				
68-3, 24–28	x	x							x							x						
69-2, 79–83	x								x	x						x						
69-3, 23–26	x	x																				Ammonite
70,CC	x	x								x				x	x	x		x?				
71-2, 9–13		x					x			x						x						
71-2, 119–123										x					x	x	x	x?				
72-1, 145–167	x	x												x	x	x	x	x?				
72-2, 104–108	x													x	x							Ammonite
73-2, 48–53	x	x													x		x					
73-2, 84–88		x					x									x		x?				
74-1, 30–34															x	x						
74-1, 89–94	x	x					x							x		x	x	x?				
74-1, 121–125	x	x															x				x	

Table 2B. Summary of bioclast occurrences in thin sections of reworked Mesozoic limestone clasts in Cores 545-10 to 545-20.

Age	Core-Section (interval in cm)	Lamellibranches	Gastropods	Echinids	Bryozoans	Ostracodes	Oncoids	Sponges	*Nauticoculina* sp.	*Trocholina* sp.	Dasyclads	Ammonites	Calpionellids	Miliolids	Brachiopods	Textularids	Lituolids	*Lenticulina* sp.
Globorotalia margaritae Zone	10-1, 143–145	x		x		x				x			x	x	x			
	10,CC	x		x				x			x				x			
	11-1, 18–21	x				x						x		x				
	11-1, 42–49	x		x	x		x	x		x		x			x			
	11-1, 46–50	x			x		x	x				x	x	x		x		
	11-1, 65–69	x				x							x[a]	x				
------	11-1, 75–79	x		x			x							x				
Globorotalia acostaensis Zone	15-1, 4–9			x			x			x							x	
	15-1, 17–21			x						x	x	x			x		x	
	15-1, 24–25	x		x	x		x	x	x	x		x	x		x			x
	15-1, 36–38	x	x	x	x		x	x		x			x	x	x	x		
	15-1, 39–42	x		x	x		x			x			x	x		x	x	x
	16-1, 0–3									Breccia								
	16-1, 29–32	x		x			x				x?		x	x		x		
	16-1, 54–59			x	x		x	x		x			x	x			x	
	16-1, 70–74		x	x	x		x	x										
	16-1, 132–137	x	x	x	x	x	x			x			x					x
	20-1, 23–26		x		x		x	x					x					

[a] Reworked.

microfauna (*Trocholina alpina, T. elongata*) do not contradict a Late Jurassic age. In some thin sections, calpionellids are numerous. Most of them are in their original lithology, except in a thin section from Sample 545-11-1, 65–69, where they are evidently reworked into a different lithology. Their bad preservation and their association with other organisms indicate an inner shelf rather than an actual pelagic environment.

At the top of Core 16 there was one composite fragment of limestone breccia containing angular clasts of various microfacies (oncoid-bioclast limestones). One clast contains calpionellids and the microfacies of all clasts suggest a Late Jurassic age. These clasts are embedded in a pelagic micrite matrix containing *Globotruncana* sp. cf. *G. bulloides, Hedbergella* sp., *Globigerinelloides* sp., and *Heterohelix* sp., indicating a Late Cretaceous depositional age for the microbreccia.

There are definite differences between the reworked limestone clasts in the Neogene and the *in situ* limestones.

A strong dolomitization characterizes the *in situ* limestone and is absent in the reworked clasts. Calpionellids occur frequently in the reworked limestones but have not been observed in the *in situ* limestones, whereas (?)*Petrascula*, for example, is frequent in the latter and absent from the reworked limestones. Taken together, these observations would suggest that the reworked limestone clasts are slightly younger than the top of the *in situ* limestones at this site.

DEPTH-VERSUS-AGE CURVE

A depth-versus-age diagram for Site 545 is shown in Figure 12. Lower Pleistocene sediments unconformably overlie upper Miocene beds. The estimated sedimentation rate for the early Pleistocene ranges from about 100 to 240 m/m.y.

The estimated rate for the late Miocene interval that precedes a 2 m.y. hiatus is in the range from about 12 to 19 m/m.y. The upper Miocene includes several redeposited units containing clasts of a limestone of Late Jurassic–Early Cretaceous age in a matrix with Neogene microfossil assemblages. Between the base of the upper Miocene and the middle Miocene is another hiatus, representing a time span of 3–5 m.y. Beneath the hiatus lies a 71-m-thick sequence of greenish clayey nannofossil chalk of middle to early Miocene age. The average sedimentation rate is between 8 and 9 m/m.y.

A regional unconformity separates lower Miocene clayey chalk from underlying Middle Cretaceous green claystone. For the Cretaceous, the accumulation rate for the claystones of late Albian–Cenomanian age was about 11 m/m.y., and for the late Aptian–middle Albian, it was about 20 m/m.y. Biostratigraphic data in the lower part of the drilled Aptian interval are confusing and suggest there may be faulting that repeats the section.

ORGANIC GEOCHEMISTRY

Carbon and Nitrogen Contents

The carbon and nitrogen contents of the sediments from Hole 545 were determined down to a sub-bottom depth of 527.5 m, including Core 56 of Lithologic Unit IIIC (Table 3); that is, the underlying limestone sequence has not been studied. The carbonate contents clearly distinguish the different lithologic units and subunits (Table 4). The amount of $CaCO_3$ in the sediments increases from the clayey foraminiferal-nannofossil ooze of Unit IA toward Unit IB and then decreases in the chalk of Unit II. There is a drop of carbonate content at the Cretaceous/Tertiary unconformity with a mean value of 30.2% in the upper part of Unit IIIA. The carbonate contents are higher again in the rest of Unit IIIA and in Unit IIIB. The most homogeneous sections, that is, those with the lowest standard deviation of the carbonate content, are Units IB and IIIB (Table 4).

The distribution of organic carbon follows a different trend (Fig. 13, Tables 3 and 4). Mean organic carbon values slightly decrease from Units IA to IB and then increase to Unit IIIA, which is the richest in organic matter at this site. Lower organic matter contents are found in Lithologic Units IIIB and IIIC. Because of a very high standard deviation of C_{org} values in Units IIIA and IIIB, the organic carbon and the noncarbonate material in the sediments of these units cannot be correlated (Table 5). The distribution of organic nitrogen follows the same pattern as the organic carbon contents, but the absolute values are too small for any significant conclusions. Only two samples from Unit IIIA contain organic nitrogen above 0.1%.

Rock-Eval Pyrolysis

A summary for 9 Cenozoic and 15 Cretaceous sediment samples studied by Rock-Eval pyrolysis is given in Table 3. Pyrolysis of the late Miocene through Pleistocene samples and of Sample 545-23-7, 0–3 cm from the early to middle Miocene yields low hydrogen- (IH) and very high oxygen-index (IO) values so that they plot outside the kerogen-type diagram (Fig. 14) adopted from Roucaché et al. (1979). The organic matter in these sedi-

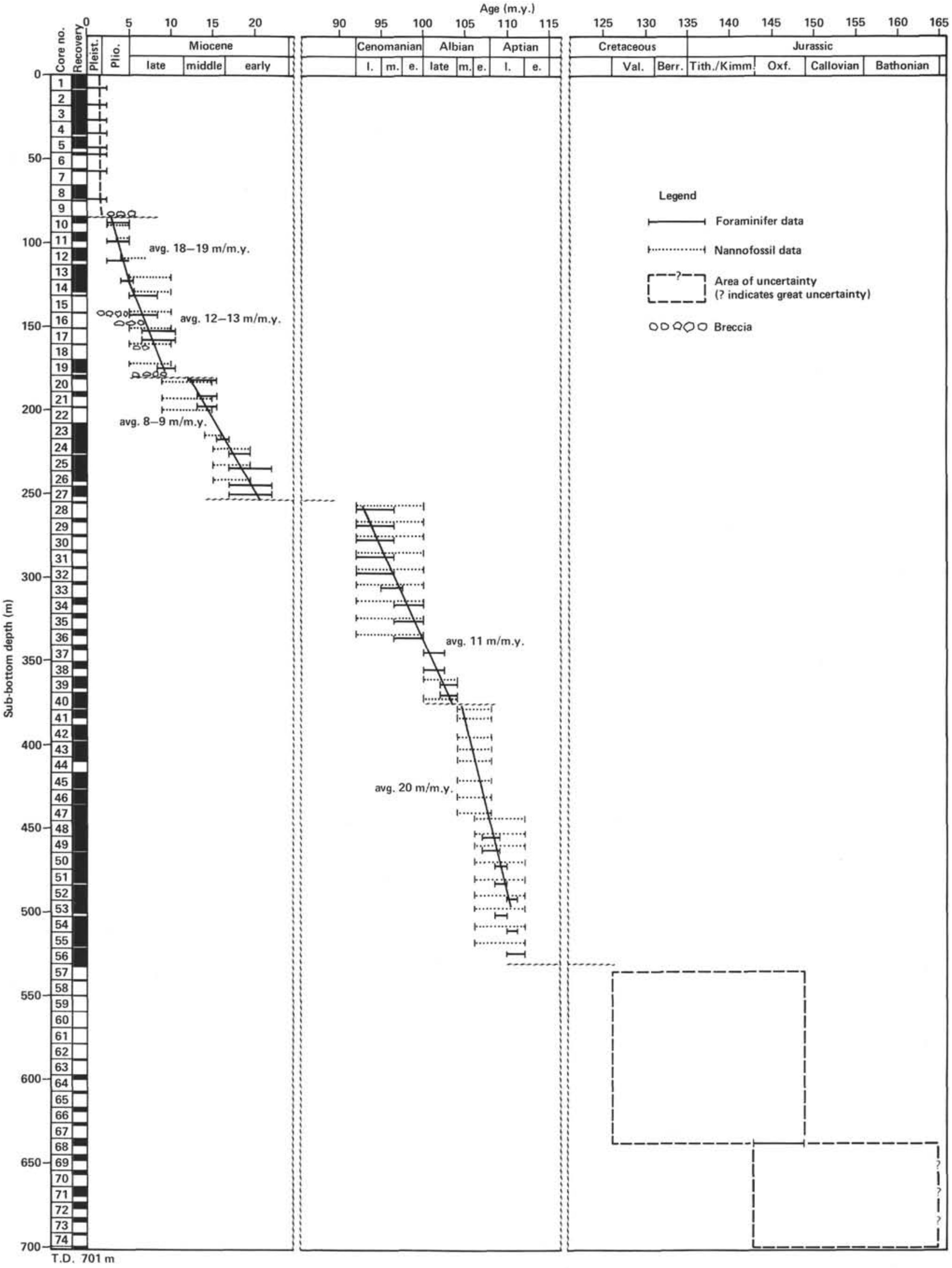

Figure 12. Depth versus age at Site 545.

Table 3. Carbon and nitrogen contents and pyrolysis data, Site 545.

							Rock-Eval pyrolysis					
Core-Section (interval in cm)	Sub-bottom depth (m)	Litho-logic unit	Age	C_{org} (%)	$CaCO_3$ (%)	N_{org} (%)	S_1	S_2 (mg/g rock)	S_3	Hydrogen index (mg HC/g C_{org})	Oxygen index (mg CO_2/g C_{org})	T_{max} (°C)
2-4, 144–150^{a}	14.4	IA	early Pleistocene	0.23	50.8	0.05						
2-5, 118–120	15.7			0.27	47.0	0.06						
2-6, 0–2	16.0			0.29	38.8	0.06	—	0.04	2.33	15	805	365
4-1, 85–86	28.3			0.35	50.3	0.05						
8-3, 144–150^{a}	69.9			0.35	45.0	0.06						
8-4, 30–32	70.3			0.21	57.0	0.04						
8-4, 118–120	71.2			0.23	66.0	0.04						
8-5, 0–2	71.5			0.19	47.9	0.05	—	0.04	1.39	21	731	371
10-2, 120–121	87.2	IB	Pliocene	0.19	61.7	0.04						
11-3, 117–120	98.2			0.11	77.9	0.02						
11-4, 0–3	98.5			0.13	78.7	0.02	—	0.02	1.09	15	842	385
12-4, 144–150^{a}	109.4			0.06	75.6	0.02						
13-5, 125–126	120.3			0.08	77.9	0.02						
14-4, 118–120	128.2		middle to late Miocene	0.08	75.6	0.02						
14-5, 0–2	128.5			0.06	77.9	0.02	—	0.02	1.01	28	1688	—
19-3, 144–150^{a}	174.5			0.16	62.7	0.04						
19-4, 118–120	175.7			0.30	53.1	0.05						
19-5, 0–2	176.0			0.13	59.1	0.04	—	0.05	1.43	38	1098	396
20-1, 130–131	180.8			0.78	70.8	0.06	0.16	0.82	2.03	105	260	442^{b}
23-3, 144–150^{a}	212.5	II	early to middle Miocene	0.10	67.9	0.03						
23-6, 117–120	216.7			0.14	62.7	0.04						
23-7, 0–3	217.0			0.10	66.0	0.03	—	0.05	1.21	53	1213	406
26-1, 73–75	237.2			~0.35^{c}	n.d.	n.d.	—	0.17	1.18	49	338	402
26-1, 118–120	237.7			0.57	51.2	0.06						
26-2, 0–2	238.0			0.67	46.0	0.06	—	0.39	1.40	58	208	418
27-3, 14150^{a}	250.5			0.59	44.1	0.07						
29-1, 22–23	265.2	IIIA	Cenomanian	~1.20^{d}	n.d.	n.d.	—	0.21	2.39	17	199	—
29-1, 118–120	266.7			1.30	28.8	0.07						
29-2, 0–2	267.0			1.01	33.6	0.07	—	0.52	3.06	52	303	416
31-1, 100–102	285.0			0.82	30.3	0.06	—	0.78	2.25	95	274	422
31-1, 140–150^{a}	285.4				0.93	28.8						
0.07							—	4.64	4.07	215	188	425
34-1, 80–81	313.3			2.16	20.5	0.13						
34-1, 140–150^{a}	313.9			0.74	29.8	0.06	—	0.85	2.31	203	550	410
34-2, 0–2	314.0			~0.42^{b}	n.d.	n.d.						
34-2, 118–120	315.2			1.09	32.6	0.08	—	2.05	3.47	132	224	428
34-3, 0–2	315.5			1.55	38.4	0.09	—	0.59	3.98	25	168	427
37-2, 118–120	343.7		late to middle Albian	2.36	32.6	0.13						
37-3, 0–2	344.0			0.73	50.8	0.05	—	6.83	2.60	327	124	422
38-1, 99–100	351.5			2.09	69.9	0.09						
38-2, 140–150^{a}	353.4			1.54	42.7	0.09	—	2.40	2.88	164	197	425
40-2, 120–121	372.2			1.46	34.8	0.08						
40-3, 118–120	373.7			1.59	42.7	0.08						
40-4, 0–2	374.0			1.45	39.3	0.08						
42-5, 140–150^{a}	396.0			1.35	41.8	0.08	—	7.11	4.05	618	352	425
43-2, 135–136	400.9			1.15	33.8	0.06						
43-4, 118–120	403.7			1.45	37.3	0.09						
43-5, 0–2	404.0			1.70	41.3	0.09	—	3.47	3.02	231	201	427
43-5, 149–150	405.5			1.50	46.2	0.08						
46-3, 140–150	430.9	IIIB	early Albian to late Aptian	0.70	42.7	0.06	—	1.41	2.45	115	199	424
46-3, 118–120	432.2			1.23	42.2	0.08						
46-5, 0–2	432.5			0.78	43.7	0.06						
49-3, 118–120	459.2			0.48	56.1	0.04	—	0.39	2.71	76	531	425
49-4, 0–2	459.5			0.51	48.7	0.04						
52-5, 118–120	490.7			0.27	52.6	0.04	—	0.36	1.98	77	421	418
52-6, 0–2	491.0			0.47	50.2	0.04						
55-5, 118–120	519.2			0.96	53.6	0.05	—	2.79	2.97	187	199	429
55-6, 0–2	519.5			1.49	53.1	0.07						
56-3, 140–150^{a}	525.9	IIIC	late Aptian	0.83	44.2	0.05						
56-4, 149–150	527.5			0.12	40.8	0.03						

Note: — = not detected.

[a] Residues from interstitial water analysis.

[b] Sample probably contaminated.

[c] Organic carbon content based on C_{org} content of noncarbonate residue and estimated carbonate content.

[d] Organic carbon content estimated from the data of a closely spaced sediment.

Table 4. Statistical characteristics of $CaCO_3$, C_{org}, and N_{org} contents in sediments from Site 545.

Lithologic unit	Age	$CaCO_3$ (%)					C_{org} (%)					N_{org} (%)				
		N	Range	Mean	Variance	S.D.	N	Range	Mean	Variance	S.D.	N	Range	Mean	Variance	S.D.
IA	early Pleistocene	15	31.9–66.0	47.0	79.33	9.22	8	0.19–0.35	0.27	0.003	0.06	8	0.04–0.06	0.05	6×10^{-5}	0.008
IB	Pliocene–late Miocene	17	53.1–77.9	69.6	60.00	7.98	11	0.06–0.78	0.19	0.039	0.21	11	0.02–0.06	0.03	2×10^{-4}	0.015
II	early-middle Miocene	15	32.9–80.8	57.3	186.23	14.13	6	0.10–0.67	0.36	0.063	0.27	6	0.03–0.07	0.05	2×10^{-4}	0.017
IIIA (upper part)	Cenomanian	11	16.6–44.7	30.2	119.54	11.47	4	0.82–1.30	1.02	0.032	0.21	4	0.06–0.07	0.07	2×10^{-5}	0.005
IIIA (lower part)	Cenomanian–Albian	23	20.5–69.9	41.2	140.48	12.12	16	0.73–2.36	1.49	0.192	0.45	16	0.05–0.13	0.09	4×10^{-4}	0.021
IIIB	Albian–late Aptian	17	36.8–56.1	48.1	25.97	5.25	9	0.27–1.49	0.77	0.140	0.40	9	0.04–0.08	0.05	2×10^{-4}	0.015
IIIC	late Aptian	2	40.8 44.2	42.5	2.89	2.40	2	0.12–0.83	0.48	0.126	0.50	2	0.03–0.05	0.04	1×10^{-4}	0.014
	Total	100					56					56				

Note: Mean $(\bar{y}) = \frac{1}{N}\sum_{i=1}^{N} y_i$; variance $= \frac{1}{N}\sum_{i=1}^{N} y_i^2 - \left(\frac{1}{N}\sum_{i=1}^{N} y_i\right)^2$; S.D. $= \sqrt{\text{var}\,\frac{N}{N\text{-}1}}$

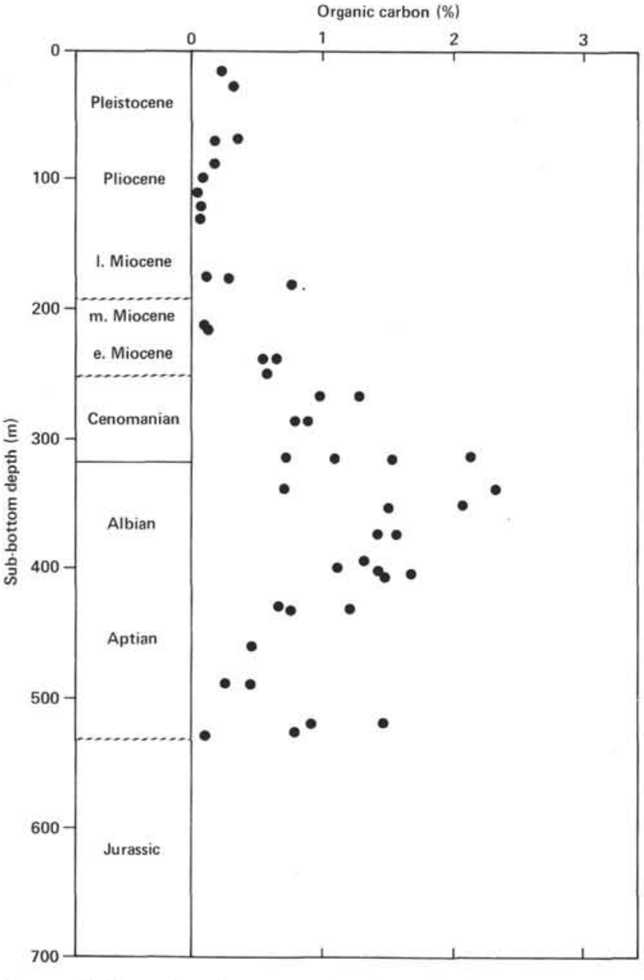

Figure 13. Organic carbon versus depth profile for sediments from Hole 545.

ments is obviously strongly oxidized, but low-temperature decomposition of carbonates in these sediments, which have undergone little diagenetic alteration, may also have contributed to the extremely high amounts of carbon dioxide in the pyrolysis products.

Table 5. Correlations between noncarbonate material and C_{org} (in total sediment) in the different lithologic units at Site 545.

Lithologic unit	Age	General lithology	N	r_s	$r_{05;N}$	Correlation
IA	early Pleistocene	Clayey foraminiferal nannofossils oozes and clays	8	0.60	0.64	No(?)
IB	Pliocene late Miocene	Clayey foraminiferal nannofossil oozes and limestones	11	0.76	0.52	Yes
II	early-middle Miocene	Clayey nannofossil chalks	6	0.92	0.83	Yes
IIIA (lower part)	Cenomanian Albian	Nannofossil-bearing silty claystones	16	−0.04	0.43	No
IIIB	Aptian	Nannofossil-bearing silty claystones	9	0.05	0.60	No

$r_2 = 1 - 6 \sum_{i=1} d_i^2/N(N^2 - 1)$ (Spearman's rank correlation coefficent), where d_i = rank difference of correlated values.

$r_{05;N}$ = critical value of Spearman's rank correlation coefficient at level of significance 0.05 and N. The correlation is significant when $|r_s| \geq r_{05;N}$.

Among the other three early to middle Miocene samples analyzed, Sample 545-20-1, 130–131 cm seems to be contaminated. This is indicated by the presence of a significant S_1 peak (volatile organic matter), the very high T_{max} value, and the total organic carbon content, which is significantly higher than that of the adjacent sediments. The two deepest Miocene samples (Core 545-26) are still hydrogen deficient, but the IO values are considerably lower than in the shallower samples. In the IH versus IO diagram (Fig. 14), these two samples plot below the kerogen type III trend line, indicating that the organic matter is of terrigenous origin and partly oxidized. The pyrolysis data of the Cenozoic samples are consistent with those obtained for sediments from the nearby Site 544.

The Cenomanian sediment samples from Cores 545-29-1, 545-29-2, and 545-31-1 exhibit IH and IO values similar to the Miocene sediment just above the unconformity and thus also plot below or close to the kerogen type III trend line in Figure 14. The three samples from Core 545-34, also of Cenomanian age, all show slightly enhanced hydrogen contents and moderate (Sections 545-34-1 and 545-34-3) or very high (Section 545-34-2) IO values (Table 3; Fig. 14). This probably indicates ei-

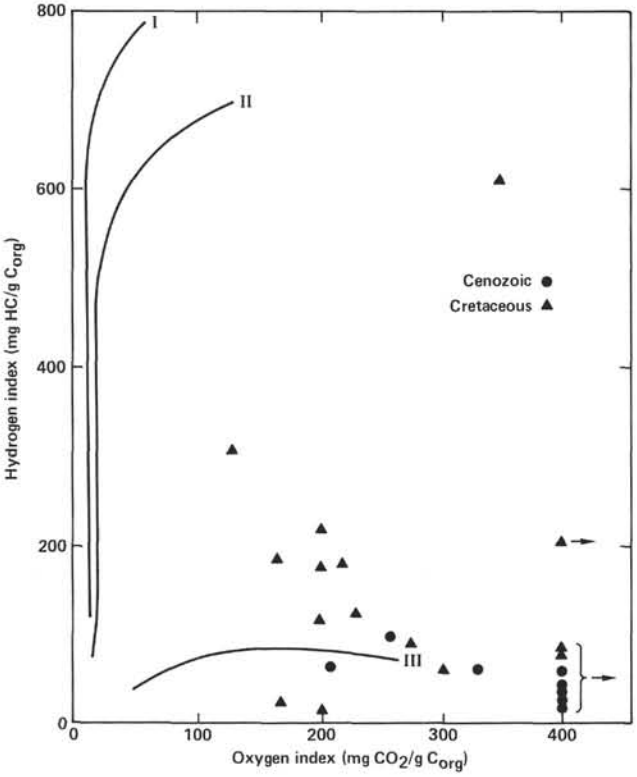

Figure 14. Results of Rock-Eval pyrolysis displayed as hydrogen index versus oxygen index diagram for sediments from Hole 545.

ther a mixture of predominantly terrigenous with some marine organic matter or well-preserved, liptinite-rich, terrigenous organic matter. The very high IO value of Sample 547-34-2, 0–2 cm is unusual, but similar results have been obtained before (e.g., Boutefeu, 1980). It is worth mentioning that Sample 545-34-1, 80–81 cm represents a dark olive green to black clast within the dark green nannofossil claystones of this lithologic unit.

The highest IH values were found in the sediments of Albian age (lower part of Lithologic Unit IIIA) except for Sample 545-37-2, 118–120 cm, which has an extremely low IH despite the fact that it has the highest organic carbon content measured among the Hole 545 sediments (2.36%). The other Albian sediments contain kerogens of mixed types II and III and indicate environmental conditions that favored preservation of organic matter during this time. Buried more deeply, these sediments should have a good potential for generation of gaseous hydrocarbons. The position of Sample 545-43-2, 135–136 cm in the IH/IO diagram (Fig. 14) is somewhat intriguing. We tend to believe that—as in Sample 545-34-2, 0–2 cm—the IO for unknown reasons is unusually high. This would mean that the kerogen in this sample actually is closer to type II than is shown in Figure 14, and thus it is dominantly of marine origin. However, a hydrogen-rich contamination cannot be fully excluded; this would shift the kerogen closer to the type III trend line.

The organic matter of the Aptian samples (Lithologic Unit IIIB) is again severely depleted in hydrogen content, and the kerogen type is similar to that of the Cenomanian samples from the upper part of Lithologic Unit IIIA, with the exception of the deepest sample investigated in this sequence (base of Lithologic Unit IIIB, which contains a mixed types II–III kerogen).

In kerogen type, the organic matter in the Cenozoic and Cenomanian samples seems to be very similar to that found in the sediments of DSDP Site 415, further south on the continental margin off Morocco (Boutefeu, 1980). There is only a limited number of samples from the Albian and Aptian of DSDP Site 416 (south of Site 545) for comparison, but some of these also show the enhanced hydrogen contents in the kerogens (Boutefeu, 1980) that appear in the sediments recovered at Site 545.

The temperatures of maximum pyrolysis yield (T_{max}) offer an interesting opportunity for comparison with DSDP Site 415. As usual, the temperature values increase rapidly in the very immature kerogens until they reach a value of about 425°C. From that point on, only a slow increase is observed with increasing depth of burial until the onset of thermal hydrocarbon generation. At DSDP Site 415, the inflection point is reached at a depth of about 900 m (Boutefeu, 1980), whereas at Site 545 it is at a depth of only 300 m (Fig. 15). Neglecting the somewhat thicker Tertiary section at Site 415, assuming comparable geothermal heat flow conditions, and keeping in mind that there is a Tertiary/Cretaceous unconformity at both sites with the uppermost Creta-

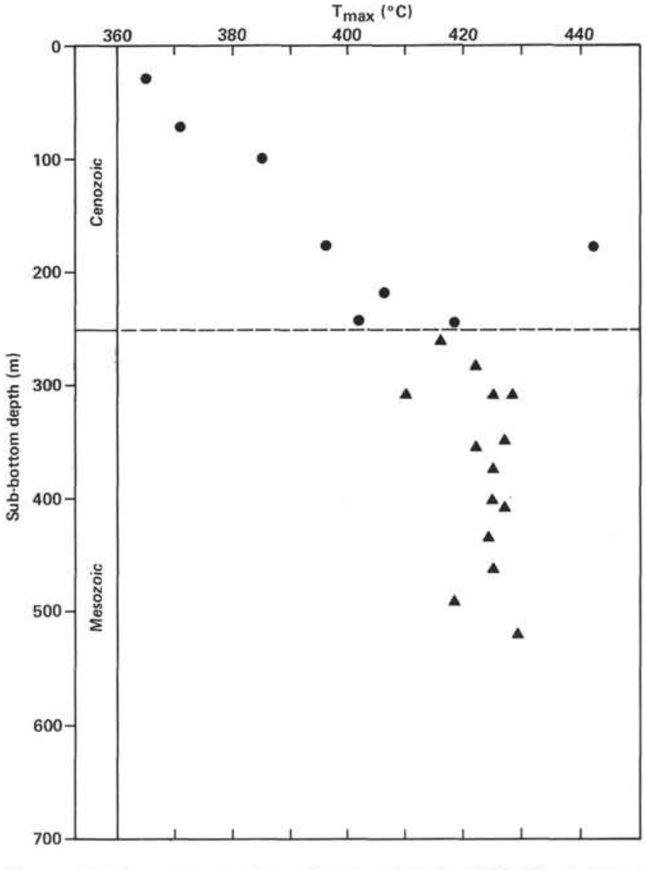

Figure 15. Temperature of maximum pyrolysis yield (T_{max}) versus depth profile for sediments from Hole 545.

ceous sediments being the Cenomanian, it may be possible that up to 600 m more sediment were eroded at Site 545 than at Site 415, at the time the unconformity was created. This has to be considered as a rough estimate only, as is shown by the considerable scatter of data points in Figure 15 and because of the low accuracy of T_{max} determination.

Gas Chromatography of Hydrocarbons

In the cores recovered from Hole 545, no gas pockets containing free hydrocarbons were observed. In the more consolidated sediments (starting at Core 545-26, early Miocene, near the lowermost Tertiary section recovered at this site), hydrocarbons dissolved in the pore water were monitored by carrier gas stripping chromatography (Table 6). The gas chromatogram of the only Cenozoic sample analyzed (Sample 545-26-1, 73–75 cm) shows isobutane dominant (Fig. 16) and small amounts of the C_2 to C_4 and C_6 *n*-alkanes. The extremely high isobutane/*n*-butane ratio indicates indigenous formation of the hydrocarbons during early diagenesis at a very low maturation level, possibly involving a specific precursor molecule.

The Cenomanian through upper Aptian green nannofossil claystone and clayey nannofossil chalk show more complex light hydrocarbon compositions. The concentrations, relative to total sediment as well as normalized to organic carbon content, vary significantly (Table 6). In many samples, hydrocarbons outside the calibrated range (Fig. 16) were detected, but they could not be identified. The highest absolute total C_2 to C_6 hydrocarbon concentration (61.6 nl/g dry sediment) was found in Sample 545-34-1, 80–81 cm, a dark olive green to black clast most probably originating from a downslope-transport event. In all samples analyzed, the isobutane/*n*-butane and isopentane/*n*-pentane ratios are close to unity, with the isoalkanes slightly predominating in most cases. This again indicates indigenous formation of the hydrocarbons at a relatively low maturation level. The reduced isobutane/*n*-butane ratio, relative to the early to middle Miocene sample, may be due to advanced maturity of the organic matter or to the absence of comparably specific precursor molecules in the Cretaceous sediments.

The gas chromatographic analysis of an obviously oxidized, yellow gray dolomitic ooze from the lower end of the Cretaceous section (Sample 545-56-4, 149–150 cm) exhibits very low hydrocarbon concentrations; the lightest hydrocarbons, ethane and propane predominate, and the isoalkane/*n*-alkane ratios at C_4 and C_5 seem to be close to unity, as in the overlying sediments. It is not clear if these hydrocarbons were formed from the low amount of organic matter still present in the oxidized sediment or if their presence is due to diffusion from the green claystone close above.

INORGANIC GEOCHEMISTRY

A summary of the inorganic geochemistry data for Site 545 is given in Table 7 and Figure 17.

PHYSICAL PROPERTIES

Physical properties measured at Site 545 include compressional-wave velocity, wet-bulk density, porosity, water content, and shear strength. These measurements are summarized in Tables 8 and 9. Variations of the physical properties are very well correlated with the lithologic units present, as shown on Figure 18.

Compressional-wave velocity gradually increases from approximately 1.5 to slightly greater than 1.6 km/s in the clayey foraminiferal nannofossil ooze and nannofossil-rich calcareous clay of Unit I (0–181 m). Density increases from 1.5 to nearly 1.9 g/cm³, but porosity decreases from 67 to about 50%. Subunit IB (85.6–181 m) contains limestone gravel layers with measured velocities of 5.6 to 6.1 km/s, densities of 2.65 to 2.69, and porosities of 1 to 3.5%. Shear strengths (Table 9) in the upper

Table 6. Light hydrocarbon (C_2–C_6) values (in nl/g sediment) detected in sediments from Hole 545 by carrier gas stripping gas chromatography.

Core-Section (interval in cm)	Sub-bottom depth (m)	Litho-logic unit	C_2	C_3	*i*-C_4	*n*-C_4	neo-C_5	*i*-C_5	*n*-C_5	cy-C_5	*i*-C_6 + *ai*-C_6	*n*-C_6 + *Me-cy*-C_5	*cy*-C_6	Total HC	Total HC (nl/g C_{org})
26-1, 73–75	237.2	II	0.4	3.6	15.6	0.1	—	—	—	—	—	0.3	—	20.0	5,714[a]
29-1, 22–23	269.2	IIIA	1.7	1.2	1.5	0.5	—	0.4	0.4	—	—	—	—	6.7	551[a]
34-1, 80–81	313.3		3.9	9.0	5.0	9.3	—	16.7	5.8	—	5.3	12.6	—	61.6	2,852
34-2, 0–2	314.0		7.7	6.9	4.1	3.7	tr	3.5	2.8	0.5	1.6	2.5	—	32.3	7,691[a]
37-2, 118–120	343.7		2.6	2.4	1.2	1.0	—	0.8	0.6	—	—	—	—	8.6	364
38-1, 99–100	351.5		7.1	10.7	5.8	6.6	0.1	7.3	6.1	0.3	3.0	5.3	tr	52.3	2,502
40-2, 120–121	372.2		3.7	6.6	4.1	4.9	tr	8.6	3.4	tr	0.9	1.0	—	36.2	2,479
43-2, 135–136	400.9		13.4	13.0	6.3	5.2	—	7.4	5.2	tr	3.7	3.7	—	56.0	4,870
43-5, 149–150	405.5		5.3	5.9	3.3	2.5	—	3.4	2.1	0.3	0.8	1.3	—	22.9	1,527
46-4, 118–120	432.2	IIIB	2.4	2.1	1.0	0.8	—	1.3	0.9	—	0.6	1.0	—	10.4	846
49-4, 0–1	459.5		0.9	0.8	0.2	0.3	—	tr	tr	—	—	—	—	2.2	440
52-6, 0–2	491.0		1.0	2.0	0.7	0.5	—	0.4	0.3	tr	0.2	0.3	—	5.4	1,149
55-5, 119–120	519.2		2.2	3.8	1.4	1.3	—	1.0	1.3	—	0.6	2.1	0.3	14.0	933[b]
56-4, 149–150	527.5	IIIC	0.4	0.4	tr	tr	—	tr	tr	—	—	—	—	0.8	667

Note: Compounds are listed in order of retention times. tr = trace; — = not detected.

[a] Organic carbon content based on C_{org} content in noncarbonate residue and estimated carbonate content.

[b] Organic carbon content estimated from a closely spaced sediment sample.

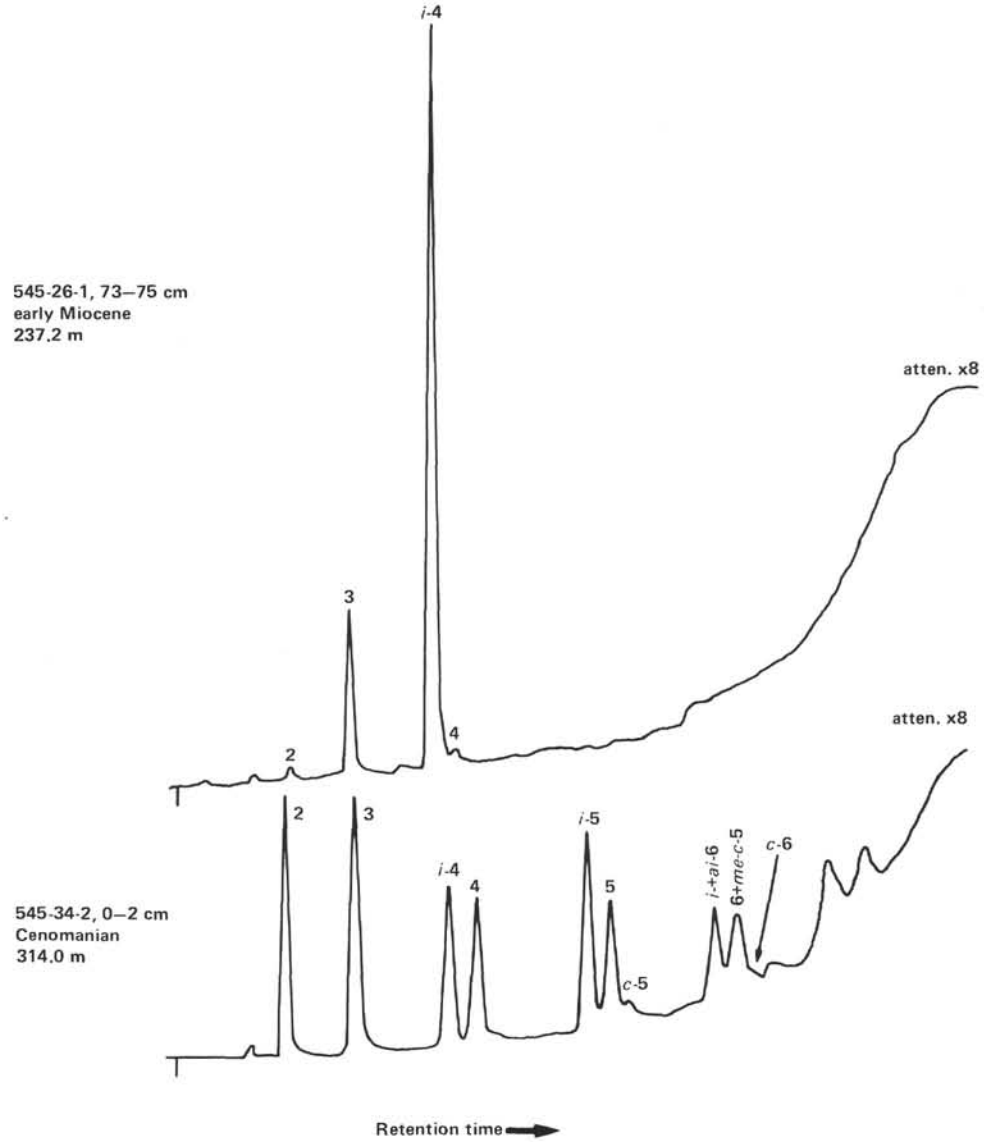

Figure 16. Gas chromatography of light hydrocarbons obtained from fresh sediment samples by carrier gas stripping. Differences in light hydrocarbon composition are shown for an early Miocene and a Cenomanian sample.

Table 7. Summary of shipboard inorganic geochemical data, Site 545.

Core-Section (interval in cm)	Sub-bottom depth (m)	pH	Alkalinity (meq/l)	Salinity (‰)	Calcium (mmoles/l)	Magnesium (mmoles/l)	Chlorinity (‰)
IAPSO standard		7.60	2.43	35.2	10.55	64.54	19.378
2-4, 144–150	14.44–14.50	7.24	5.96	35.3	7.98	51.72	19.311
8-3, 144–150	69.94–70.00	7.21	8.05	35.1	6.28	49.65	19.378
12-4, 144–150	109.44–109.50	7.25	4.70	34.2	9.95	45.08	19.311
19-3, 144–150	174.44–174.50	7.42	2.41	35.1	12.75	42.16	19.176
23-3, 144–150	212.44–212.50	7.15	2.97	35.1	15.05	40.58	19.412
27-3, 144–150	250.44–250.50	7.16	3.58	35.1	17.49	38.74	19.412
31-1, 140–150	285.40–285.50	7.78	4.98	33.0	18.36	41.46	18.332
34-1, 140–150	313.90–314.00	7.39	3.66	34.1	18.24	41.70	18.771
38-2, 140–150	353.40–353.50	7.24	3.74	34.9	18.97	39.71	19.311
42-5, 140–150	395.90–396.0	7.20	3.13	35.8	18.92	40.06	19.412
46-3, 140–150	430.90–431.0	a	a	35.2	19.15	40.43	19.412
56-3, 140–150	525.90–526.0	a	a	36.0	13.27	50.61	19.446

[a] Insufficient quantity of pore water obtained for analyses.

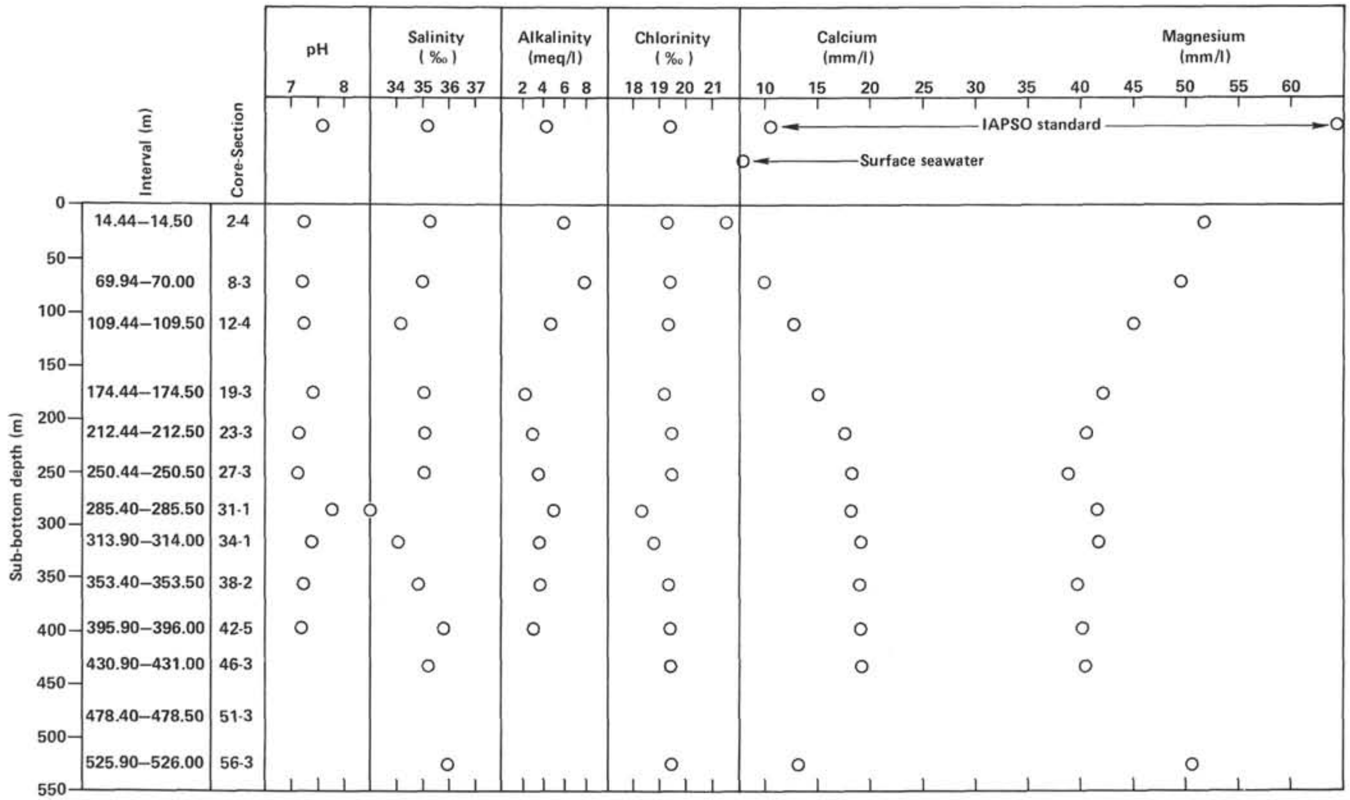

Figure 17. Interstitial water chemistry, Site 545. Insufficient pore water obtained for analysis from Core 51.

130 m of Unit I increase generally with depth. Anomalously low values at 38 and 117 m may reflect the highly disturbed nature of these soft sediments.

Unit II (181–252 m) is a green gray clayey foraminiferal-nannofossil chalk in which velocities increase slightly from 1.57 to near 1.7 km/s. In this unit densities are approximately 1.8 g/cm^3 and porosities average near 53%.

Subunit IIIA (252–418.2 m) consists of nannofossil-bearing and nannofossil claystone. In the upper 100 m of the unit, vertical velocities range from 1.66 to 1.87 km/s, but the measured horizontal velocities are 0.04 to 0.09 km/s higher. Gravimetrically determined densities range from 1.82 to 1.97 g/cm^3, and porosities are between 45 and 55%.

Between 350 and 418 m vertical velocities increase more rapidly to nearly 2.1 km/s, and horizontal velocities are 0.11 to 0.26 km/s higher than vertical velocities. Densities increase from approximately 1.95 to 2.14 g/cm^3, but porosities decrease from 46 to 33% in this unit.

Subunit IIIB (418.2–520.2 m) is dominantly a nannofossil claystone containing pervasive small-scale faults and folds. In this unit measured velocities become more variable, ranging from 2.07 to 2.40 km/s for vertical velocities, with horizontal velocities are 0.10 to 0.21 km/s higher. Densities range from 2.16 to 2.26 g/cm^3, and porosities vary from 33 to 26%.

Subunit IIIC (520.7–530.7 m) consists of fragmented, muddy nannofossil ooze and slightly fractured, clayey nannofossil chalk. The two samples measured from this unit show considerably lower velocities (1.8 to 2.2 km/s) than the overlying sediments. Densities are 2.15 and 2.02 g/cm^3, and porosities are 32 and 43%.

Unit IV (530.7–701 m) is limestone that is highly variable in composition. Subunit IVB contains terrigenous debris, calcareous sandstone, and calcareous shale. The variability of composition is reflected in the wide ranges of the measured physical properties. Velocities vary from 3.3 to 5.5 km/s. Densities range from 2.2 to 2.64 g/cm^3, and porosities vary from 25 to about 4%.

SEISMIC STRATIGRAPHY

Site 545 lies at the foot of the steeply sloping Mazagan Escarpment in 3150 m water depth (Figs. 1 and 19). Seismic coverage near Site 545 is good and includes 24-fold and migrated multichannel lines (*Meteor* 53-01 to *M* 53-10, *Valdivia VA* 79-02) and good quality single-channel records of *Vema* cruise 3013 (Fig. 20). Seismic and bathymetric measurements were made during the approach to Site 545 from the position of Site 544, trying to follow along the multichannel line *M* 53-08. The attempt to occupy proposed Site MAZ-4 at shotpoint (SP) 740 of line *M* 53-08 was unsuccessful owing to insufficient satellite fixes. Site 545 lies about 750 m west of line *M* 53-08 (SP 725) (Fig. 21).

Seismic Sequences

For the following discussion of the seismic sequences, line *M* 53-08 has been chosen because sound penetration on the profile made by *Glomar Challenger* is not deep enough. Figure 21 shows the seismic record of line

Table 8. Physical properties, Site 545.

Core-Section (interval in cm)	Sub-bottom depth (m)	Velocity		GRAPE		Density (g/cm^3)	Porosity (%)	Water content (%)	Acoustic impedance $(10^5 g \cdot cm^{-2} s^{-1})$
		Horizontal (km/s)	Vertical	Density (g/cm^3)	Porosity (%)				
2-1, 112–114	9.6	1.45				1.58	66.8	42.3	2.30[a]
2-4, 93–95	13.9	1.49				1.61	65.3	40.6	2.40[a]
3-2, 93–95	20.4	1.52				1.65	62.9	38.0	2.51[a]
4-1, 117–119	28.7	1.52				1.72	59.4	34.6	2.62[a]
5-1, 117–119	38.2	1.54				1.77	56.5	31.9	2.72[a]
6-1, 8–10	46.6	1.51							
7-1, 73–75	56.7	1.53				1.71	59.7	34.9	2.61[a]
8-3, 116–118	69.7	1.58				1.79	55.1	30.8	2.82[a]
10-2, 76–78	86.8	1.57				1.83	52.4	28.6	2.87[a]
11-1, 33–36	94.4	6.08				2.69	1.0	0.4	16.36[a]
11-1, 93–95	94.9	1.59				1.82	53.2	29.2	2.89[a]
11-4, 133–135	99.8	1.61				1.85	51.2	27.7	2.98[a]
12-5, 118–120	110.7	1.60				1.84	51.6	28.1	2.94[a]
13-3, 73–75	116.7	1.60				1.85	51.3	27.7	2.95[a]
14-2, 88–90	124.9	1.61				1.84	51.7	28.1	2.96[a]
14-4, 55–57	127.6	1.60				1.81	53.2	29.4	2.89[a]
16-1, 125–127	142.8	5.67	5.60	2.66	2.6	2.65	3.2	1.2	14.84
19-1, 91–93	170.9	1.66				1.89	48.6	25.8	3.14[a]
19-3, 118–120	174.2	1.63							
20-2, 50–52	181.5	1.57				1.80	51.9	28.9	2.83[a]
21-2, 116–118	191.7	1.59				1.84	51.0	27.8	2.92[a]
22-1, 55–57	199.1	1.63							
23-1, 117–119	209.2	1.65							
24-2, 110–112	220.1	1.65	1.63	1.82	53.1	1.80	54.2	30.2	2.94
25-3, 23–25	230.2	1.78	1.75	1.83	52.3	1.81	52.3	29.0	3.17
25-5, 27–30	233.3	1.78	1.56	1.88	49.5	1.86	50.1	27.0	2.90
26-3, 53–55	240.0	1.63	1.61	1.72	59.0	1.71	55.3	32.3	2.75
27-3, 80–82	249.8	1.67	1.66	1.88	49.0	1.78	56.6	31.9	2.95
28-1, 62–64	256.1	1.80	1.71	1.89	48.7	1.82	54.4	29.9	3.10
29-1, 67–69	265.7	1.76	1.70	1.88	49.3	1.87	51.2	27.4	3.18
31-1, 71–73	284.7	1.70	1.66	1.92	46.5	1.88	49.9	26.6	3.13
32-1, 16–18	293.7	1.75	1.71	1.90	47.6	1.86	51.6	27.7	3.19
34-3, 33–35	315.8	1.82	1.76	1.98	43.0	1.94	46.3	23.8	3.41
36-2, 61–63	333.6	1.84	1.78	2.00	41.9	1.96	45.0	23.0	3.49
38-1, 15–17	350.7	1.91	1.87	2.04	39.5	1.97	44.7	22.7	3.68
39-1, 47–49	360.5	1.97	1.76	1.97	43.9	1.93	45.8	23.8	3.39
40-2, 94–96	372.0	2.06	1.80	2.01	40.3	1.97	42.2	21.4	3.55
41-2, 52–54	381.0	2.08	1.97			2.09	35.8	17.1	4.12
42-3, 26–28	391.8	2.13	1.98	2.03	40.1	2.04	36.7	18.0	4.03
43-2, 43–45	399.9	2.28	2.09	2.11	35.1	2.13	32.5	15.2	4.46
44-1, 58–60	408.1	2.25	2.07	2.16	32.5	2.14	33.4	15.6	4.42
45-3, 71–73	420.7	2.36	2.23	2.17	31.6	2.18	30.1	13.8	4.87
46-2, 75–77	428.8	2.28	2.16	2.22	28.8	2.16	32.9	15.2	4.66
47-1, 85–87	436.9	2.38	2.28	2.17	31.9	2.19	30.2	13.8	4.98
48-2, 43–46	447.4	2.18	2.07	2.17	31.8	2.16	32.7	15.1	4.48
49-2, 4–6	456.6	2.53	2.36	2.23	28.3	2.25	27.1	12.1	5.31
50-1, 56–58	465.1	2.37	2.17	2.17	32.0	2.19	30.4	13.9	4.75
51-3, 30–32	477.3	2.29	2.17	2.18	31.3	2.18	31.5	14.4	4.74
52-2, 89–92	485.9	2.42	2.26	2.21	29.7	2.20	28.8	13.1	4.96
53-3, 16–18	496.2	2.60	2.40	2.24	26.9	2.25	26.5	11.8	5.40
54-2, 32–34	504.3	2.31	2.18	2.16	32.1	2.17	32.1	14.8	4.74
55-2, 93–95	514.4	2.55	2.34	2.27	25.9	2.26	26.3	11.6	5.29
56-3, 96–98	525.5	2.19	2.05	2.17	31.8	2.15	32.1	14.9	4.41
56-5, 122–124	528.7	1.81	1.80	2.03	40.3	2.02	43.2	21.4	3.63
57-1, 7–9	531.1	3.33	3.28	2.22	28.7	2.20	25.0	11.4	7.22
59-1, 30–32	550.3	4.72	4.16	2.42	16.5	2.46	18.4	7.5	10.23
63-1, 77–79	588.8	3.71	3.64	2.27	25.8	2.32	22.8	9.8	8.44
66-1, 136–138	617.9	5.53	5.36	2.63	4.4	2.61	4.5	1.7	13.98
67-1, 29–31	626.3	4.77	4.54	2.50	12.0	2.48	18.1	7.3	11.25
68-1, 86–88	636.4	3.36	3.30	2.53	10.5	2.50	13.6	5.4	8.25
69-1, 46–48	645.5	5.44	5.29	2.67	2.0	2.64	4.4	1.6	13.96
70-1, 38–40	654.9	4.43	4.27	2.56	8.5	2.54	9.7	3.8	10.85
71-2, 73–75	666.2	4.93	4.80	2.63	4.3	2.60	5.8	2.2	12.49
72-2, 63–65	675.6	4.34	4.28	2.59	6.5	2.58	7.2	2.8	11.04
73-1, 55–57	683.1	4.04	3.80	2.58	7.4	2.56	8.5	3.3	9.74
74-1, 53–55	692.0	4.61	4.38	2.61	5.8	2.61	6.2	2.4	11.44
75-1, 24–26	700.8	4.13	3.90			2.57	8.7	3.4	10.03

[a] Value computed using horizontal velocity.

M 53-08 and a line drawing with the interpreted seismic sequences. The correlation of seismic reflectors and seismic sequences with the drilling results is presented on Figure 22. We recognized five seismic sequences at Site 545. (For a discussion of the regional seismic stratigraphy, see the regional synthesis chapter by Winterer and Hinz, this volume.)

The uppermost sequence, Ma 1.3, is 0.22 s (2-way traveltime) thick and is subdivided by an unconformity at 0.11 s beneath the seafloor.

Sequence Ma 1.2 shows a pattern of parallel to subparallel reflectors that slope slightly downward. It thins toward the east by progressive onlapping on an unconformity and finally pinches out near the foot of the escarpment. At the projected site location, Sequence Ma 1.2 has a thickness of 0.09 s. The reflection pattern of Sequence Ma 1.2, as well as that of the underlying subsequent Ma 1.1, suggests more or less uniform sedimentation into a steadily subsiding basin. This deep-water basin had already been subdivided by erosion into depressions and highs before deposition of Sequence Ma 1.2. During this period of intensive erosion, Sequence Ma 1.1 was completely eroded at Site 545.

Sequence Ma 2.1 forms a landward-thinning wedge, only about 0.1 s thick at Site 545. Seaward of Site 545, Sequence Ma 2.3 is distinguished by a seaward-dipping,

Table 9. Shear strength of sediments, Site 545.

Core-Section (interval in cm)	Sub-bottom depth (m)	Shear strength (kPa)
2-1, 122-124	9.7	5
2-4, 130-132	14.3	4
3-2, 120-122	20.7	8
4-1, 125-127	28.8	12
5-1, 129-131	38.3	2
7-1, 68-70	56.7	19
8-3, 123-125	69.7	33
10-2, 81-83	86.8	32
11-1, 98-100	95.0	33
11-4, 137-139	99.9	41
12-5, 129-131	110.8	36
13-3, 78-80	116.8	19
14-2, 93-95	124.9	83
14-4, 60-62	127.6	95

subparallel pattern, probably downsloping onto an unconformity (reflector B) and toplapping against the erosional unconformity beneath Sequence Ma 1.1 (reflector R). The reflection pattern of Sequence Ma 2.3 indicates deposition in deep water onto a former continental slope, after a period of erosion or nondeposition.

Deposition onto a former slope is also assumed for the underlying Sequence Ma 2.2, the lower boundary of which is not clearly defined. Sequence Ma 2.2 is represented by discontinuous and seaward-dipping reflection elements.

The interpreted Sequence Ma 2.1 is highly speculative. The same speculation, unfortunately, holds true for the steeply downsloping seaward limit of Unit Ma 3. This seismic unit, represented by a few flat-lying discontinuous reflections, is interpreted as the Mesozoic carbonate platform. The discontinuous seismic pattern we interpret as caused by intensive block faulting.

Correlation of Recognized Seismic Sequences with the Drilling Results

A linear increase of velocity with depth can be assumed according to the sonic velocity measurements in the Hamilton Frame velocimeter. The sonic velocities measured on sediments of Cores 1 to 40 (drilling depth 0-370 m sub-bottom) and of Cores 40 to 56 (370-530 m sub-bottom depth) have been approximated by:

$$V_z = 1500[V_0] + 0.77[g]\ Z \text{ (Cores 1–40), and}$$
$$V_z = 1420[V_0] + 1.75[G]\ Z \text{ (Cores 40–56),}$$

where V_0 (m/s) is the velocity at seafloor, V_z (m/s) is the velocity at a depth Z(m) below seafloor and $g(s^{-1})$ the velocity gradient. For the stratigraphic interpretation of the recognized seismic sequences, the reflection times, $t = 2(1/g\ ln[(V_0 + g\ Z)/V_0]$, of drilled geological bound-

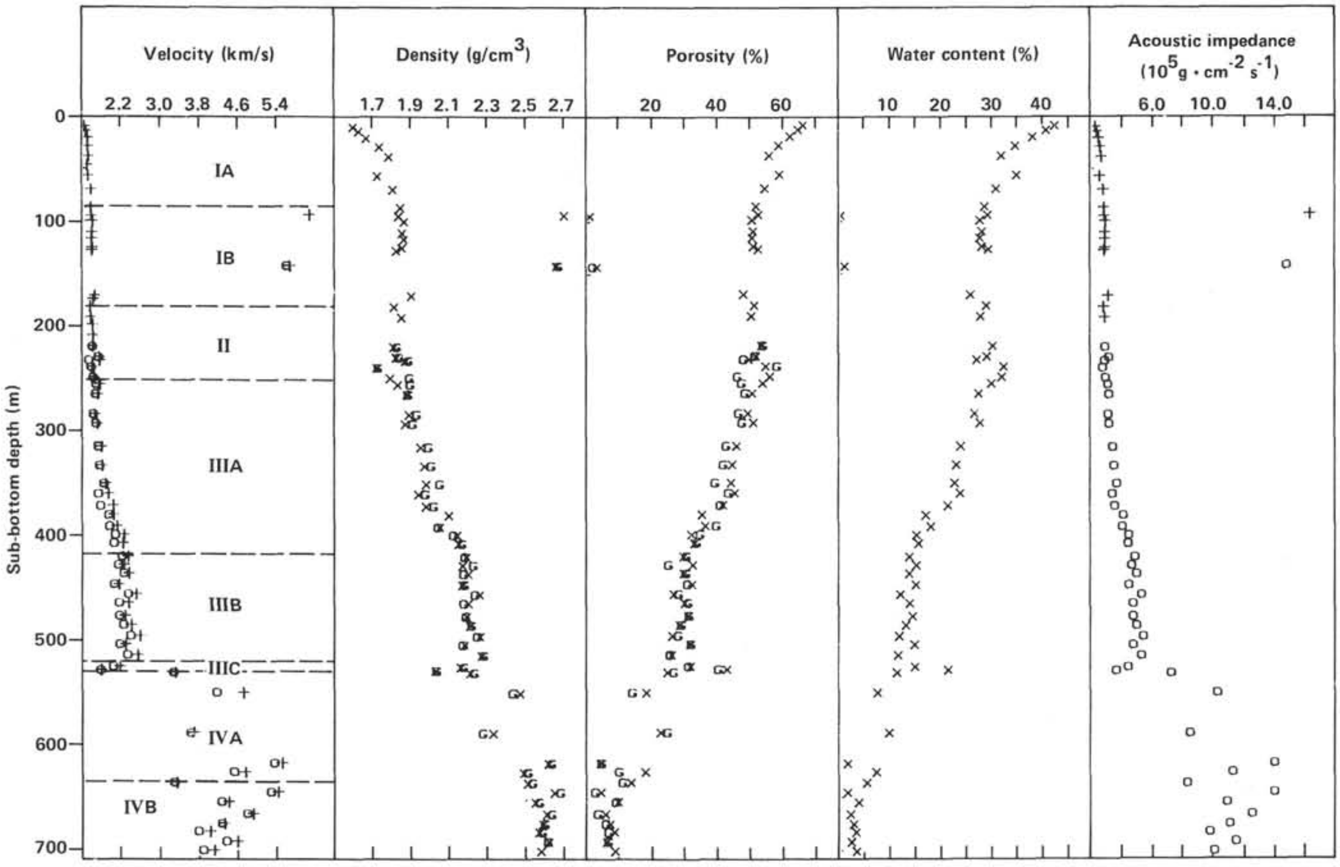

Figure 18. Physical properties versus depth, Hole 545. +, o represent horizontal and vertical values, respectively. X, G represent gravimetric (immersion) and GRAPE values, respectively.

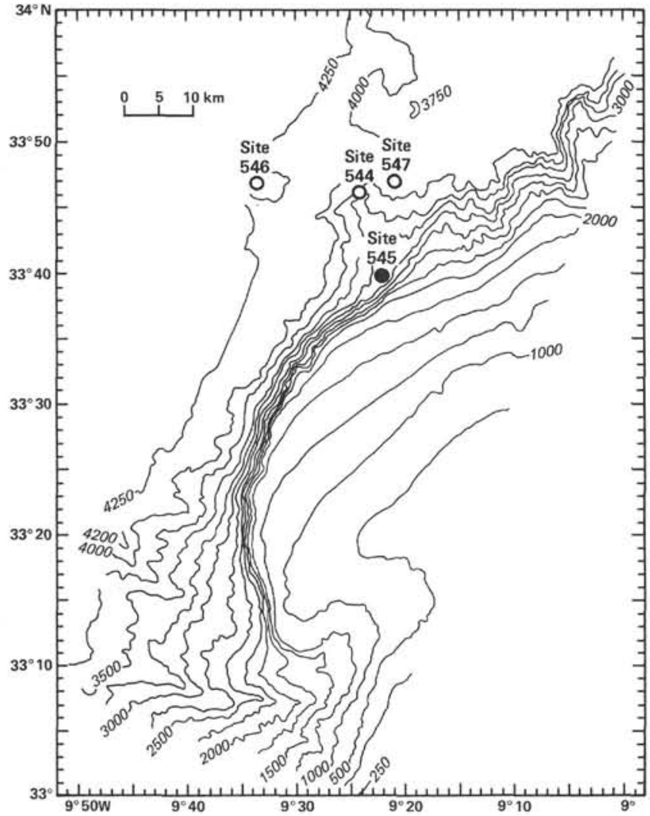

Figure 19. Bathymetric map of the Mazagan continental margin segment, from echo sounding of *Meteor* cruises 9/1967, 39/1975, 53/1980, the *Valdivia* West Africa cruise 1979 and the SEAZAGAN seabeam survey of *Jean Charcot* (Auzende et al., this volume). Depths in m.

aries were calculated and compared with the reflection seismic data.

The following correlation between seismic sequences and drilled lithostratigraphic units can be established (Fig. 22):

Sequence Ma 1.3 correlates well with the Pleistocene and upper Miocene to lower Pliocene clayey nannofossil ooze.

Sequence Ma 1.2 represents the lower to middle Miocene clayey radiolarian-bearing nannofossil chalk. The erosional unconformity which forms the lower boundary of Sequence Ma 1.2 at Site 545 represents the hiatus (about 70 m.y.) drilled at 252 m beneath the seafloor.

Sequence Ma 1.1, completely eroded at Site 545, is interpreted as Paleogene. If this interpretation is correct, the lower boundary of Ma 1.1 could be correlated with an early Eocene erosional event, a Paleocene boundary (Lancelot and Winterer, 1980), and/or with a Cretaceous unconformity perhaps caused by a global fall in sea level postulated by Vail et al. (1977). Although its true stratigraphic level is uncertain, the lower boundary of Ma 1.1 separates the Cretaceous from Tertiary strata. At Site 545, this unconformity merges with a younger surface of erosion, probably of Oligocene age, which forms the lower boundary of Sequence Ma 1.2.

Sequences Ma 2.3 and Ma 2.2 correlate with the Cenomanian through upper Aptian nannofossil claystone.

The lower boundary of Sequence Ma 2.2 is difficult to define near Site 545, probably because of side echoes and diffractions from the steeply dipping slope. The top of the seaward-dipping reflectors of seismic Sequence Ma 3, which probably represent the block- and downfaulted Upper to Middle Jurassic dolomitized limestone, lies somewhere between 0.565 and 0.57 s beneath the seafloor. Table 10 summarizes the seismostratigraphic results.

SUMMARY AND CONCLUSIONS

Although we were unable to core through the entire column of sedimentary strata to basement, the drilling at Site 545 returned valuable scientific dividends. The bit refused to rotate at a depth of 701 m, after having cut 75 cores from a sequence of Neogene and Middle Cretaceous slope sediment replete with evidences of gravity flow phenomena that, in turn, overlie Jurassic platform dolomitic limestone and sandstone.

We intended to drill exactly at planned Site MAZ-4, but the uncertainties of fine-scale navigation on *Challenger* placed Site 545 about 1 km west of MAZ-4, though still in a very congruent position with relation to the foot of the Mazagan Escarpment and the acoustic stratigraphic section at MAZ-4.

Neogene Sediments

The hole spudded in Pleistocene sediments. Both the *Challenger* seismic profile across the site and the nearby *Meteor* 53-08 line show a bumpy topography that is most plausibly explained by erosion of upper Pleistocene (and Recent?) sediments (Figs. 5 and 21). The *Meteor* profile (Fig. 21) suggests that at least 50 m of section may be missing at the top of the column at Site 544.

Lower Pleistocene sediments are about 86 m thick and consist of nannofossil-rich calcareous claystone at the top, grading downward to clayey foraminiferal nannofossil ooze. Terrigenous quartz and mica decrease from about 4% at the top to only a trace at the base. The sediments are well oxidized and are mainly shades of yellow-brown. Siliceous fossils occur commonly in the uppermost part of the unit.

At 85.6 m, the bit met the highest of a series of limestone gravel beds, and the nannofossils in the ooze beneath the top gravel bed indicate middle to late Pliocene age. A hiatus probably separates the gravel from the overlying lower Pleistocene ooze. Five intervals of gravel are intercalated in the lower Pliocene and upper Miocene section between 85.6 and 181 m depth, ranging in thickness from just a single layer of pebbles to about 3 m. The gravel consists of pebbles and cobbles (and perhaps even boulders) of mainly white, skeletal, oncoidal, and intraclastic wackestone and packstone, commonly with peloidal texture. Some clasts have grainstone texture. The white clasts contain a shallow-water fauna of corals, echinoderms, thick-shelled bivalves, and algae, probably of Late Jurassic age. Some of these rocks have calpionellids of Tithonian or Berriasian age in the micrite matrix. A few pink limestone clasts, with *Bositra*(?), are identical to the Middle to Upper Jurassic limestone cored at Site 544. One clast contains calpio-

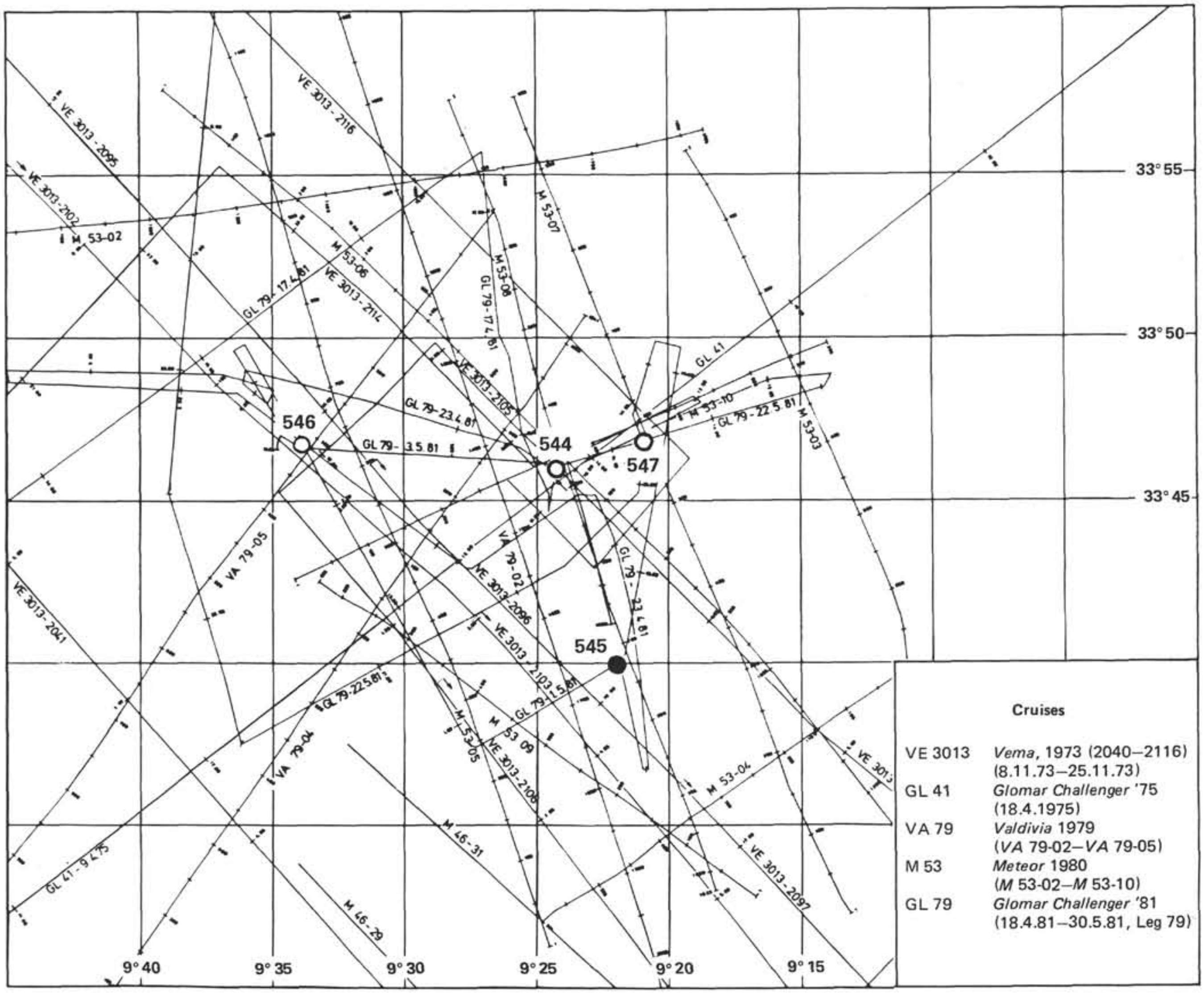

Figure 20. Location of seismic lines around Site 545.

nellid-bearing peloids in a Santonian micrite matrix. The evidence, then, is that the Mazagan Escarpment lay partly bare during late Miocene and Pliocene times, and occasional debris flows sluiced coarse debris down the face of the escarpment onto the slopes below. The escarpment exposes a section of carbonate rocks ranging in age from Middle to Late Jurassic to at least Santonian. The cross section (Fig. 23) shows the buried escarpment and outcrops of Upper Cretaceous strata a little farther up. These latter beds must in turn rest on or next to Jurassic strata nearby, beyond the line of section.

The hiatus at the base of this gravelly unit, which cuts out the lower part of the upper Miocene, correspond fairly closely to the hiatus recorded at Site 544. During the time interval across the hiatus, erosion probably removed a cover of middle Miocene ooze that had blanketed the escarpment, and during the late Miocene, currents probably continued to sweep across the outcrops, where dissolution, bioerosion, and gravity processes combined to deface the slope.

Beneath the hiatus is a thickness of 71 m of greenish clayey nannofossil chalk of middle and early Miocene age. The chalk also contains radiolarians and sponge spicules. Clay increases downward. Glauconite is present in most smear slides. A few layers of intraclastic gravel occur in the lower part of the unit. The cross section (Fig. 23) shows this unit overlapped upslope by the overlying upper Miocene gravels. We interpret this unit to represent a time of increased productivity of overlying waters, probably with penecontemporaneous erosion of ooze recently deposited higher on the slope. Although the average sedimentation rate is between 10 and 20 m/m.y. (0.9–1.8 g/cm^2 per 10^3 yr.), the rate may have been very uneven. Terrigenous influx was relatively high (40–65%) and suggests a more humid climate in Morocco than at present.

The unconformity that separates lower Miocene clayey chalk from underlying Middle Cretaceous claystone at Site 545 can be traced on most seismic records in the region as the Red reflector. At Site 545, at least two

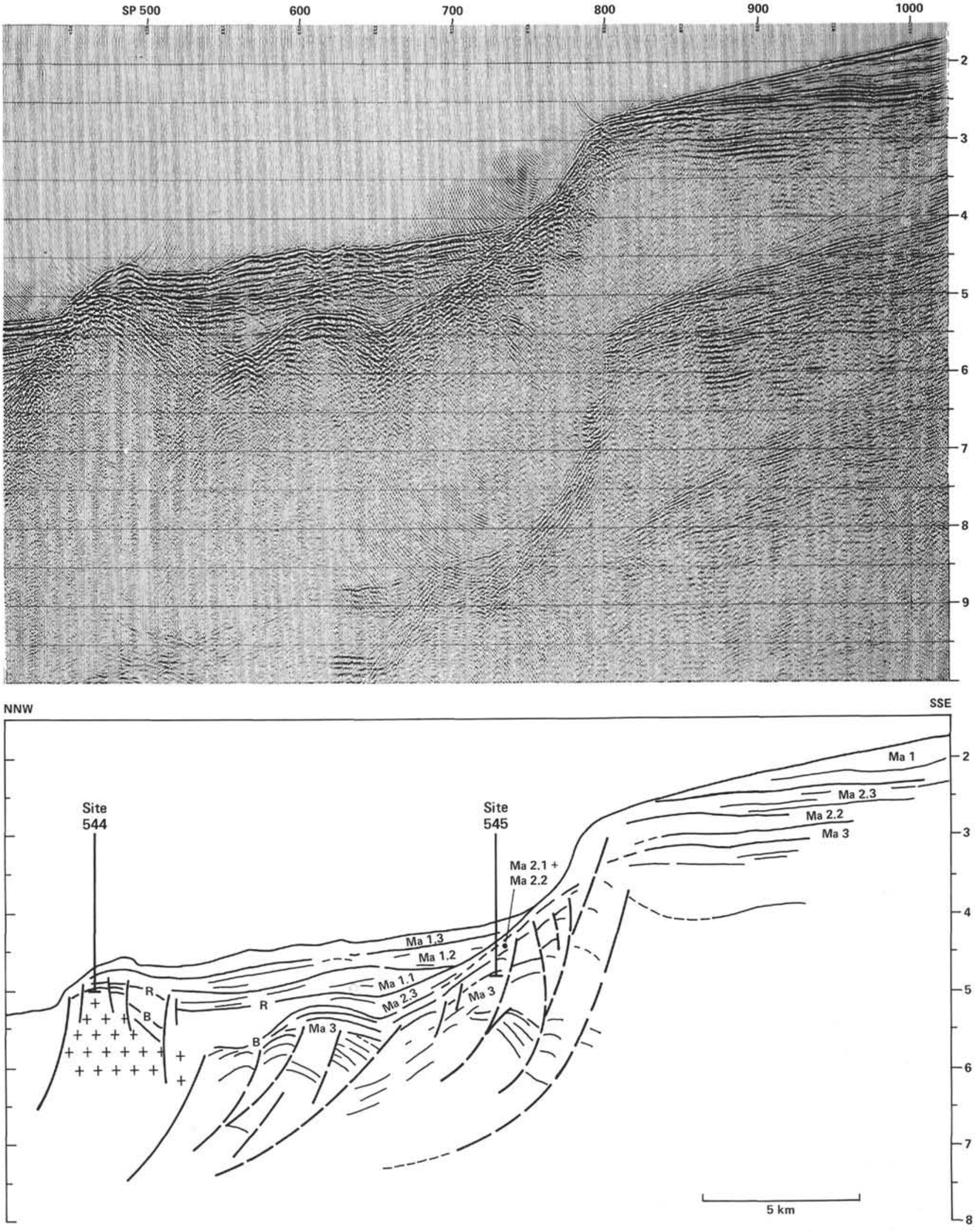

Figure 21. Seismic record of *Meteor* Line *M* 53-08 and line drawing with reflectors and identified seismic sequences near Site 545. Location of the profile is indicated in Figure 20.

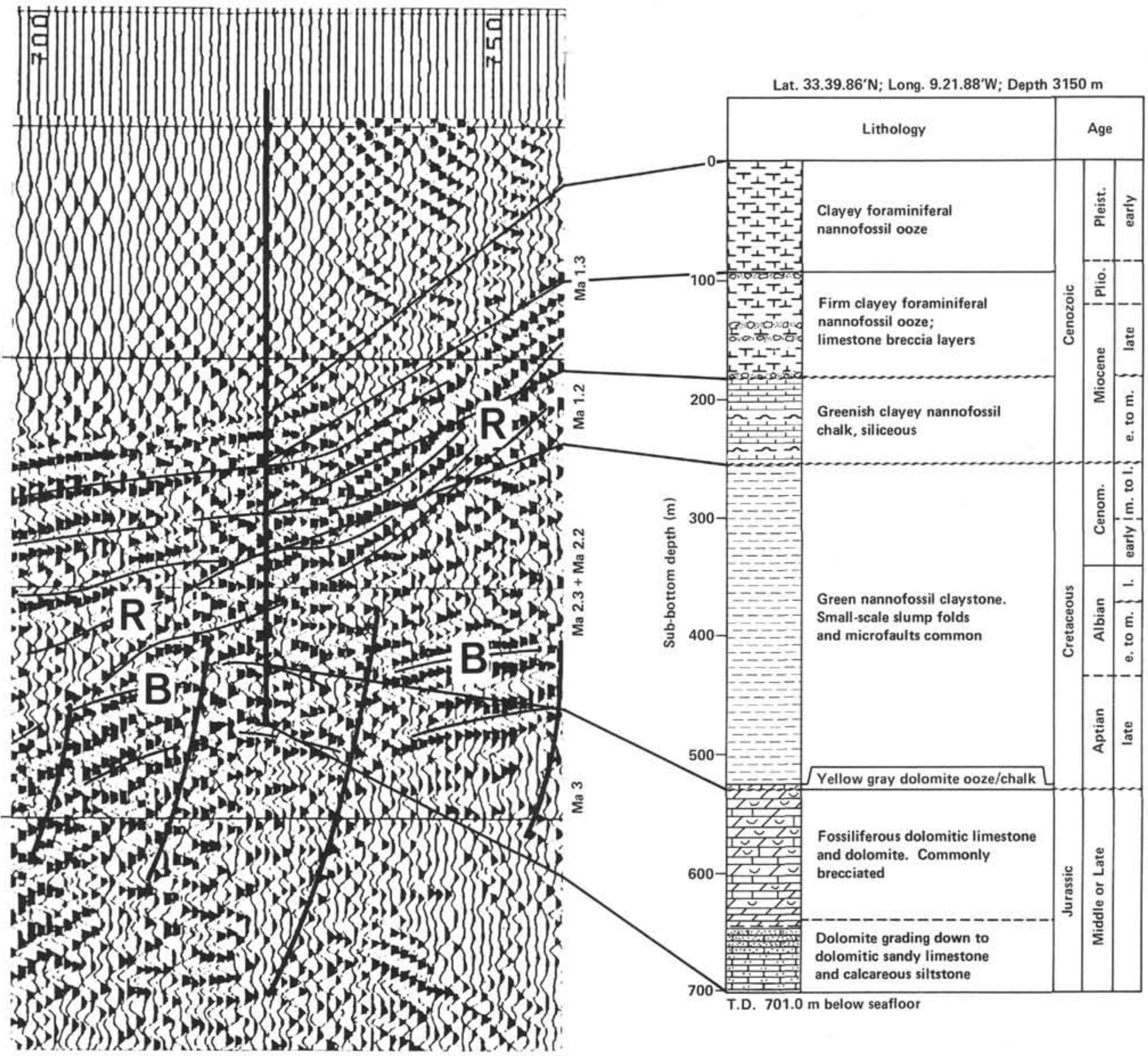

Figure 22. Correlation of seismic sequences and reflectors with the drilling results of Site 545. B, Blue reflector; R, Red reflector.

hiatuses are merged into one: seaward, the Cenozoic section expands to include Eocene and Paleocene beds beneath the hiatus that occurred before the middle Miocene, and these rest in turn unconformably on the Middle Cretaceous, as learned at Site 547.

Cretaceous Rocks

A section of middle or upper Cenomanian to upper Aptian green claystone 279 m thick was cored at Site 545, although the presence of slumps and low-angle faults in the section suggests that this is probably greater than the "true" stratigraphic, that is, undisturbed, thickness. The dominant lithology is nannofossil-bearing claystone, but the carbonate content ranges from about 10 to as much as 70%, and some intervals are thus clayey nannofossil chalk. Three subdivisions are recognized:

A. Fairly soft gray green nannofossil clay/claystone and clayey nannofossil chalk, more indurated downward, and including clayey conglomerate and pebbly claystone beds. Middle Cenomanian to middle Albian (166.2 m).

B. Similar to A, but without clay-pebble conglomerate. Pervasive microfracturing throughout. Middle Albian to upper Aptian (102 m).

C. Highly deformed claystone. Lower upper Aptian (10.6 m).

Bedding tends to be wispy and discontinuous, and burrows are omnipresent. Small-scale slumps and microfaults are common. The mud-supported pebble conglomerate beds are ungraded.

At a depth of about 400 m (middle Albian), there are two beds of fissile black claystone, each only a few tens of centimeters thick, devoid of signs of burrowing and with as much as 2.3% organic carbon.

The claystone is composed chiefly of illite and mixed-layer clays, along with kaolinite in the upper 120 m of the formation. The bulk density increases from about

Table 10. Correlation of seismic sequences and lithologic units, Site 545.

Seismic sequences	Reflection time beneath seafloor (s)	Sub-bottom depth (m)	Interval velocity (km/s)	Drilling results
			1.56	lower Pleistocene foraminiferal nannofossil ooze (Lithologic Unit IA)
Ma 1.3	0.11	86		
				upper Miocene to Pliocene clayey nannofossil ooze (Lithologic Unit IB)
	0.22	180	1.71	
Ma 1.2			1.62	lower to middle Miocene clayey radiolarian-bearing nannofossil chalk (Lithologic Unit II)
	0.31	253		
Ma 2.3 +				upper Cenomanian through upper Aptian nannofossil claystone (Lithologic Unit III)
Ma 2.2 Ma 3	0.565–0.57	531	2.14–2.18	
				Upper to Middle Jurassic dolomitized limestone (Lithologic Unit IV)
		701 (T.D.)		

1.8 at the top to 2.1 at the base, and porosity decreases from about 50 to about 30%. The sound velocity begins to increase rather suddenly at a depth of about 370 m, from a value of about 1.7 km/s to values that increase irregularly to about 2.3 km/s near the base of the unit. The change is at about the level in the upper Albian where there are layers of claystone–pebble conglomerate.

Biostratigraphic data in the lower part of the unit are confusing and suggest that there may be faulting that repeats the section. The foraminifers in Sample 545-52,CC may belong to a zone younger than the zone represented by the foraminifers in Sample 545-53,CC; these suggest faulting at about 500 m. The abundance of shears near the bedding plane in this part of the formation makes it likely that this is a very low angle fault, essentially a thrust or slide.

The rate of accumulation for the Cretaceous claystone was from about 10 to 20 m/m.y., which is not high for terrigenous sediments on a continental slope. For comparison, the lower Miocene off the Tarfaya coast, opposite the Canary Islands, accumulated on the continental slope at a rate about ten times as fast as the Cretaceous sediments on the Mazagan slope.

The boundary between the two lowest subunits in the Cretaceous is a zone of intense shearing, which we interpret as a low-angle fault zone, nearly parallel to bedding, in which younger beds have been displaced downdip over older.

We interpret the Cretaceous claystone beds as deposits on the continental slope at bathyal depths, but well above the calcite compensation depth. Radiolarians and sponge spicules are abundant and planktonic microfossils rare for a brief interval during the middle Albian, signaling perhaps a short-lived rise in carbonate dissolution levels. This corresponds with the interval where the thin black shales occur, and this in turn suggests unusual conditions—perhaps high rates of burial of organic matter. These features are the only local manifestations of a mid-Cretaceous "oceanic anoxic event" (Schlanger and Jenkyns, 1976), but considering that at that time the depth for this area was probably in the range of 1500–2500 m, perhaps only an expanded oxygen-poor zone would have reached as deep as Site 545.

As shown on the cross section (Fig. 23), there is a large structural low between Sites 544 and 545, and the Cretaceous claystone filled up this low region nearly to the rim formed by the structural high at Site 544. The Cretaceous generally rests with unconformity on faulted, and perhaps eroded, Jurassic carbonate rocks, and the lower fault zone is interpreted as a décollement surface. The faults and slump features higher in the formation also record effects of gravity-driven movements down the original continental slope, which has probably been but little steepened since Cretaceous times.

The correlation of the Cretaceous beds below the Mazagan Escarpment with the strata on the Mazagan Plateau labeled Cretaceous on the cross section (Fig. 23) is speculative, since no physical connection can be shown.

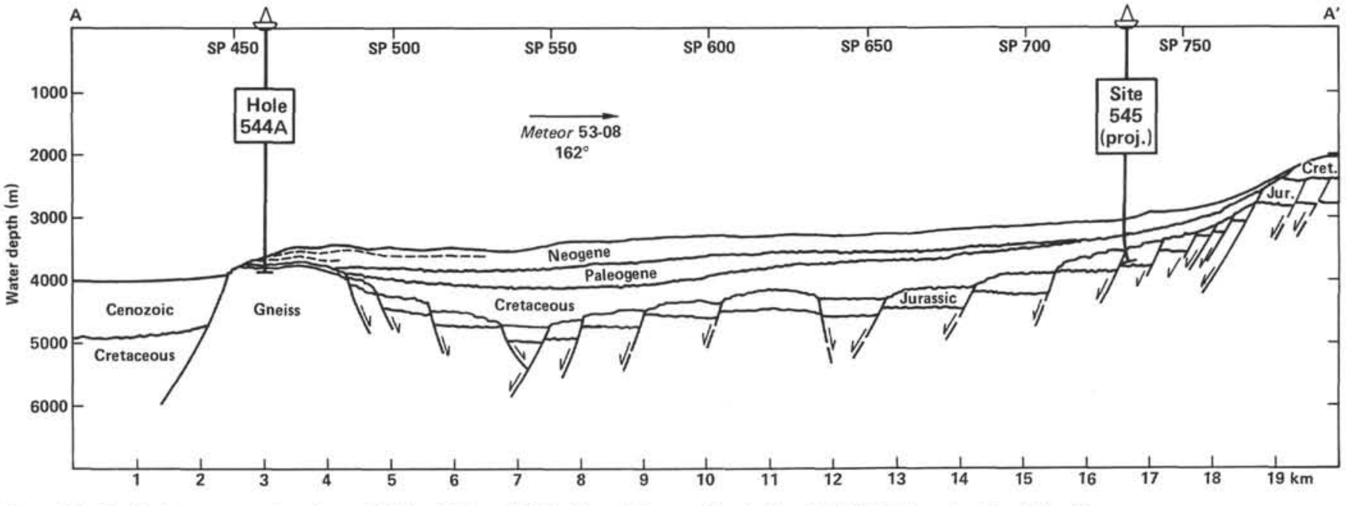

Figure 23. Geologic cross section through Sites 544 and 545, along *Meteor* seismic line *M* 53-08 (Line A–A′ of Fig. 2).

The labeled beds on the Plateau may be much older, and their seismic response suggests they may be carbonate rather than claystone.

During Leg 50, mid-Cretaceous claystones showing slumps and low-angle faults very like those at Site 545 were cored at Site 415, about 350 km south of the Mazagan area, on the lower continental slope (Lancelot and Winterer, 1980); these were interpreted by Price (1980) as slide sheets rooted in thrust faults that originated during epeirogenic uplift of the continental terrace at the western end of the Atlas mountain chain during Late Cretaceous times. The evidence from Site 545 suggests that epeirogeny is not necessary, but rather that only a relatively steep slope is needed for clayey sediments to slump and slide.

Jurassic Rocks

The section of Jurassic limestone, dolomite, and sandstone at Site 545 (Unit IV) which is at least 170 m thick, comprises two subunits, with gradational contact between:

A. Skeletal intraclast grainstone, in part leached, micritized, and dolomitized (47.8 m), overlying, packstone and grainstone (commonly with coral fragments), oolitic grainstone, skeletal intraclast grainstone, coral boundstone, and very fine grained peloid grainstone (57 m).

B. Skeletal wackestone and peloidal packstone, with subordinate oolitic grainstone, calcitic sandstone, and shale. Detrital quartz and feldspar are present throughout and increase in abundance downward (65.5 m).

The hole was terminated in Unit IV B and we have no good clues to the strata that lie at deeper levels.

The fossils in the limestone represent mainly very shallow water environments, mostly in high-energy zones. Dasycladacean algae, coral fragments, bryozoans, bivalves, benthic foraminifers, and echinoderms are all represented. The lower sandy unit also contains ammonites and shows Zoophycos burrows, suggesting slightly deeper water—or perhaps simply a muddier seafloor. No sign of the pelagic elements seen in the red limestone at Site 544 are seen at Site 545.

Many particles are micritized, probably by boring algae. Cementation by bladed sparry calcite suggests an original fibrous aragonite or high-Mg calcite-rim cement, developed in a submarine environment. Much of the limestone is weakly to moderately dolomitized, and the upper part is commonly brecciated. It is not clear whether the brecciation was caused by solution collapse or by infilling of joints and open fractures, perhaps on a depositional slope.

Seismic velocities are quite variable in the carbonate sequence, ranging from 3.3 to nearly 5.4. Measured porosity values are mainly between 5 and 10%. A high impedance contrast exists between the limestone ($7\text{-}14 \times 10^5\ g \cdot cm^{-2}\ s^{-1}$) and the overlying Cretaceous claystone (about $5 \times 10^5\ g \cdot cm^{-2}\ s^{-1}$). This gives rise to the Blue seismic reflector.

The age range of the carbonate sequence is only loosely constrained by the shipboard paleontological data. An ammonite in the lower part of the sequence, in Core 68, was determined as *Sowerbyceras* sp. by Renz (this volume), suggesting an Oxfordian age. A Late Jurassic age is suggested for the upper part of the succession by the presence of *Trocholina alpina* and a questionable *Pseudocyclammina lituus*. Rare lituolid foraminifers in the lower half of the unit suggest a late Dogger to Oxfordian age.

Because red Oxfordian oncolitic skeletal limestone like that drilled at Site 544 is known from dredge samples from the Mazagan Escarpment only a few kilometers to the southeast (Renz et al., 1976), we had expected to drill this limestone at Site 545, and its absence is puzzling. If the upper part of the limestone at Site 545 is Upper Jurassic, and if the lower part is Oxfordian and Dogger(?), we should have met the red limestone. Two contrasting possibilities are open:

1. The paleontological data are not firm, and the rocks are all either older or younger than the red Oxfordian limestone.

2. The red limestone is a lateral facies equivalent of part of the section drilled.

In support of the first possibility is the plausible idea that the Mazagan carbonate succession records progressive deepening as the continental margin subsides. In this view, the shallow-water succession drilled at Site 545 is overlain by slightly deeper water red limestone, but these rocks are missing here at the Cretaceous/Jurassic hiatus because of post-Oxfordian erosion.

The second hypothesis takes the view that there was some local relief in the Mazagan area during Late Jurassic time, and that the limestones in the middle part of the cored section at Site 545 were deposited in a different environmental setting from the contemporaneous red limestone.

The geologic cross section (Fig. 23) depicts the carbonate rocks at Site 545 as tilted fault blocks, significantly eroded before the Cretaceous beds were deposited, but much less faulted schemes are equally plausible. At the present stage of analysis of the drilling data and seismic records, it is not possible to choose between these models.

A detailed summary of the lithologic and biostratigraphic successions at Site 545 is shown in Figure 24.

REFERENCES

Boutefeu, A., 1980. Pyrolysis study of organic matter from Deep Sea Drilling Project Sites 370 (Leg 41), 415, and 416 (Leg 50). *In* Lancelot, Y., Winterer, E. L., et al., *Init. Repts. DSDP*, 50: Washington (U.S. Govt. Printing Office), 555–566.

Burst, J. F., 1968a. Glauconite pellets; their mineral nature and application to stratigraphic interpretation. *Am. Assoc. Pet. Geol. Bull.*, 42:310–327.

_______, 1968b. Mineral heterogeneity in 'glauconite' pellets. *Am. Mineral.*, 43:481–497.

Chamberlain, C. K., 1978. Recognition of trace fossils in cores. *In* Basan, P. B. (Ed.), *Trace Fossil Concepts.* Soc. Econ. Paleont. Mineral. Short Course, No. 5:133–183.

Gartner, S., 1977. Calcareous nannofossil biostratigraphy and revised zonation of the Pleistocene. *Mar. Micropaleontol.*, 2:1–25.

Lancelot, Y., and Winterer, E. L., 1980. Evolution of the Moroccan Oceanic Basin and adjacent continental margin—a synthesis. *In* Lancelot, Y., Winterer, E. L., et al., *Init. Repts. DSDP*, 50: Washington (U.S. Govt. Printing Office), 801–821.

Matthews, D. J., 1939. *Tables of the Velocity of Sound in Pure Water and in Sea Water:* London (Admiralty Hydrographic Department).

Okada, H., and Bukry, D., 1980. Supplementary modification and introduction of Code Numbers to the low-latitude coccolith biostratigraphic zonation. *Mar. Micropaleontol.*, 5:321-325.

Powers, M. C., 1953. A new roundness scale for sedimentary particles. *J. Sed. Pet.*, 23:117-119.

Price, I., 1980. Gravity tectonics on a passive margin: Deep Sea Drilling Project Site 415 in relation to regional seismic data. *In* Lancelot, Y., Winterer, E. L., et al., *Init. Repts. DSDP*, 50: Washington (U.S. Govt. Printing Office), 759-771.

Renz, O., Imlay, R., Lancelot, Y., and Ryan, W. B. F., 1975. Ammonite-rich Oxfordian limestones from the base of the continental slope off Northwest Africa. *Eclogae Geol. Helv.*, 68:431-448.

Roucaché, J., Deroo, G., and Boulet, R., 1979. Caractérisation par différentes méthodes physico-chimique de types de matière organique dans des sédiments du Crétacé d'Atlantique en mer profonde. *Rev. Inst. Fr. Pet.*, 31:191-220.

Schlanger, S. O., and Jenkyns, H. C., 1976. Cretaceous anoxic events: causes and consequences. *Geol. Mjnb.*, 55:179-184.

Seilacher, A., 1967. Bathymetry of trace fossils. *Mar. Geol.*, 5:413-428.

Sliter, W. V., 1980. Mesozoic foraminifers and deep-sea benthic environments from DSDP Sites 415 and 416, eastern North Atlantic. *In* Lancelot, Y., Winterer, E. L., et al., *Init. Repts. DSDP*, 50: Washington (U.S. Govt. Printing Office), 353-427.

Stainforth, R. M., Lamb, J. L., Luterbacher, H., Beard, J. H., and Jeffords, R. M., 1975. *Cenozoic Planktonic Foraminiferal Zonation and Characteristics of Index Forms. Univ. Kansas Paleontol. Contrib.*, 62.

Thierstein, H. R., 1976. Mesozoic calcareous nannoplankton biostratigraphy of marine sediments. *Mar. micropaleontol.*, 1:325-362.

Vail, P. R., Mitchum, R. M., Todd, R. G., et al., 1977. Seismic stratigraphy and global changes of sea level. *In* Payton, C. E. (Ed.), *Seismic Stratigraphy—Application to Hydrocarbon Exploration.* Am. Assoc. Pet. Geol. *Mem.*, 26:45-212.

van Hinte, J. E., 1976. A Cretaceous time scale. *Am. Assoc. Pet. Geol. Bull.*, 60:498-516.

Date of Acceptance: October 26, 1983

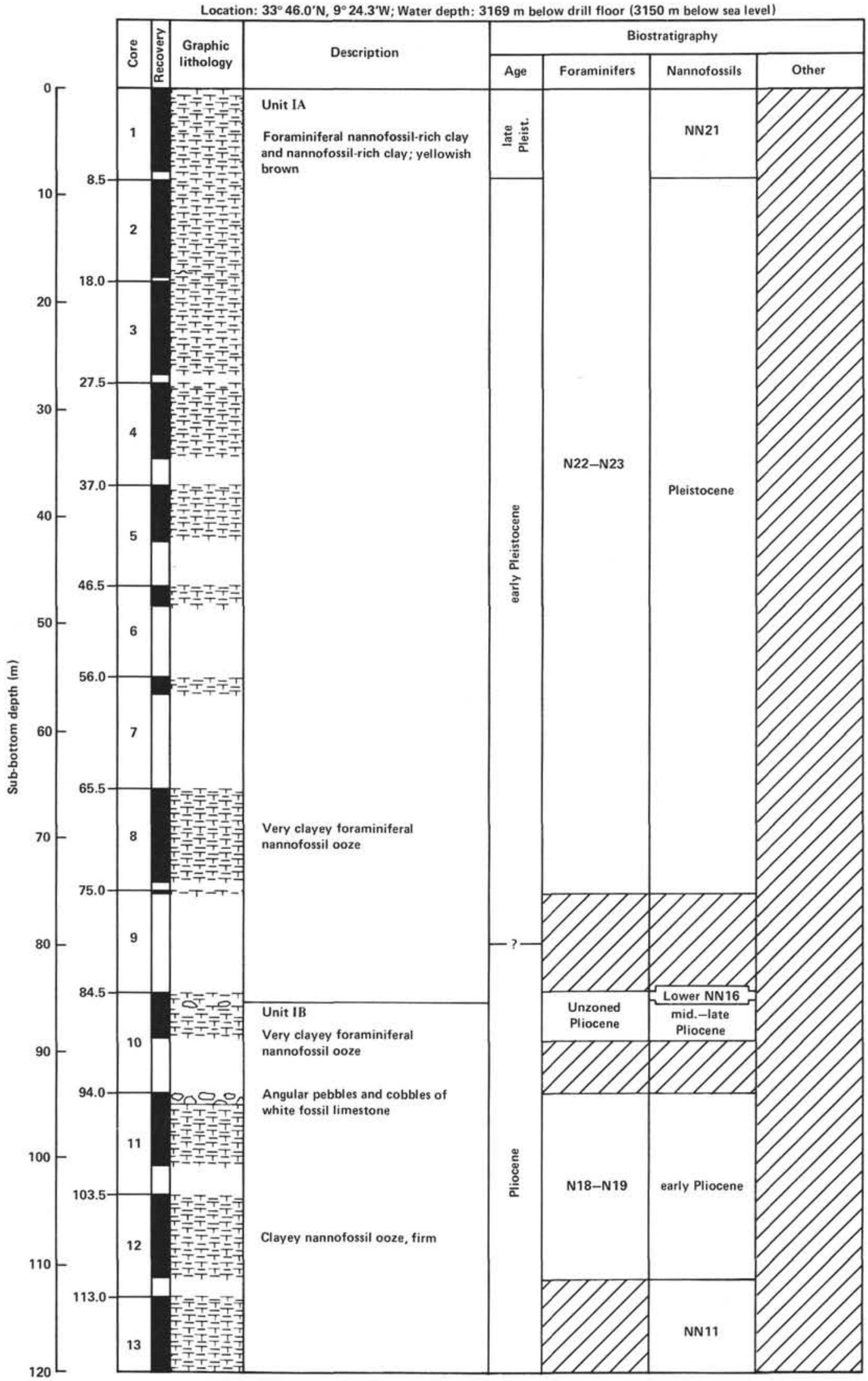

Figure 24. Detailed graphic log of Site 545.

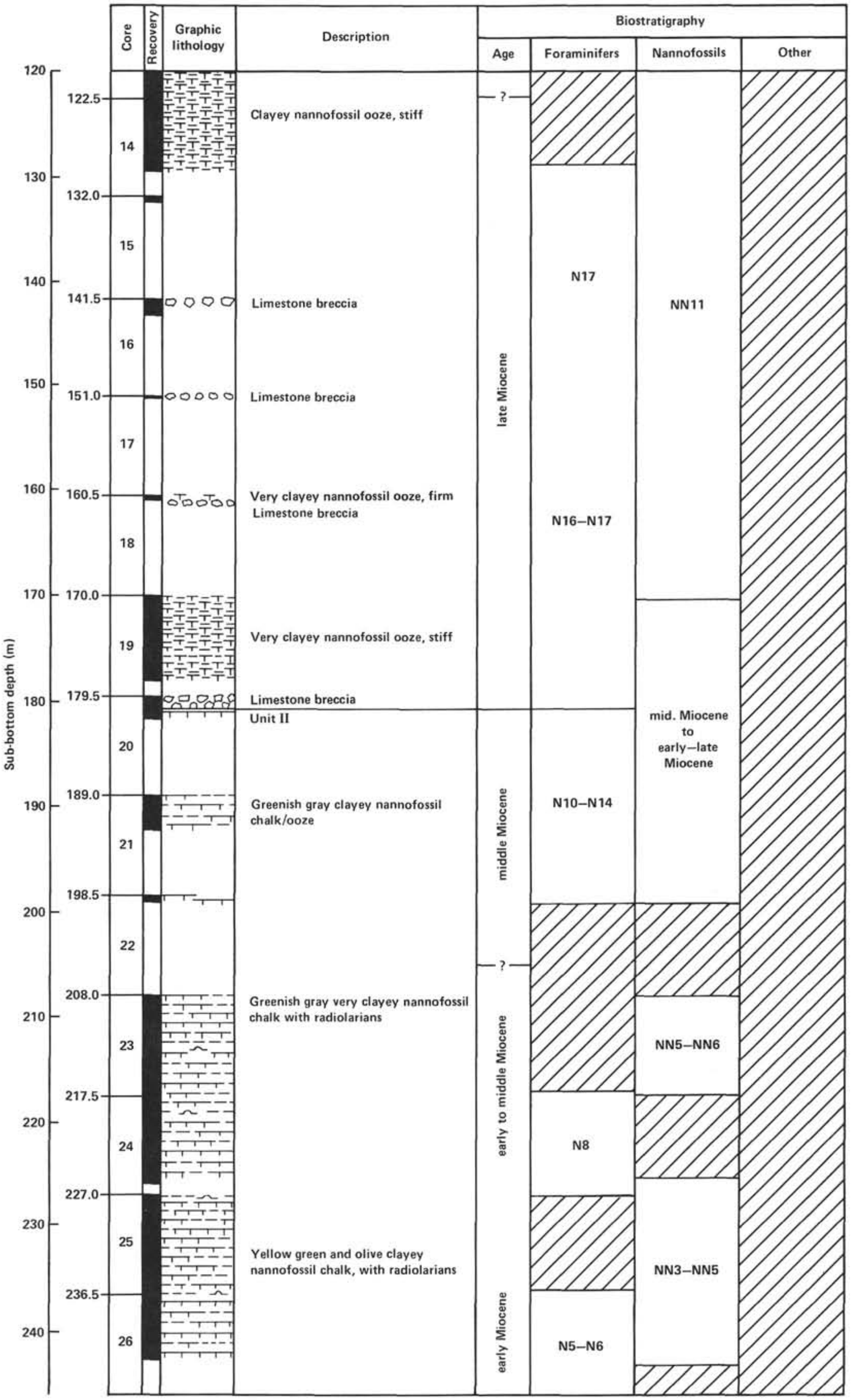

Figure 24. (Continued).

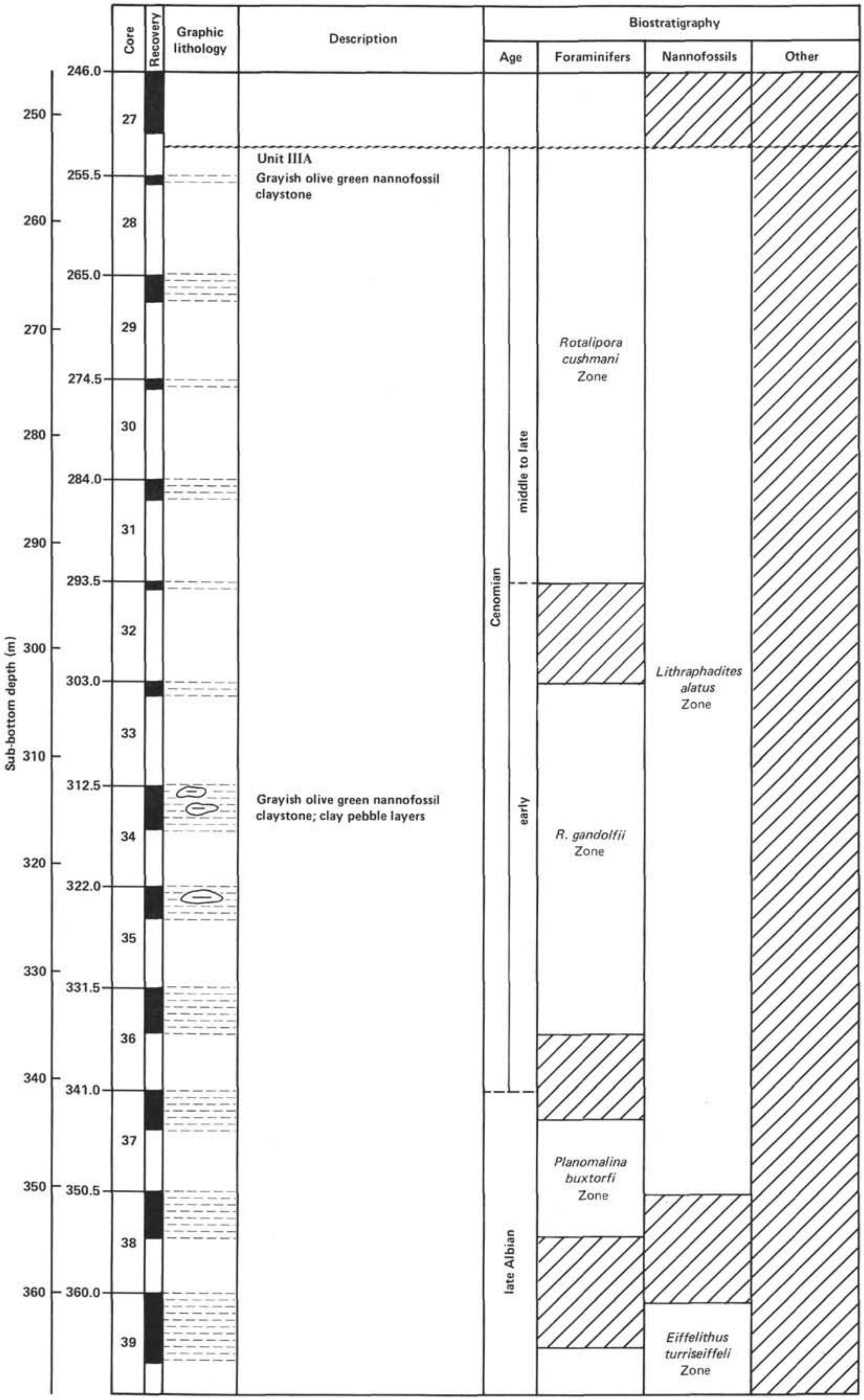

Figure 24. (Continued).

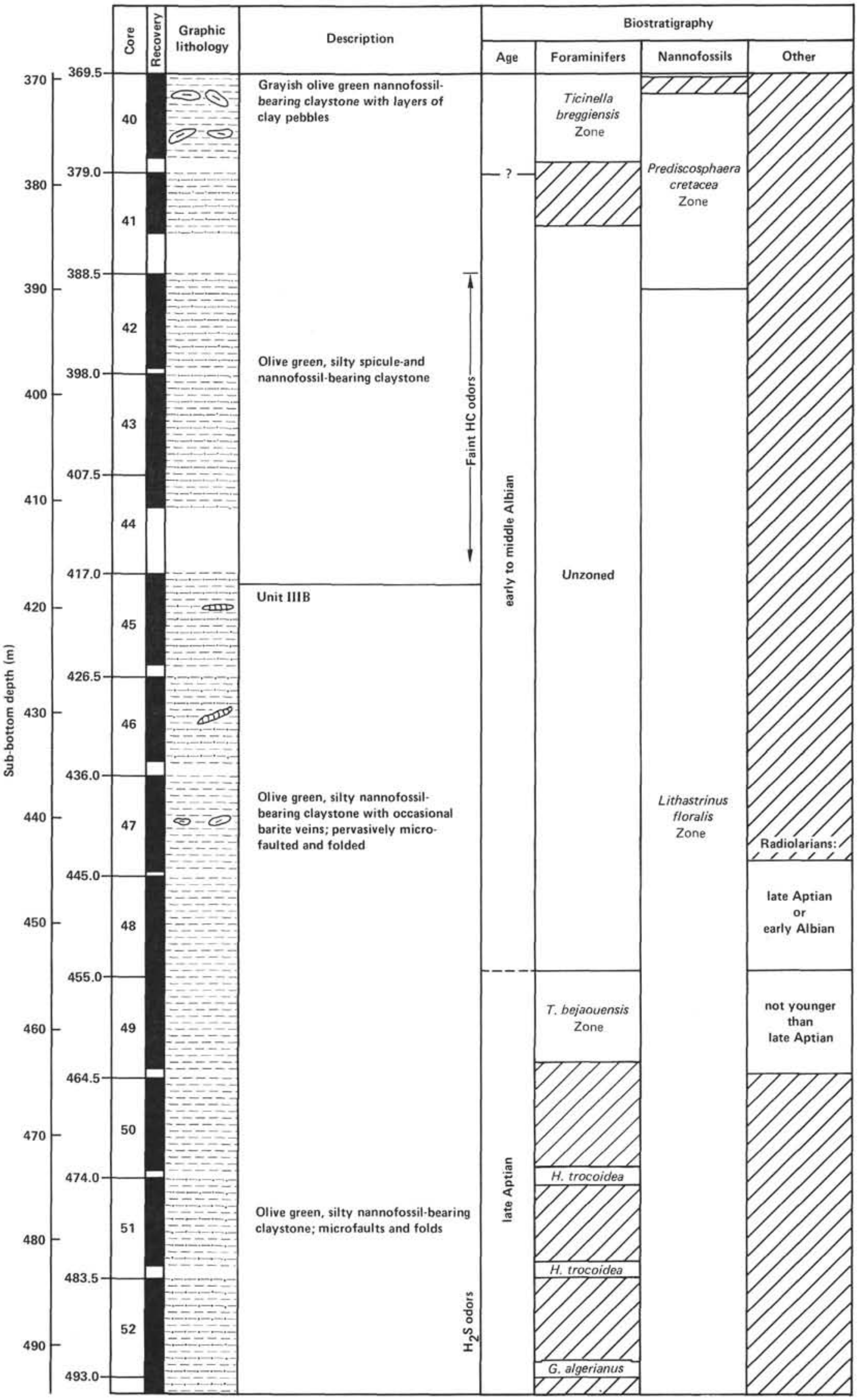

Figure 24. (Continued).

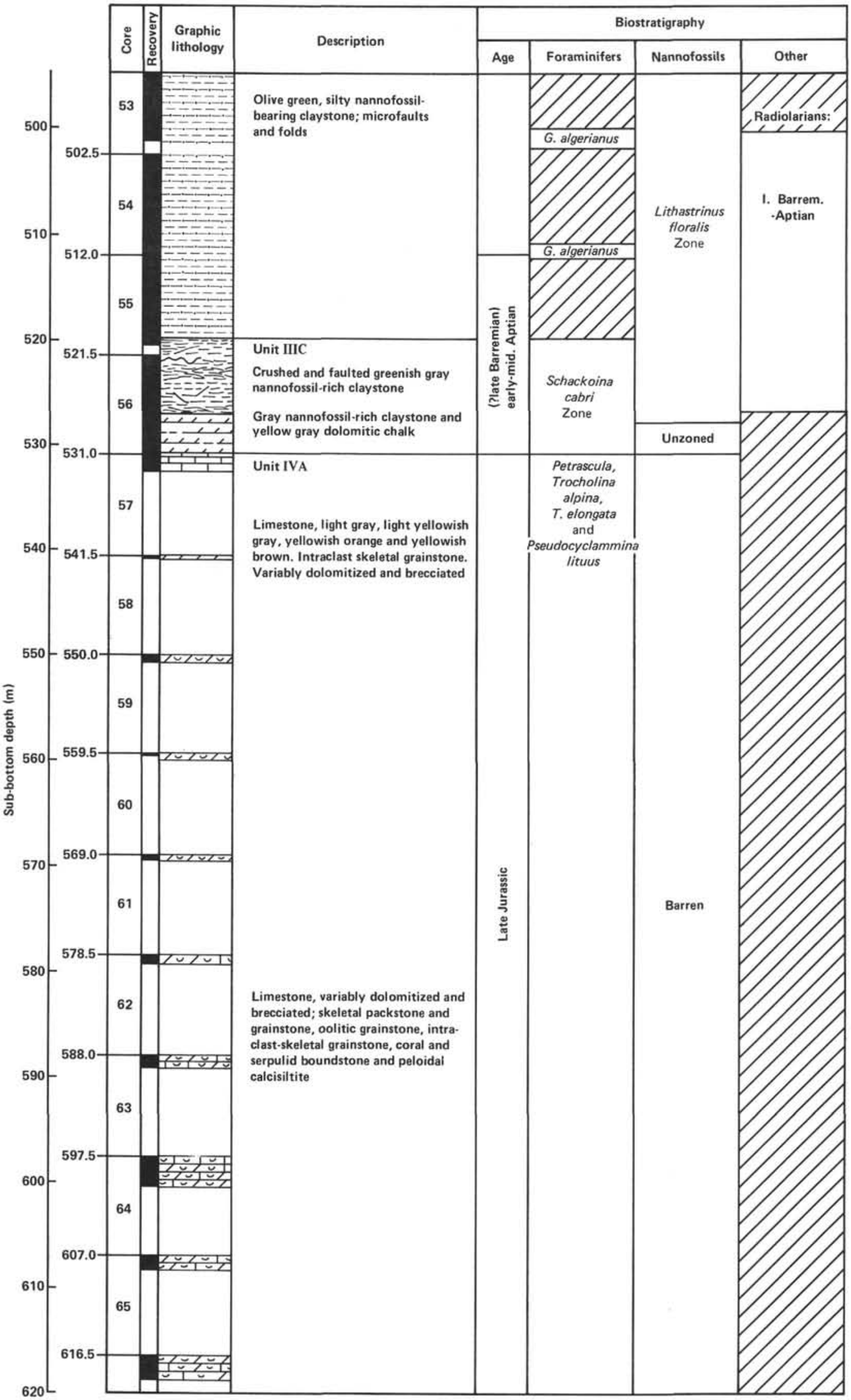

Figure 24. (Continued).

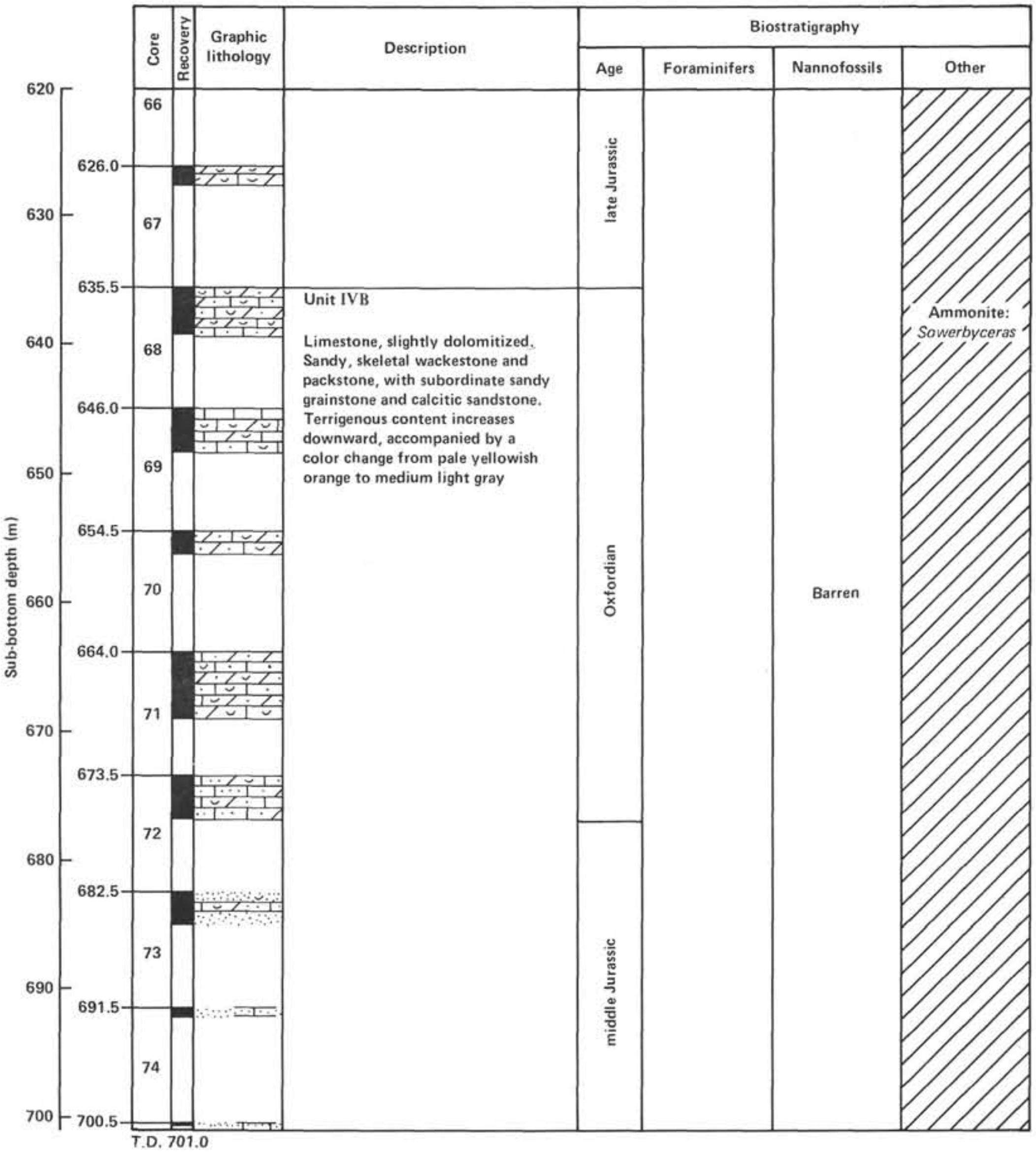

Unit IVB

Limestone, slightly dolomitized. Sandy, skeletal wackestone and packstone, with subordinate sandy grainstone and calcitic sandstone. Terrigenous content increases downward, accompanied by a color change from pale yellowish orange to medium light gray

Figure 24. (Continued).

SITE 545 HOLE CORE 1 CORED INTERVAL 0.0–8.5 m sub-bottom

TIME – ROCK UNIT | BIOSTRATIGRAPHIC ZONE | FOSSIL CHARACTER: FORAMINIFERS, NANNOFOSSILS, RADIOLARIANS, DIATOMS | SECTION | METERS | GRAPHIC LITHOLOGY | DRILLING DISTURBANCE | SEDIMENTARY STRUCTURES | SAMPLES | LITHOLOGIC DESCRIPTION

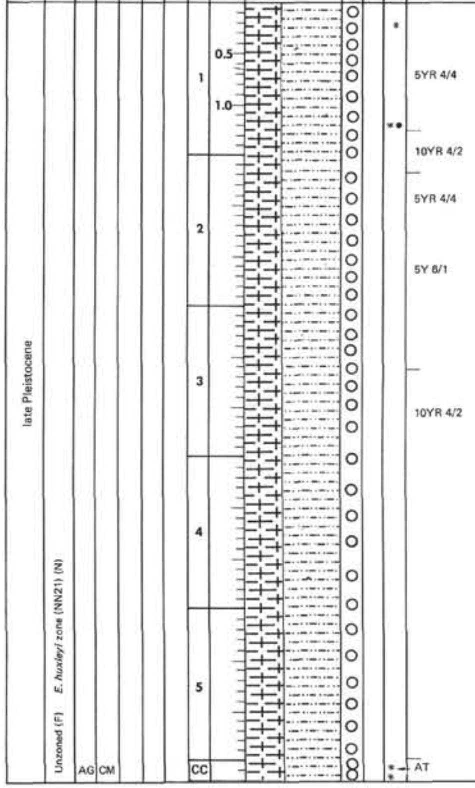

Soupy, dark yellowish brown (10YR 4/2) and light olive (5Y 6/1) FORAMINIFER-NANNOFOSSIL-RICH CLAY rich in silt and fine sand sized quartz, mica, and framoidal pyrite (often as burrow fillings.)

SMEAR SLIDE SUMMARY (%):

	1, 25	1, 120	CC	CC (AT)
	D	D	D	D
Texture:				
Sand	15	5	20	–
Silt	15	20	10	–
Clay	70	75	70	–
Composition:				
Quartz	5	3	3	50
Feldspar	–	–	–	Tr
Mica	1	3	1	30
Heavy minerals	–	–	–	Tr
Clay	15	15	10	–
Glauconite	–	–	–	Tr
Pyrite	1	2	Tr	2
Carbonate dolom.	Tr	2	Tr	–
Foraminifers	15	5	25	–
Calc. nannofossils	60	70	60	–
Sponge spicules	Tr	Tr	–	–
Plant debris	–	–	–	Tr
Tintinids	–	–	–	Tr

ORGANIC CARBON AND CARBONATE (%):

	1, 120–121
Carbonate	39.3

SITE 545 HOLE CORE 2 CORED INTERVAL 8.5–18.0 m sub-bottom

TIME – ROCK UNIT | BIOSTRATIGRAPHIC ZONE | FOSSIL CHARACTER: FORAMINIFERS, NANNOFOSSILS, RADIOLARIANS, DIATOMS | SECTION | METERS | GRAPHIC LITHOLOGY | DRILLING DISTURBANCE | SEDIMENTARY STRUCTURES | SAMPLES | LITHOLOGIC DESCRIPTION

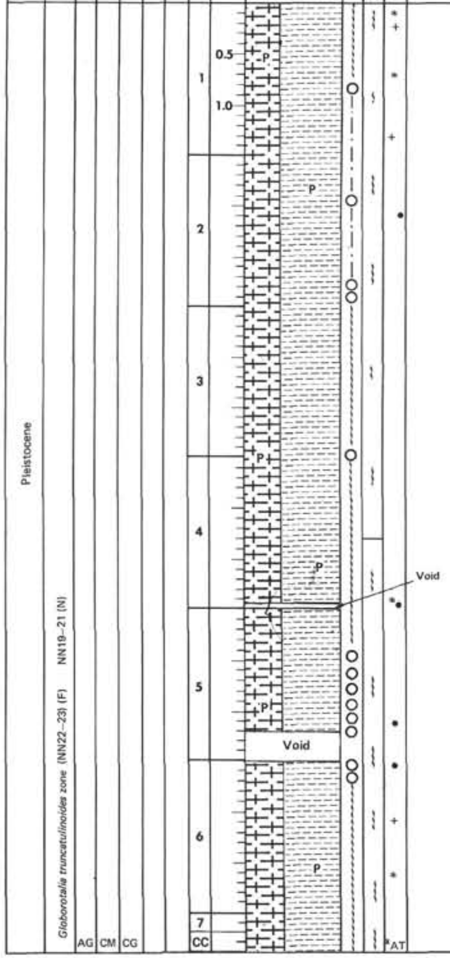

Section 1 through Section 4, 130 cm: mostly highly disturbed, pale brown (5YR 5/2) and pale yellowish brown (10YR 6/2) VERY FORAMINIFER-NANNOFOSSIL-RICH CLAY with 0.5–1 cm thick light olive gray (5Y 5/2).

Section 4, 130 cm through Section 6, 124 cm: grayish orange pink (5YR 7/2) to pale yellowish brown (10YR 6/2).

Section 6, 124–150 cm: light brown (5YR 6/4). Light olive gray (5Y 5/2) and dark gray (N3) pyritic burrow fills throughout.

SMEAR SLIDE SUMMARY (%):

	1, 10	1, 70	4, 140	6, 114	CC (AT)
	D	D	D	D	D
Texture:					
Sand	5	5	5	10	–
Silt	30	15	20	20	–
Clay	65	80	75	70	–
Composition:					
Quartz	10	5	5	5	60
Feldspar	–	Tr	–	–	–
Mica	Tr	3	2	3	30
Heavy minerals	–	–	–	–	Tr
Clay	20	20	10	20	–
Glauconite	–	–	–	–	Tr
Pyrite	Tr	Tr	1	1	Tr
Carbonate Dolom.	–	–	2	3	–
Foraminifers	–	10	5	15	–
Calc. nannofossils	60	60	75	60	–
Diatoms	–	–	–	–	Tr
Radiolarians	Tr	Tr	–	–	2
Sponge spicules	5	2	–	Tr	5
Plant debris	–	–	–	–	Tr

ORGANIC CARBON AND CARBONATE (%):

	2, 60–61	4, 144–150	5, 118–120	6, 0–2
Carbonate	41.3	50.8	47.0	38.8

SITE 545 HOLE CORE 3 CORED INTERVAL 18.0–27.5 m sub-bottom

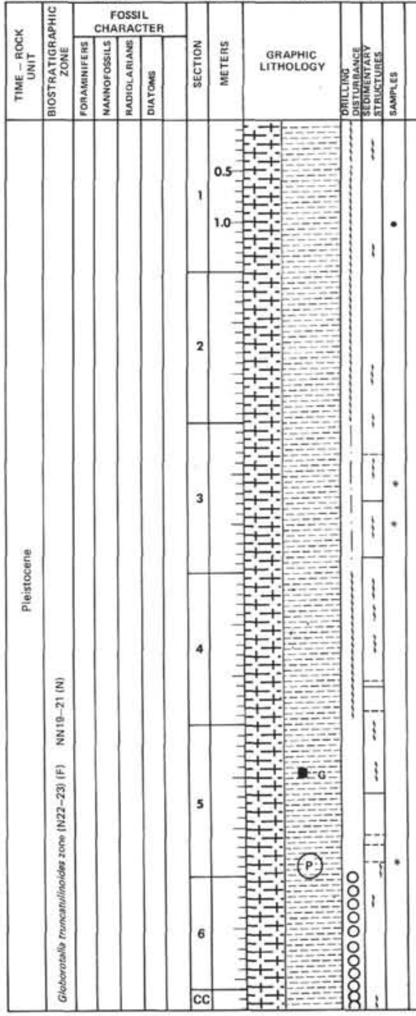

LITHOLOGIC DESCRIPTION

Mostly highly disturbed, dark yellowish brown (10YR 4/2) and pale yellowish brown (10YR 6/2) FORAMINIFER-NANNOFOSSIL-RICH CLAY. Light greenish gray (5G 8/1) and light olive gray (5Y 5/2) layers up to 1 cm thick occur at approximately 4 cm intervals between 1.5 and 4.5 m. Color interlayering of dark and pale yellowish brown on a 40–60 cm scale occurs below 3.0 m; contacts are both sharp and gradational.

SMEAR SLIDE SUMMARY (%):

	3, 60	3, 100	5, 133
	D	D	D
Texture:			
Sand	4	3	3
Silt	18	17	17
Clay	78	80	80
Composition:			
Quartz	2	3	2
Mica	Tr	1	Tr
Clay	63	61	62
Pyrite	Tr	Tr	Tr
Dolomite	1	1,5	1
Foraminifers	6	3	5
Calc. nannofossils	28	2.5	29

ORGANIC CARBON AND CARBONATE (%):

	1, 100–101
Carbonate	31.9

SITE 545 HOLE CORE 4 CORED INTERVAL 27.5–37.0 m sub-bottom

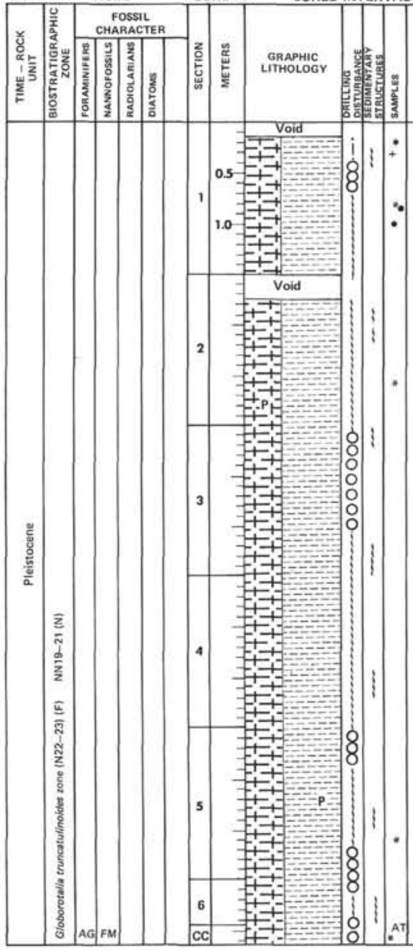

LITHOLOGIC DESCRIPTION

Highly disturbed to soupy, mostly pale yellowish brown (10YR 6/2) NANNOFOSSIL-RICH CLAY (Section 1) and FORAMINIFER-NANNOFOSSIL-RICH CLAY (Section 2–Core-Catcher).

SMEAR SLIDE SUMMARY (%):

	1, 20	1, 80	2, 100	5, 100	CC (AT)
	D	D	D	D	D
Texture:					
Sand	3	3	5	5	–
Silt	18	18	18	17	–
Clay	79	79	77	78	–
Composition:					
Quartz	2	1,5	1	1	60
Mica	1	Tr	Tr	Tr	20
Heavy minerals	–	–	–	–	Tr
Clay	57	49	56	56	–
Glauconite	–	–	–	–	Tr
Pyrite	Tr	Tr	–	Tr	Tr
Dolomite	2	2	1	1	–
Foraminifers	3	3	7	7	–
Calc. nannofossils	35	44	34	34	–
Radiolarians	–	–	–	–	Tr
Sponge spicules	–	–	–	–	1

ORGANIC CARBON AND CARBONATE (%):

	1, 85–86	1, 100–101
Carbonate	50.3	36.8

SITE 545 HOLE CORE 5 CORED INTERVAL 37.0–46.5 m sub-bottom

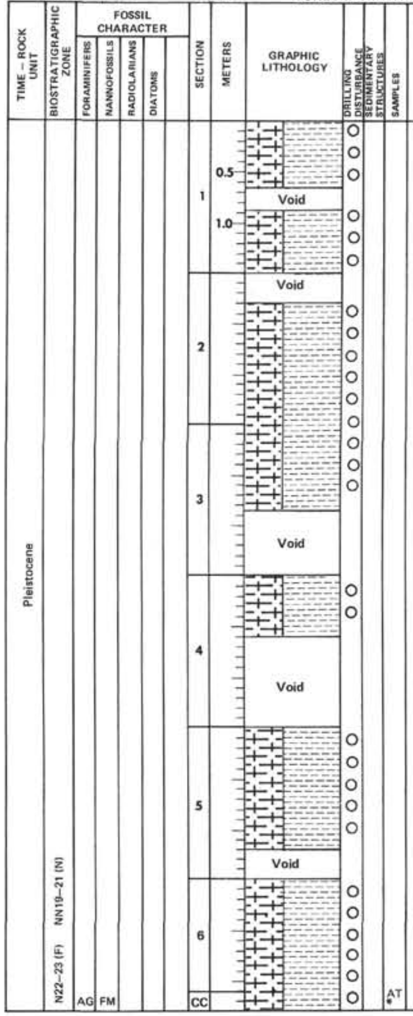

LITHOLOGIC DESCRIPTION

Soupy, dark yellowish brown (10YR 4/2) and pale yellowish brown (10YR 6/2) FORAMINIFER-NANNOFOSSIL-RICH CLAY.

SMEAR SLIDE SUMMARY (%):

	CC (AT)
	D
Composition:	
Quartz	50
Mica	30
Glauconite	Tr
Pyrite	10
Plant debris	3
Dinoflagellates	5

SITE 545 HOLE CORE 6 CORED INTERVAL 46.5–56.0 m sub-bottom

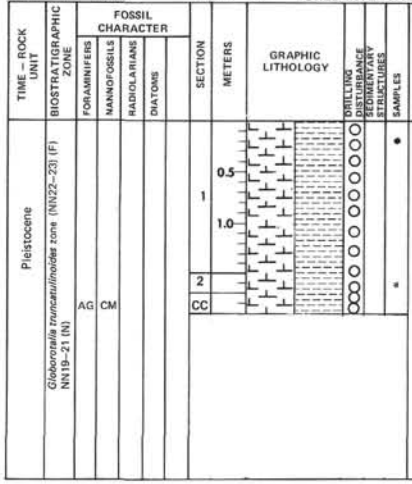

LITHOLOGIC DESCRIPTION

Soupy, pale brown (5YR 5/2) and dark yellowish brown (10YR 4/2) FORAMINIFER-NANNOFOSSIL-RICH CLAY with abundant pyrite and dolomite in fine sand and silt fraction.

SMEAR SLIDE SUMMARY (%):

	2, 10
	D
Texture:	
Sand	2
Silt	16
Clay	82
Composition:	
Quartz	1.5
Mica	Tr
Clay	56
Pyrite	Tr
Dolomite	1.5
Foraminifers	3
Calc. nannofossils	37

ORGANIC CARBON AND CARBONATE (%):

	1, 20–21
Carbonate	41.3

SITE 545 HOLE CORE 7 CORED INTERVAL 56.0–65.5 m sub-bottom

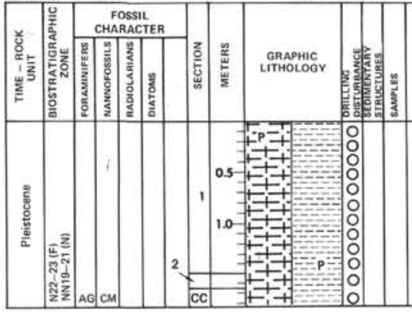

LITHOLOGIC DESCRIPTION

Soupy, pale brown (5YR 5/2) and dark yellowish brown (10YR 4/2) FORAMINIFER-NANNOFOSSIL-RICH CLAY with minor blebs of pyrite.

SITE 545 HOLE CORE 8 CORED INTERVAL 65.5–75.0 m sub-bottom

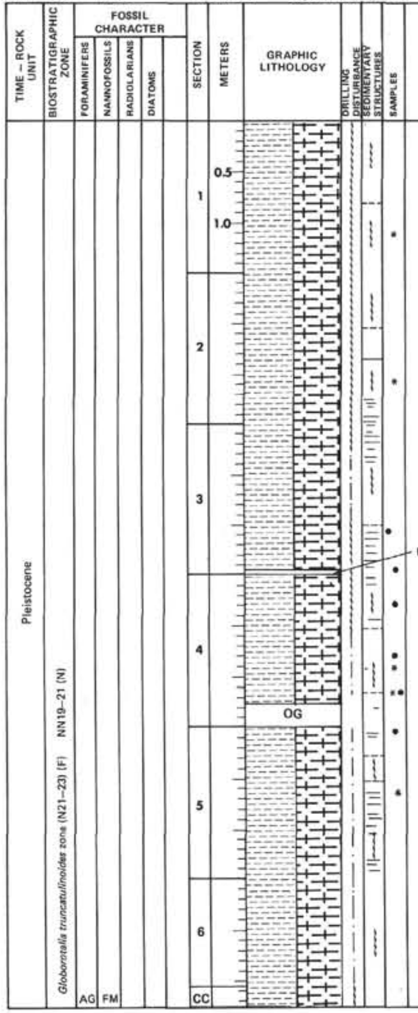

LITHOLOGIC DESCRIPTION

Moderately to highly deformed, pale yellowish brown (10YR 6/2) and light olive gray (5Y 5/2) VERY CLAYEY FORAMINIFERAL NANNOFOSSIL OOZE with regular light olive gray (5Y 5/2) interlayers of up to 1 cm thickness composing between 15 and 30% of the sediment.

SMEAR SLIDE SUMMARY (%):

	1, 110	2, 110	4, 90	4, 120	5, 60
	D	D	D	D	D
Texture:					
Sand	6	4	6	5	4
Silt	20	23	30	24	23
Clay	74	73	64	71	73
Composition:					
Quartz	1	1	1	1	1
Mica	Tr	Tr	–	–	–
Clay	50	48	40	46	44
Glauconite	–	Tr	–	Tr	–
Dolomite	–	Tr	1	Tr	1
Foraminifers	8	7	9	9	7
Calc. nannofossils	41	44	49	44	47
Iron oxides	–	Tr	–	–	Tr

ORGANIC CARBON AND CARBONATE (%):

	3, 110–111	3, 144–150	4, 30–32
Carbonate	52.6	45.0	57.0
	4, 79–80	4, 118–120	5, 0–2
Carbonate	59.0	66.0	47.9

SITE 545 HOLE CORE 9 CORED INTERVAL 75.0–84.5 sub-bottom

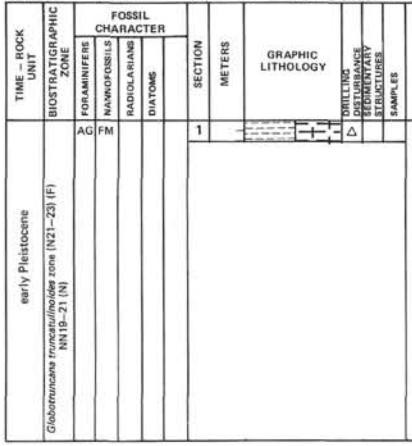

LITHOLOGIC DESCRIPTION

Slab (2 cm thick) of dark yellowish brown (10YR 4/2) VERY CLAYEY FORAMINIFERAL NANNOFOSSIL OOZE with a 1 cm thick pyrite nodule.

SITE 545 HOLE CORE 10 CORED INTERVAL 84.5–94.0 m sub-bottom

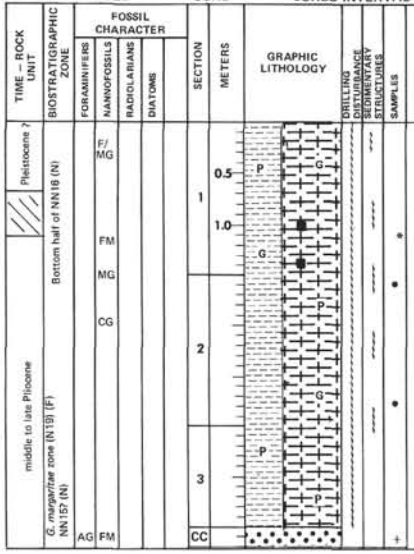

LITHOLOGIC DESCRIPTION

Highly disturbed, pale yellowish brown (10YR 6/2) VERY CLAYEY FORAMINIFERAL NANNOFOSSIL OOZE with occasional pyrite burrow fillings and dispersed glauconite throughout.

At Section 1, 106 and 143 cm pebble sized clasts of GLAUCONITE-BEARING SKELETAL WACKESTONE. Biostratigraphy: *Calpionella alpina*, *Tintinopsella* sp., *Crassiollaria* sp. to late Tithonian.

In Core-Catcher an 8 cm long clast of BIOCLAST PELOID GRAINSTONE with coral bioclasts (4x4 cm) bored by bivalves and encrusted foraminifers. Biostratigraphy: *Thaumatoporella parvovesiculifera*, *Protopeneoplis strata* to Late Jurassic(?).

SMEAR SLIDE SUMMARY (%):

	1, 108
	D
Composition:	
Glauconite	Tr
Dolomite	Tr
Carbonate unspec.	99
Calc. nannofossils	1

ORGANIC CARBON AND CARBONATE (%):

	2, 6–7	2, 120–121
Carbonate	66.0	61.7

SITE 545 HOLE CORE 11 CORED INTERVAL 94.0–103.5 m sub-bottom

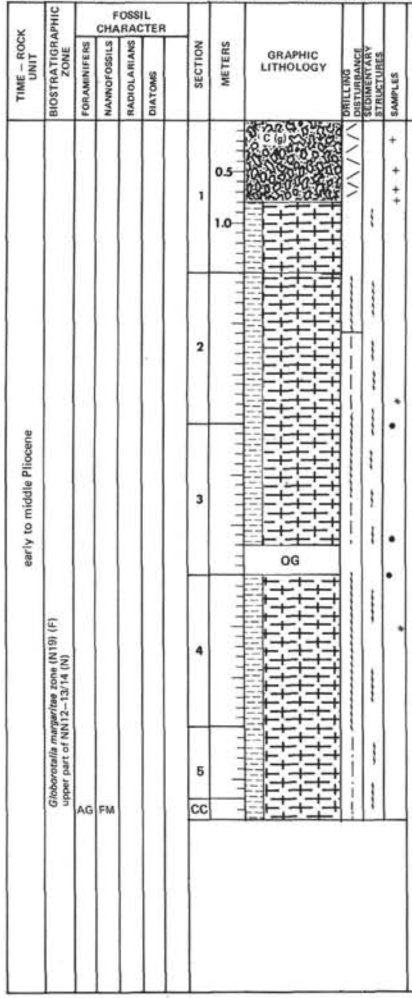

LITHOLOGIC DESCRIPTION

Section 1, 0–80 cm: highly fractured, 6–8 cm sized, light greenish gray (5GY 8/1) and blue white (5B 9/1) pebbles of SKELETAL GRAINSTONE with coral and bivalve bioclasts, glauconite, some pebbles show borings.

Section 2 through Core-Catcher: mostly highly disturbed, firm, pale yellowish brown (10YR 6/2) CLAYEY FORAMINIFERAL NANNOFOSSIL OOZE with 30% pinkish gray (5YR 8/1) color interlayers on a 1 cm scale, and occasional light olive gray (5Y 5/2) pyrite-rich layers.

Biostratigraphy of reworked limestone clasts: *Trocholina alpina* to Late Jurassic, early Cretaceous. *Calpionella alpina* to Tithonian-Berriasian.

SMEAR SLIDE SUMMARY (%):

	2, 127	4, 50
	D	D
Texture:		
Sand	4	6
Silt	36	35
Clay	60	59
Composition:		
Quartz	1	1.5
Mica	Tr	Tr
Clay	24	21
Dolomite	2	1
Foraminifers	7	10
Calc. nannofossils	66	66

THIN SECTION/PEEL SUMMARY (%):

	1, 46–50	1, 65–69
Texture:		
Rudite	30	–
Arenite	60	70
Silt	10	30
Composition:		
Micrite	5	25
Sparite	25	5
Intraclasts		
Oncoids		
Coated grains	45	70
Ooids		
Peloids		
Skeletal grains:		
Crinoids	Tr	Tr
Bivalves	10	Tr
Ammonites	Tr	–
Forams	Tr	Tr
Dasyclads	Tr	–
Tubiphytes	Tr	–
Siliceous sponges	15	–
Calpionellids	–	Tr
Beleninites	–	Tr
Structure:		
Vugs	Tr	–
Bioturbation	–	Tr

ORGANIC CARBON AND CARBONATE (%):

	3, 6–7	3, 117–120	4, 0–3
Carbonate	77.3	77.9	72.7

SITE 545 HOLE CORE 12 CORED INTERVAL 103.5–113.0 m sub-bottom

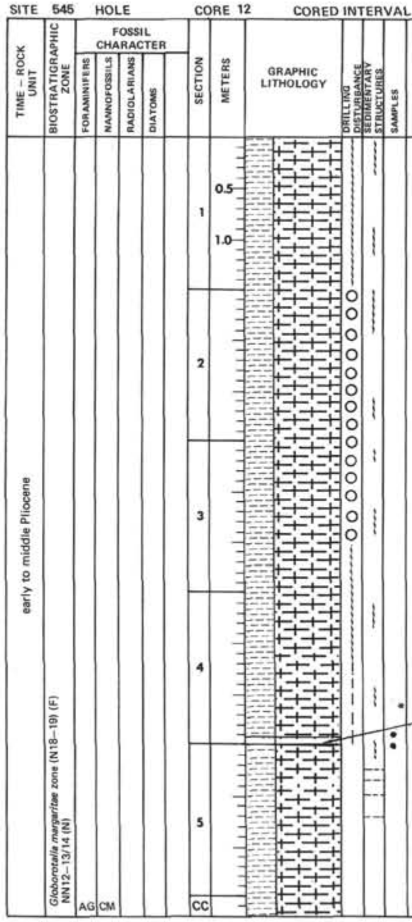

LITHOLOGIC DESCRIPTION

Partly strongly disturbed pale yellowish brown (10YR 6/2) CLAYEY FORAMINIFERAL NANNOFOSSIL OOZE with light olive gray (5Y 6/1) thin pyrite-rich layers and with pinkish gray (5YR 8/1) intervals.

SMEAR SLIDE SUMMARY (%):

	4, 110
	D
Texture:	
Sand	3
Silt	35
Clay	62
Composition:	
Foraminifers	10
Calc. nannofossils	75

ORGANIC CARBON AND CARBONATE (%):

	4, 144–150	5, 3–4
Carbonate	75.6	73.9

SITE 545 HOLE CORE 13 CORED INTERVAL 113.0–122.5 m sub-bottom

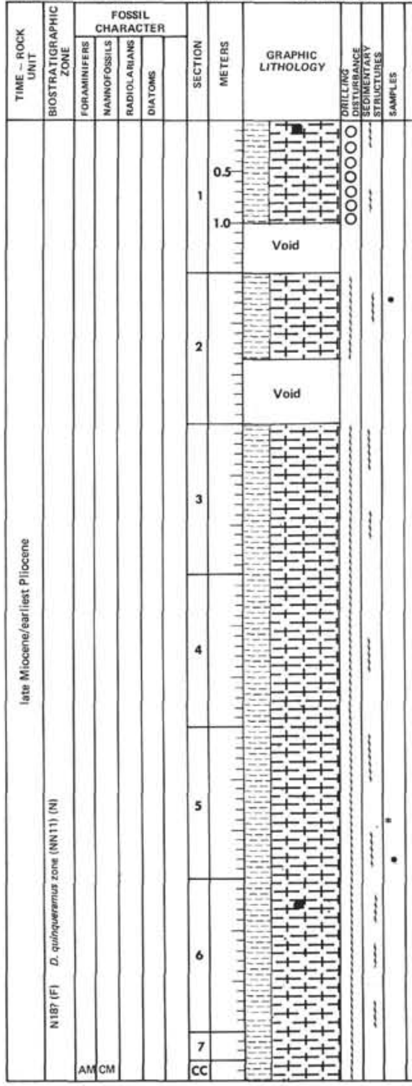

LITHOLOGIC DESCRIPTION

Highly disturbed, pale yellowish brown (10YR 6/2) and grayish orange pink (5YR 7/2) CLAYEY FORAMINIFERAL NANNOFOSSIL OOZE with occasional pyrite specks.

In Section 1, 13 and and Section 6, 30 cm pebble sized clasts of glauconite-bearing PELOID GRAINSTONE.

SMEAR SLIDE SUMMARY (%):

	5, 90
	D
Texture:	
Sand	2
Silt	33
Clay	65
Composition:	
Quartz	1
Clay	25
Dolomite	Tr
Foraminifers	6
Calc. nannofossils	67

ORGANIC CARBON AND CARBONATE (%):

	2, 25–26	5, 125–126
Carbonate	69.9	77.9

SITE 545 HOLE CORE 14 CORED INTERVAL 122.5–132.0 m sub-bottom

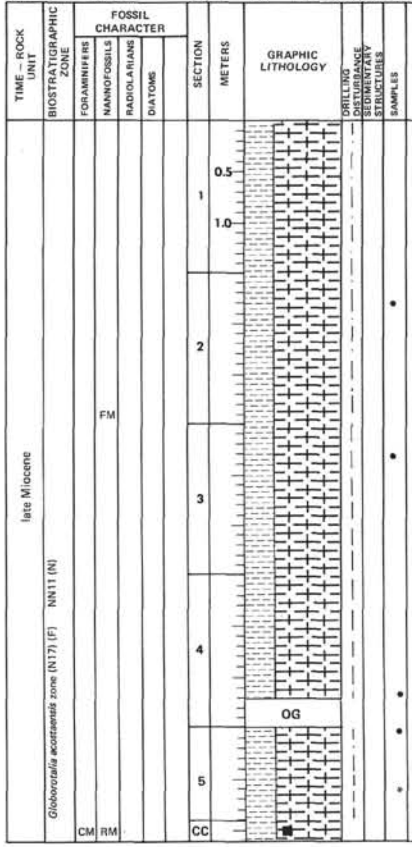

LITHOLOGIC DESCRIPTION

Moderately to slightly disturbed pinkish gray (5YR 8/1) and grayish orange pink (5YR 7/2) CLAYEY FORAMINIFERAL NANNOFOSSIL OOZE with occasional pyrite-rich laminae and burrow fillings.

In Core-Catcher pebble-sized fragment of PELOID GRAINSTONE.

SMEAR SLIDE SUMMARY (%):

	5, 60
	D
Texture:	
Sand	2
Silt	30
Clay	38
Composition:	
Quartz	1
Mica	Tr
Clay	25
Dolomite	1
Foraminifers	5
Calc. nannofossils	68

ORGANIC CARBON AND CARBONATE (%):

	2, 30–31	3, 30–31
Carbonate	70.4	68.4
	4, 118–120	5, 0–2
Carbonate	75.6	77.9

SITE 545 HOLE CORE 15 CORED INTERVAL 132.0–141.5 m sub-bottom

TIME – ROCK UNIT	BIOSTRATIGRAPHIC ZONE	FOSSIL CHARACTER: FORAMINIFERS	FOSSIL CHARACTER: NANNOFOSSILS	FOSSIL CHARACTER: RADIOLARIANS	FOSSIL CHARACTER: DIATOMS	SECTION	METERS
late Miocene	Reworked *Globotruncana* aff. *undulata* to Coniacian–Santonian *Globorotalia acostaensis* zone (N17) (F) *D. quinqueramus* zone (NN11) (N)	AG	FM			1	

GRAPHIC LITHOLOGY

DRILLING DISTURBANCE SEDIMENTARY STRUCTURES SAMPLES

+ + + + +

LITHOLOGIC DESCRIPTION

Section 1, 0–2 cm: pale yellowish brown (10YR 6/2) CLAYEY NANNOFOSSIL OOZE highly fractured, light colored to white pebbles of SKELETAL and PELOID WACKESTONES, PACKSTONES, and GRAINSTONES. The pebbles represent several shallow water facies including glauconite-bearing, bioturbated peloid grainstone with quartz; foraminiferal skeletal wackestones with *Tubiphytes* and coral fragments; well sorted oolitic grainstones.

Biostratigraphy of reworked limestone clasts: *Pseudocyclammina* sp. *lituolids, Salpingoporella* sp., *Trocholina* sp. *Thaumatoporella* sp., *Trocholina alpina, Trocholina elongata, Nahtiloculina* sp., *Cramicolasia* sp., *Caplonella* sp., *Tintinopsella* sp. Late Jurassic(?).

THIN SECTION/PEEL SUMMARY (%):

	1, 24–26	1, 39–42
Texture:		
Rudite	15	–
Arenite	85	40
Silt	–	60
Composition:		
Micrite	–	65
Sparite	40	–
Intraclasts	10	–
Oncoids Coated grains Ooids	10	15
Skeletal grains:		
Crinoids	10	5
Bivalves	15	Tr
Gastropods	Tr	Tr
Ammonites	Tr	–
Serpulids	Tr	–
Forams	Tr	Tr
Spiculae	–	3
Tubiphytes	10	10
Calpionellids	–	3
Reef builders:		
corals, sil. sponges	5	–

SITE 545 HOLE CORE 16 CORED INTERVAL 141.5–151.0 m sub-bottom

TIME – ROCK UNIT	BIOSTRATIGRAPHIC ZONE	FOSSIL CHARACTER: FORAMINIFERS	FOSSIL CHARACTER: NANNOFOSSILS	FOSSIL CHARACTER: RADIOLARIANS	FOSSIL CHARACTER: DIATOMS	SECTION	METERS
late Miocene	*Globorotalia acostaensis* zone (N17) (F) *D. quinqueramus* zone (NN11) (N)	FG	FM			1	0.5 1.0

GRAPHIC LITHOLOGY

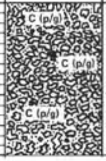

DRILLING DISTURBANCE SEDIMENTARY STRUCTURES SAMPLES

+ + + + +

LITHOLOGIC DESCRIPTION

Highly fractured coarse limestone breccia containing:

- greenish gray (5GY 6/1) to light greenish gray (5GY 8/1) LIMESTONE BRECCIA;
- yellowish gray (5Y 8/1) to white (N9) SKELETAL PACKSTONES GRAINSTONES with oncoids, echinoderms, corals, and gastropods;
- yellowish gray (5Y 8/1) dolosparite; and
- pale olive (10Y 6/2) and grayish olive (10Y 4/2) glauconitic grainstones.

Biostratigraphy of limestone clasts first generation: *Calp. alpina, Tintinopsella, Crassicollaria* sp. to Tithonian. Second generation: *globotruncana* cf. *bulloides* to Santonian to Maastrichtian.

THIN SECTION/PEEL SUMMARY (%):

	1, 6–9	1, 29–32	1, 70–74	1, 84–89
Texture:				
Rudite	100	–	100	–
Arenite	–	30	–	85
Silt	–	70	–	15
Composition:				
Micrite	Tr	55	–	15
Sparite	–	–	40	–
Intraclasts	100	–	10	Tr
Oncoids	–	–	–	15
Peloids	–	–	–	60
Skeletal grains:			–	
Crinoids	–	30	Tr	3
Bivalves	–	Tr	5	1
Gastropods	–	–	Tr	–
Brachipods	–	–	–	Tr
Serpulids	–	–	Tr	–
Forams	Tr	Tr	–	–
Tubiphytes	–	Tr	10	2
Sil. sponges		–	30	2
and corals	–	–	5	–
Bryozoans	–	–	–	2
Calpionellids	–	5	–	–
Structure:				
Porosity	–	10	–	–

SITE 545 HOLE CORE 17 CORED INTERVAL 151.0–160.5 m sub-bottom

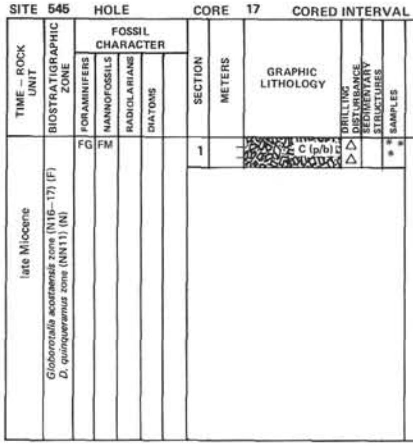

LITHOLOGIC DESCRIPTION

Drilling breccia of SKELETAL PACKSTONE to BOUNDSTONE as in Core 16, embedded in pale yellowish brown (10YR 6/2) VERY CLAYEY NANNOFOSSIL OOZE.

SMEAR SLIDE SUMMARY (%):

	1, 3	1, 5	1, 20
	M	D	D
Texture:			
Sand	6	2	3
Silt	33	30	16
Clay	61	68	81
Composition:			
Quartz	1.5	1.5	1
Mica	Tr	Tr	Tr
Clay	30	30	31
Dolomite	1	1	1
Foraminifers	10	3	3
Calc. nannofossils	57	64	64

SITE 545 HOLE CORE 18 CORED INTERVAL 160.5–170.0 m sub-bottom

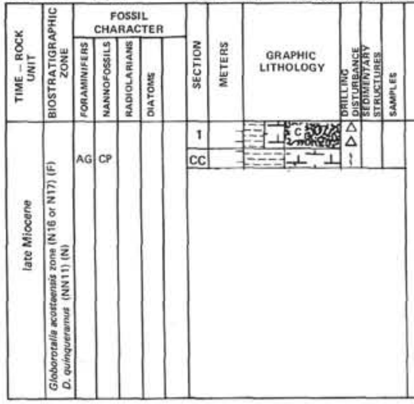

LITHOLOGIC DESCRIPTION

Section 1: drilling breccia of the facies seen in Core 15, embedded in pale yellowish brown (10YR 6/2) and light olive gray (5Y 6/1) VERY CLAYEY NANNOFOSSIL OOZE with minor greenish gray (5G 6/1) pyrite filled burrow tubes and glauconite.

Core-Catcher: highly disturbed VERY CLAYEY NANNOFOSSIL OOZE intermixed pale yellowish brown (10YR 6/2) and light olive gray (5Y 6/1).

SITE 545 HOLE CORE 19 CORED INTERVAL 170.0–179.5 m sub-bottom

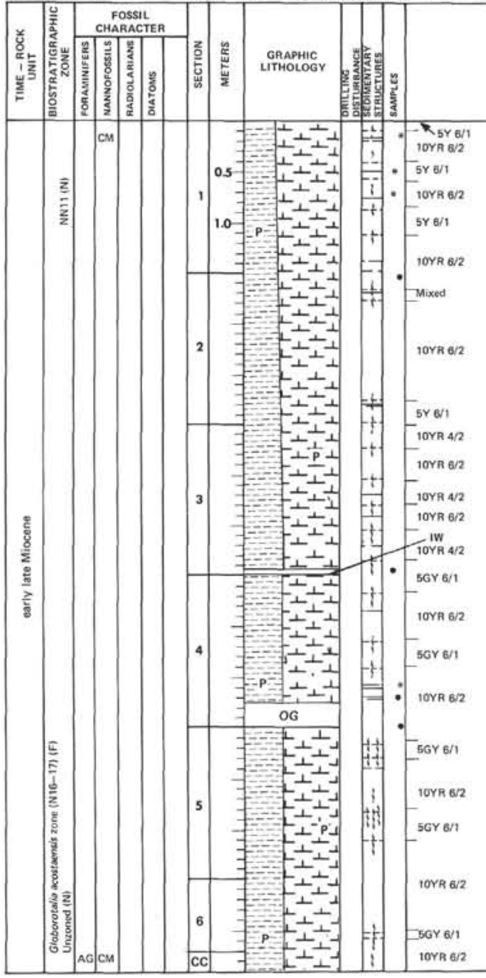

LITHOLOGIC DESCRIPTION

Undisturbed, very firm dark yellowish brown (10YR 4/2) and light olive gray (5Y 6/1) VERY CLAYEY NANNOFOSSIL OOZE in alternating intervals. Common greenish gray (5G 6/1) glauconitic laminae *and dark gray (N4) pyrite-rich burrow fillings and blebs throughout.*

Dusky brown (5YR 2/2) nannofossil-rich clay layers occur between Section 4, 105 and 120 cm. Three cm thick foraminifer-rich layers occur at Section 3, 47–50 cm and Section 6, 32–35 cm.

SMEAR SLIDE SUMMARY (%):

	1, 17	1, 50	1, 70	4, 109
	D	D	D	M
Texture:				
Sand	1	4	2	2
Silt	28	25	25	20
Clay	71	71	73	78
Composition:				
Quartz	1	1	1	5
Mica	Tr	Tr	Tr	1
Clay	37	37	37	50
Pyrite	Tr	–	–	–
Dolomite	1	1	2	3
Foraminifers	2	5	4	1
Calc. nannofossils	60	56	56	41

ORGANIC CARBON AND CARBONATE (%):

	2, 3–4	3, 144–150	4, 118–120	5, 0–2
Organic carbon	0.16	0.30	0.13	–
Carbonate	–	62.7	53.1	–
$CaCO_3$	62.0	–	–	55.1

SITE 545 HOLE CORE 20 CORED INTERVAL 179.5–189.0 m sub-bottom

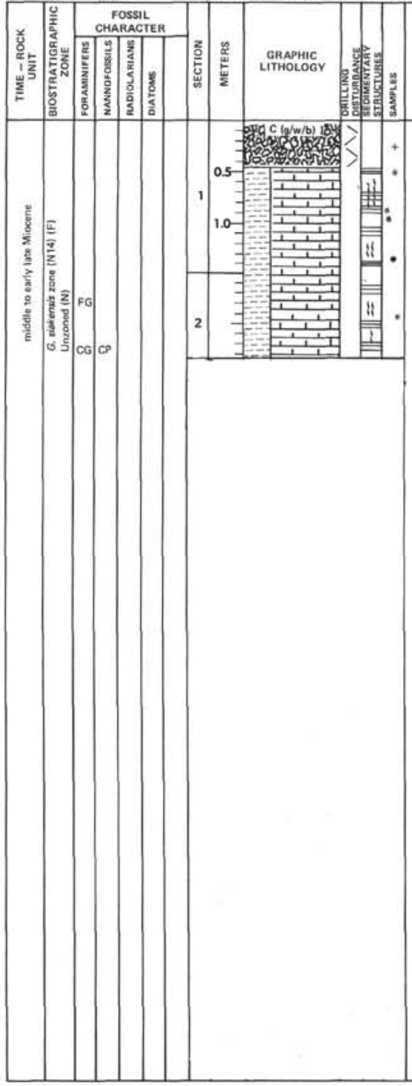

LITHOLOGIC DESCRIPTION

Section 1, 0–45 cm: highly fragmented LIMESTONE BRECCIA containing: GRAINSTONE with coral, calcified siliceous sponge and echinoderm debris; WACKESTONE with oncoids, forams and gastropods; BOUNDSTONE with calcified siliceous sponges, crusts, and skeletal debris.

Reworked fossils: hexactinellid sponges, Tybiphytes, *Calp. alpina*, *Cramicolasia* to Late Jurassic.

Section 1, 45 cm through Section 2, 82 cm: undisturbed, firm, (light) greenish gray (5GY 8/1–6/1) and light olive gray (5Y 5/2) CLAYEY NANNOFOSSIL CHALK with alternations at 10–20 cm intervals. Abundant pyrite and glauconite laminae.

At Section 1, 43, 83, and 98 cm – 1 cm thick layers of olive black (5Y 2/1) NANNOFOSSIL-RICH CLAYSTONE.

SMEAR SLIDE SUMMARY (%):

	1, 50 D	1, 80 M	1, 88 D	1, 99 M	2, 40 D
Texture:					
Silt	30	19	25	20	27
Clay	70	81	75	80	73
Composition:					
Quartz	Tr	2.5	1.5	2.5	0.5
Feldspar	–	Tr	–	–	–
Mica	–	1	0.8	Tr	–
Clay	25	51	26	51	24
Glauconite	–	1.5	Tr	2	–
Pyrite	–	–	Tr	Tr	Tr
Dolomite	0.5	1.5	1.5	1	0.5
Foraminifers	2	0.5	1	5	0.5
Calc. nannofossils	72	43	68	39	74
Diatoms	–	–	–	–	Tr
Radiolarians	–	–	0.5	–	0.5
Sponge spicules	–	–	1.0	–	0.5
Silicoflagellates	–	–	–	–	Tr

THIN SECTION/PEEL SUMMARY (%):

	1, 23–26
Texture:	
Rudite	20
Arenite	25
Silt	55
Composition:	
Micrite	45
Intraclasts	Tr
Oncoids	10
Peloids	Tr
Skeletal grains:	
Crinoids	5
Gastropods	Tr
Brachipods	Tr
Serpulids	Tr
Forams	Tr
Tubiphytes	5
Sil. sponges	20
Calpionellids	Tr
Bioturbation	Tr
Structure:	
Porosity	15

ORGANIC CARBON AND CARBONATE (%):

	1, 130–131
Organic carbon	0.78
Carbonate	70.8

SITE 545 HOLE CORE 21 CORED INTERVAL 189.0–198.5 m sub-bottom

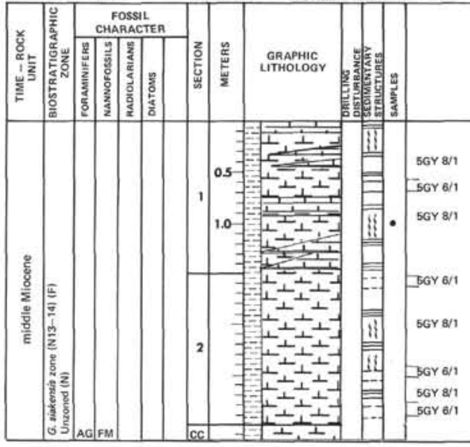

LITHOLOGIC DESCRIPTION

Undisturbed, light greenish gray (5GY 8/1) and greenish gray (5GY 6/1) CLAYEY NANNOFOSSIL OOZE and CHALK with traces of original sedimentary lamination in places, but mostly destroyed by bioturbation which is picked out in shades of greenish gray.

ORGANIC CARBON AND CARBONATE (%):

	1, 100–101
Carbonate	79.3

SITE 545 HOLE CORE 22 CORED INTERVAL 198.5–208.0 m sub-bottom

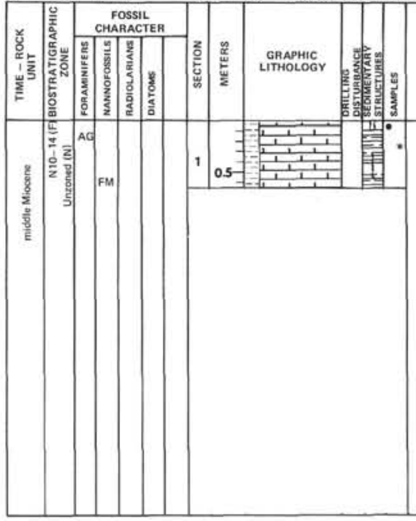

LITHOLOGIC DESCRIPTION

Undisturbed, light greenish gray (5GY 8/1) and greenish gray (5GY 6/1) CLAYEY NANNOFOSSIL CHALK with abundant siliceous microfossils: sponge spicules, radiolarians, silicoflagellates, and with pyrite and glauconite. Well laminated.

SMEAR SLIDE SUMMARY (%):

	1, 24 D
Texture:	
Sand	10
Silt	5
Clay	85
Composition:	
Quartz	Tr
Mica	Tr?
Clay	10
Glauconite	Tr
Pyrite	Tr
Foraminifers	10
Calc. nannofossils	80

ORGANIC CARBON AND CARBONATE (%):

	1, 5–6
Carbonate	80.8

SITE 545 HOLE CORE 23 CORED INTERVAL 208.0–217.5 m sub-bottom

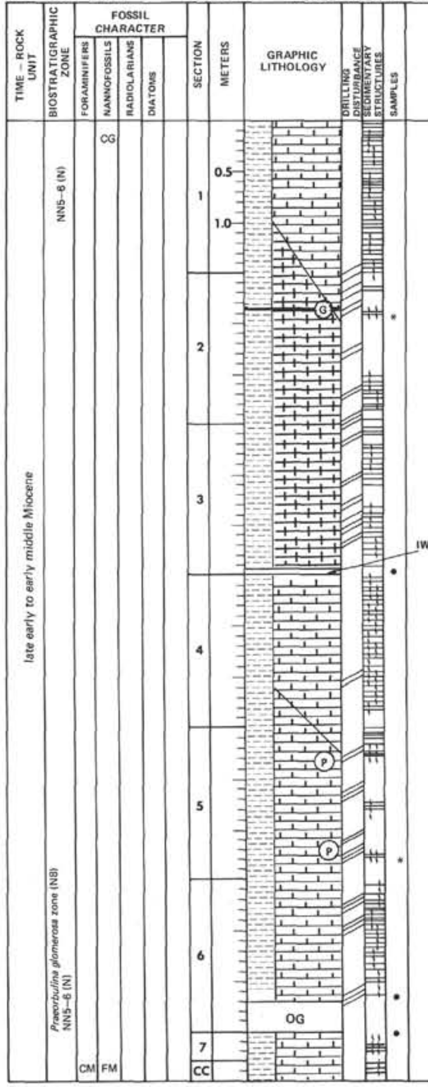

LITHOLOGIC DESCRIPTION

Slightly fractured, greenish gray (5GY 6/1) and light greenish gray (5GY 8/1) VERY CLAYEY NANNOFOSSIL CHALK and VERY CLAYEY FORAMINIFERAL NANNOFOSSIL CHALK. Thin lamination throughout. Burrows throughout filled with olive gray (5Y 4/1) and dark gray (N4) pyrite-rich sediment.

At Section 2, 40–46 cm concentration of sand-sized glauconite *in situ*.

At Section 5, 118–125 cm and Section 6, 24–41 cm dusky yellowish brown (10YR 2/2) FORAMINIFER-NANNOFOSSIL-RICH CLAYSTONE.

SMEAR SLIDE SUMMARY (%):

	2, 45 D	5, 130 M
Texture:		
Sand	15	10
Silt	35	20
Clay	50	70
Composition:		
Quartz	2	5
Mica	2	2
Clay	20	50
Glauconite	Tr	–
Pyrite	Tr	5
Micronodules	5	–
Dolomite	1	2
Foraminifers	20	5
Calc. nannofossils	50	30

ORGANIC CARBON AND CARBONATE (%):

	3, 144–150	6, 117–120	7, 0–3
Carbonate	–	–	66.0
$CaCO_3$	67.9	62.7	–

SITE 545 HOLE CORE 24 CORED INTERVAL 217.5–227.0 m sub-bottom

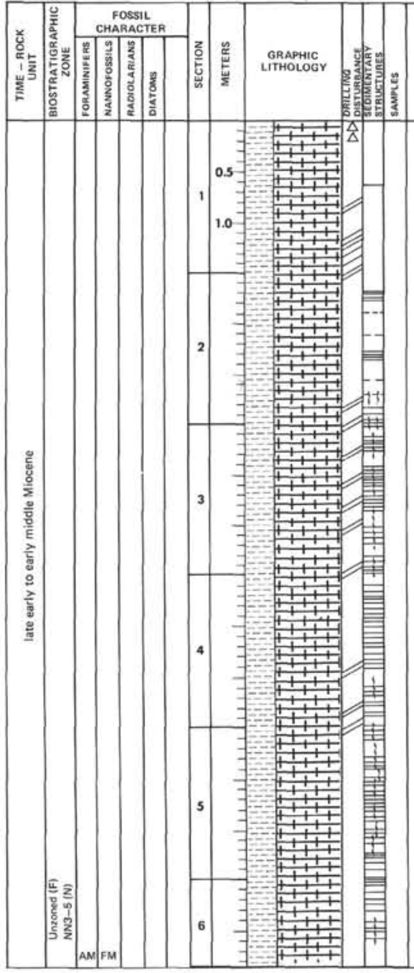

LITHOLOGIC DESCRIPTION

Slightly fractured, greenish gray (5Y 6/1) and olive gray (5Y 4/1) CLAYEY FORAMINIFERAL NANNOFOSSIL CHALK. Extensively bioturbated with olive gray (5Y 4/1), also pyritic burrows. Olive gray (5Y 4/1) intervals at Section 1, 25–63 cm and Section 6, 37–45 cm preserve traces of sedimentary lamination. Sand-sized glauconite common, especially in layers between Section 4, 120–135 cm.

SITE 545 HOLE CORE 25 CORED INTERVAL 227.0–236.5 m sub-bottom

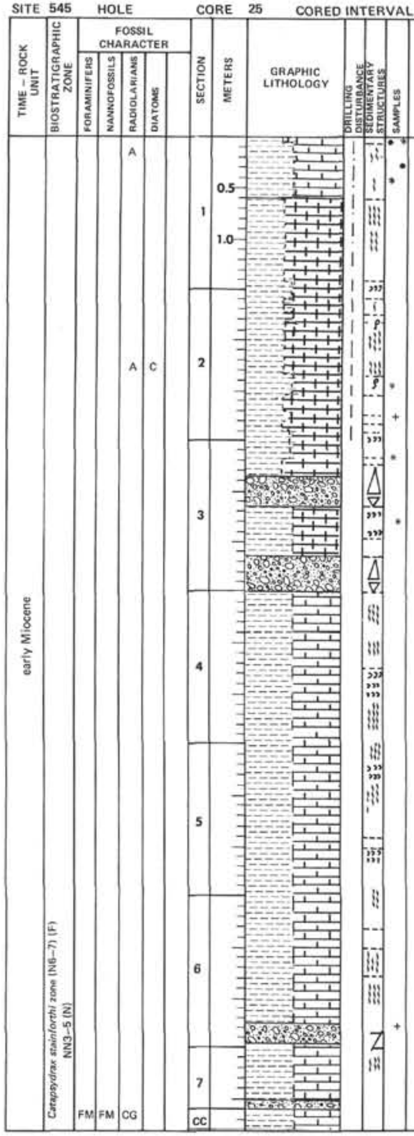

LITHOLOGIC DESCRIPTION

Section 1, 0–7 cm: pale green (10G 6/2) VERY CLAYEY NANNOFOSSIL CHALK.

Section 1, 7–60 cm: dusky yellow green (5GY 5/2) SLIGHTLY SILICEOUS VERY CLAYEY NANNOFOSSIL CHALK. Softer and more clayey than above, with bioturbation picked out in pale olive (10Y 6/2).

Section 1, 60 cm–Section 3, 36 cm and 63–115 cm: mostly light greenish gray (5G 8/1) SLIGHTLY SILICEOUS VERY CLAYEY FORAMINIFERAL NANNOFOSSIL CHALK with 10–30 cm layers of dusky yellow green (5GY 5/2) softer, more clayey sediment and two layers of moderate olive brown color (5Y 4/4), which contain sand-sized glauconite (Section 3, 0–17 cm and 63–115 cm.

Section 4, 0 cm–Core-Catcher: mostly pale green (5G 7/2) SLIGHTLY SILICEOUS VERY CLAYEY NANNOFOSSIL CHALK with moderate olive brown (5Y 4/4) bioturbation; slightly softer and dusky yellow green (5GY 5/2) below Section 5 with pale olive bioturbation. Light greenish gray (5G 8/1) layers rich in glauconite occur throughout.

Section 3, 36–61 cm, 115–150 cm, and Section 6, 126–141 cm: CONGLOMERATE – texturally a clayey conglomerate with clast support. Phenoplasts up to 5 cm in diameter of grayish yellow green (5GY 7/2) and moderate olive brown (5Y 4/4) penecontemporaneous sediment plus small pebble to sand-sized glauconite in moderate olive brown (5Y 4/4) slightly siliceous very clayey foraminiferal-nannofossil chalk. Base of units not sharp and maximum clast size occurs about 8–10 cm above base of unit.

Section 6, 128–141 cm: 30° dipping, 2 cm broad zone of normal faults with slight rotational element (beds above faults for 2 m dip at up to 15°).

SMEAR SLIDE SUMMARY (%):

	1, 2 D	1, 40 D	2, 94 D	3, 15 D	3, 80 D
Texture:					
Sand	2	5	7	10	6
Silt	25	22	22	22	25
Clay	73	73	71	71	69
Composition:					
Quartz	1	1	1	1	0.5
Mica	–	Tr	Tr	–	–
Clay	32	42	40	38	33
Glauconite	–	0.5	1	5	0.5
Dolomite	0.8	0.5	Tr	Tr	Tr
Foraminifers	5	3	7	10	10
Calc. nannofossils	59	48	45	43	52
Diatoms	–	Tr	Tr	–	–
Radiolarians	0.5	3	4	2.5	2
Sponge spicules	1.0	1.5	2	1	0.7
Fish remains	–	–	–	Tr	Tr

ORGANIC CARBON AND CARBONATE (%):

	1, 4–5	1, 30–31
Carbonate	65.0	51.6

SITE 545 HOLE CORE 26 CORED INTERVAL 236.5–246.0 m sub-bottom

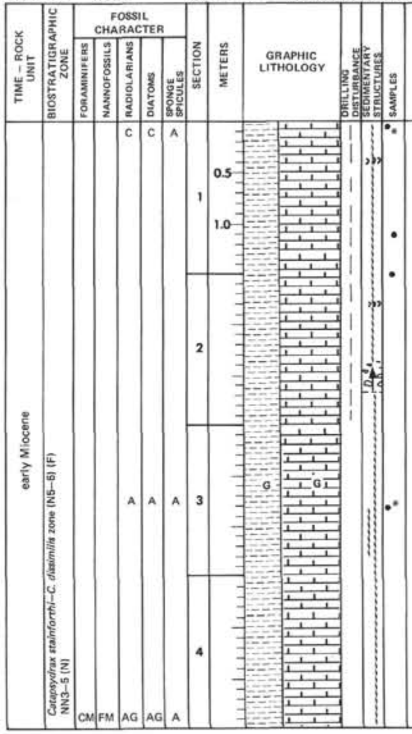

LITHOLOGIC DESCRIPTION

Slightly disturbed to undisturbed dusky yellowish green (5GY 5/2) and pale olive (10Y 6/2) SILICEOUS VERY CLAYEY NANNOFOSSIL CHALK with common burrows: chondrites often cutting other larger planolites, occasional zoophycus.

In Section 2, 95–114 cm plastically deformed intraformational pebbles with glauconite pebbles and sand.

Radiolarians and sponge spicules abundant throughout.

SMEAR SLIDE SUMMARY (%):

	1, 10 D	3, 80 D
Texture:		
Sand	6	7
Silt	24	20
Clay	70	73
Composition:		
Quartz	1	1.5
Clay	37	44
Glauconite	0.5	0.5
Pyrite	–	Tr
Dolomite	0.5	Tr
Foraminifers	4	3
Calc. nannofossils	50	44
Diatoms	1	1
Radiolarians	3	5
Sponge spicules	1.3	1.5
Fish remains	Tr	Tr

ORGANIC CARBON AND CARBONATE (%):

	1, 6–7	1, 118–120	2, 0–2	3, 80–81
Organic carbon	–	0.57	0.67	–
Carbonate	55.1	51.2	46.0	47.2

SITE 545 HOLE CORE 27 CORED INTERVAL 246.0–255.5 m sub-bottom

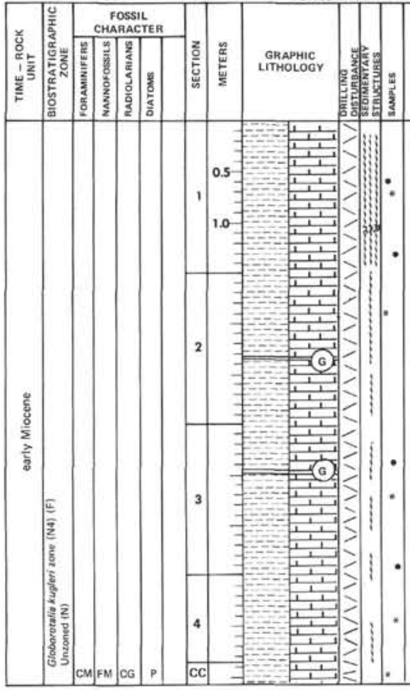

LITHOLOGIC DESCRIPTION

Heavily fractured due to swell of ocean to 2–7 cm long pieces, which are fused together along downwards concave clay seams.

Pale olive (10Y 6/2) and moderate olive green (5Y 4/4) and dusky yellowish green (5GY 5/2) SLIGHTLY SILICEOUS VERY CLAYEY NANNOFOSSIL CHALK, with heavy bioturbation especially in Section 1. Burrows are filled with darker to black pyrite and/or glauconite rich sediment. Glauconitic sands in Section 2, 81–86 cm and Section 3, 45 cm.

SMEAR SLIDE SUMMARY (%):

	1, 75	2, 40	3, 75	4, 44
	D	D	D	D
Texture:				
Sand	5	4	1	3
Silt	20	20	15	18
Clay	75	76	84	79
Composition:				
Quartz	1	1.5	1	1.5
Mica	Tr	Tr	Tr	Tr
Clay	49	50	54	54
Glauconite	Tr	0.8	–	0.5
Dolomite	0.5	0.7	1	0.8
Foraminifers	3	3.5	1	3
Calc. nannofossils	41	39	41	38
Diatoms	Tr	–	–	Tr
Radiolarians	3	3	0.5	1.5
Sponge spicules	2	1.5	1.0	0.4
Silicoflagellates	Tr	–	–	–
Fish remains	Tr	Tr	–	Tr
Plant debris	–	–	–	Tr

ORGANIC CARBON AND CARBONATE (%):

	1, 65–66	1, 130–131	3, 43–44	3, 144–150
Organic carbon	–	–	–	0.59
Carbonate	44.7	40.8	32.9	44.1

SITE 545 HOLE CORE 28 CORED INTERVAL 256.5–265.0 m sub-bottom

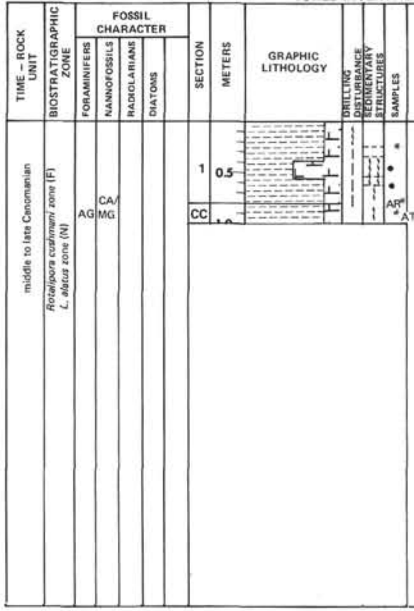

LITHOLOGIC DESCRIPTION

Section 1, 0–34 and 57–82 cm and Core-Catcher: slightly disturbed, grayish olive green (5GY 3/2) and grayish olive (10Y 4/2) NANNOFOSSIL CLAYSTONE.

Section 1, 34–57 cm: slightly disturbed, grayish-olive (10Y 4/2) and greenish gray (5GY 6/1) FORAMINIFER-NANNOFOSSIL-RICH CLAYSTONE with thin color laminae.

SMEAR SLIDE SUMMARY (%):

	1, 25	CC (AT)	CC (AR)
	D	D	D
Texture:			
Sand	1	–	–
Silt	7	–	–
Clay	92	–	–
Composition:			
Quartz	Tr	70	Tr
Mica	–	Tr	Tr
Heavy minerals	–	Tr	–
Clay	79	–	–
Glauconite	–	10	Tr
Pyrite	–	10	Tr
Dolomite	3	–	–
Foraminifers	2.5	–	99
Calc. nannofossils	14.5	–	–
Sponge spicules	0.5	–	–
Fish remains	–	–	Tr
Plant debris	–	10	–

ORGANIC CARBON AND CARBONATE (%):

	1, 47–48	1, 65–66
Carbonate	47.7	16.6

SITE 545 HOLE CORE 29 CORED INTERVAL 265.0–274.5 m sub-bottom

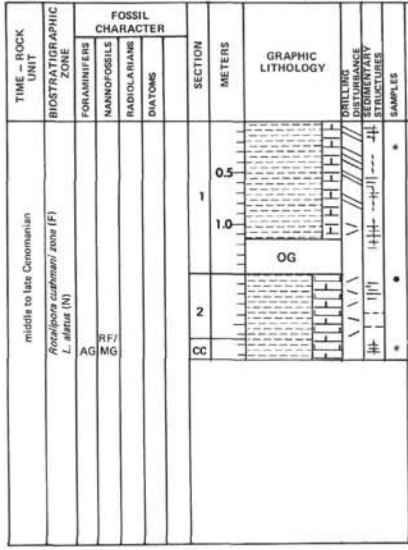

LITHOLOGIC DESCRIPTION

Slightly fractured, grayish olive green (5GY 3/2) and grayish green (10GY 5/2) NANNOFOSSIL CLAYSTONE with fine laminae at mm scale.

(Similar drilling disturbance as in Core 27.)

SMEAR SLIDE SUMMARY (%):

	1, 25	CC
	D	D
Texture:		
Sand	0	3
Silt	14	14
Clay	86	83
Composition:		
Quartz	0.5	0.7
Clay	74	73
Glauconite	–	Tr
Dolomite	2.5	2
Foraminifers	0.8	3
Calc. nannofossils	21.7	20
Radiolarians	Tr	–
Sponge spicules	0.5	0.6
Plant debris	–	0.5

ORGANIC CARBON AND CARBONATE (%):

	1, 3–4	1, 118–120	2, 0–2
Organic carbon	–	1.30	1.01
Carbonate	17.1	28.8	33.6

SITE 545 HOLE CORE 30 CORED INTERVAL 274.5–284.0 m sub-bottom

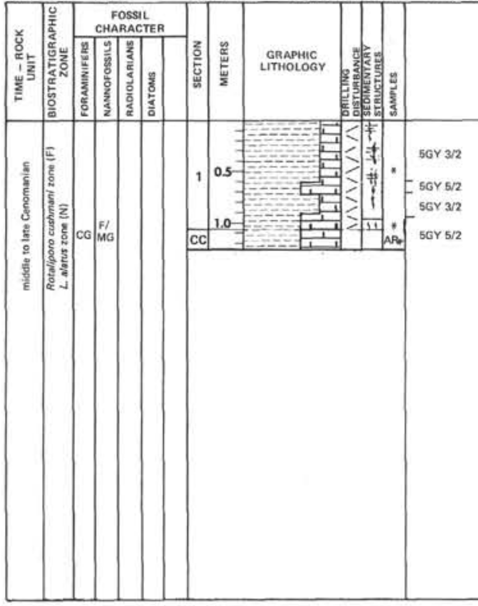

LITHOLOGIC DESCRIPTION

Fused drilling cakes of 2 cm thickness of grayish olive green (5GY 3/2) and dusky yellowish green (5GY 5/2) firm NANNOFOSSIL CLAYSTONE to NANNOFOSSIL-RICH CLAYSTONE with thin olive black wispy laminae <1 mm throughout. Stretched burrows in 93–103 cm. Pyrite common.

SMEAR SLIDE SUMMARY (%):

	1, 50	1, 100	CC (AR)
	D	D	D
Texture:			
Sand	2	3	–
Silt	11	19	–
Clay	87	78	–
Composition:			
Quartz	0.7	0.5	2
Feldspar	–	Tr	–
Mica	Tr	–	Tr
Heavy minerals	–	–	Tr
Clay	70	58	–
Pyrite	–	–	Tr
Micronodules	–	–	Tr
Dolomite	1.0	3	–
Carbonate unspec.	–	–	3
Foraminifers	0.7	1	96
Calc. nannofossils	16.3	36	–
Radiolarians	–	Tr	–
Sponge spicules	0.8	0.7	–
Fish remains	–	–	Tr

ORGANIC CARBON AND CARBONATE (%):

	1, 55–56	1, 65–66
Carbonate	18.0	44.7

SITE 545 HOLE CORE 31 CORED INTERVAL 284.0–293.5 m sub-bottom

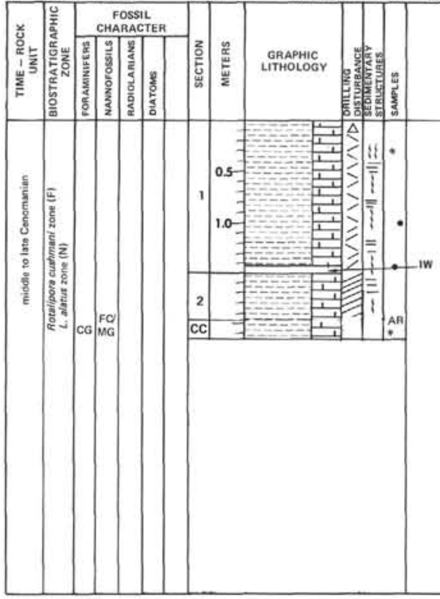

LITHOLOGIC DESCRIPTION

Fused drilling cakes of dusky yellowish green (5GY 5/2) to grayish olive green (5GY 3/2).

Firm NANNOFOSSIL CLAYSTONE with some bioturbation in Section 1, 30–42 cm. Indistinct laminae of black and olive black color throughout.

SMEAR SLIDE SUMMARY (%):

	1, 30	CC (AR)
	D	D
Texture:		
Sand	2	–
Silt	15	–
Clay	83	–
Composition:		
Quartz	0.5	2
Feldspar	–	Tr
Mica	–	Tr
Clay	64	–
Glauconite	–	Tr
Pyrite	–	Tr
Dolomite	2	–
Foraminifers	1	95
Calc. nannofossils	32	–
Sponge spicules	0.5	–
Fish remains	–	Tr

ORGANIC CARBON AND CARBONATE (%):

	1, 100–102	1, 145–150
Organic carbon	0.82	0.93
Carbonate	30.3	28.8

SITE 545 HOLE CORE 32 CORED INTERVAL 293.5–303.0 m sub-bottom

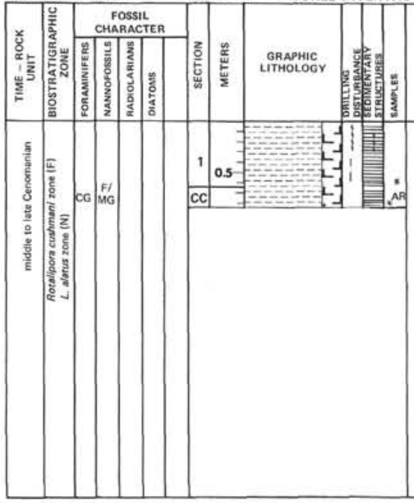

LITHOLOGIC DESCRIPTION

Slightly disturbed, grayish olive green (5GY 4/1) and dark greenish gray (5GY 4/1) NANNOFOSSIL CLAYSTONE with minor burrows at 10 cm, fine lamination throughout.

SMEAR SLIDE SUMMARY (%):

	1, 60	CC (AR)
	D	D
Texture:		
Sand	1	–
Silt	10	–
Clay	89	–
Composition:		
Quartz	0.5	6
Feldspar	–	Tr
Mica	–	Tr
Clay	74	–
Volcanic glass	–	Tr
Glauconite	–	2
Pyrite	–	2
Micronodules	–	Tr
Dolomite	1	–
Foraminifers	1	90
Calc. nannofossils	23	–
Sponge spicules	0.7	–

SITE 545 HOLE CORE 33 CORED INTERVAL 303.0–312.5 m sub-bottom

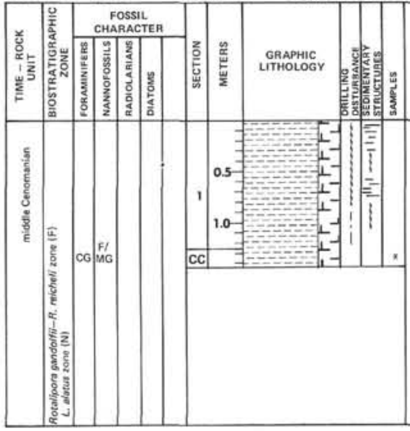

LITHOLOGIC DESCRIPTION

Highly disturbed grayish olive green (5GY 3/2) NANNOFOSSIL CLAYSTONE.

SMEAR SLIDE SUMMARY (%):

	CC
	D
Composition:	
Quartz	3
Feldspar	Tr
Mica	Tr
Heavy minerals	Tr
Glauconite	Tr
Pyrite	2
Micronodules	Tr
Dolomite	2
Foraminifers	90
Fish remains	Tr

SITE 545 HOLE CORE 34 CORED INTERVAL 312.5–322.0 m sub-bottom

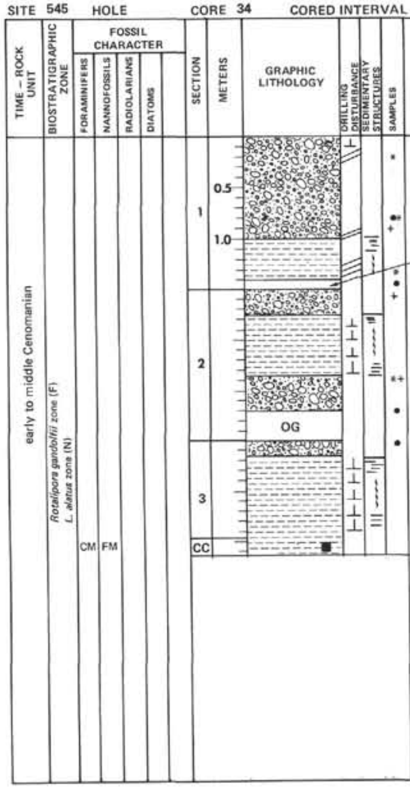

LITHOLOGIC DESCRIPTION

Section 1, 0–100 cm; Section 2, 0–25 and 35–120 cm; and Section 3, 0–15 cm: slightly fractured dusky yellowish brown (10YR 2/2) grayish yellow green (5GY 7/2) and light olive gray (5Y 5/2) CLAYSTONE CONGLOMERATE and PEBBLY CLAYSTONE. Clasts subrounded to well rounded, compact to elongate, very coarse sand to cobble-sized, no visible organization. Clasts:

1. Dusky yellowish brown (10YR 2/2) CLAYSTONE, with occasional glauconite-rich burrows.

2. Grayish yellow green (5GY 7/2) NANNOFOSSIL CALCAREOUS MUDSTONE containing fragments of 1.

3. Light olive gray (5Y 5/2) NANNOFOSSIL MUDSTONE with approximately 20% of quartz silt. Matrix of conglomerate as claystone at Section 1, 100–140 cm; Section 2, 25–85 cm; and Section 3, 15–102 cm: drilling cakes of grayish olive green (5GY 3/2) NANNOFOSSIL CLAYSTONE slightly fissile, with occasional burrows.

SMEAR SLIDE SUMMARY (%):

	1, 22	1, 80	1, 133	2, 22	2, 85
	M	M	D	M	M
Texture:					
Sand	1	2	3	3	2
Silt	20	9	15	9	25
Clay	79	88	82	88	73
Composition:					
Quartz	Tr	4	1	4	2
Feldspar	–	Tr	–	–	–
Mica	Tr	Tr	Tr	Tr	–
Clay	55	75	66	–	58
Glauconite	Tr	–	–	Tr	Tr
Pyrite	–	–	1	Tr	Tr
Dolomite	–	1	–	1	1
Carbonate unspec.	20	–	–	–	10
Foraminifers	–	1.5	1	3	1.5
Calc. nannofossils	25	18	30	16	27
Sponge spicules	Tr	Tr	1	Tr	Tr
Plant debris	–	–	1	–	Tr

ORGANIC CARBON AND CARBONATE (%):

	1, 80–81	1, 140–150	2, 118–120	3, 0–2
Organic carbon	2.16	0.74	1.09	1.55
Carbonate	20.5	29.8	32.6	38.4

SITE 545 HOLE CORE 35 CORED INTERVAL 322.0–331.5 m sub-bottom

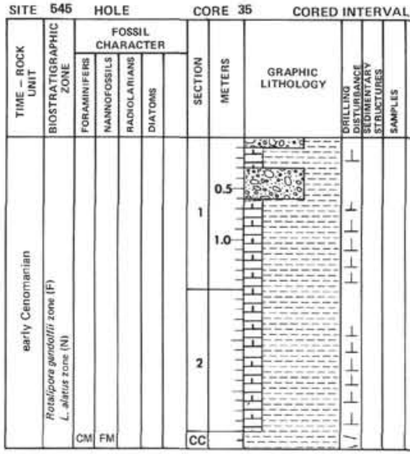

LITHOLOGIC DESCRIPTION

Section 1, 0–10 and 30–60 cm: undisturbed, light olive gray (5Y 5/2), light olive brown (5Y 5/6) and grayish yellow green (5GY 7/2) PEBBLY CLAYSTONE. Pebbles of same type as in Core 34.

Section 1, 10–30 and 60–150 cm; Section 2, 0–140 cm; and Core-Catcher: 2–5 cm long fused drilling cakes of grayish olive (10Y 4/2) and grayish olive green (5GY 3/2) NANNOFOSSIL CLAYSTONE wtih small spots of dusky yellowish green (10GY 3/2) bioturbation especially in Section 2, 0–40 cm and Core-Catcher.

SITE 545 HOLE CORE 36 CORED INTERVAL 331.5–341.0 m sub-bottom

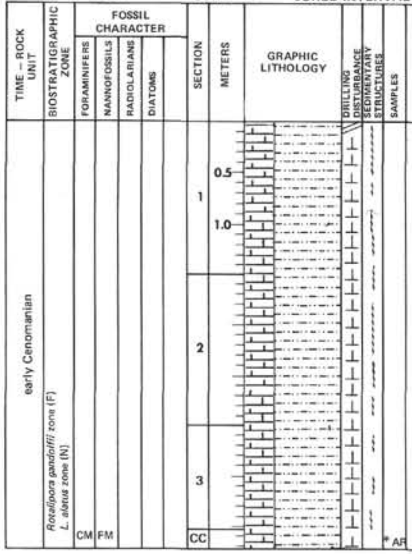

LITHOLOGIC DESCRIPTION

Mostly fused drilling cakes of grayish olive green (5GY 3/2) NANNOFOSSIL MUDSTONE, with dark gray (N4) burrow fillings in Section 1, 10–35 and 100–130 cm and in Section 2, 30–70 cm, minor amount throughout. White, thin calcite "veins" or "shell fragments" occur clustered throughout the core. Pyrite probably 1–2% of total rock.

SMEAR SLIDE SUMMARY (%)

	CC (AR)
	D
Composition:	
Quartz	6
Feldspar	Tr
Mica	Tr
Glauconite	Tr
Pyrite	Tr
Carbonate unspec.	70
Foraminifers	20
Fish remains	Tr

SITE 545 HOLE CORE 37 CORED INTERVAL 341.0–350.5 m sub-bottom

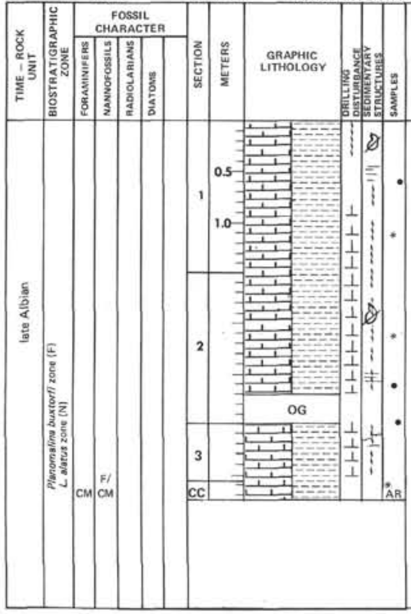

LITHOLOGIC DESCRIPTION

Mostly drilling cakes of grayish olive (10Y 4/2) NANNOFOSSIL-RICH CLAYSTONE with occasional black pyritic layers and black planolites and chondrite-like ichnofossils. Occasional thin calcitic or aragonitic "shell fragments" or "veins" throughout.

SMEAR SLIDE SUMMARY (%):

	1, 110	2, 60	CC (AR)
	D	D	D
Texture:			
Sand	2	2	–
Silt	22	22	–
Clay	76	76	–
Composition:			
Quartz	1	1.2	20
Feldspar	–	–	Tr
Mica	Tr	Tr	Tr
Clay	53	58	–
Glauconite	–	–	Tr
Pyrite	–	–	2
Dolomite	2	2	–
Carbonate unspec.	4	4	50
Foraminifers	1.5	0.7	20
Calc. nannofossils	37	33	–
Sponge spicules	0.5	0.5	–
Fish remains	Tr	Tr	–
Plant debris	Tr	Tr	–

ORGANIC CARBON AND CARBONATE (%):

	1, 60–61	2, 118–120	3, 0–2
Organic carbon	–	2.36	0.73
Carbonate	53.6	32.6	50.8

SITE 545 HOLE CORE 38 CORED INTERVAL 350.5–360.0 m sub-bottom

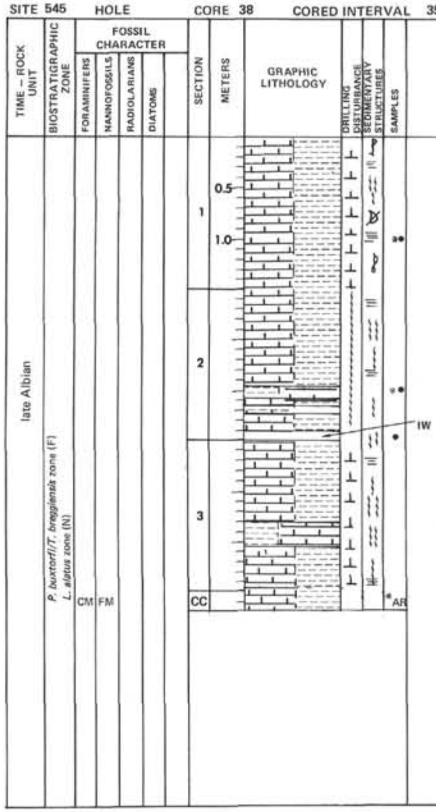

LITHOLOGIC DESCRIPTION

Sections 1–Section 2, 85, 87–92, 102–115, 120–130 cm and Section 3, 104–140 cm grayish olive green (5GY 3/2) NANNOFOSSIL-RICH CLAYSTONE with original sedimentary lamination picked out by lighter, sometimes slight olive gray (5Y 5/2) CHALK. Pyrite-rich layers and burrow-fills are abundant, 1–2 mm in diameter and dark gray. Aragonite shell debris.

Section 2, 85–87, 92–102, 115–120 cm and Section 3, 80–104 cm mostly light olive gray (5Y 5/2) CHALK with grayish olive green (5GY 3/2) bioturbation.

SMEAR SLIDE SUMMARY (%):

	1, 100	2, 100	CC (AR)
	D	D	D
Texture:			
Sand	3	4	–
Silt	18	50	–
Clay	79	46	–
Composition:			
Quartz	1.5	2	30
Feldspar	–	–	2
Mica	–	–	Tr
Clay	49	31	–
Glauconite	–	–	Tr
Pyrite	1	–	5
Micronodules	–	–	Tr
Dolomite	3	3	–
Carbonate unspec.	5	30	35
Foraminifers	0.5	Tr	30
Calc. nannofossils	39	33	–
Sponge spicules	–	Tr	–
Fish remains	–	–	Tr

ORGANIC CARBON AND CARBONATE (%):

	1, 99–100	2, 100–101	2, 140–150
Organic carbon	2.09	–	1.54
Carbonate	69.9	66.5	42.7

SITE 545 HOLE CORE 39 CORED INTERVAL 360.0–369.5 m sub-bottom

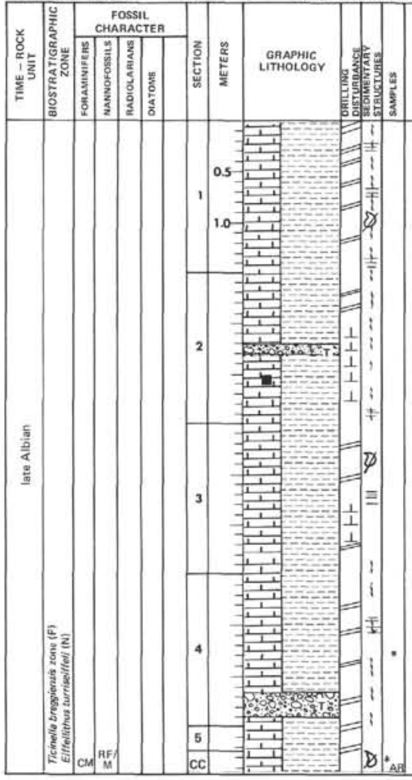

LITHOLOGIC DESCRIPTION

Slightly fractured, grayish olive green (5GY 3/2) NANNOFOSSIL-RICH CLAYSTONE with common bioturbation throughout. Most of the burrow traces are flattened due to compaction. A faint lamination throughout the core shows a general inclination of 15° to core axis. Individual laminae of 2–5 mm scale, burrows may be concentrated in 1–2 cm thick zones parallel with lamination.

Section 4, 115–139 cm: soft deformed PEBBLE CONGLOMERATE with paler color than matrix and irregular outline.

Occasional pieces of thin "shells" or calcite "veins".

SMEAR SLIDE SUMMARY (%):

	4, 80	CC (AR)
	D	D
Texture:		
Sand	2	–
Silt	18	–
Clay	80	–
Composition:		
Quartz	0.5	15
Feldspar	–	Tr
Clay	67	–
Glauconite	–	Tr
Pyrite	–	1
Micronodules	–	Tr
Dolomite	1	–
Carbonate unspec.	8	50
Foraminifers	1	30
Calc. nannofossils	22	–
Sponge spicules	0.7	–
Plant debris	Tr	–

ORGANIC CARBON AND CARBONATE (%):

	2, 61–62
Carbonate	24

SITE 545 HOLE CORE 40 CORED INTERVAL 369.5–379.0 m sub-bottom

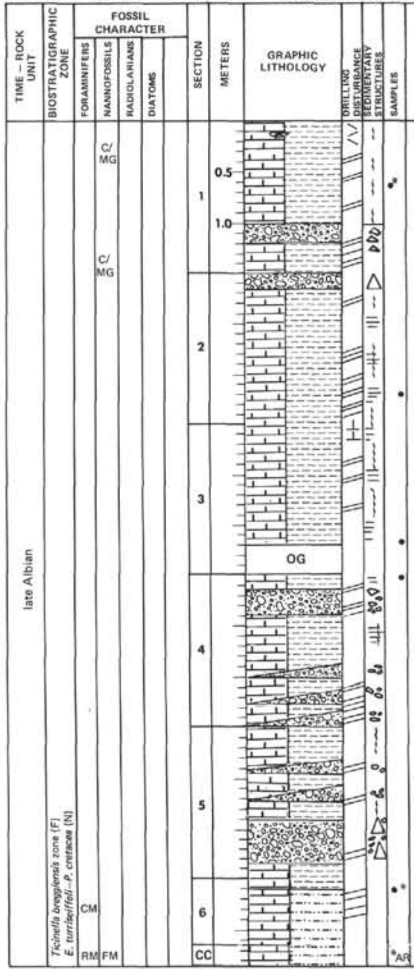

LITHOLOGIC DESCRIPTION

Main lithology Section 1 through 6: slightly fractured, grayish olive green (5GY 3/2) to grayish olive (10Y 4/2) NANNOFOSSIL-RICH CLAYSTONE with fine lamination of olive gray (5Y 3/2) and common burrowing throughout.

In Section 1, 102–119 cm; Section 2, 0–15 cm; Section 4, 12–39 98–99, 123–124, and 139–144 cm; and Section 5, 41–43, 70–72, and 89–131 cm: PEBBLY CLAYSTONE CONGLOMERATES.

Pebbles are pale green (5G 7/2), greenish black (5GY 2/1), and dark greenish gray (5GY 4/1). Some beds show grading and amalgamation, general clast alignment consistent with lamination in claystone and dipping 15° to core axis. Pebble beds often seem to rework underlying sediment.

SMEAR SLIDE SUMMARY (%):

	1, 60	6, 10	CC (AR)
	D	D	D
Texture:			
Sand	–	2	–
Silt	42	27	–
Clay	58	71	–
Composition:			
Quartz	0.8	2	60
Feldspar	–	–	5
Mica	–	–	Tr
Clay	42	63	–
Glauconite	–	–	5
Pyrite	–	–	2
Micronodules	–	–	Tr
Dolomite	2	2	–
Carbonate unspec.	30	20	15
Foraminifers	1	1	10
Calc. nannofossils	25	13	–
Sponge spicules	Tr	Tr	–

ORGANIC CARBON AND CARBONATE (%):

	1, 66–67	2, 120–121	3, 118–120
Organic carbon	–	1.46	1.59
Carbonate	57.6	34.8	42.7

	4, 0–2	6, 12–14
Organic carbon	1.45	–
Carbonate	39.3	34.8

SITE 545 HOLE CORE 41 CORED INTERVAL 379.0–388.5 m sub-bottom

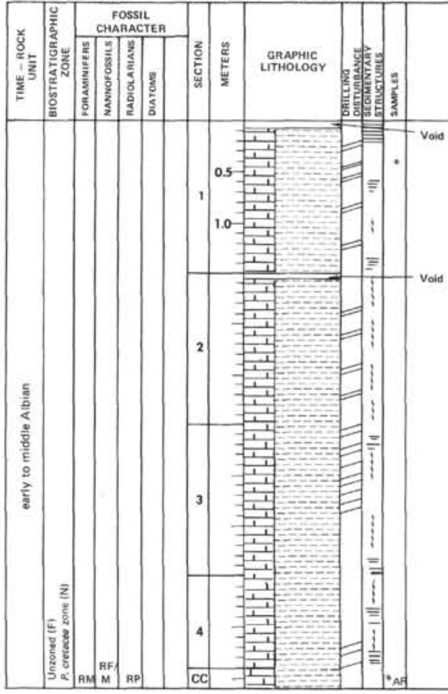

LITHOLOGIC DESCRIPTION

Slightly fractured, olive gray (5Y 3/2) NANNOFOSSIL-RICH CLAYSTONE, with poor lamination in Section 1, 0–27 cm and slight bioturbation. Dip of sedimentary structures 15–20° to core axis.

SMEAR SLIDE SUMMARY (%):

	1, 40	CC (AR)
	D	D
Composition:		
Quartz	2,5	20
Feldspar	–	5
Clay	67	–
Dolomite	2	–
Carbonate unspec.	12	5
Foraminifers	0,5	–
Calc. nannofossils	15	–
Radiolarians	–	2
Sponge spicules	Tr	1
Fish remains	–	1
Aggregated material	–	65

SITE 545 HOLE CORE 42 CORED INTERVAL 388.5–398.0 m sub-bottom

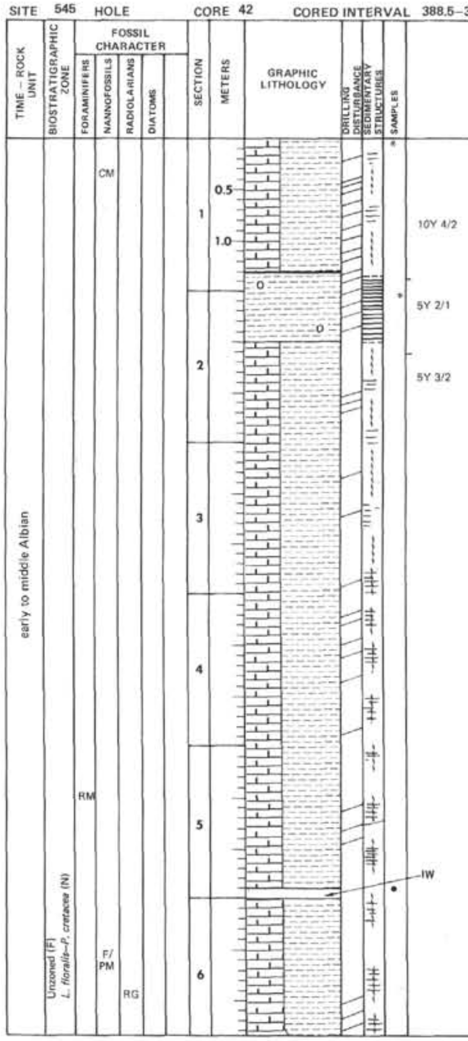

LITHOLOGIC DESCRIPTION

Slightly fractured, grayish olive (10Y 4/2) and olive gray (5Y 3/2) NANNOFOSSIL-RICH CLAYSTONE.

In Section 1, 135–150 cm and Section 2, 0–45 cm olive black (5Y 2/1) NANNOFOSSIL CLAYSTONE with grayish yellow (5Y 8/4) flattened patches, laminated. ("BLACK SHALE".)

Lamination dips 10° to core axis.

SMEAR SLIDE SUMMARY (%):

	2, 1
	D
Composition:	
Quartz	4
Clay	69
Glauconite	0.5
Calc. nannofossils	25
Sponge spicules	2
Fish remains	Tr

ORGANIC CARBON AND CARBONATE (%):

	5, 140–150
Organic carbon	1.35
Carbonate	40.8

SITE 545 HOLE CORE 43 CORED INTERVAL 398.0–407.5 m sub-bottom

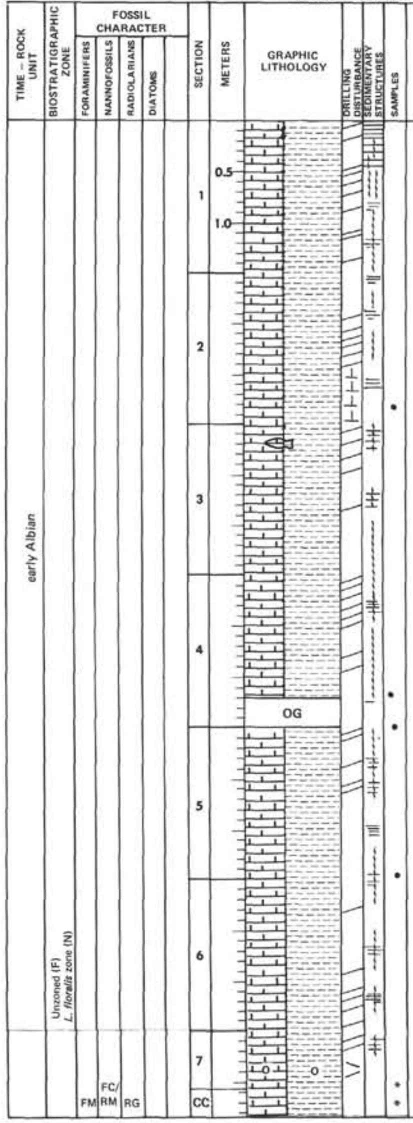

LITHOLOGIC DESCRIPTION

Slightly fractured, grayish olive (10Y 4/2) to olive gray (5Y 3/2) SILTY NANNOFOSSIL-RICH CLAYSTONE with some burrowing throughout and a faint lamination.

SMEAR SLIDE SUMMARY (%):

	7, 50	CC
	D	D
Texture:		
Sand	2	3
Silt	23	25
Clay	75	72
Composition:		
Quartz	0.9	2
Mica	–	Tr
Clay	56	51
Glauconite	Tr	–
Dolomite	2	2
Carbonate unspec.	22	22
Calc. nannofossils	19	19
Radiolarians	–	2
Sponge spicules	0.5	1.5

ORGANIC CARBON AND CARBONATE (%):

	2, 135–136	4, 118–120
Organic carbon	1.15	1.45
Carbonate	33.8	37.3
	5, 0–2	5, 149–150
Organic carbon	1.70	1.50
Carbonate	41.3	46.2

SITE 545 HOLE CORE 44 CORED INTERVAL 407.5–417.0 m sub-bottom

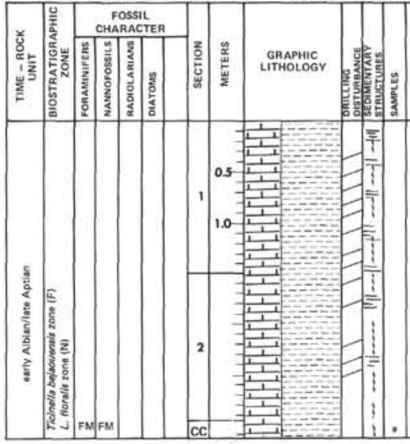

LITHOLOGIC DESCRIPTION

Slightly fractured, grayish olive (10Y 4/2) SILTY SLIGHTLY SILICEOUS NANNOFOSSIL-RICH CLAYSTONE with weak color lamination. Bedding picked out by compacted darker-colored burrow. Dip of bedding: 7°.

SMEAR SLIDE SUMMARY (%):

	CC (Coarse fraction)
	D
Composition:	
Quartz	15
Feldspar	Tr
Mica	Tr
Heavy minerals	Tr
Aggregates	60
Glauconite	Tr
Pyrite	Tr
Radiolarians	25

SITE 545 HOLE CORE 45 CORED INTERVAL 417.0–426.5 m sub-bottom

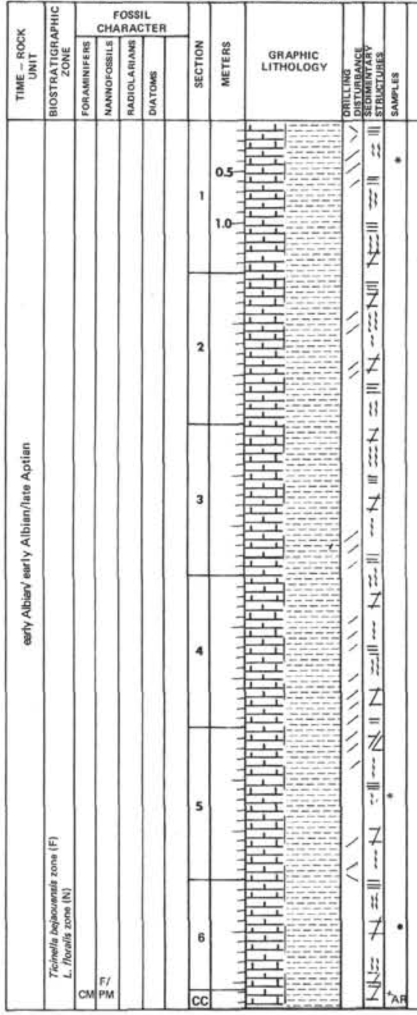

LITHOLOGIC DESCRIPTION

Slightly fractured, greenish gray (5G 6/1) to grayish olive green (5GY 3/2) SILTY NANNOFOSSIL-RICH CLAYSTONE with slight color mottling (bioturbation) and small scaled syndepositional faulting at Section 1, 120–150 cm; Section 2, 135–140 cm; Section 3, 20–40, 65–80 cm; Section 4, 0–40 cm; and Section 5, 0–20 cm. Some layers show dips up to 30° to core axis.

In Section 4, 47–98 cm, several greenish black (5GY 2/1) layers showing interval irregular (slump) folding.

Barite vein (1 cm thick) at Section 5, 5 cm.

SMEAR SLIDE SUMMARY (%):

	1, 37	5, 66	CC (AR)
	D	D	D
Texture:			
Sand	6	4	–
Silt	32	22	–
Clay	62	74	–
Composition:			
Quartz	2.5	2.5	40
Feldspar	–	–	2
Mica	Tr	Tr	Tr
Clay	50	50	–
Glauconite	–	–	Tr
Pyrite	–	Tr	2
Dolomite	2	1	–
Carbonate unspec.	22	13	Tr
Foraminifers	1	0.5	–
Calc. nannofossils	18	30	–
Radiolarians	–	Tr	50
Sponge spicules	4	1.5	

ORGANIC CARBON AND CARBONATE (%):

	6, 47–50
Carbonate	47.2

SITE 545 HOLE CORE 46 CORED INTERVAL 426.5–436.0 m sub-bottom

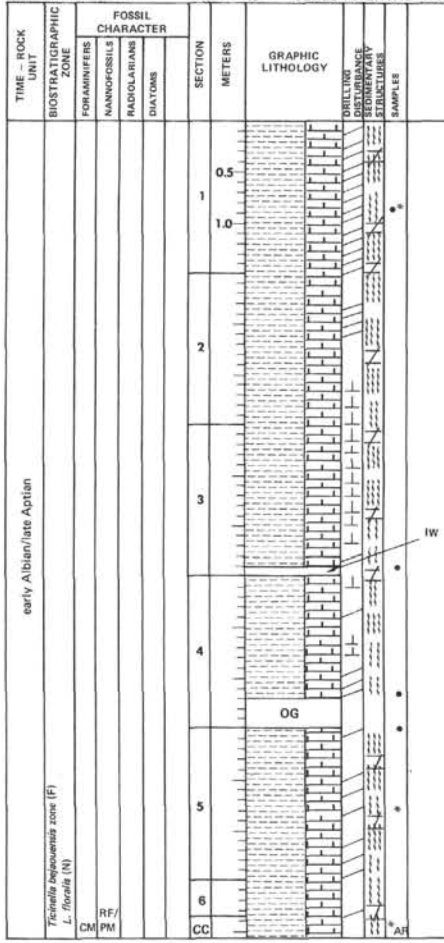

LITHOLOGIC DESCRIPTION

Slightly fractured and drilling cakes of dark greenish gray (5GY 4/1) and grayish olive green (5GY 3/2) NANNOFOSSIL-RICH CLAYSTONE, SLIGHTLY SILICEOUS with heavy bioturbation throughout.

Burrows are flattened by compaction (height/width ≈ 1/3) and show dips between 30 and 35° to core axis.

Smear slides show presence of sponge spicules and radiolarians.

SMEAR SLIDE SUMMARY (%):

	1, 80	5, 80	CC (AR)
Texture:			
Sand	2	4	–
Silt	30	28	–
Clay	68	68	–
Composition:			
Quartz	1	2	40
Feldspar	–	–	Tr
Mica	–	–	Tr
Clay	49	50	–
Glauconite	Tr	Tr	Tr
Pyrite	–	–	20
Dolomite	2	2	–
Carbonate unspec.	16	9	2
Foraminifers	0.5	1	–
Calc. nannofossils	30	32	–
Radiolarians	Tr	Tr	50
Sponge spicules	1.0	3.5	

ORGANIC CARBON AND CARBONATE (%):

	1, 89–90	3, 140–150
Organic carbon	–	0.70
Carbonate	49.2	42.7
	4, 118–120	5, 0–2
Organic carbon	1.23	0.78
Carbonate	42.2	43.7

SITE 545 HOLE CORE 47 CORED INTERVAL 436.0–445.5 m sub-bottom

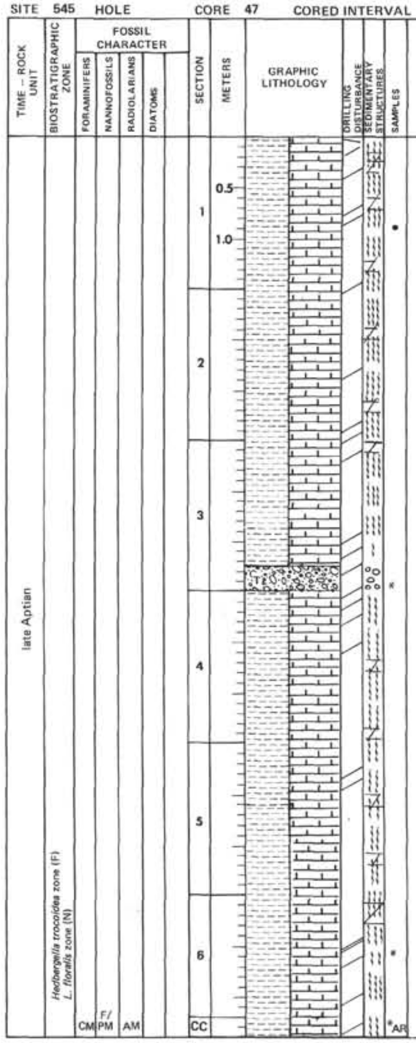

LITHOLOGIC DESCRIPTION

Slightly fractured, dusky yellowish brown (5GY 5/2) and dark greenish gray (5GY 4/1) in Sections 1–3, and greenish gray (5GY 6/1) in Sections 4–Core-Catcher. NANNOFOSSIL-RICH CLAYSTONE with abundant bioturbation mostly as flattened, subhorizontal, slightly darker, brownish wisps and blebs. Dip 15–30° to core axis.

Section 3, 127–150 cm: PEBBLY CLAYSTONE CONGLOMERATE with light gray (N7) granules and small pebbles of chalk floating in dark greenish gray (5GY 4/1) slightly siliceous nannofossil-rich claystone.

SMEAR SLIDE SUMMARY (%):

	3, 147	6, 56	CC (AR)
	D	D	D
Texture:			
Sand	1.5	2	–
Silt	20	26	–
Clay	78.5	72	–
Composition:			
Quartz	1.5	1	25
Clay	48	46	–
Glauconite	Tr	–	–
Pyrite	Tr	–	–
Dolomite	1	2	–
Carbonate unspec.	12	18	–
Calc. nannofossils	35	32	–
Radiolarians	0.5	0.5	40
Sponge spicules	2	1	
Aggregated material	–	–	33

ORGANIC CARBON AND CARBONATE (%):

	1, 90–91
Carbonate	50.6

SITE 545 HOLE CORE 48 CORED INTERVAL 445.5–455.0 m sub-bottom

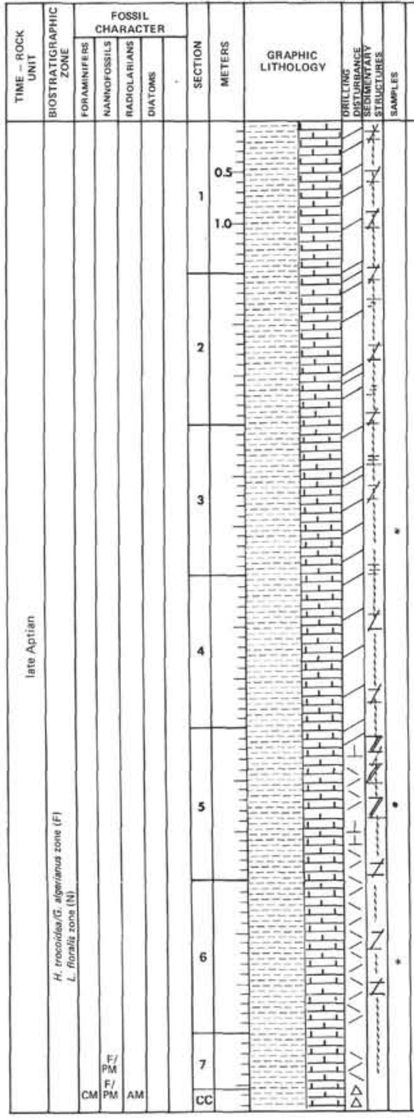

LITHOLOGIC DESCRIPTION

Slightly fractured and some highly fragmented grayish green (10GY 6/4) to greenish gray (5GY 6/1) NANNOFOSSIL SLIGHTLY SILICEOUS-RICH CLAYSTONE with 10–15% flattened burrows of planolites and chondrites-type, often enriched in pyrite.

The dips are variable and rapidly changing from 7–22° to core axis.

Several slickensides are broken up due to drilling in Section 5, 10–97 cm.

SMEAR SLIDE SUMMARY (%):

	3, 107	6, 80
	D	D
Texture:		
Sand	1	1.5
Silt	25	23
Clay	74	75
Composition:		
Quartz	1.5	1.5
Clay	44	51
Glauconite	1	Tr
Dolomite	1	2
Carbonate unspec.	11	10
Calc. nannofossils	41	33
Radiolarians	Tr	0.5
Sponge spicules	1.0	1.5
Fish remains	Tr	–

ORGANIC CARBON AND CARBONATE (%):

	5, 74–75
Carbonate	36.8

SITE 545 HOLE CORE 49 CORED INTERVAL 455.0–464.5 m sub-bottom

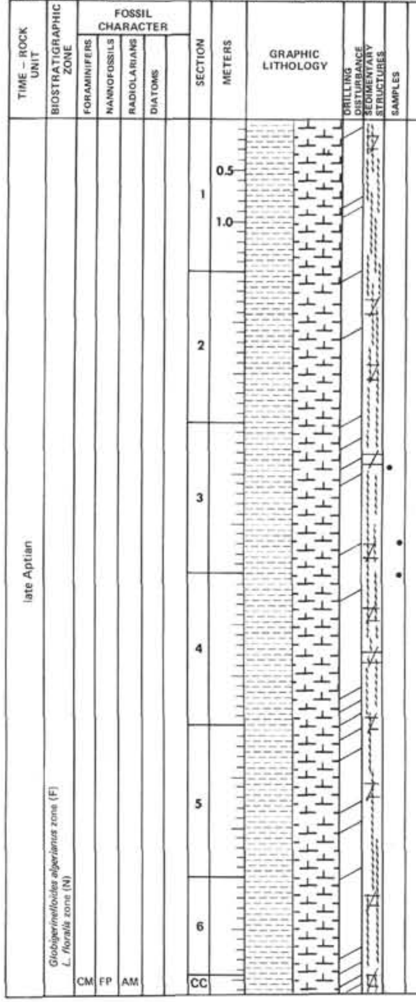

LITHOLOGIC DESCRIPTION

Slightly fractured, greenish gray (5G 5/2) and light olive gray (5Y 5/2) SLIGHTLY SILICEOUS NANNOFOSSIL-RICH CLAYSTONE with abundant bioturbation. Burrows are flattened and mostly oriented parallel to bedding. Dips around 10–15°.

Series of microfractures occur in Section 3, 36–44 cm and in Section 4, 80–90 cm. Slickensides and listric surfaces occur throughout the core but are probably accentuated by drilling.

ORGANIC CARBON AND CARBONATE (%):

	3, 42–43	3, 118–120	4, 0–2
Organic carbon	–	0.48	0.51
Carbonate	54.6	56.1	48.7

SITE 545 HOLE CORE 50 CORED INTERVAL 454.5–474.0 m sub-bottom

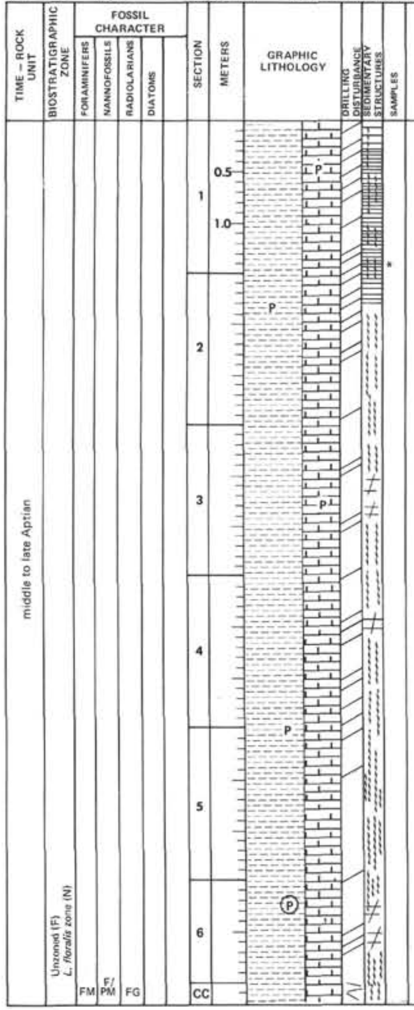

LITHOLOGIC DESCRIPTION

Slightly fractured grayish olive green (5GY 3/2) to olive gray (5Y 3/2) SILTY NANNOFOSSIL-RICH CLAYSTONE. An indistinct irregular layering of lighter and darker colors occurs throughout the core – probably strongly flattened burrows.

This layering is cut by several steeply dipping postdepositional faults (especially in Section 3, 80–90 cm).

The layering dips 13–20°.

Pyrite nodules up to 5 mm across in Section 6, 20–30 cm. Fine pyrite abundant throughout.

SMEAR SLIDE SUMMARY (%):

	1, 140 D
Texture:	
Sand	1
Silt	16
Clay	83
Composition:	
Quartz	3
Clay	68
Dolomite	1
Carbonate unspec.	5
Calc. nannofossils	23
Sponge spicules	Tr

SITE 545 HOLE CORE 51 CORED INTERVAL 474.0–483.5 m sub-bottom

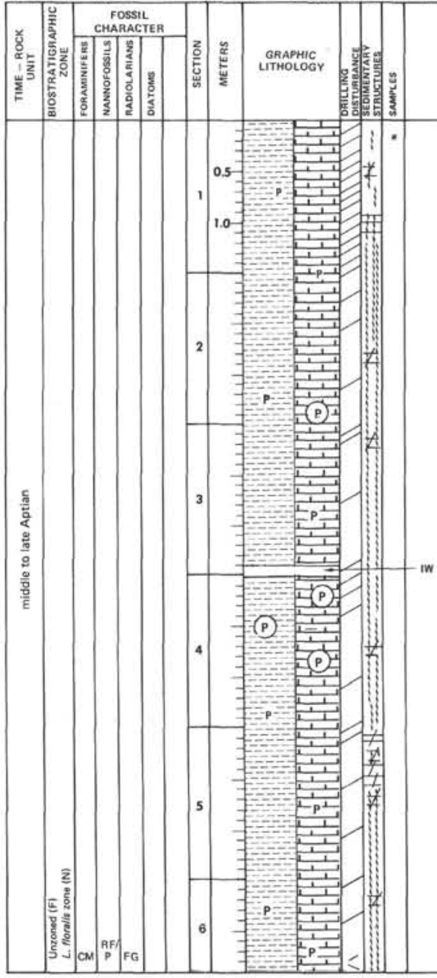

LITHOLOGIC DESCRIPTION

Slightly fractured, dark greenish gray (5GY 4/1), grayish olive (10Y 4/2) and grayish green (5G 5/2). SILTY NANNOFOSSIL-RICH CLAYSTONE.

Abundant subhorizontal, flattened darker burrows occur from Section 1, 100 cm–Core-Catcher. They are generally rich in pyrite.

Larger pyrite concretions occur especially at Section 2, 140 cm and Section 4, 18, 40, and 82 cm.

Sharp bounded faults occur at Section 5, 17, 42, and 57 cm.

SMEAR SLIDE SUMMARY (%):

	1, 15 D
Texture:	
Sand	1
Silt	15
Clay	84
Composition:	
Quartz	2
Mica	Tr
Clay	49
Glauconite	Tr
Pyrite	1
Dolomite	1
Carbonate unspec.	10
Foraminifers	0.5
Calc. nannofossils	35

SITE 545 HOLE CORE 52 CORED INTERVAL 683.5–493.0 m sub-bottom

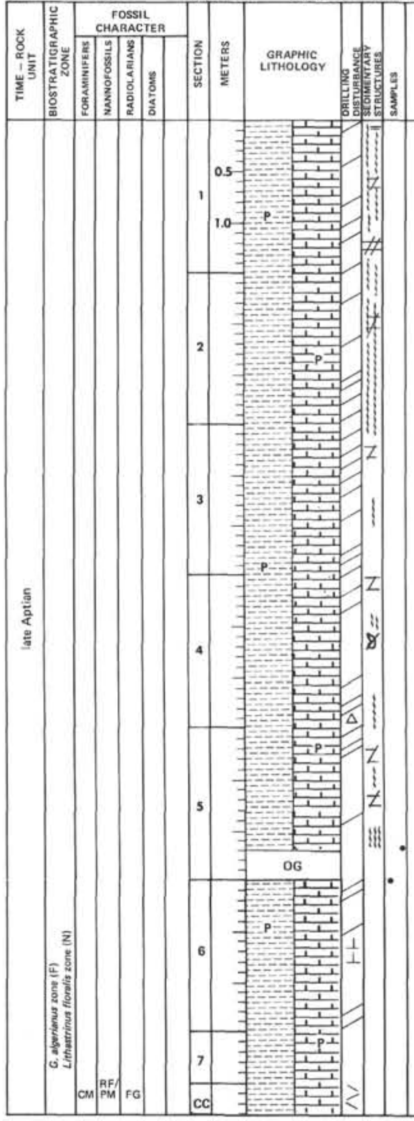

LITHOLOGIC DESCRIPTION

Slightly fractured, greenish gray (5GY 6/1) NANNOFOSSIL-RICH CLAYSTONE with abundant flattened subhorizontal bioturbation. Burrows consist mostly of 2–4 m diameter tubes and minor 2 cm sized patches. Soft sediment deformation at a cm scale is common throughout the core.

At Section 1, 120–128 cm a shear zone, dipping 50° to core axis is filled with barite.

Pyrite is common throughout.

A syndepositional fault at Section 5, 20–30 cm.

ORGANIC CARBON AND CARBONATE (%):

	5, 118–120	6, 0–2
Organic carbon	0.27	0.47
Carbonate	52.6	50.2

SITE 545 HOLE CORE 53 CORED INTERVAL 493.0–502.5 m sub-bottom

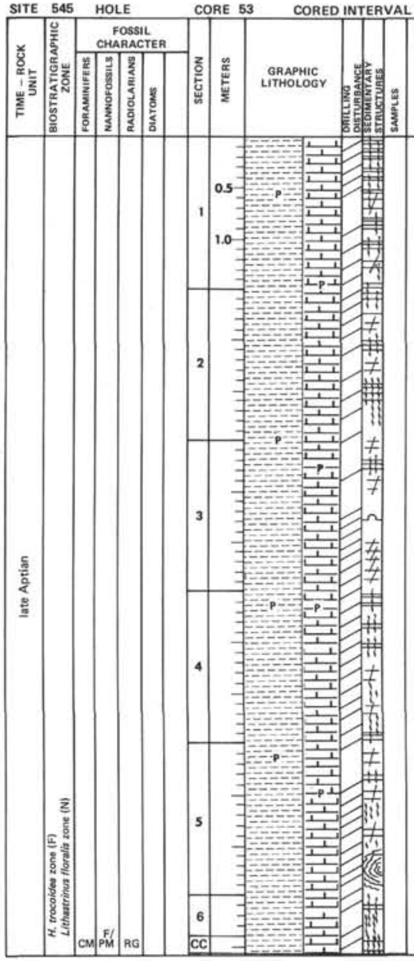

LITHOLOGIC DESCRIPTION

Slightly fractured, greenish gray (5G 6/1) and grayish olive green (5GY 3/2) NANNOFOSSIL-RICH CLAYSTONE. Gradational color changes occur due to the interlayering of more grayer and more greener laminae. Most laminae represent 1–3 mm thick flattened and stretched burrows. Occasionally large burrows (1 cm diameter). Pyrite abundant throughout.

Syndepostional deformation is present throughout but increasing downward. It consists of soft sediment deformation, syndepositional faulting, slumping, and folding (especially at Section 2, 33–55 and 70–88 cm and Section 3, 120–140 cm). Large slump fold at Section 5, 115–140 cm. Dip of laminae≈20° to core axis.

SITE 545 HOLE CORE 54 CORED INTERVAL 502.5–512.0 m sub-bottom

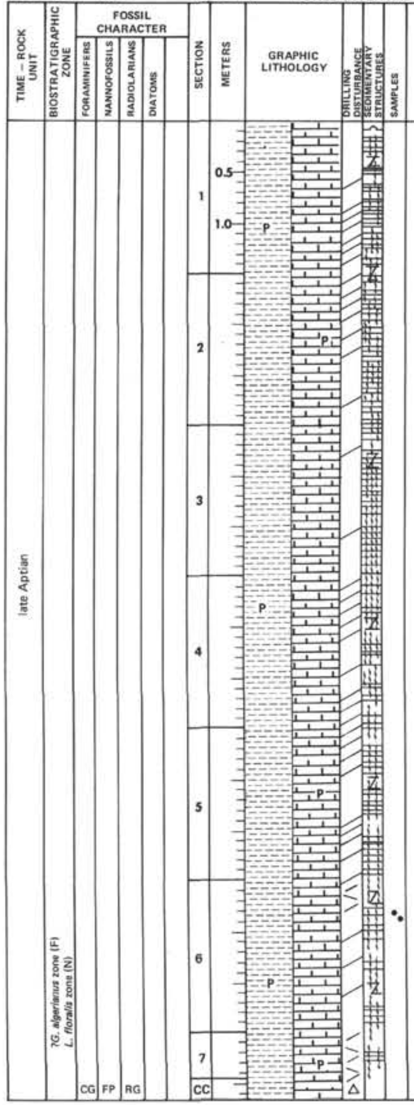

LITHOLOGIC DESCRIPTION

Slightly fractured, dark greenish gray (5GY 4/1) to greenish gray (5GY 6/1) NANNOFOSSIL-RICH CLAYSTONE with olive gray (5Y 4/1) pyrite-rich burrows, flattened and deformed by soft sediment deformation. Pyrite common throughout, incipient reduction rings becoming more common in lower part of core.

Minor syndepositional faults with more offsets.

ORGANIC CARBON AND CARBONATE (%):

	6, 27–30	6, 39–42
Carbonate	47.2	47.7

SITE 545 HOLE CORE 55 CORED INTERVAL 512.0–521.5 m sub-bottom

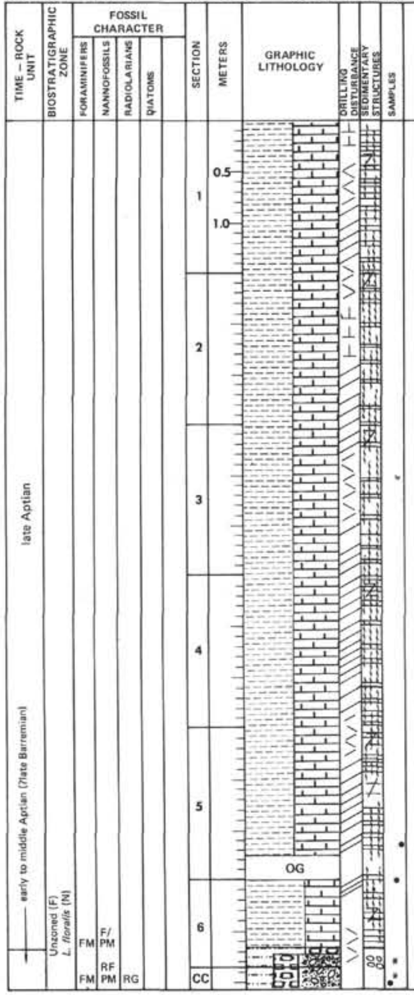

LITHOLOGIC DESCRIPTION

Section 1 through Section 6, 65 cm: slightly to highly fragmented, greenish gray (5GY 6/1) NANNOFOSSIL-RICH CLAYSTONE. Abundant bioturbation appears as flattened, irregular layers of brownish olive, slightly darker, often pyrite-rich sediment, rare microfaulting. Dip~15° to core axis.

Sharp fault contact at Section 6, 65 cm.

Section 6, 65 cm–Core-Catcher: BRECCIA with highly deformed and fractured, olive gray (5Y 4/1) CALCAREOUS MUD and scattered olive green (5Y 4/1) clasts of NANNOFOSSIL CLAYSTONE and light olive gray (5Y 6/1) clasts of CALCAREOUS CHALK (microsparite with quartz silt) showing microfractures.

SMEAR SLIDE SUMMARY (%):

	3, 50	6, 85	CC
	D	D	D
Texture:			
Sand	1	2	–
Silt	26	27	60
Clay	73	71	40
Composition:			
Quartz	3	3	2
Clay	40	54	40
Glauconite	Tr	Tr	–
Pyrite	–	1	–
Dolomite	2	2	–
Carbonate unspec.	13	13	58
Foraminifers	25	–	–
Calc. nannofossils	38	27	–

ORGANIC CARBON AND CARBONATE (%):

	5, 118–120	6, 0–2	CC, 15–16
Organic carbon	0.96	1.49	–
Carbonate	53.6	53.1	42.2

SITE 545 HOLE CORE 56 CORED INTERVAL 521.5–531.0 m sub-bottom

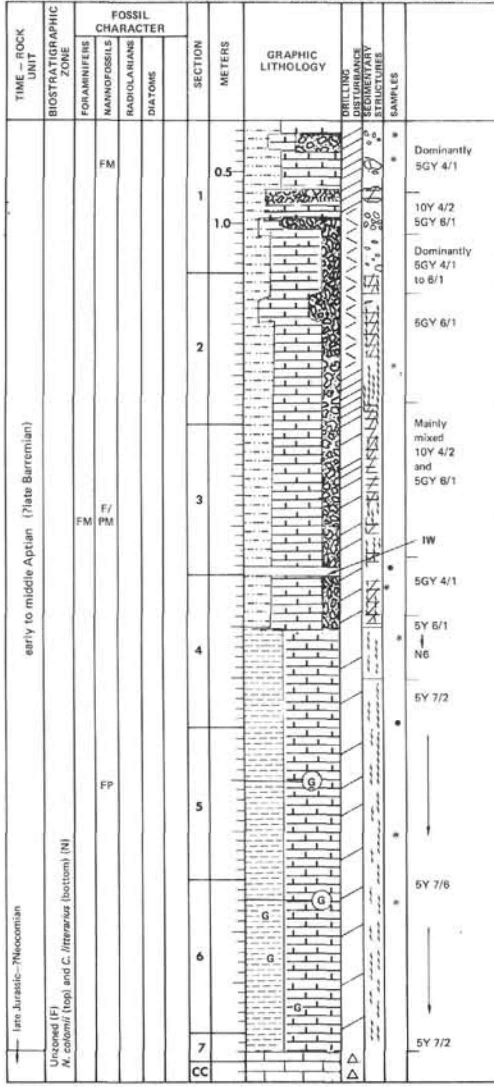

LITHOLOGIC DESCRIPTION

Section 1 through 4, 40 cm: slightly to highly fragmented dominantly dark greenish gray (5GY 4/1) VERY MUDDY NANNOFOSSIL OOZE with clasts of grayish olive (10Y 4/2) VERY MUDDY NANNOFOSSIL CHALK and light gray (N6–N7) MICROSPARITE pebbles. This interval is intensely faulted, and pervasively fractured forming a mosaic of very angular FAULT BRECCIA.

Section 4, 40–50 cm: sheared underlying lithology.

Section 4, 50 cm through Section 7, 20 cm: slightly fractured, yellowish gray (5Y 7/2) to moderate yellow (5Y 7/6) VERY CLAYEY NANNOFOSSIL CHALK with common limonitized pyrite speckles, laminae and scattered coarse grains of glauconite.

Section 7, 20–25 cm and Core-Catcher: highly fragmented, yellowish gray (5Y 8/1) SKELETAL GRAINSTONE and SKELETAL WACKESTONE with micritized bioclasts (echinoderm remains, mollusc shell fragments, coral fragments, dasycladaceaus) and intraclasts.

SMEAR SLIDE SUMMARY (%):

	1, 16	1, 36	2, 90	4, 10	4, 60	5, 100	6, 20
	D	D	D	D	D	D	D
Texture:							
Sand	3	2	3	–	2	1	3
Silt	12	15	12	15	15	20	40
Clay	85	83	85	85	83	79	57
Composition:							
Quartz	4	3	3	1	3	1.5	3
Feldspar	–	–	–	–	Tr	–	–
Mica	–	–	–	Tr	–	–	–
Clay	56	48	52	55	56	58.5	54
Glauconite	–	–	–	Tr	Tr	–	–
Pyrite	–	–	–	Tr	–	–	–
Dolomite	3	–	3	–	3	6	40
Carbonate unspec.	5	10	7	8	8	10	–
Foraminifers	–	Tr	Tr	–	–	Tr	–
Calc. nannofossils	32	38	35	34	29	23	–
Radiolarians	–	–	–	–	Tr	–	–
Sponge spicules	–	–	–	1.5	–	–	–
Limonite sand	–	–	–	–	–	–	3

ORGANIC CARBON AND CARBONATE (%):

	3, 140–150	4, 149–150
Organic carbon	0.83	0.12
Carbonate	44.2	40.8

SITE 545 HOLE CORE 57 CORED INTERVAL 531.0–540.5 m sub-bottom

TIME – ROCK UNIT | BIOSTRATIGRAPHIC ZONE | FOSSIL CHARACTER: FORAMINIFERS, NANNOFOSSILS, RADIOLARIANS, DIATOMS, ALGAE | SECTION | METERS | GRAPHIC LITHOLOGY | DRILLING DISTURBANCE | SEDIMENTARY STRUCTURES | SAMPLES | LITHOLOGIC DESCRIPTION

late Jurassice (?Neocomian)

Protopeneroplis (F)
Petrascula (Algae)

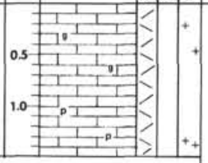

Highly fragmented skeletal limestones: 0–68 and 130–150 cm white dolomitized SKELETAL GRAINSTONE with shallow water components: corals, clasycladaceaus, bryozoans, hydrozoans, benthic forams, pelsparitic intraclasts. At 68–130 cm light olive gray (5Y 6/1) to white (N9) dolomitized INTRACLASTIC SKELETAL PACKSTONE with echinoderms. High porosity.

THIN SECTION/PEEL SUMMARY (%):

	1, 22–25	1, 45–50	1, 133–135	1, 139–142
Texture:				
Rudite	5	20	–	–
Arenite	65	80	80	80
Silt	30	–	20	20
Composition:				
Micrite	50	–	–	20
Sparite	–	5	–	–
Intraclasts	–	15	–	20
Coated grains	Tr	–	–	–
Ooids	–	–	–	40
Skeletal grains:				
Crinoids	15	20	15	–
Bivalves	5	Tr	–	–
Gastropods	–	Tr	–	–
Forams	–	1	–	2
Dasyclads	10	3	–	2
Others	–	20	20	–
Tubiphytes	5	–	–	Tr
Dolomite	–	–	55	–
Porosity	15	35	10	15

SITE 545 HOLE CORE 58 CORED INTERVAL 540.5–550.0 m sub-bottom

TIME – ROCK UNIT | BIOSTRATIGRAPHIC ZONE | FOSSIL CHARACTER: FORAMINIFERS, NANNOFOSSILS, RADIOLARIANS, DIATOMS | SECTION | METERS | GRAPHIC LITHOLOGY | DRILLING DISTURBANCE | SEDIMENTARY STRUCTURES | SAMPLES | LITHOLOGIC DESCRIPTION

late Jurassic (?Neocomian)

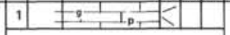

At 0–5 cm highly fragmented yellowish gray (5Y 8/1) dolomitized SKELETAL GRAINSTONE with shallow water components: coated grains, superficial ooids, dasycladaceaus, foraminifera. High porosity.

At 5–12 cm moderately fragmented light olive gray (5Y 6/1) to white (N9) dolomitized SKELETAL PACKSTONE with echinoderm remains. Occurrence of hematite stained calcite veins.

SITE 545 HOLE CORE 59 CORED INTERVAL 550.0–559.5 m sub-bottom

TIME – ROCK UNIT | BIOSTRATIGRAPHIC ZONE | FOSSIL CHARACTER: FORAMINIFERS, NANNOFOSSILS, RADIOLARIANS, DIATOMS | SECTION | METERS | GRAPHIC LITHOLOGY | DRILLING DISTURBANCE | SEDIMENTARY STRUCTURES | SAMPLES | LITHOLOGIC DESCRIPTION

late Jurassic (?Neocomian)

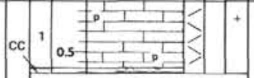

Highly fragmented light gray (N7) highly dolomitized SKELETAL PACKSTONE with shallow water components: echinoderm remains, dasycladaceaus fragments. High porosity.

At 55 cm 3 mm thick laminae of reddish iron oxide between solution surfaces.

THIN SECTION/PEEL SUMMARY (%):

	1, 10–13
Texture:	
Arenite	100
Composition:	
Micritic part, unspec.	20
Skeletal grains:	
Crinoids	15
Bivalves	Tr
Dasyclads	Tr
Tubiphytes	Tr
Dolomite	55
Porosity	10

SITE 545 HOLE CORE 60 CORED INTERVAL 559.5–569.0 m sub-bottom

TIME – ROCK UNIT | BIOSTRATIGRAPHIC ZONE | FOSSIL CHARACTER: FORAMINIFERS, NANNOFOSSILS, RADIOLARIANS, DIATOMS | SECTION | METERS | GRAPHIC LITHOLOGY | DRILLING DISTURBANCE | SEDIMENTARY STRUCTURES | SAMPLES | LITHOLOGIC DESCRIPTION

late Jurassic (?Neocomian)

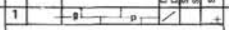

Highly fragmented greenish gray (5GY 6/1) dolomitized SKELETAL PACKSTONE with echinoderm remains and pink patches of micrite from 0–3 cm.

From 5–15 cm white (N9) dolomitized SKELETAL GRAINSTONE with shallow water components (corals, dasycladaceaus) and ammonite shells. High porosity. Presence of pale reddish brown (10R 5/4) clay seams.

THIN SECTION/PEEL SUMMARY (%):

	1, 13–15
Texture:	
Rudite	20
Arenite	80
Composition:	
Intraclasts	20
Skeletal grains:	
Crinoids	10
Bivalves	10
Gastropods	Tr
Ammonites	Tr
Serpulids	Tr
Forams	2
Dasyclads	5
Reef builders	5
Tubiphytes	5
Porosity	40

SITE 545 HOLE CORE 61 CORED INTERVAL 569.0–578.5 m sub-bottom

TIME – ROCK UNIT	BIOSTRATIGRAPHIC ZONE	FOSSIL CHARACTER: FORAMINIFERS	NANNOFOSSILS	RADIOLARIANS	DIATOMS	SECTION	METERS	GRAPHIC LITHOLOGY	DRILLING DISTURBANCE	SEDIMENTARY STRUCTURES	SAMPLES	LITHOLOGIC DESCRIPTION
late Jurassic (?Neocomian)						1	0.5					

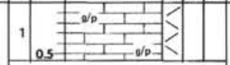

Highly fragmented white (N9) to very light gray (N8) dolomitized SKELETAL GRAINSTONE/PACKSTONE with coated shallow water components. High porosity. Occurrence of low relief stylolites both irregular asastomosing and parallel to the bedding with moderate red (5YR 4/1) and light olive gray (5Y 5/2) clay seams.

From 28–42 cm brecciation of the grainstones: rotated, angular fragments in a moderate red (5R 4/6) matrix of dolomite and clay residue.

SITE 545 HOLE CORE 62 CORED INTERVAL 578.5–588.0 m sub-bottom

TIME – ROCK UNIT	BIOSTRATIGRAPHIC ZONE	FOSSIL CHARACTER: FORAMINIFERS	NANNOFOSSILS	RADIOLARIANS	DIATOMS	ALGAE	SECTION	METERS	GRAPHIC LITHOLOGY	DRILLING DISTURBANCE	SEDIMENTARY STRUCTURES	SAMPLES	LITHOLOGIC DESCRIPTION
late Jurassic (?Neocomian)	*Salpingoporella pygmaea*(?) (Algae)						1	0.5				+ +	

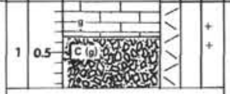

Highly fragmented white to very light gray (N9–N8) dolomitized SKELETAL GRAINSTONE with coated shallow water components and pelmicritic intraclasts. High porosity. Pressure solution seams parallel to bedding.

At 36–52 cm LIMESTONE BRECCIA very light gray (N9–N8) angular fragments of grainstone, single superficial ooids and serpulid tubes in a yellowish gray (5Y 8/1) matrix of dolomite.

At 52–83 cm LIMESTONE BRECCIA white to very light gray (N9–N8) angular fragments of pelmicrite, coral debris, oncoids, grainstone in stylolitic contact.

THIN SECTION/PEEL SUMMARY (%):

	1, 23–27	1, 41–43
Texture:		
Rudite	20	25
Arenite	80	75
Composition:		
Sparite	–	5
Intraclasts	15	25
Coated grains	–	Tr
Ooids	–	Tr
Skeletal grains:		
Crinoids	15	20
Bivalves	5	5
Forams	–	5
Dasyclads	1	–
Others	20	5
Tubiphytes	5	–
Porosity	40	35

SITE 545 HOLE CORE 63 CORED INTERVAL 588.0–597.5 m sub-bottom

TIME – ROCK UNIT	BIOSTRATIGRAPHIC ZONE	FOSSIL CHARACTER: FORAMINIFERS	NANNOFOSSILS	RADIOLARIANS	DIATOMS	SECTION	METERS	GRAPHIC LITHOLOGY	DRILLING DISTURBANCE	SEDIMENTARY STRUCTURES	SAMPLES	LITHOLOGIC DESCRIPTION
late Jurassic (?Neocomian)						1	0.5 1.0				+ +	

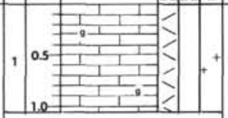

Highly fragmented white (N9) to yellowish gray (5Y 8/1) dolomitized SKELETAL GRAINSTONE with coated shallow water components and pelsparitic intraclasts.

From 22–48 and 93–108 cm brecciation: angular fragments of grainstone in stylolitic contact with moderate red (5R 4/6) to moderate reddish brown (10R 4/6) clay seams.

THIN SECTION/PEEL SUMMARY (%):

	1, 11–14	1, 53–57	1, 61–64
Texture:			
Rudite	30	40	30
Arenite	60	40	70
Silt	10	20	–
Composition:			
Micrite	5	20	–
Sparite	–	10	20
Intraclasts	20	–	30
Oncoids	10	–	–
Coated grains	–	10	–
Peloids	–	10	–
Skeletal grains:			
Crinoids	10	–	30
Bivalves	Tr	–	5
Gastropods	–	Tr	–
Serpulids	–	–	Tr
Forams	–	–	Tr
Dasyclads	–	–	Tr
Corals	10	20	–
Tubiphytes	–	20	5
Dolomite	45	–	–
Porosity	–	–	10
Structure:			
Veins	Tr	–	

SITE 545 HOLE CORE 64 CORED INTERVAL 597.5–607.0 m sub-bottom

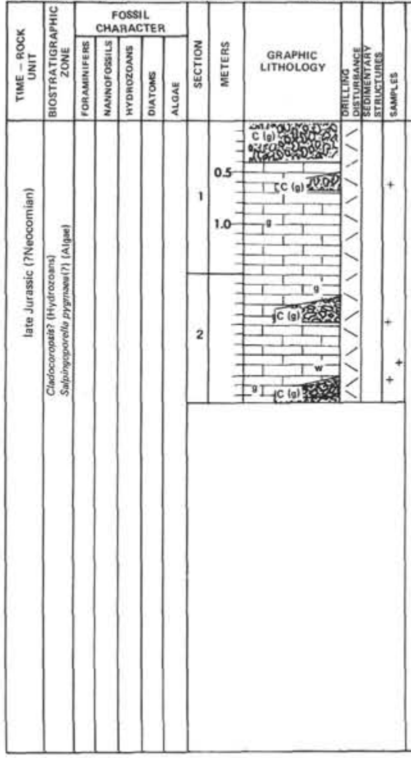

LITHOLOGIC DESCRIPTION

Highly fragmented white (N9), very light gray (N8) to very pale orange (10YR 8/2) LIMESTONE of different facies:

1. Section 1, 0–40 and 61–69 cm; Section 2, 32–48 and 119–127 cm: LIMESTONE BRECCIA with pelsparitic intraclasts in a moderate (5R 4/6) to moderate brown (5YR 4/4) dolomitic matrix; stylolitic grain contacts.

2. Section 1, 40–59, 69–77, and 130–150 cm; Section 2, 0–57, 67–93, 99–103, and 108–119 cm: dolomitized shallow water SKELETAL GRAINSTONE with alternating predominance of peloids and coated grains.

3. Section 1, 59–61 cm; Section 2, 57–67 cm: OOLITIC GRAINSTONE, slightly dolomitized.

4. Section 2, 93–99 and 103–108 cm: grayish orange (10YR 7/4) to light brown (5YR 5/6) slightly laminated PELMICRITE.

Section 1, 103–130 cm: SKELETAL GRAINSTONES with a grayish orange (10YR 7/4) dolomite matrix.

THIN SECTION/PEEL SUMMARY (%):

	1, 62–66	2, 47–51	2, 88–91	2, 105–108
Texture:				
Rudite	5	15	25	30
Arenite	95	85	75	70
Composition:				
Sparite	30	30	35	40
Intraclasts	–	15	20	10
Oncoids	5		15	–
Coated grains	–	40	–	15
Ooids	60		25	–
Peloids	–	Tr	–	–
Skeletal grains:	–	15	–	–
Crinoids	2	Tr	5	15
Bivalves	Tr	Tr	–	3
Gastropods	–	Tr	–	–
Ammonites	–	Tr	–	–
Forams	–	Tr	Tr	Tr
Dasyclads	Tr	Tr	–	Tr
Tubiphytes	Tr	–	–	15
Thaumatoporella	–	Tr	–	–
Coral debris	–	–	Tr	–
Porosity	3	–	–	–

SITE 545 HOLE CORE 65 CORED INTERVAL 607.0–616.5 m sub-bottom

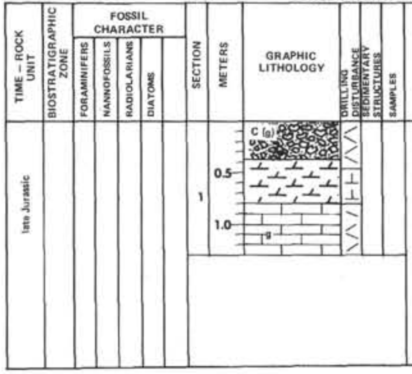

LITHOLOGIC DESCRIPTION

At 0–38 and 113–129 cm: highly fragmented LIMESTONE BRECCIA very pale orange (10YR 8/2) fragments of grainstone and very light gray (N8) coral debris in a moderate yellowish brown (10YR 4/2) dolomite matrix.

At 38–80 cm: moderately fragmented moderate yellowish brown (10YR 5/4), moderate red (5R 5/4), pale reddish brown (10R 5/4) pale red (10R 6/2) DOLOSTONE showing components, irregular color banding and black blebs.

At 80–90 cm: coarse GRAINSTONE with angular clasts of pelsparite, coral debris and coated grains in a sparry matrix.

At 90–113 cm: fine-grained grayish yellow (5Y 8/4) to yellowish gray (5Y 7/2) DOLOSTONE with calcareous particles. Occurrence of moderate yellowish brown (10YR 4/2) dolomite veins and moderate red (5R 5/4) stylolites.

SITE 545 HOLE CORE 66 CORED INTERVAL 616.5–626.0 m sub-bottom

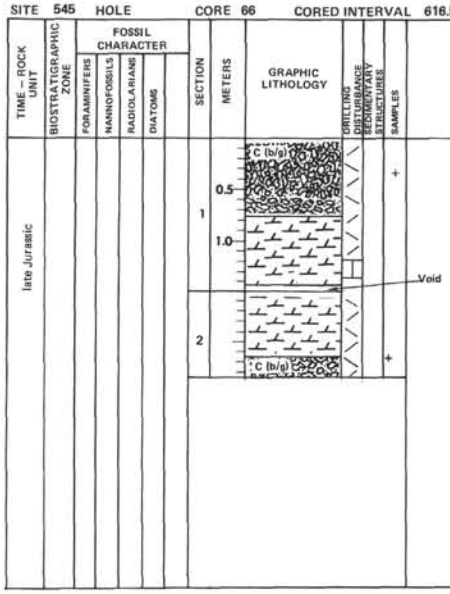

LITHOLOGIC DESCRIPTION

Section 1, 0–73 cm; Section 2, 67–87 cm highly fragmented yellowish gray (5Y 7/2) LIMESTONE BRECCIA with near reef rock fragments: boundstone pods pelsparitic intraclasts, coated grains in a grayish orange (10YR 7/2) dolomite matrix; high porosity.

Section 1, 73–147 cm,; Section 2, 0–67 cm moderately and highly fractured fine grained yellowish gray (5Y 7/2) DOLOMITE. Downwards increasing content of shell fragments, oncoids, and tubiphytes; occasionally solution cavities of dissolved shells; fracturing by stylolitization.

THIN SECTION/PEEL SUMMARY (%):

	1, 39–49	2, 67–69
Texture:		
Rudite	50	50
Arenite	50	Tr
Silt	–	50
Composition:		
Micrite	–	50
Sparite	30	–
Intraclasts	10	–
Ooids	30	–
Peloids	Tr	–
Skeletal grains:		
Crinoids	20	Tr
Bivalves	10	–
Serpulids	–	50
Bryozoan fragments	Tr	–

SITE 545 HOLE CORE 67 CORED INTERVAL 626.0–635.5 m sub-bottom

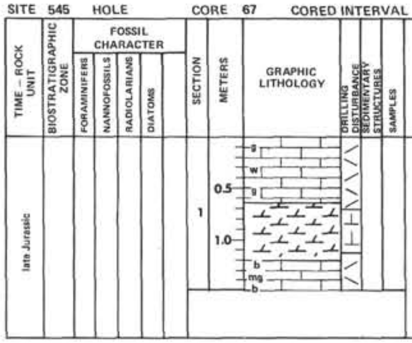

LITHOLOGIC DESCRIPTION

At 0–17, 41–65, and 136–141 cm highly fragmented very pale orange (10YR 8/2) SKELETAL GRAINSTONE with coated shallow water bioclasts and intraclasts in a sparry matrix.

At 17–41 and 141–143 cm highly fragmented grayish yellow green (5GY 7/2) MICROSPARITE.

At 65–119 cm moderately fragmented dark yellowish orange (10YR 6/6) mm scale laminated DOLOMITE. Dolomicrospar with 30–40% calcite microspar, lamination generated by FeS stained interlayers.

At 119–133 and 143–150 cm highly fragmented very pale orange (10YR 8/2) SKELETAL BOUNDSTONE (clast?): corals of thecosmilia-type in pelmicritic sediment with shell debris of bivalves.

SITE 545 HOLE CORE 68 CORED INTERVAL 635.5–645.0 m sub-bottom

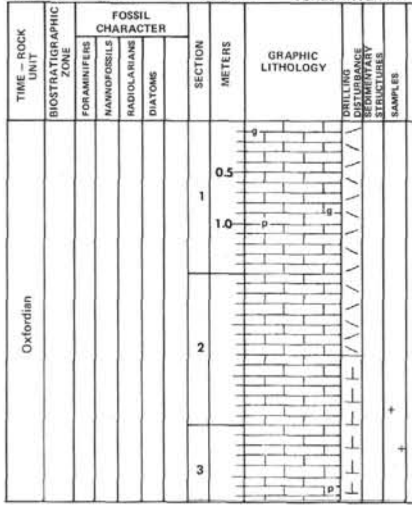

LITHOLOGIC DESCRIPTION

Section 1, 0–96 cm highly fragmented very pale orange (10YR 8/2) dolomitized SKELETAL GRAINSTONE with shallow water components: *coral fragments, echinoderm remains, peloids.*

Section 1, 96–150 cm; Section 2; and Section 3 moderately fragmented very pale orange (10YR 8/2) dolomitized SKELETAL PACKSTONE with shallow water components in pelmicritic matrix: coral fragments, *echinoderm fragments, serpulids, shell debris of gastropods* and bivalves; occasionally thin layers of coarser bioclasts.

At Section 1, 96–105 cm occurrence of veins filled with light brown (5YR 6/4) dolomitic clay.

THIN SECTION/PEEL SUMMARY (%):

	2, 134–139	3, 24–28
Texture:		
Arenite	45	80
Silt	55	20
Composition:		
Micrite	55	–
Sparite	–	20
Skeletal grains:		
Crinoids	40	70
Bivalves	5	5
Coral fragments	–	5

SITE 545 HOLE CORE 69 CORED INTERVAL 645.0–654.5 m sub-bottom

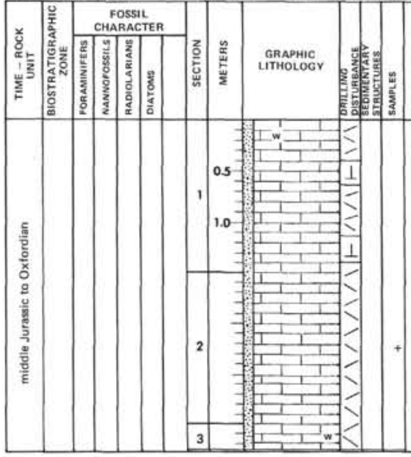

LITHOLOGIC DESCRIPTION

Highly to moderately fragmented dark yellowish orange (10YR 8/6) to very pale orange (10YR 8/2) SANDY DOLOMITIZED SKELETAL WACKESTONE. Coated shallow water bioclasts (corals, echinoderms, serpulids, shell fragments of bivalves and ammonites) in a matrix of pelmicritic sediment.

From Section 2, 80 cm downwards occurrence of angular terrigenous quartz grains.

THIN SECTION/PEEL SUMMARY (%):

	2, 79–83
Texture:	
Arenite	25
Silt	75
Composition:	
Micrite	70
Skeletal grains:	
Crinoids	10
Serpulids	5
Quartz grains	10
Dolomite	5

SITE 545 HOLE CORE 70 CORED INTERVAL 654.5–664.0 m sub-bottom

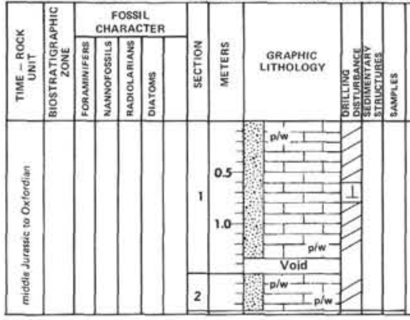

LITHOLOGIC DESCRIPTION

Moderately to slightly fragmented very pale orange (10YR 8/2) to grayish orange (10YR 7/4) and yellowish gray (5Y 7/2) SLIGHTLY SANDY DOLOMITIZED SKELETAL PACKSTONE and SKELETAL WACKESTONE with terrigenous components: angular clasts of terrigenous quartz and feldspar (minor) and echinoderm remains, ammonite and bivalve shells in pelmicritic matrix.

Section 1, 44–76 cm light brown (5YR 5/6) and light olive gray (5Y 5/2) interval of MUDDY SKELETAL PACKSTONES and MUDDY SKELETAL WACKESTONE with increasing content of reworked dolomitized limestone clasts downwards.

Section 1, 0–5, 78, and 122 cm pressure solution surfaces.

SITE 545 HOLE CORE 71 CORED INTERVAL 664.0–673.5 m sub-bottom

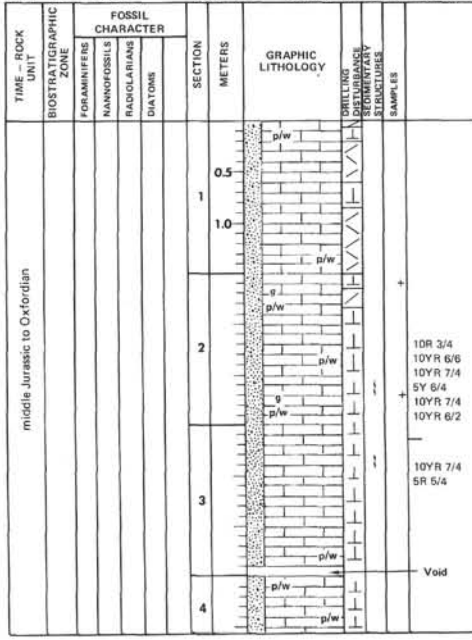

LITHOLOGIC DESCRIPTION

Highly to moderately fragmented yellowish gray (5Y 7/2) to dusky yellow (5Y 6/4) SANDY DOLOMITIZED SKELETAL PACKSTONE and SKELETAL WACKESTONE with terrigenous components: angular quartz grains and feldspar (minor) and echinoderm remains frequently concentrated in layers.

In Section 2, 9–13 and 118–125 cm occurrence of OOLITIC GRAINSTONE with terrigenous quartz grains.

The sediment is slightly burrowed.

THIN SECTION/PEEL SUMMARY (%):

	2, 9–13	2, 119–123
Texture:		
Arenite	70	70
Silt	30	30
Composition:		
Micrite	30	30
Intraclasts	Tr	Tr
Ooids	35	30
Skeletal grains:		
Crinoids	Tr	25
Bivalves	Tr	Tr
Gastropods	–	Tr
Forams	Tr	10
Aptychi	Tr	–
Quartz grains	35	5
Porosity	10	–

SITE 545 HOLE CORE 72 CORED INTERVAL 673.5–682.5 m sub-bottom

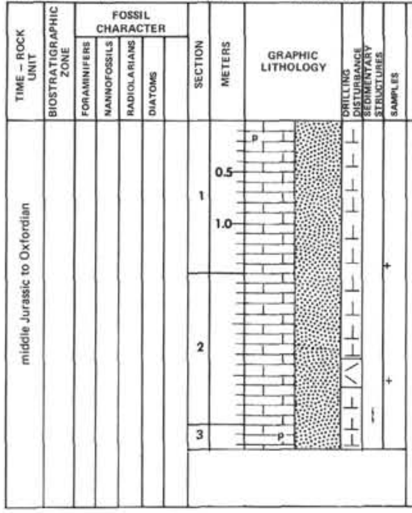

LITHOLOGIC DESCRIPTION

Highly to moderately fragmented pale yellowish brown (10YR 6/2), moderate yellowish brown (10YR 5/4) and grayish red (10R 4/2) to moderate reddish brown (10R 4/6) (patches) VERY SANDY SKELETAL PACKSTONE and VERY CALCAREOUS SANDSTONE. Angular grains of quartz, feldspar, granite, fragments of bivalve and ammonite shells, coated grains and forams in a matrix of pelmicritic sediment.

Section 1, 30–100 cm occurrence of fractures filled with calcite.

Section 2 sediment is burrowed teichichuus and zoophycos at 144–146 cm.

THIN SECTION/PEEL SUMMARY (%):

	1, 142–147	2, 104–108
Texture:		
Arenite	95	75
Silt	5	25
Composition:		
Micrite	5	25
Ooids	20	–
Skeletal grains:		
Crinoids	20	10
Bivalves	5	2
Forams	Tr	2
Quartz grains	50	60

SITE 545 HOLE CORE 73 CORED INTERVAL 682.5–691.5 m sub-bottom

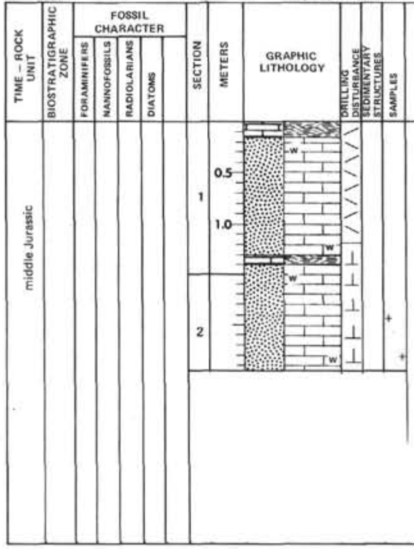

LITHOLOGIC DESCRIPTION

Highly to moderately fragmented light olive gray (5Y 6/1) VERY SANDY WACKESTONE. Angular quartz grains, ooids and bioclasts in a slightly dolomitized pelsparitic matrix.

Section 1, 0–13 and 130–139 cm dark greenish gray (5GY 4/1) soft CALCAREOUS CLAYSTONE.

Section 2, 22 and 43 cm layers of quartz sand.

Section 2, 48–55 cm occurrence of burrowing.

THIN SECTION/PEEL SUMMARY (%):

	2, 49–53	2, 84–88
Texture:		
Arenite	65	5
Silt	35	95
Composition:		
Micrite	35	95
Intraclasts	2	–
Ooids	–	Tr
Skeletal grains:		
Crinoids	10	–
Bivalves	10	1
Ammonites	3	–
Forams	Tr	Tr
Spiculae	Tr	Tr
Dolomite	–	2
Quartz grains	40	3

SITE 545 HOLE CORE 74 CORED INTERVAL 691.5–700.5 m sub-bottom

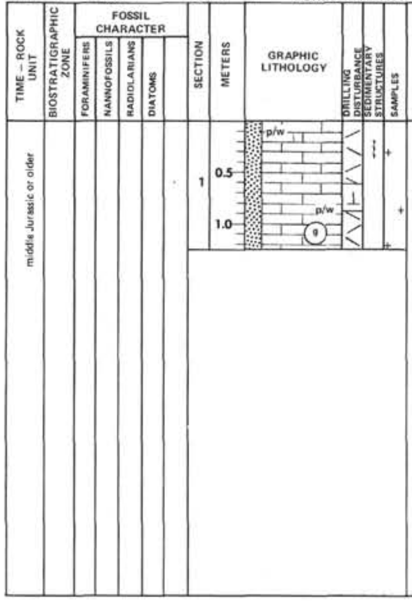

LITHOLOGIC DESCRIPTION

Highly to moderately fragmented medium light gray (N6) SANDY SKELETAL PACKSTONE and WACKESTONE: angular grains of quartz and feldspar, echinoderm remains, foraminifera, ooids, shell fragments of bivalves, gastropods and ammonites in a pelmicritic matrix.

At 20–30 cm sediment is bioturbated.

At 70 cm occurrence of a coal clast.

At 113 cm reworked clasts of skeletal grainstone.

THIN SECTION/PEEL SUMMARY (%):

	1, 30–34	1, 89–94	1, 121–125
Texture:			
Arenite	10	30	90
Silt	90	70	10
Composition:			
Micrite	90	70	10
Sparite	–	–	15
Ooids	Tr	0.5	30
Peloids	–	Tr	–
Skeletal grains:			
Crinoids	–	5	10
Bivalves	2	5	–
Gastropods	–	Tr	–
Forams	Tr	0.5	5
Spiculae	Tr	–	–
Tubiphytes	1	Tr	–
Dolomite	1	–	–
Quartz grains	5	20	30

SITE 545 HOLE CORE 75 CORED INTERVAL 700.5–701.0 m sub-bottom

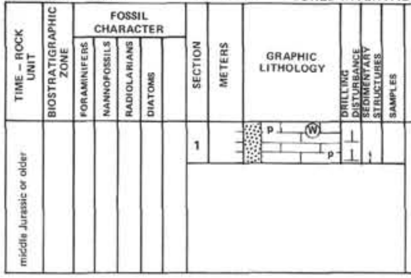

LITHOLOGIC DESCRIPTION

Moderately fragmented medium light gray (N7) bioturbated SANDY SKELETAL PACKSTONE. Angular quartz grains and bioclasts in a pelmicritic matrix.

At 1–3 cm reworked clast of SKELETAL WACKESTONE which shows soft deformation.

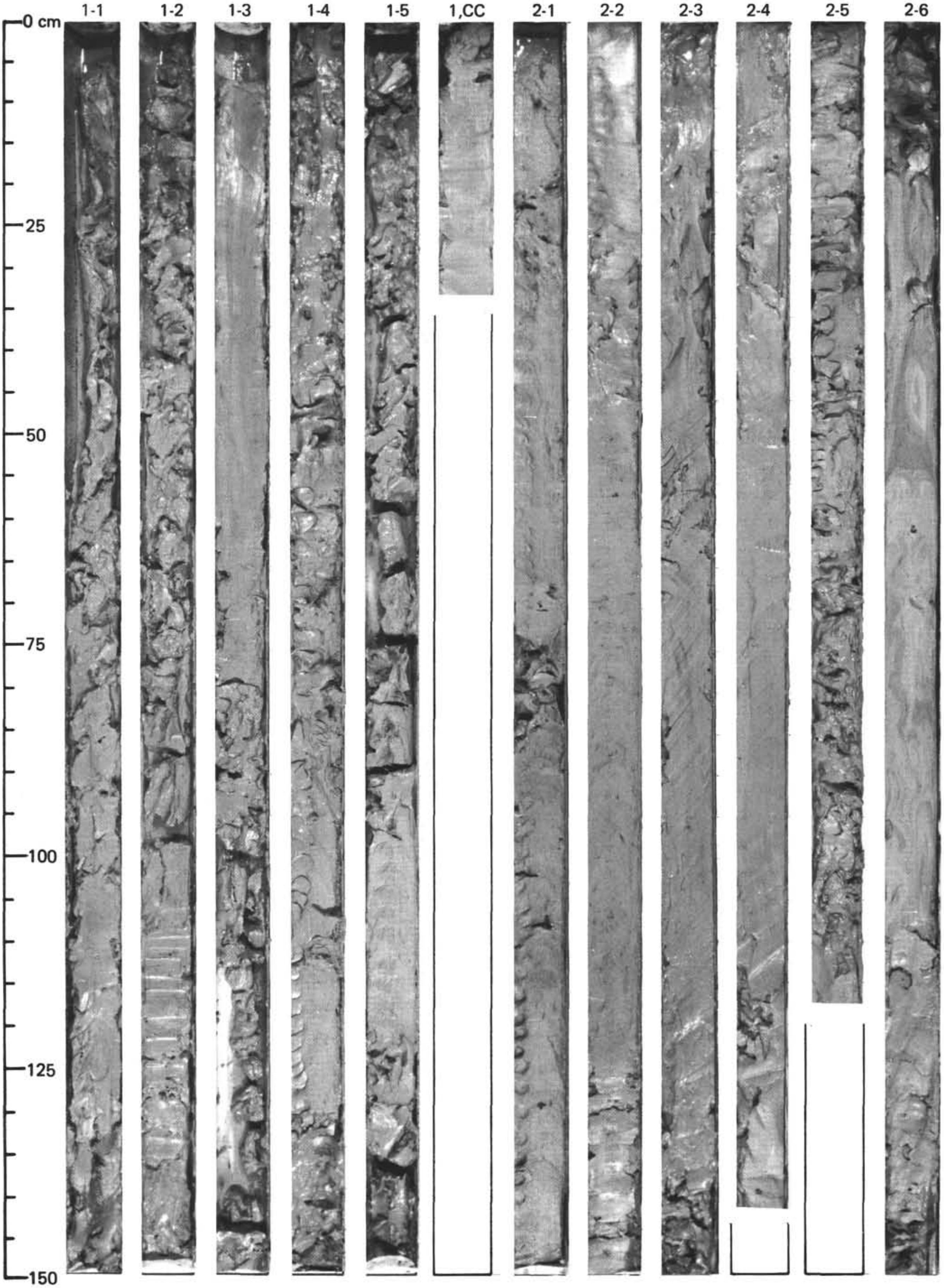
1-1
1-2
1-3
1-4
1-5
1,CC
2-1
2-2
2-3
2-4
2-5
2-6
0 cm
25
50
75
100
125
150

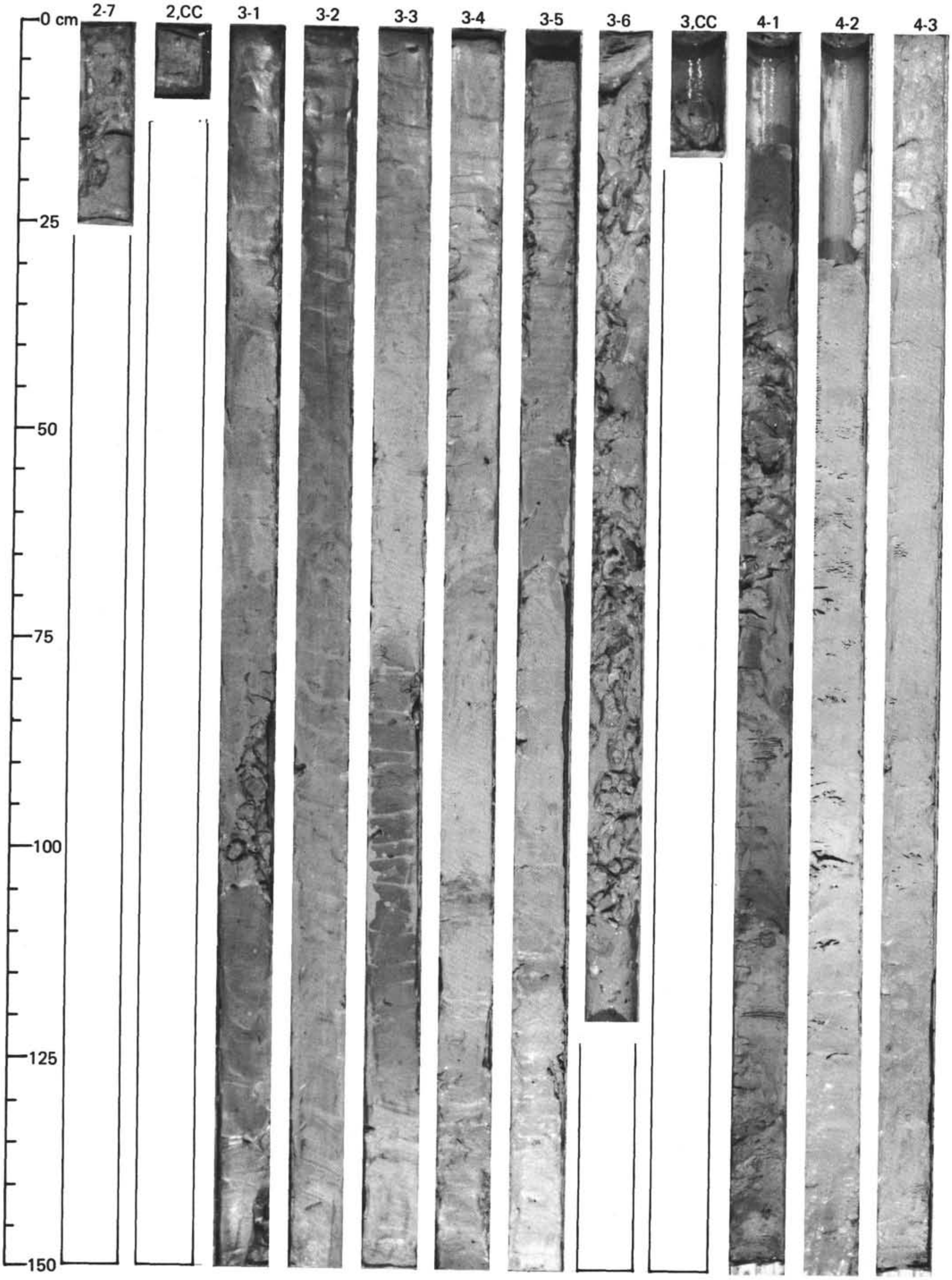
0 cm
25
50
75
100
125
150
2-7
2,CC
3-1
3-2
3-3
3-4
3-5
3-6
3,CC
4-1
4-2
4-3

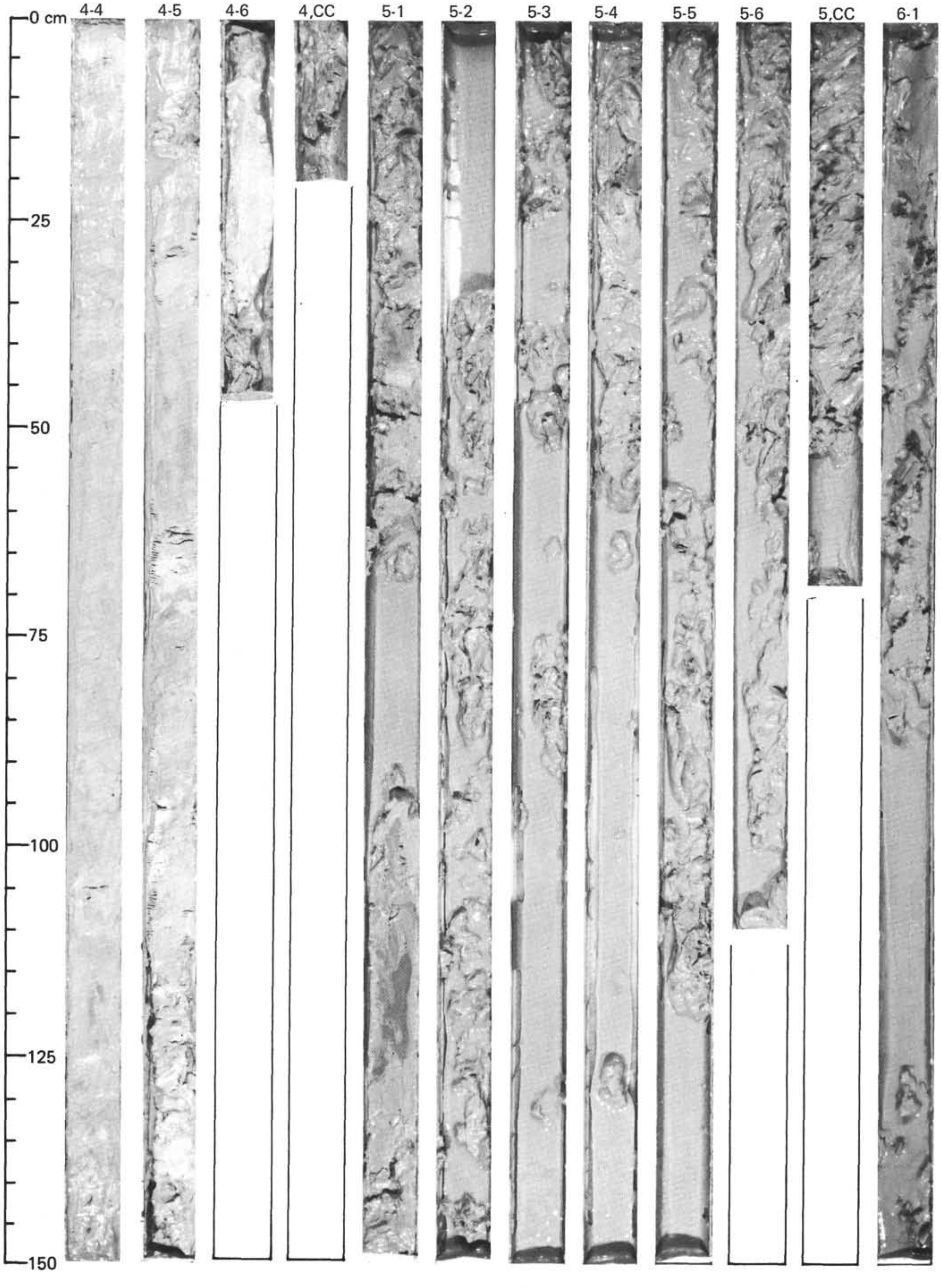
0 cm
25
50
75
100
125
150
4-4
4-5
4-6
4,CC
5-1
5-2
5-3
5-4
5-5
5-6
5,CC
6-1

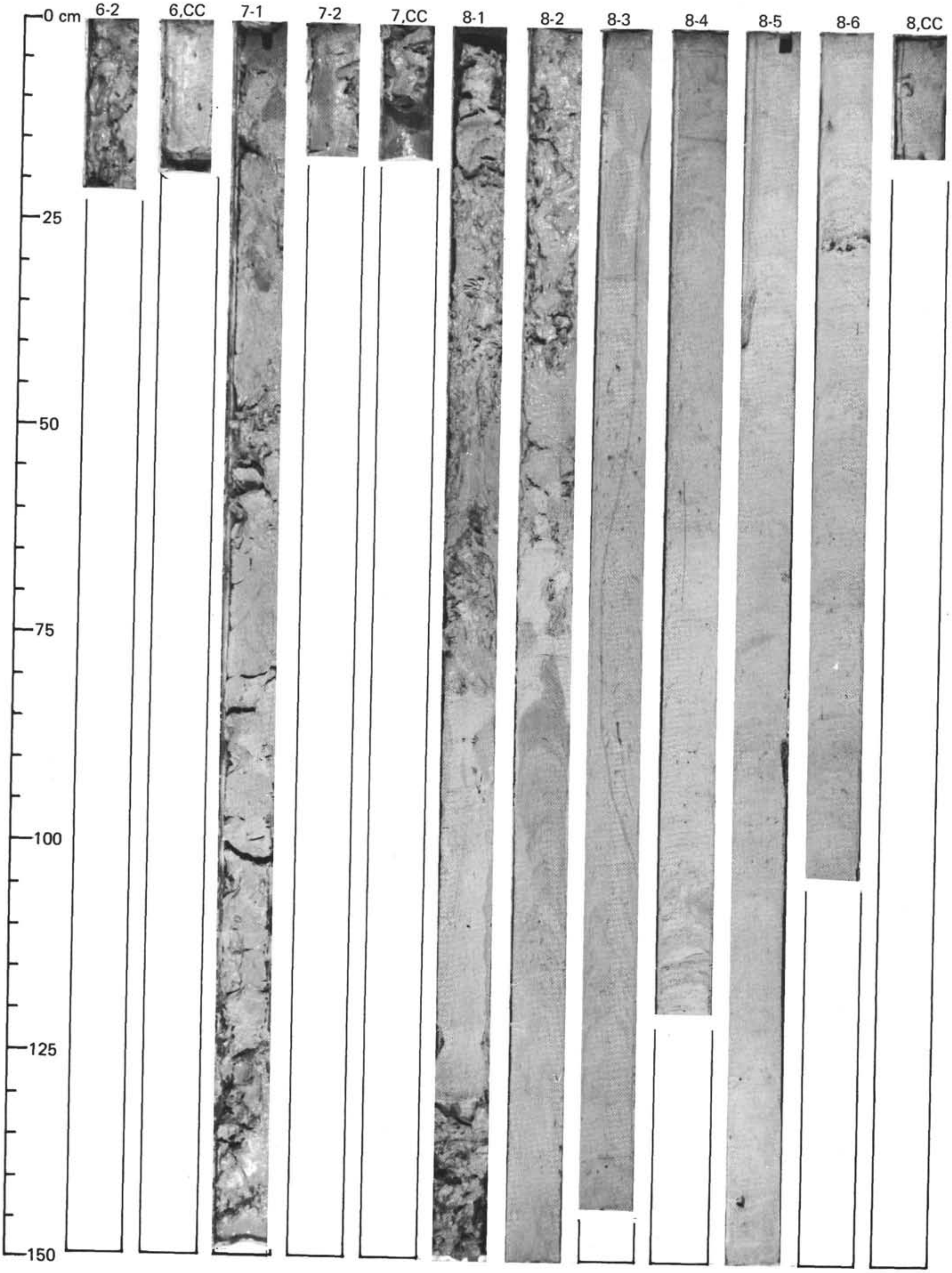
0 cm
25
50
75
100
125
150
6-2
6,CC
7-1
7-2
7,CC
8-1
8-2
8-3
8-4
8-5
8-6
8,CC

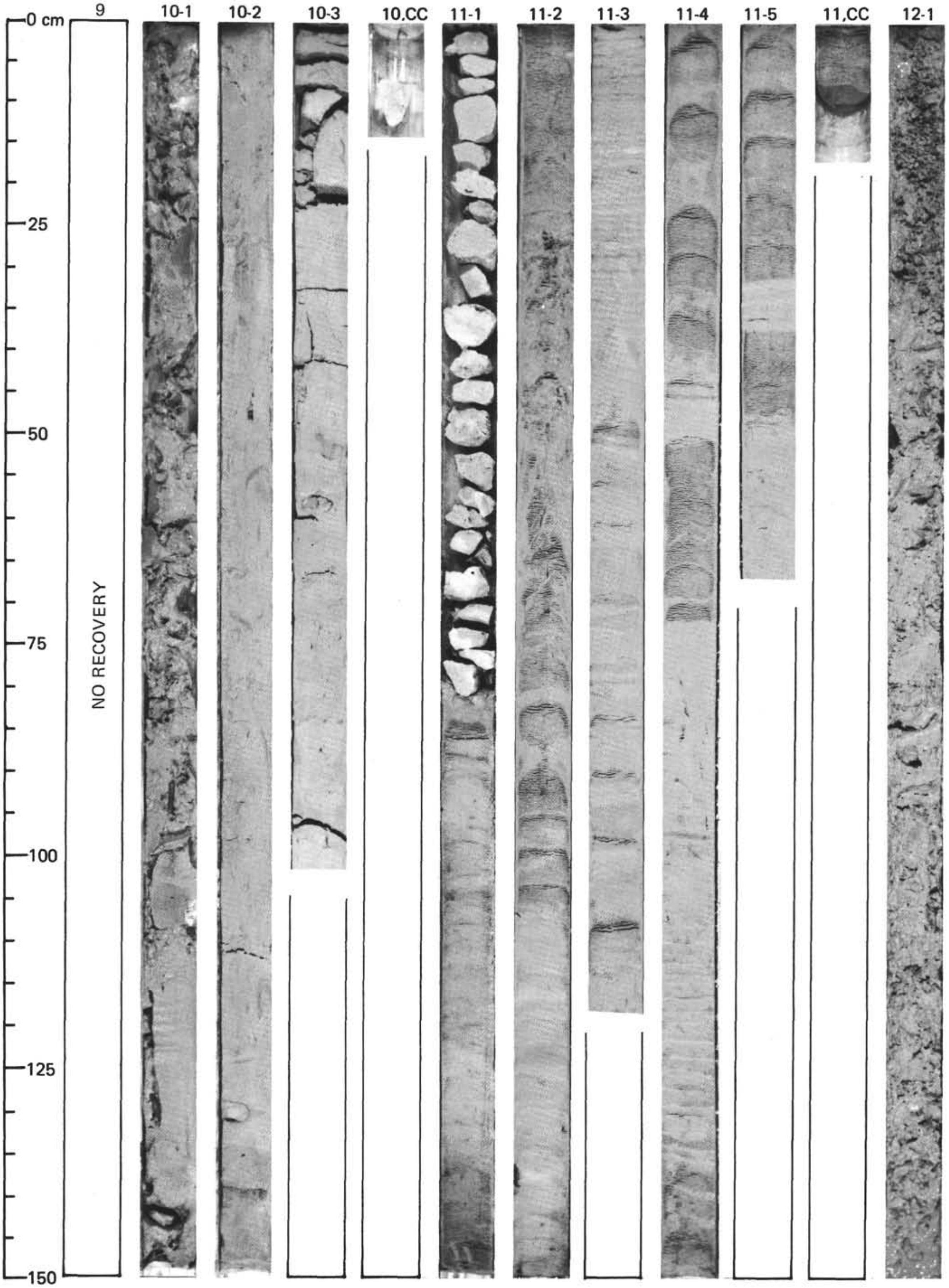
0 cm
25
50
75
100
125
150
9
10-1
10-2
10-3
10,CC
11-1
11-2
11-3
11-4
11-5
11,CC
12-1
NO RECOVERY

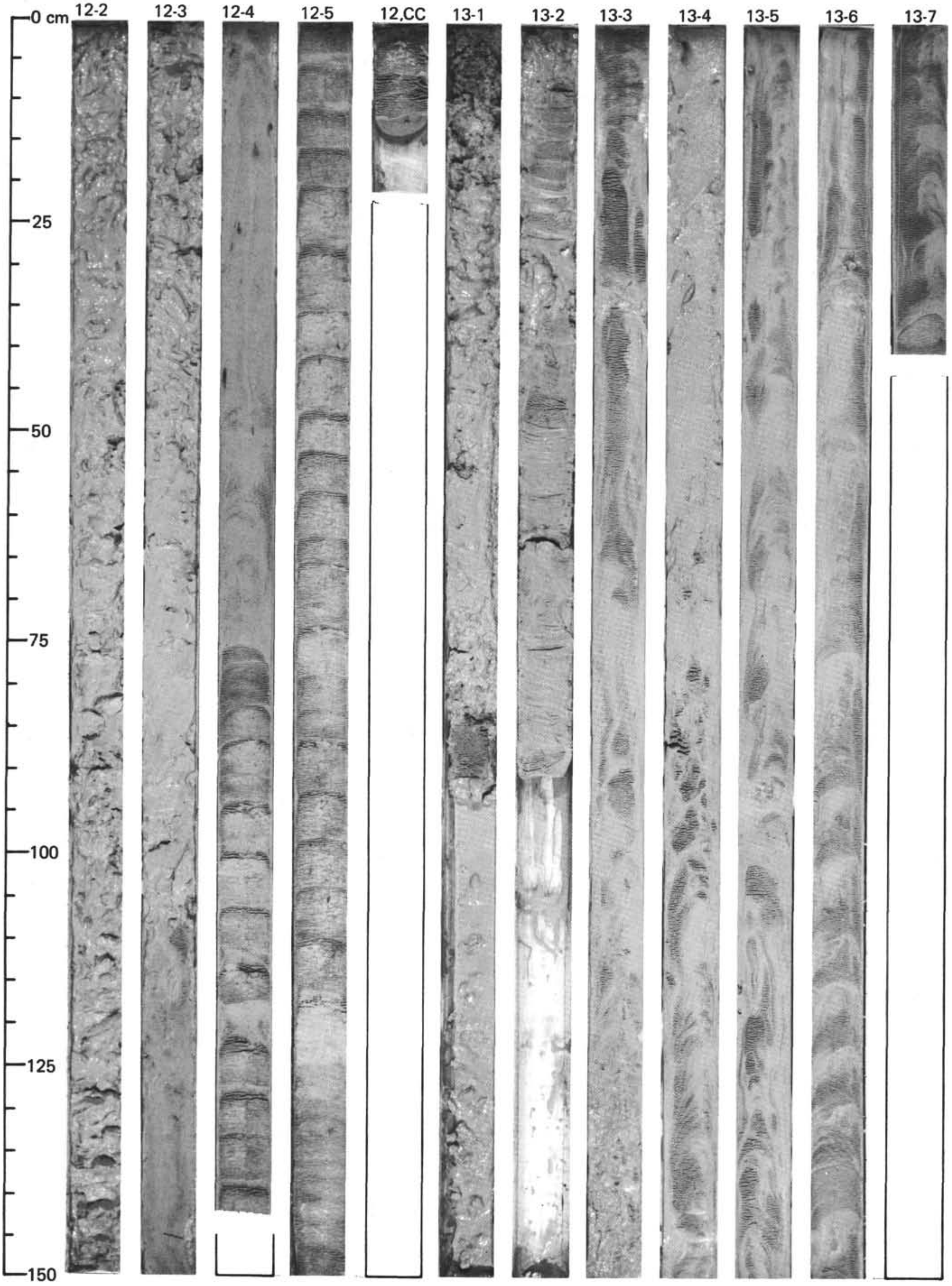
0 cm
25
50
75
100
125
150
12-2
12-3
12-4
12-5
12,CC
13-1
13-2
13-3
13-4
13-5
13-6
13-7

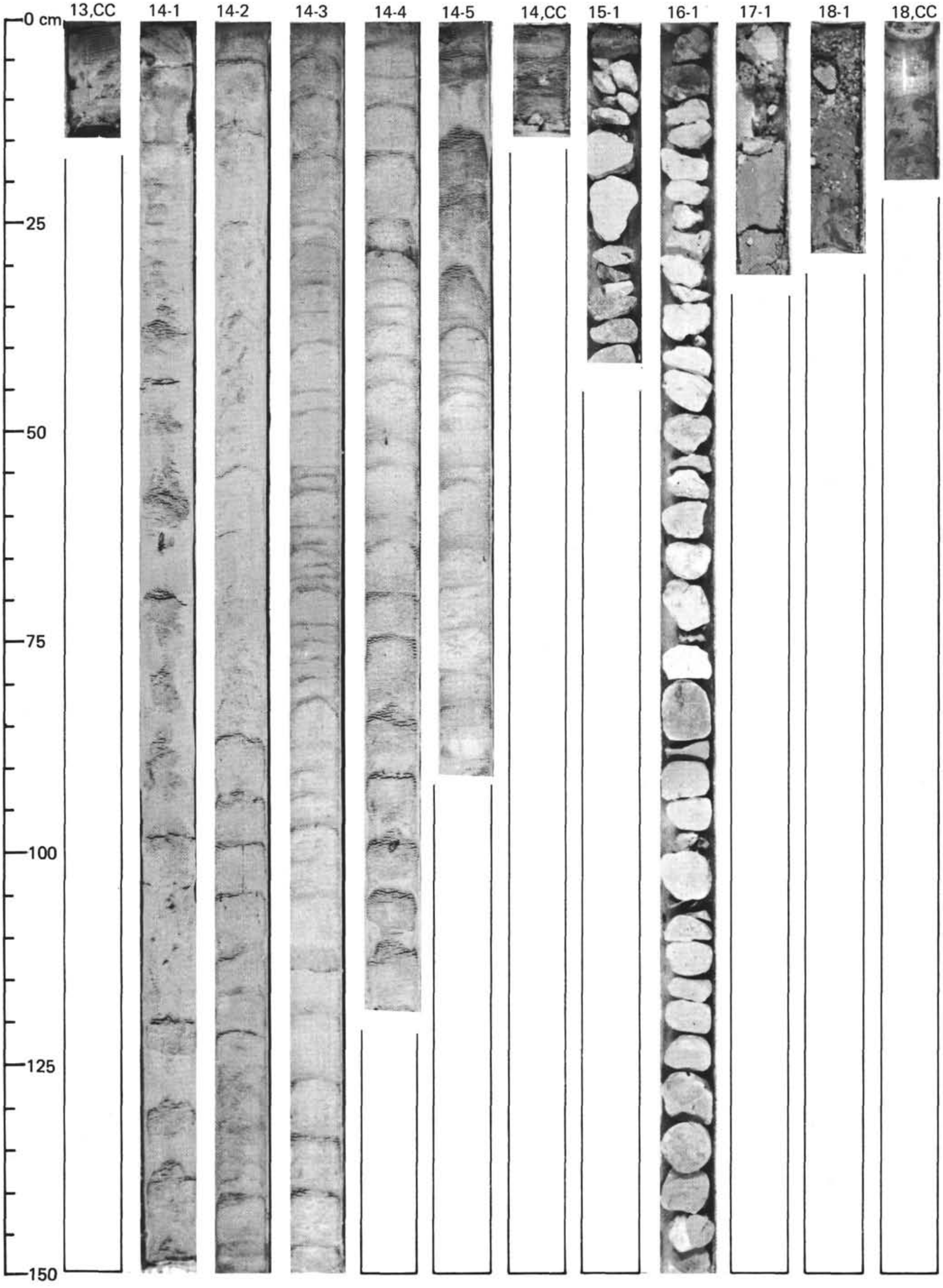
0 cm
25
50
75
100
125
150
13,CC
14-1
14-2
14-3
14-4
14-5
14,CC
15-1
16-1
17-1
18-1
18,CC

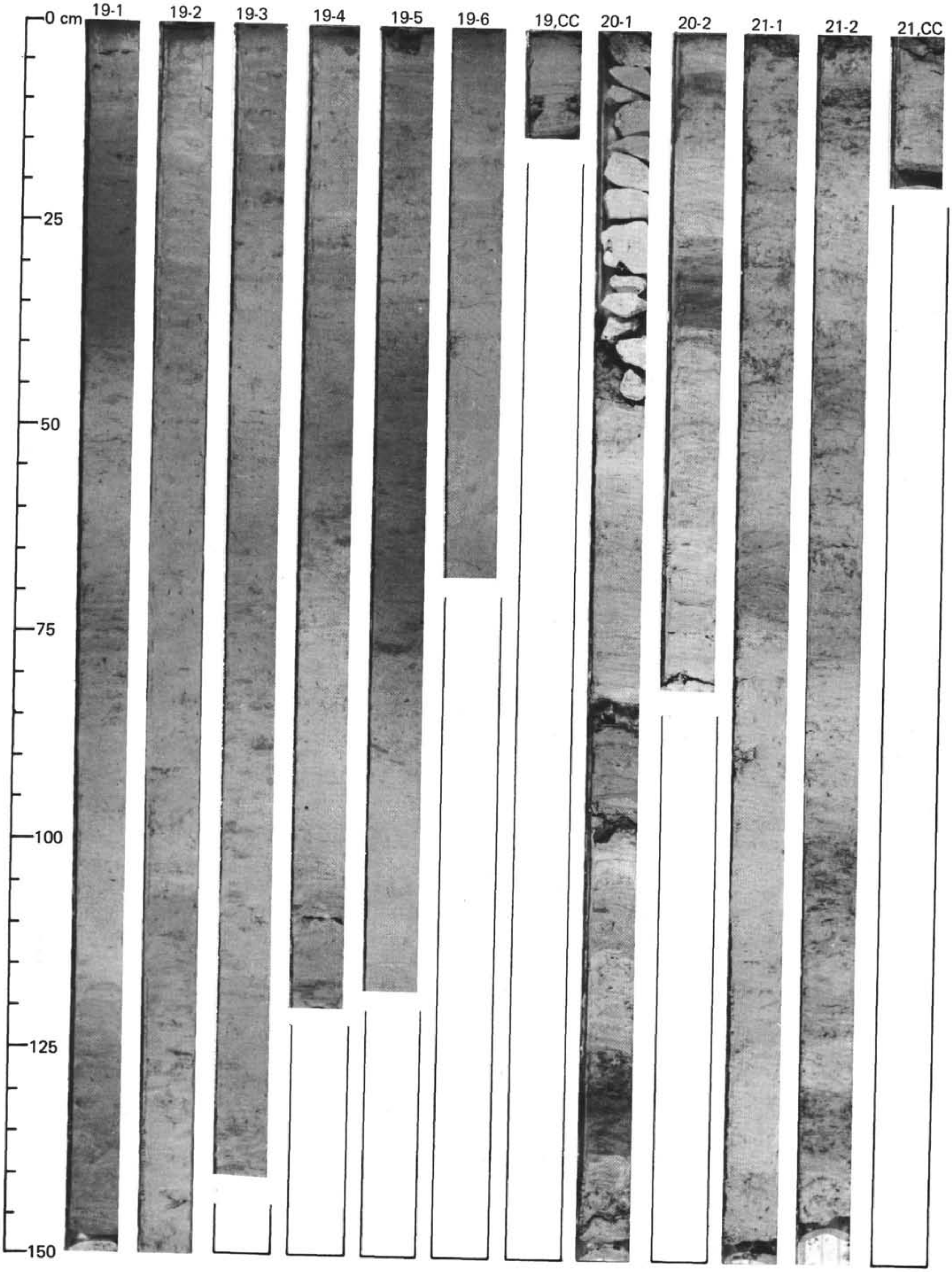
0 cm
25
50
75
100
125
150
19-1
19-2
19-3
19-4
19-5
19-6
19,CC
20-1
20-2
21-1
21-2
21,CC

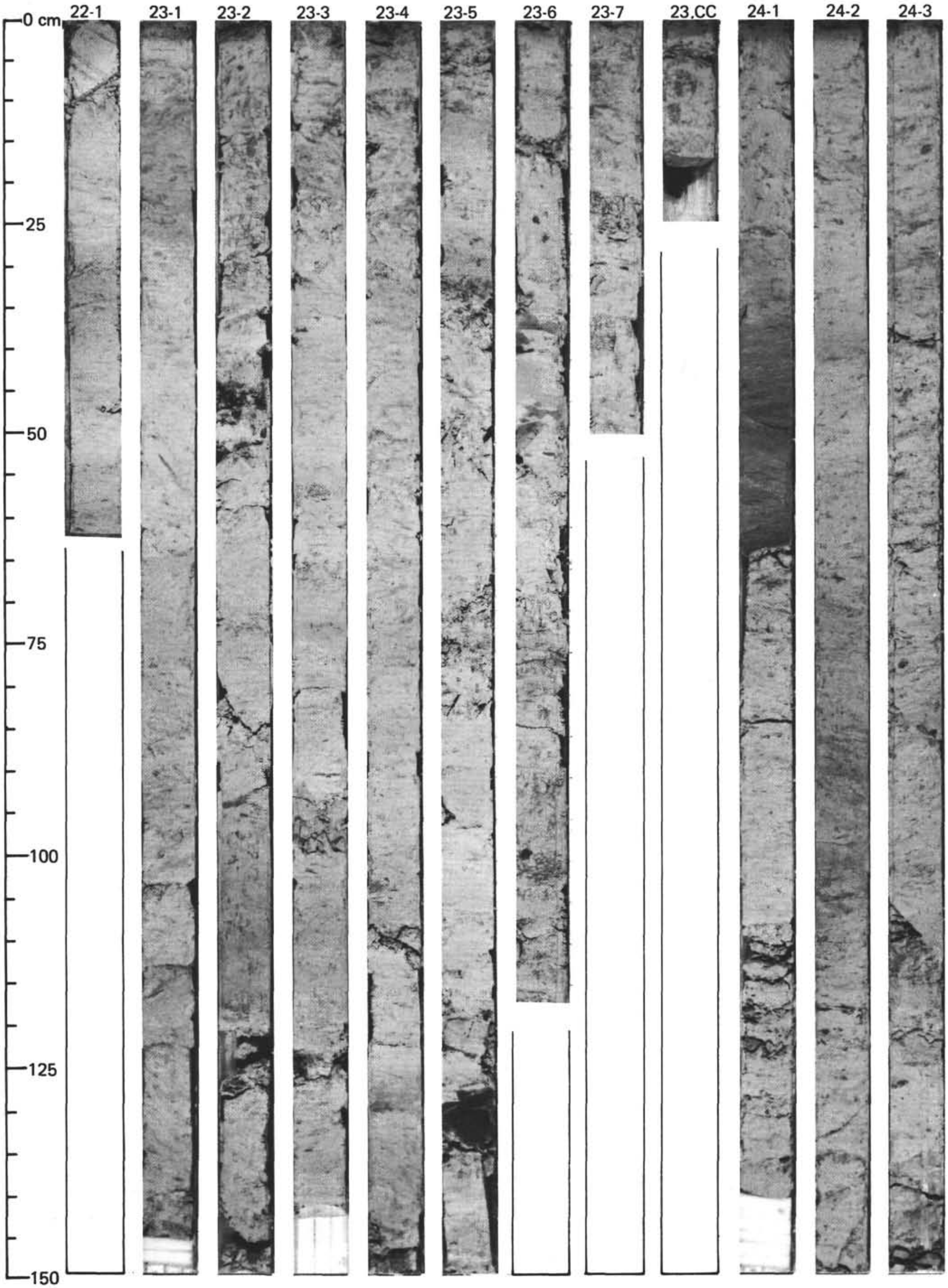
0 cm
25
50
75
100
125
150
22-1
23-1
23-2
23-3
23-4
23-5
23-6
23-7
23,CC
24-1
24-2
24-3

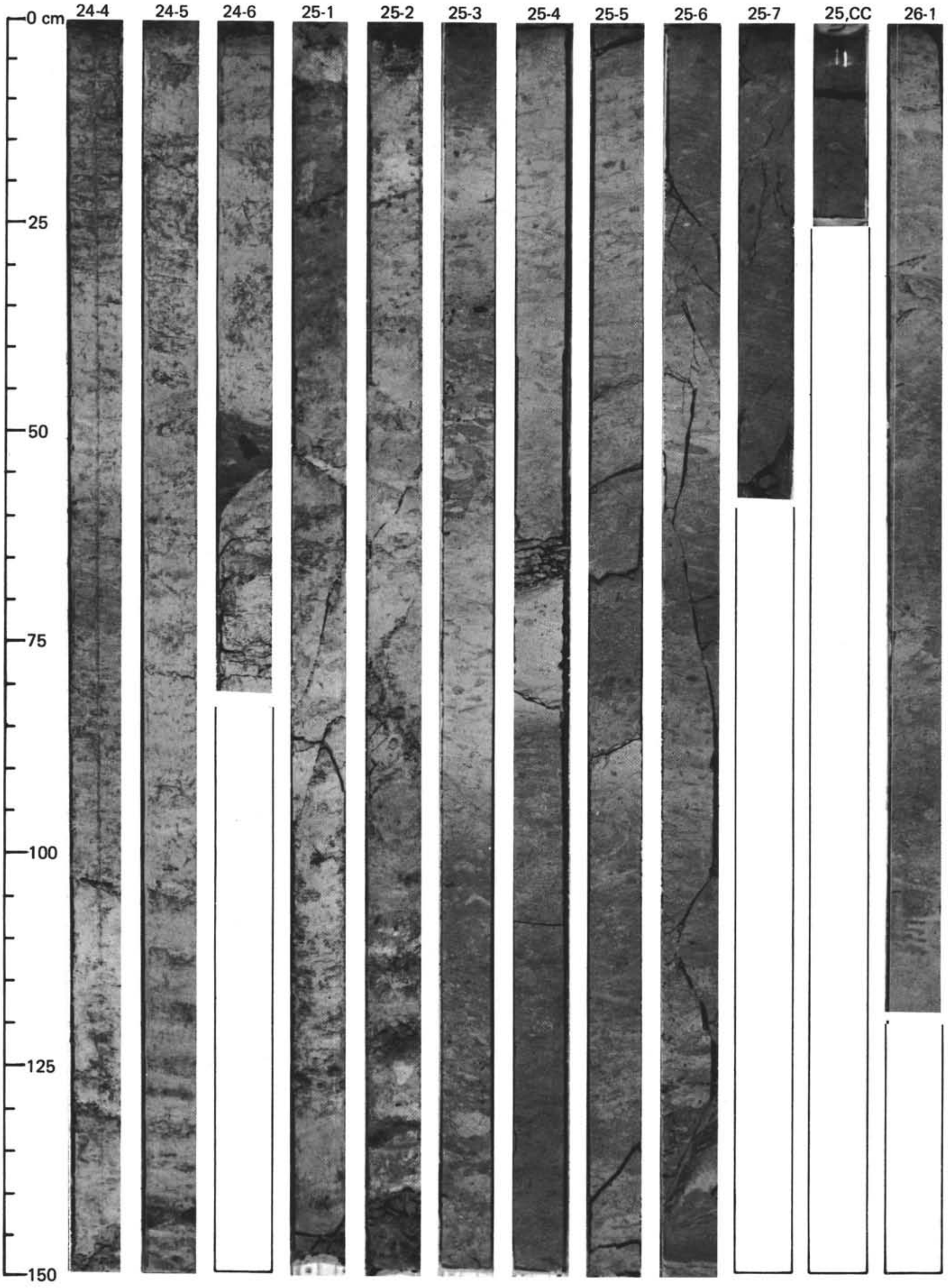
0 cm
25
50
75
100
125
150
24-4
24-5
24-6
25-1
25-2
25-3
25-4
25-5
25-6
25-7
25,CC
26-1

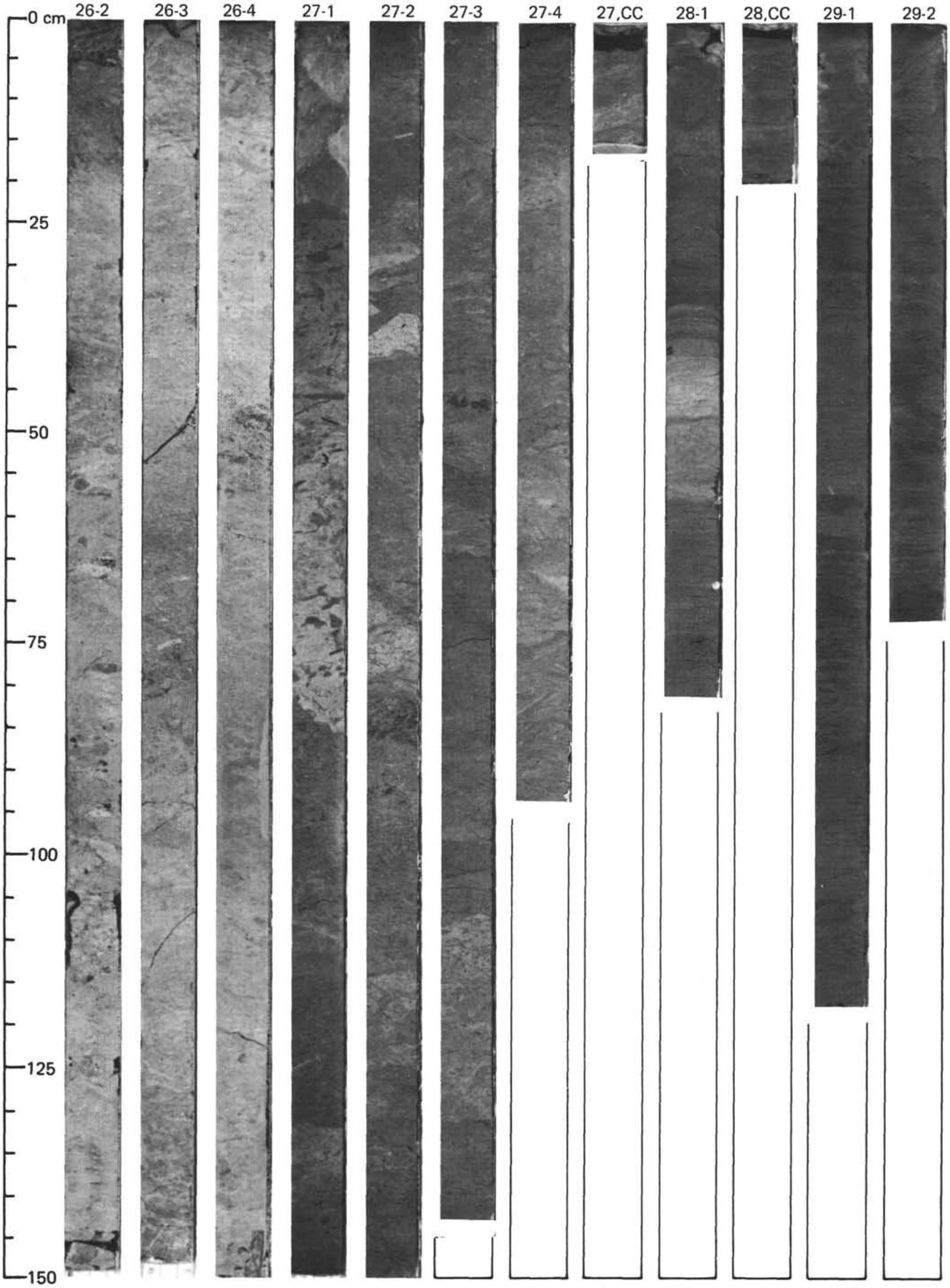
0 cm
25
50
75
100
125
150
26-2
26-3
26-4
27-1
27-2
27-3
27-4
27,CC
28-1
28,CC
29-1
29-2

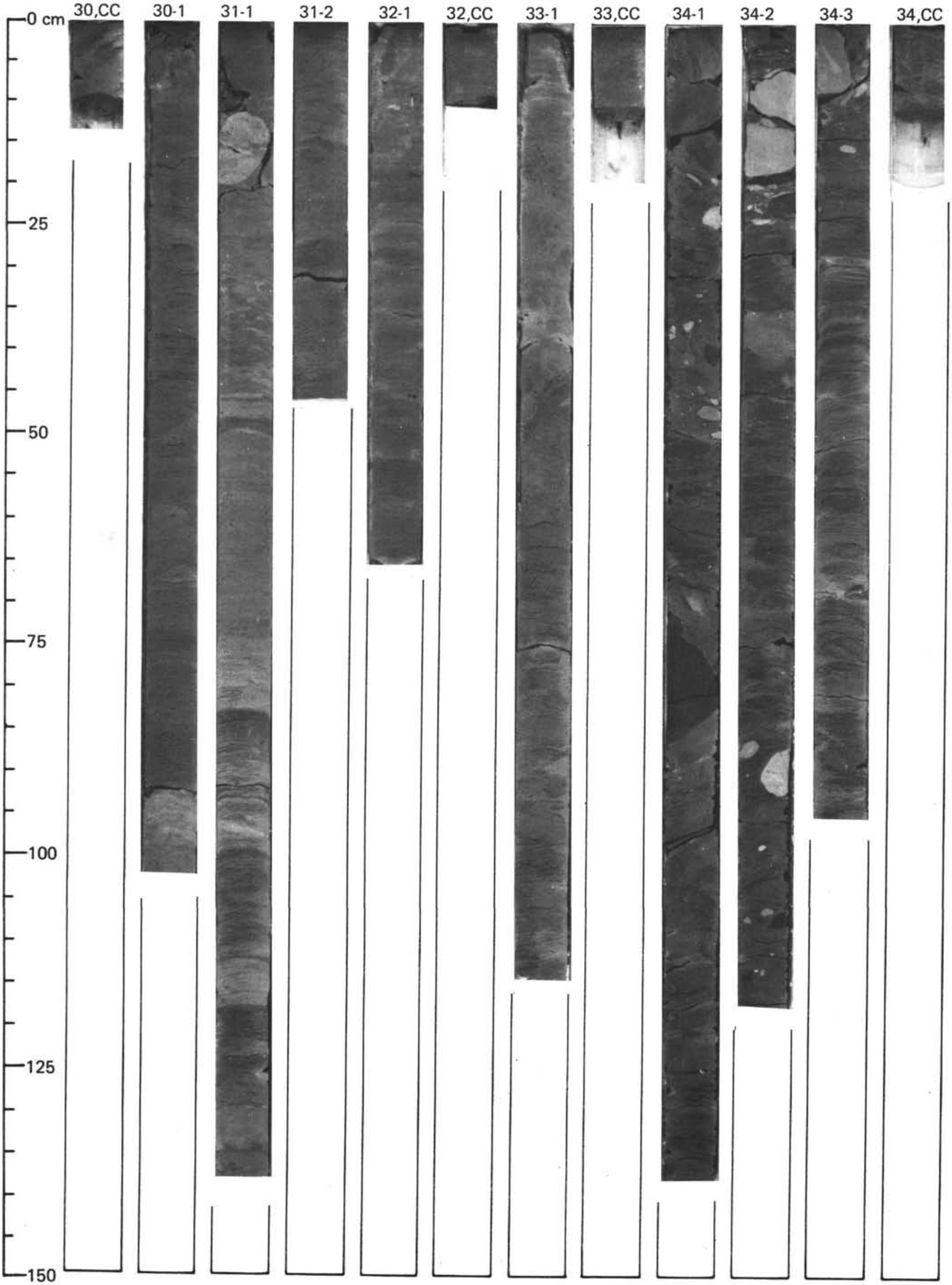
0 cm
25
50
75
100
125
150
30,CC
30-1
31-1
31-2
32-1
32,CC
33-1
33,CC
34-1
34-2
34-3
34,CC


35-1
35-2
35,CC
36-1
36-2
36-3
36,CC
37-1
37-2
37-3
37,CC
38-1
0 cm
25
50
75
100
125
150

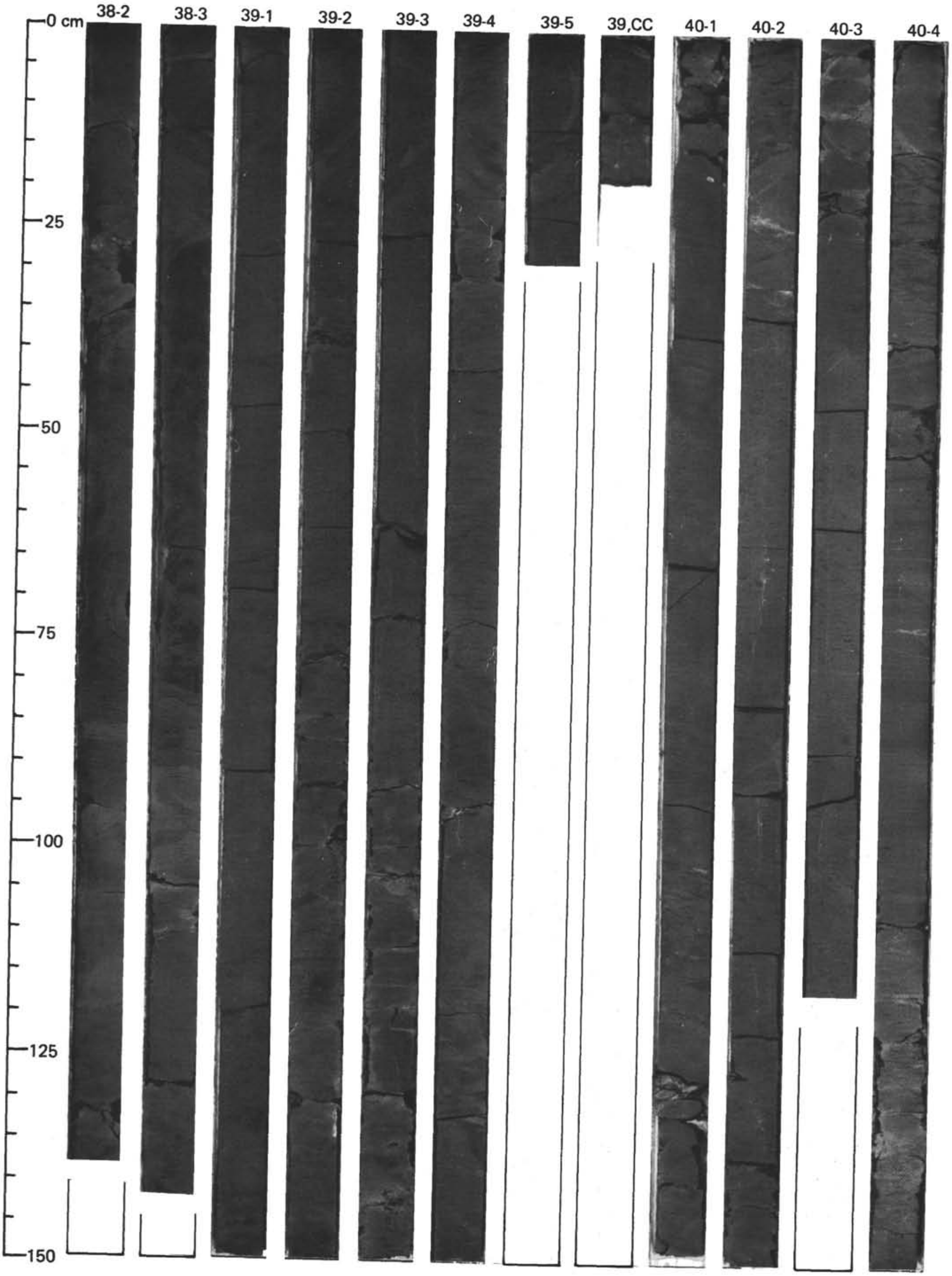
0 cm
25
50
75
100
125
150
38-2
38-3
39-1
39-2
39-3
39-4
39-5
39,CC
40-1
40-2
40-3
40-4

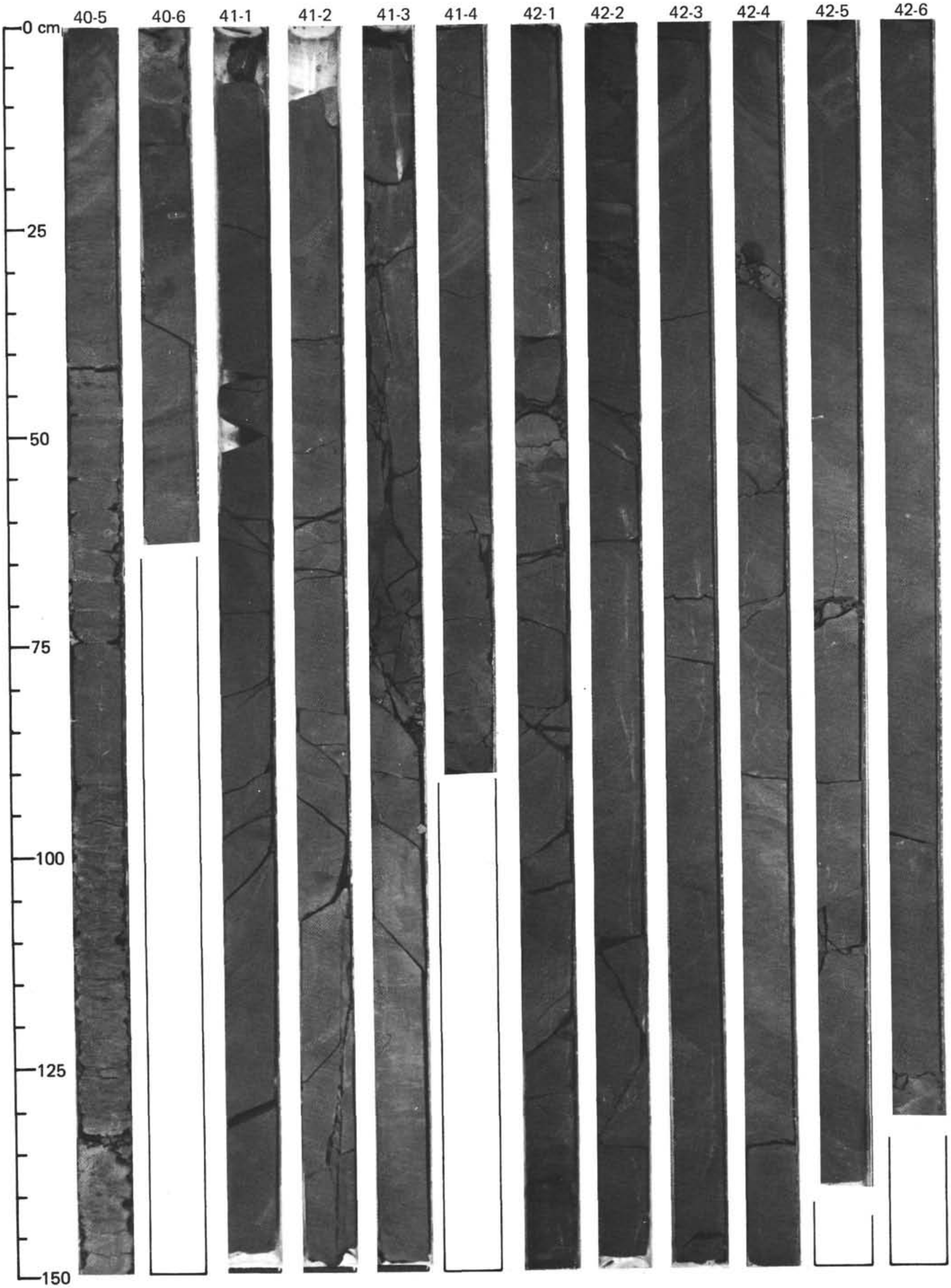
40-5
40-6
41-1
41-2
41-3
41-4
42-1
42-2
42-3
42-4
42-5
42-6
0 cm
25
50
75
100
125
150

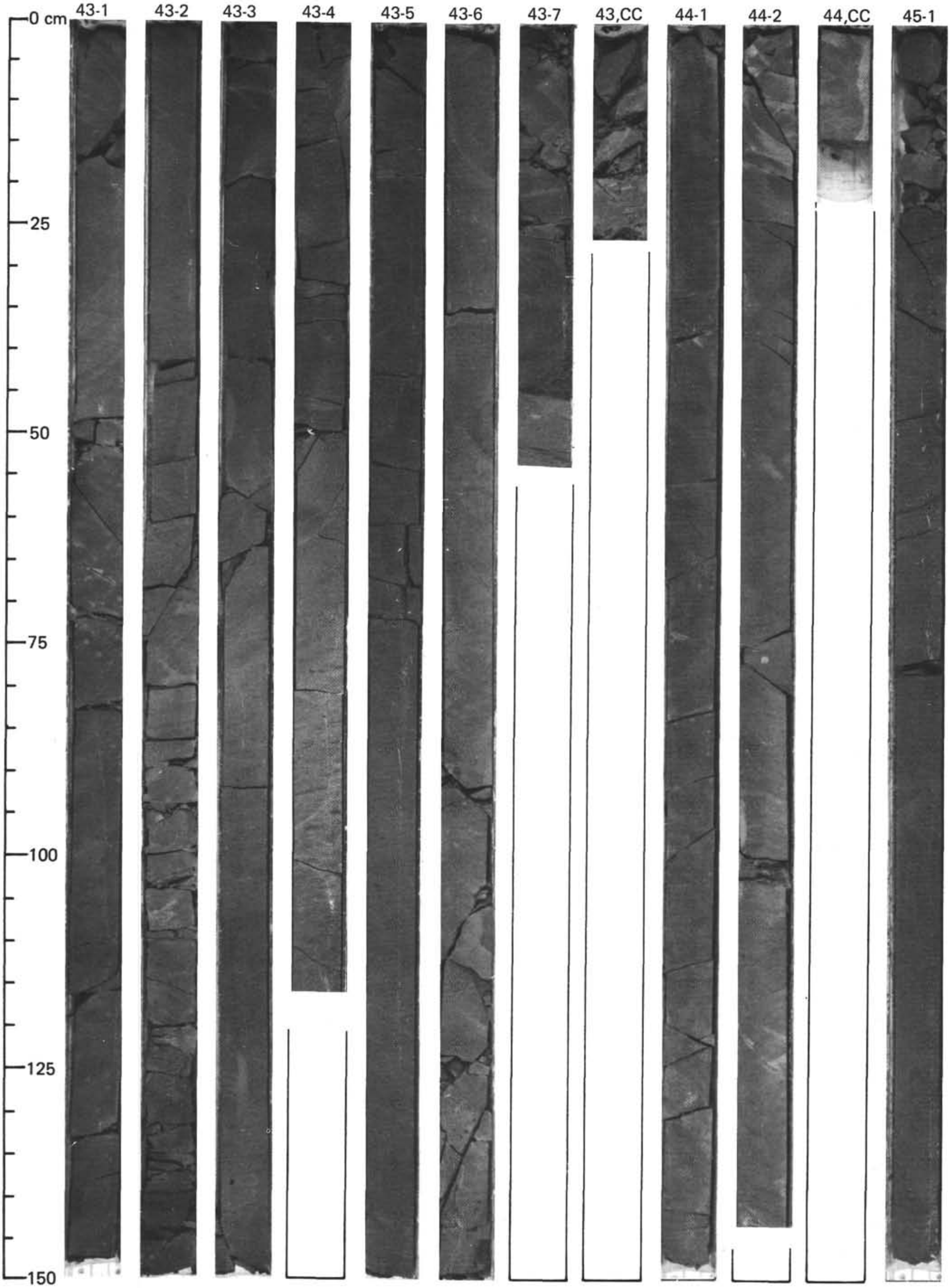
0 cm
25
50
75
100
125
150
43-1
43-2
43-3
43-4
43-5
43-6
43-7
43,CC
44-1
44-2
44,CC
45-1

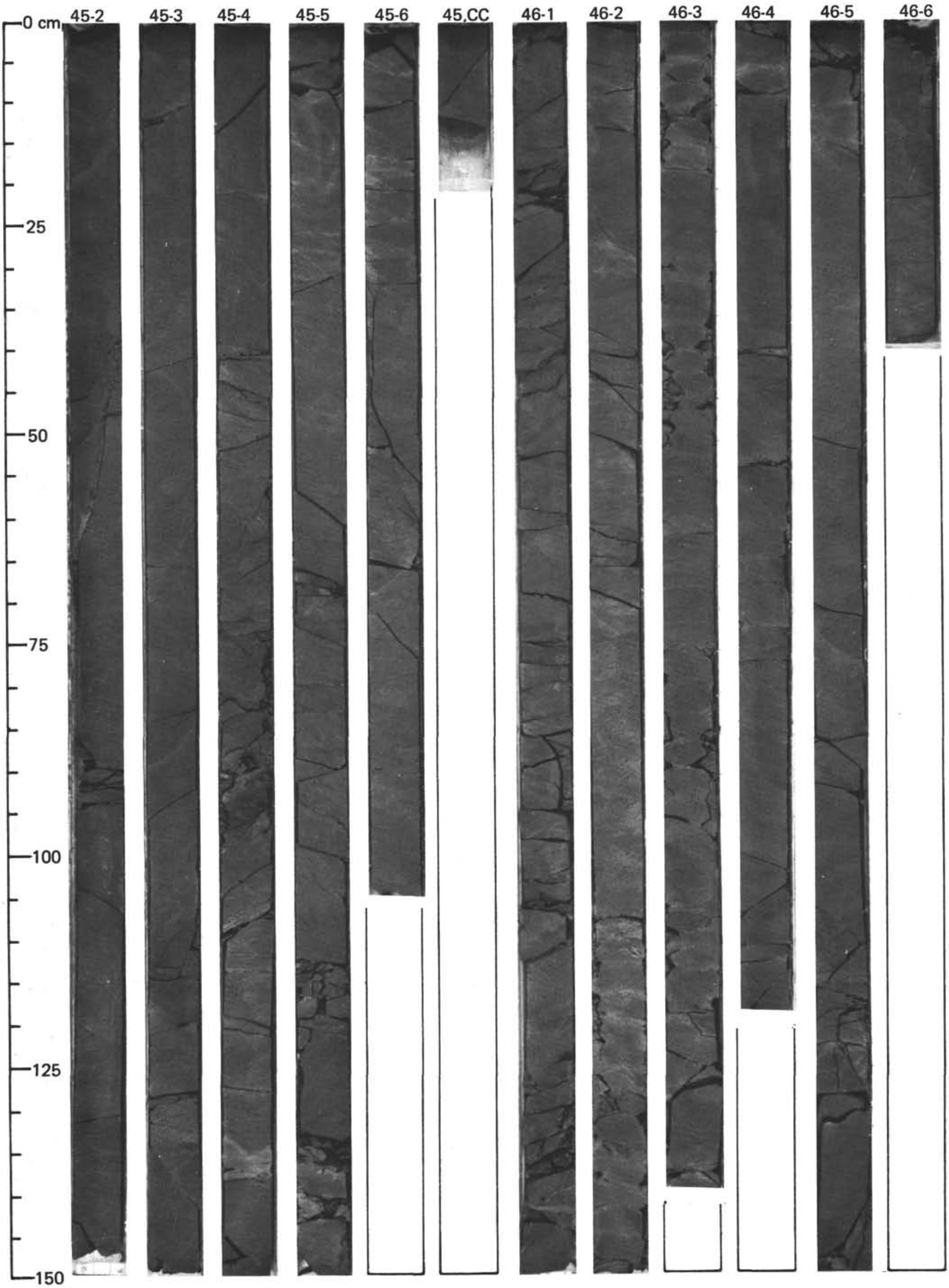
0 cm
25
50
75
100
125
150
45-2
45-3
45-4
45-5
45-6
45,CC
46-1
46-2
46-3
46-4
46-5
46-6

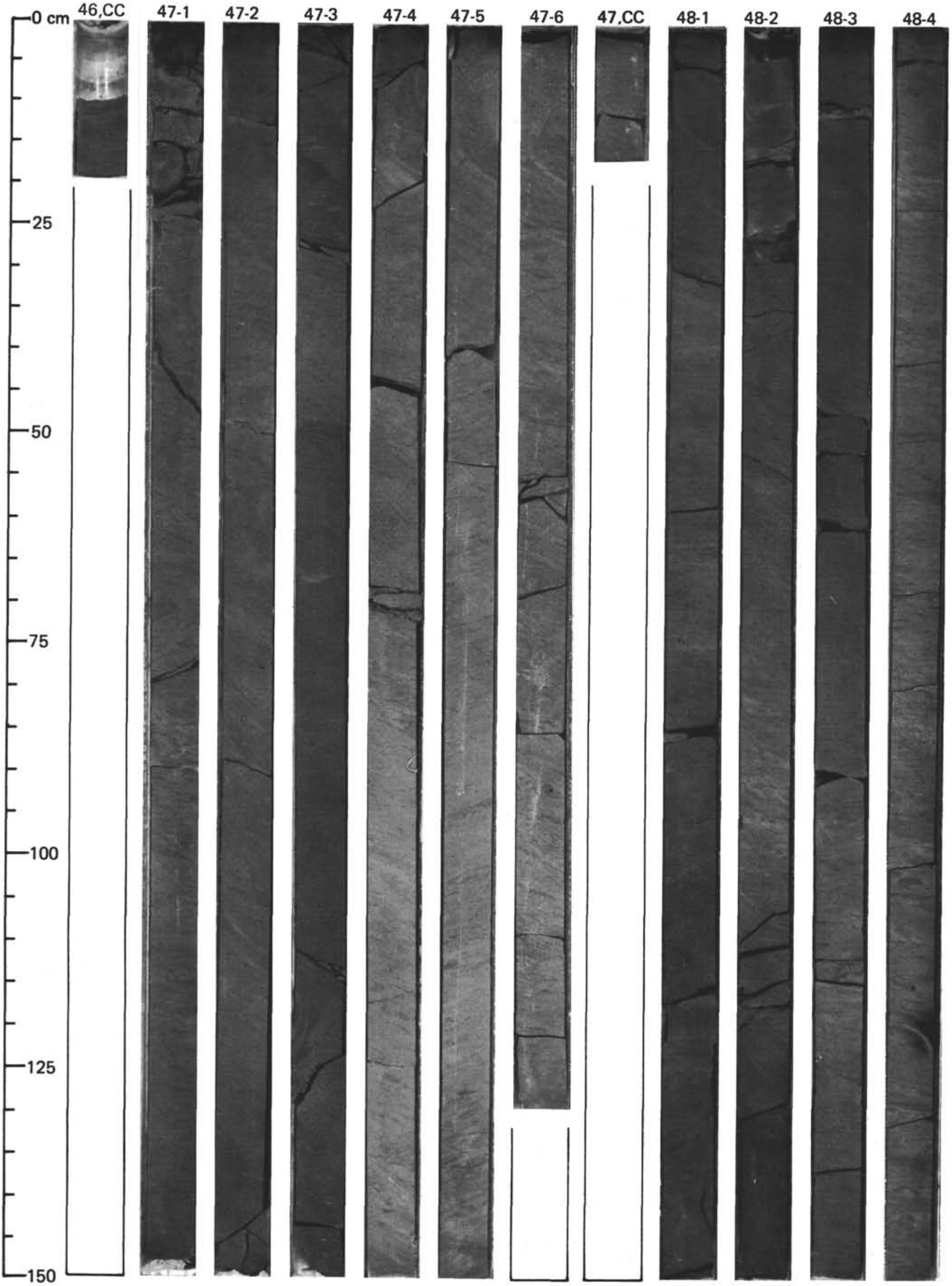
0 cm
25
50
75
100
125
150
46,CC
47-1
47-2
47-3
47-4
47-5
47-6
47,CC
48-1
48-2
48-3
48-4

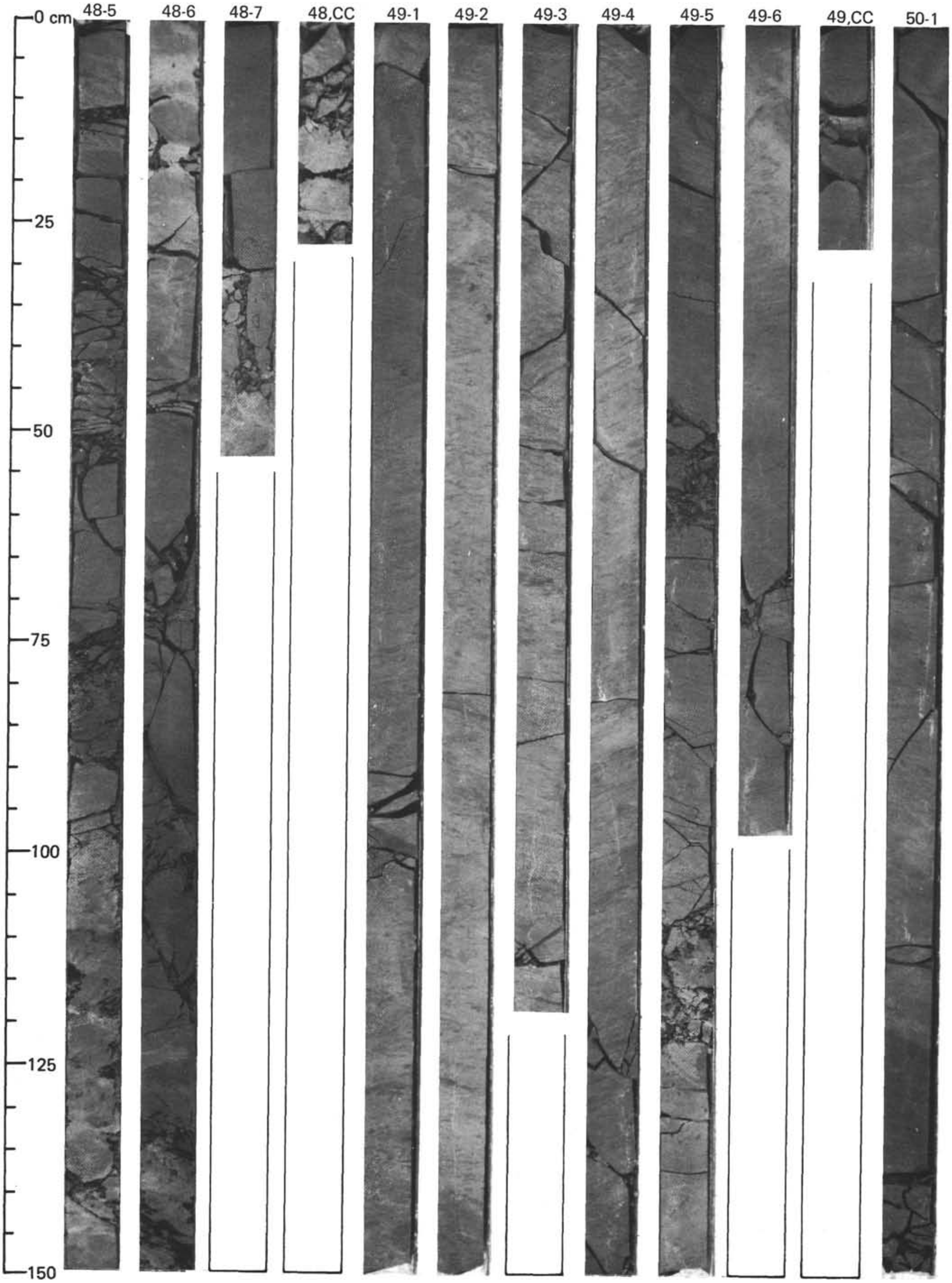
0 cm
25
50
75
100
125
150
48-5
48-6
48-7
48,CC
49-1
49-2
49-3
49-4
49-5
49-6
49,CC
50-1

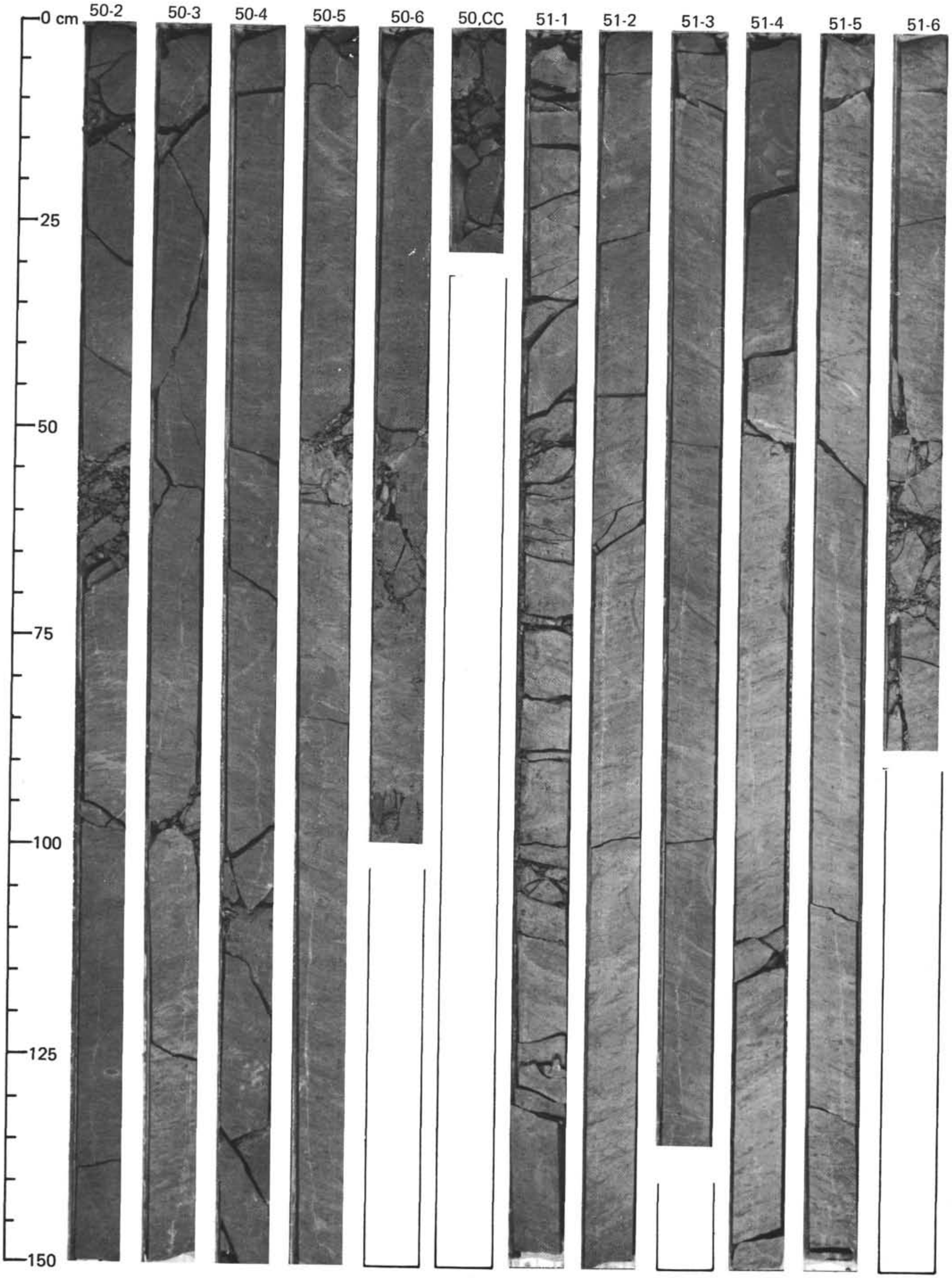
0 cm
25
50
75
100
125
150
50-2
50-3
50-4
50-5
50-6
50,CC
51-1
51-2
51-3
51-4
51-5
51-6

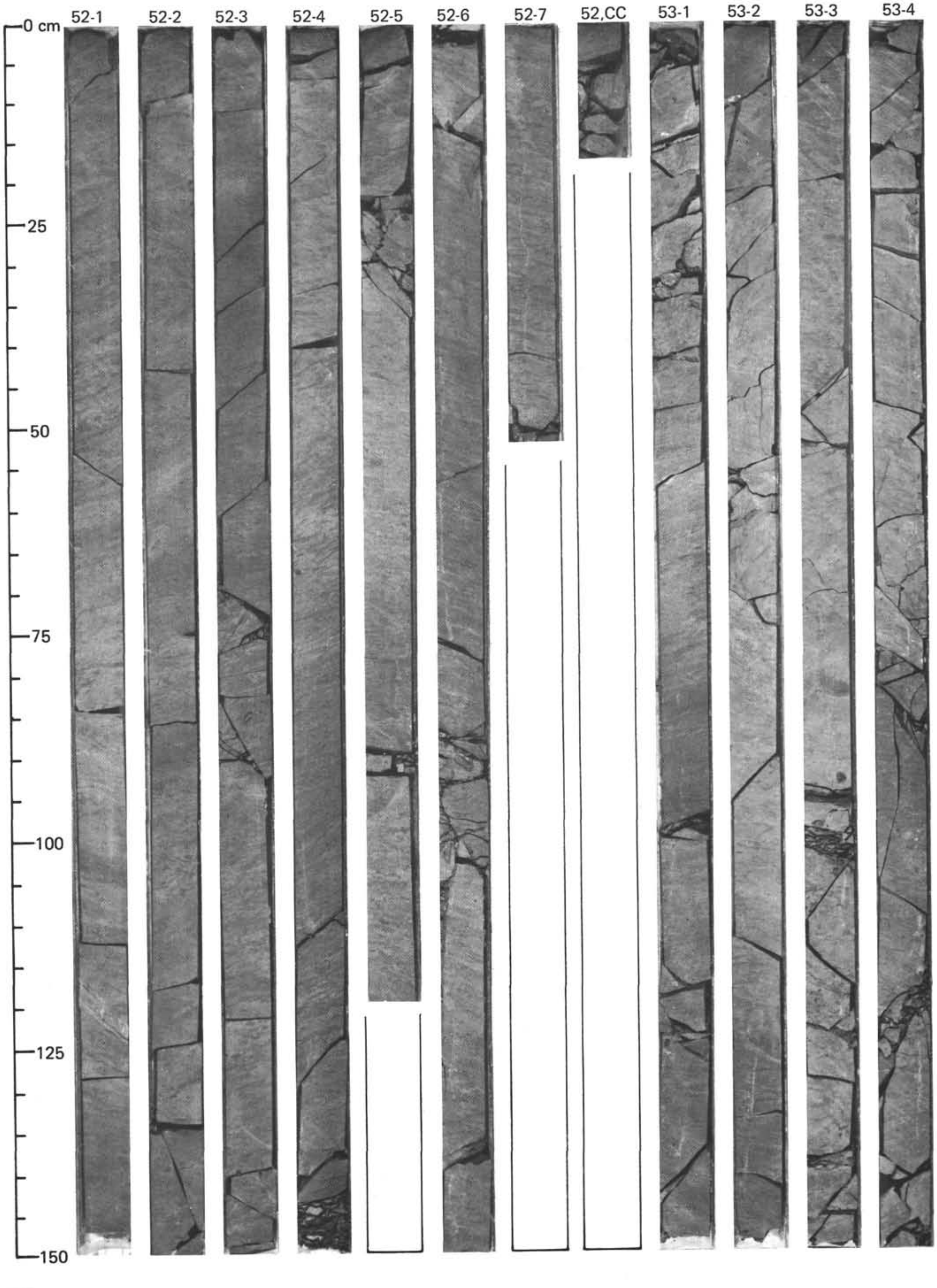
52-1
52-2
52-3
52-4
52-5
52-6
52-7
52,CC
53-1
53-2
53-3
53-4
0 cm
25
50
75
100
125
150

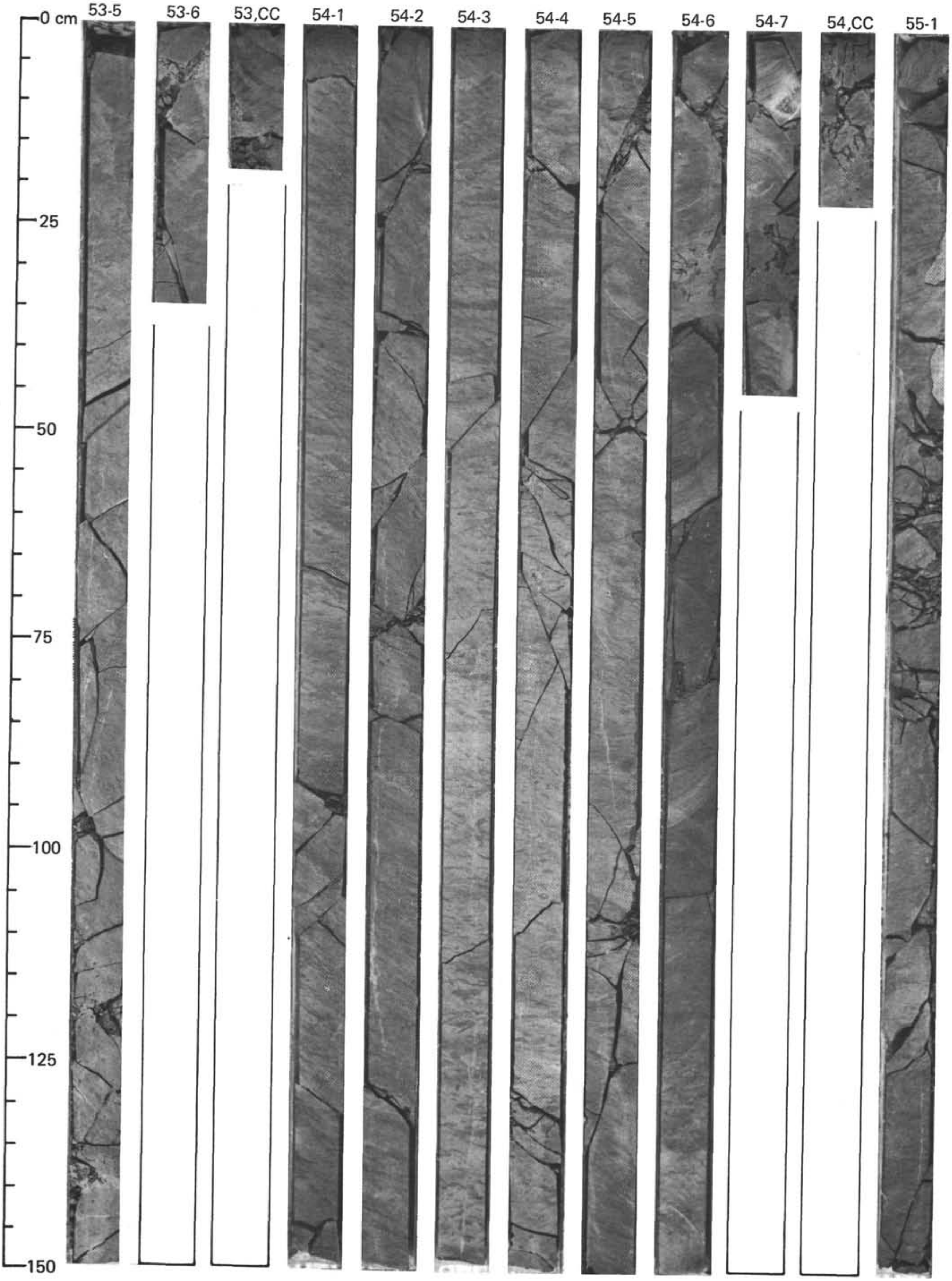
0 cm
25
50
75
100
125
150
53-5
53-6
53,CC
54-1
54-2
54-3
54-4
54-5
54-6
54-7
54,CC
55-1

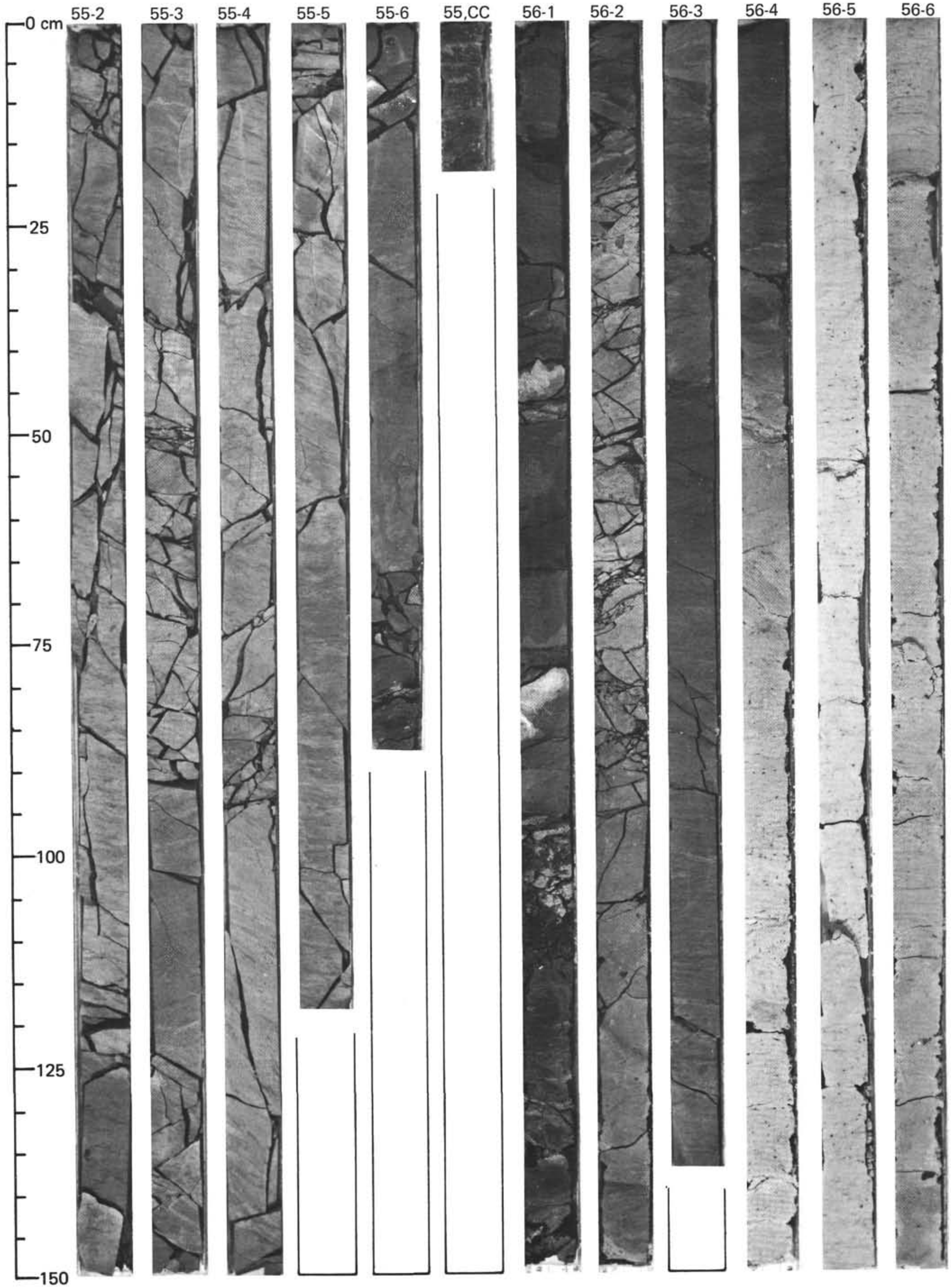
55-2
55-3
55-4
55-5
55-6
55,CC
56-1
56-2
56-3
56-4
56-5
56-6
0 cm
25
50
75
100
125
150

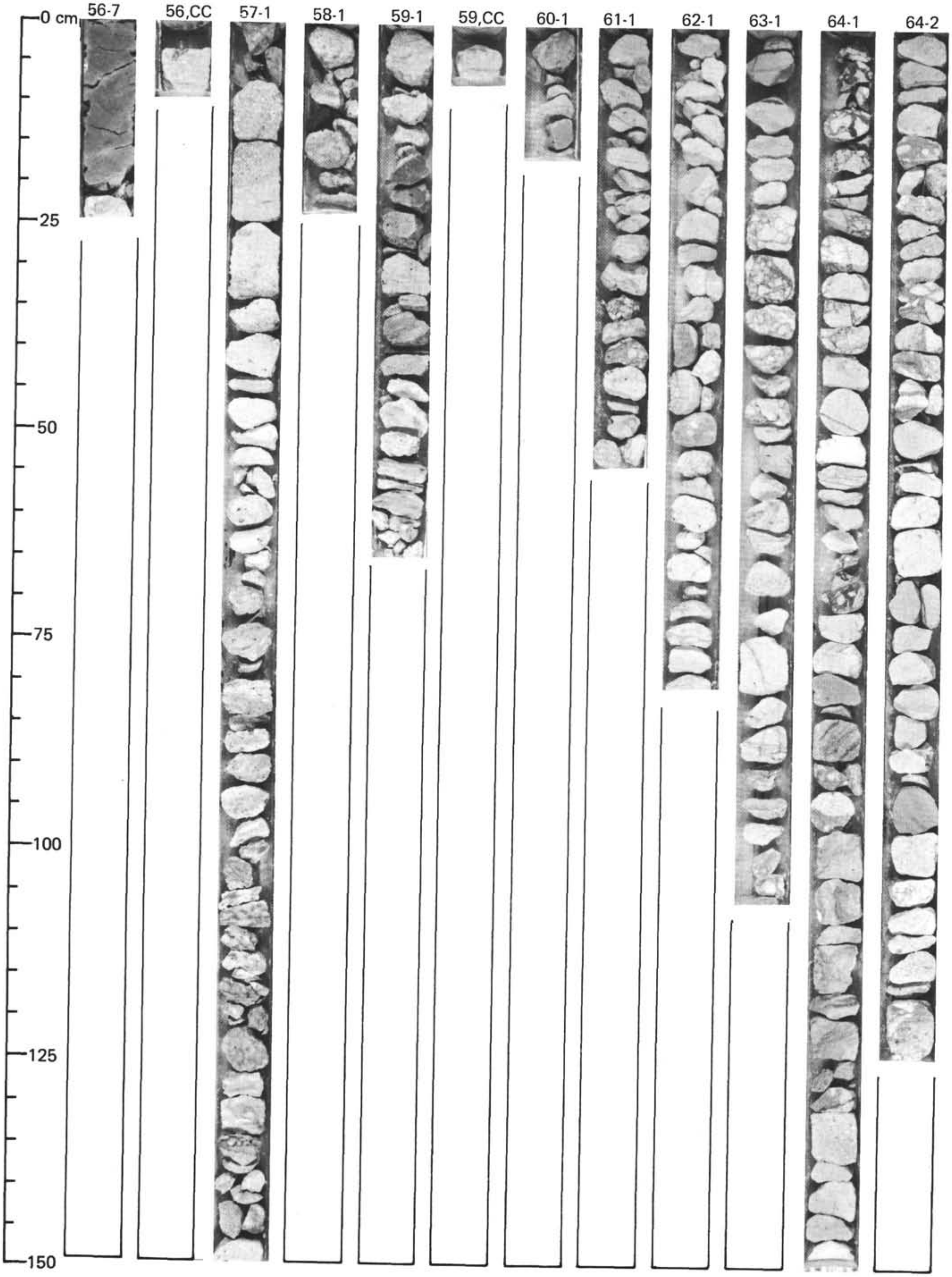
0 cm
25
50
75
100
125
150
56-7
56,CC
57-1
58-1
59-1
59,CC
60-1
61-1
62-1
63-1
64-1
64-2

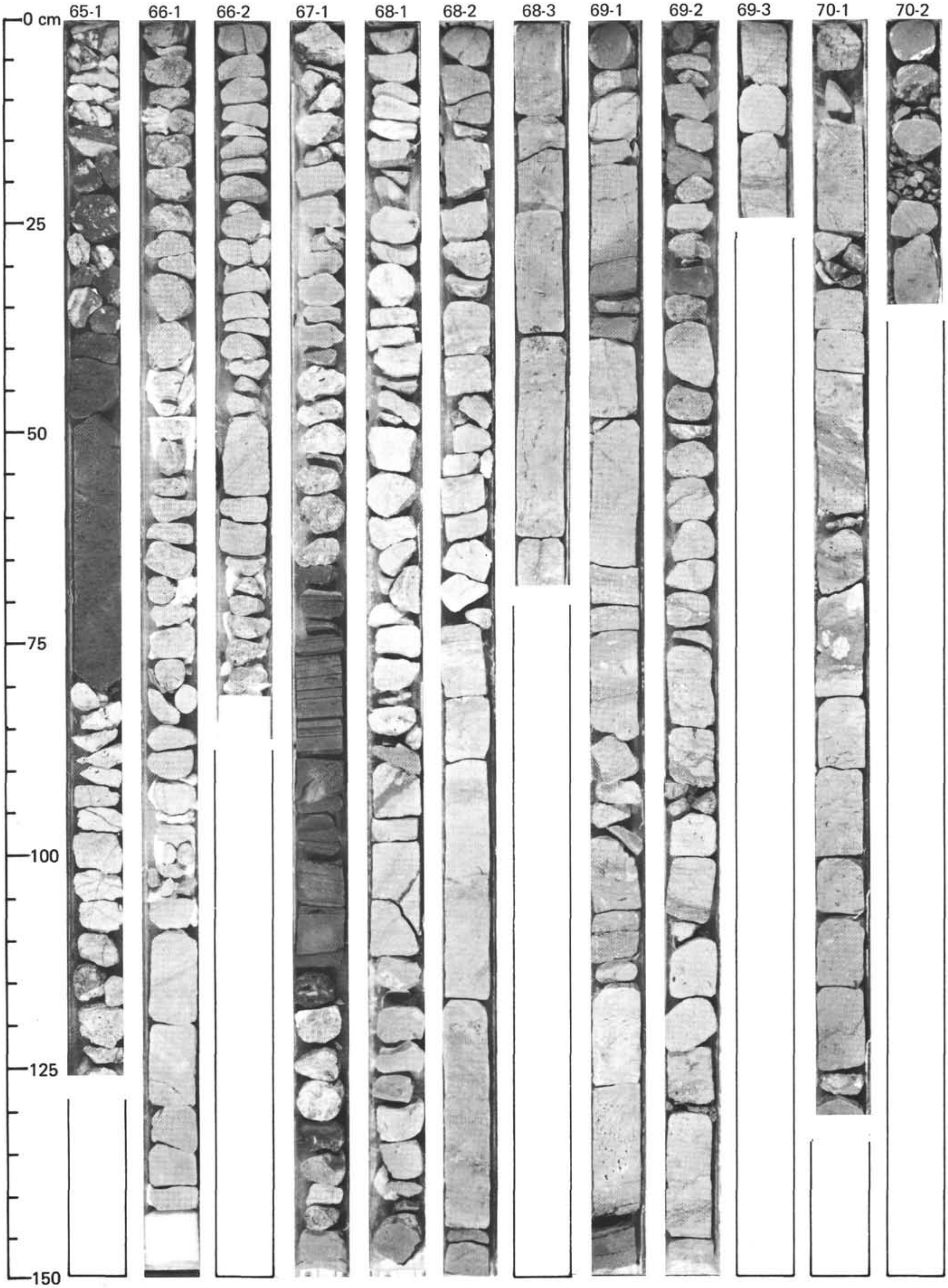
0 cm
25
50
75
100
125
150
65-1
66-1
66-2
67-1
68-1
68-2
68-3
69-1
69-2
69-3
70-1
70-2

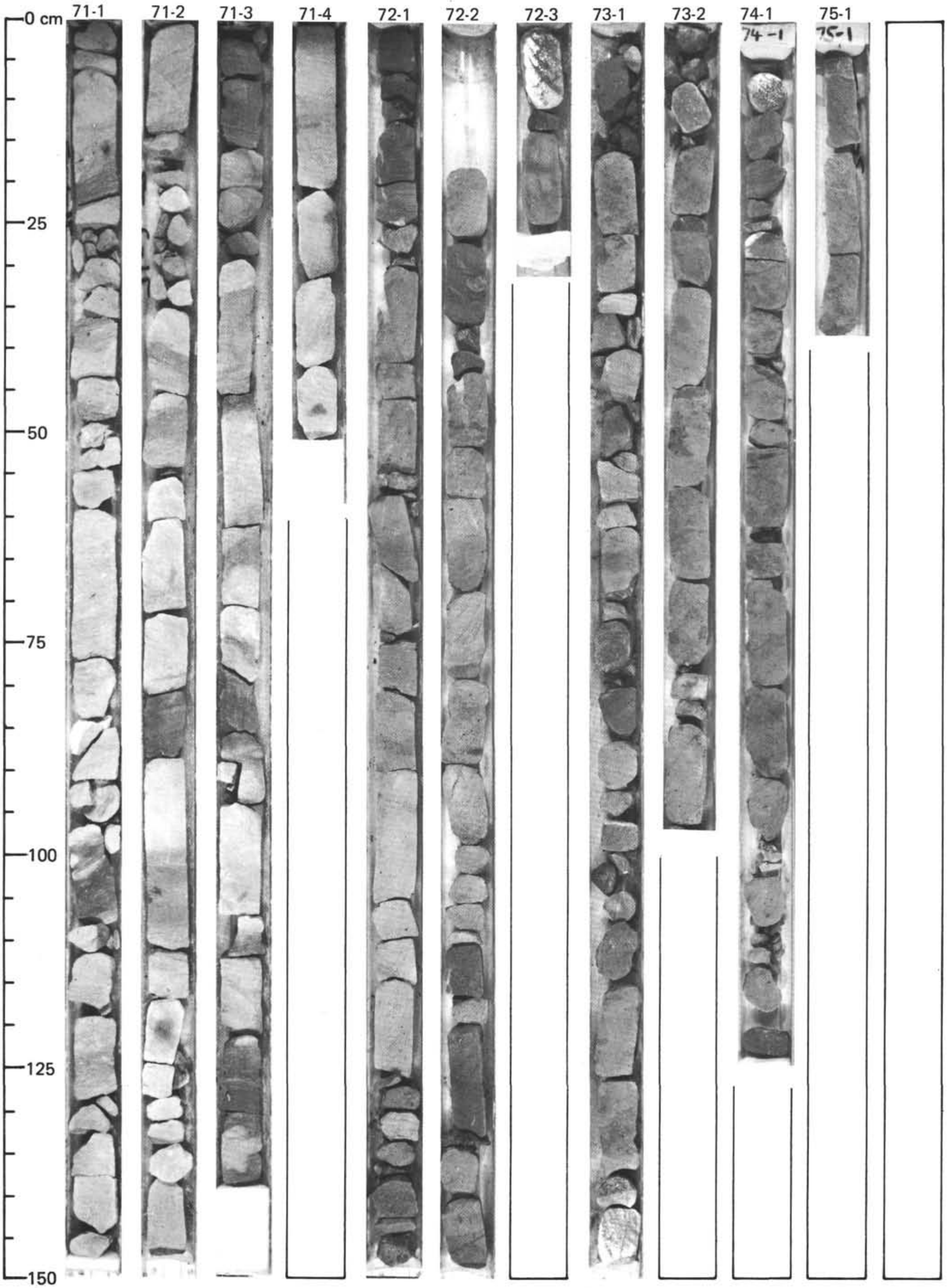
0 cm
25
50
75
100
125
150
71-1
71-2
71-3
71-4
72-1
72-2
72-3
73-1
73-2
74-1
75-1
74-1
75-1